TECHNICAL TRANSACTIONS
CZASOPISMO TECHNICZNE

ENVIRONMENTAL ENGINEERING
ŚRODOWISKO

ISSUE 1-Ś (11)
ZESZYT 1-Ś (11)

YEAR 2016 (113)
ROK 2016 (113)

WYDAWNICTWO POLITECHNIKI KRAKOWSKIEJ

TECHNICAL TRANSACTIONS
ENVIRONMENTAL ENGINEERING

CZASOPISMO TECHNICZNE
ŚRODOWISKO

ISSUE 1-Ś (11)
YEAR 2016 (113)

ZESZYT 1-Ś (11)
ROK 2016 (113)

Basic version of each Technical Transactions magazine is its online version
Pierwotną wersją każdego zeszytu Czasopisma Technicznego jest jego wersja online
www.ejournals.eu/Czasopismo-Techniczne www.technicaltransactions.com www.czasopismotechniczne.pl

TECHNICAL TRANSACTIONS | CZASOPISMO TECHNICZNE
ENVIRONMENT ENGINEERING | ŚRODOWISKO
1-Ś/2016
DOI: 10.4467/2353737XCT.16.191.5940

RAJA ABOU ACKL, PAUL UWE THAMSEN*

EXPERIMENTAL AND NUMERICAL INVESTIGATIONS ON AIR ENTRAINMENT IN PUMP SUMP FOR WET PIT PUMPING STATIONS

BADANIA EKSPERYMENTALNE I NUMERYCZNE NAD PORYWANIEM POWIETRZA W STUDZIENCE ŚCIEKOWEJ DLA STACJI POMP MOKRYCH

Abstract

This paper presents a detailed study carried out in order to predict the influence of various design parameters and operating conditions on the performance of the wet pit pumping station. The method is based on the use of physical and numerical models to reproduce and understand the flow conditions inside the wet pit and their effect on the air entrainment. The research starts with developing a representative model for the wet pit pumping station, goes through conducting the numerical and experimental studies as well as the validation of the results, and ends with providing a valuable easy-to-enforce preliminary design and operating recommendations.

Keywords: air entrainment, CFD, pumping station wet pit

Streszczenie

W niniejszym artykule przedstawiono szczegółowe badania przeprowadzone w celu przewidywania wpływu różnych parametrów projektowych i warunków pracy na działanie stacji pomp mokrych. Metoda ta opiera się na wykorzystaniu wzorów fizycznych i numerycznych w celu odtworzenia i zrozumienia warunków przepływu wewnątrz pompy mokrej oraz ich wpływu na porywanie powierza. Badanie rozpoczyna się od opracowania reprezentatywnego modelu stacji pomp mokrych, następnie skupia się na przeprowadzeniu badań eksperymentalnych i numerycznych oraz walidacji wyników, kończąc na przedstawieniu cennych i łatwych do wdrożenia rekomendacji dotyczących wykonania projektu wstępnego i eksploatacji.

Słowa kluczowe: porywanie powietrza, CFD, stacja pomp, pompa mokra

* M.Sc. Raja Abou Ackl, Prof. D.Sc. Ph.D. Eng. Paul Uwe Thamsen, Chair of of Fluid System Dynamics, Department of Fluid Dynamics and Technical Acoustics, Technische Universität Berlin.

1. Introduction

In many places, lifting systems represent central components of a wastewater system. Pumping stations with circular wet-pit design are the most popular for smaller pump stations due to their relatively simple construction techniques as well as a smaller footprint for a given sump volume [1].

This type of pumping stations is equipped with submersible pumps located, in this case, directly in the wastewater collection pit. The wastewater passes through the pump station untreated and loaded with all kind of solids. Thus, the role of the pump sump is to provide an optimal operation environment for the pumps in addition to the transportation of the sewage solids. Bad design of the pit may affect the overall performance of the station in terms of poor flow conditions inside the pit, non-uniform and disturbed inflow at the pump inlet, as well as air entrainment to the pump. Therefore, understanding the effects of design criteria concerning pumping station performance is important in order to fulfil the wastewater transport maintenance-free and as energy efficient as possible.

The aim of this article is to explain a method evaluating the impact of various design and operating conditions on the performance of the pump station concerning the air entrainment to the pump as well as inside the pit.

2. Air entrainment in wet pit pumping stations

Due to the 'intermittently' working conditions of the wet pit pumping stations, the height between the inlet pipe and the free liquid surface in the pit changes constantly. This means that the wastewater forms a free jet falling on to the sump wastewater surface (Fig. 1). Depending on the velocity and the height of the falling jet, air bubbles may be entrained beneath the surface by the plunging jet [2–4].

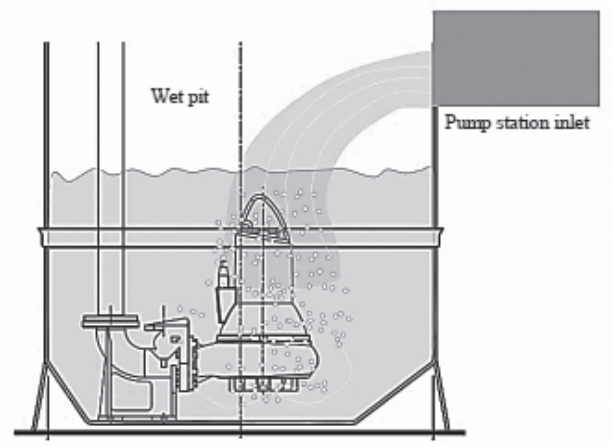

Fig. 1. Typical air entrainment in wet well pumping station

The air entrainment by plunging jets takes place when the jet impact velocity exceeds a critical value, which is a function of the inflow conditions [2–3]. The maximum penetration depth of the air bubbles depends on many parameters, such as the impact diameter of the jet, the velocity at the water surface, the jet instability and the free surface deformation [4, 6]. Therefore, it is difficult to predict theoretically. Entrained air caused by the impacting jet has an influence on the liquid flow field and on the debris transport in the sump [5]. Moreover, the performance of the pump will be affected if the air bubbles enter it. In general, centrifugal pumps can pump water with up to 5–10% gas content [7]. Yet, lower amounts of gas already influence the pumping system operation, changing the power consumption and hydraulic head, which reduce the efficiency of the system. Furthermore, vibrations arise that will damage the bearings. Thus, air entrainment of all amounts should be avoided and be considered during the design process.

Most of the studies on the mechanism of air entrainment and the penetration depth of a plunging jet are based on experimental investigations for jets from nozzles falling into a receiving reservoir or for a velocity that is not applicable in the wastewater system, see example publications [2, 6, 8, 18]. Moreover, the flow inside the pump sumps is irregular and very complicated with three dimensional patterns, due to the flow induced by the suction effect of the working pumps, in addition to the interaction between the tight space and the flow in the sump.

Thus, the conclusions and the formulas derived from these studies are not, or at least partly, applicable in the case of an impinging jet into a wet pit pumping station.

3. Methodology

The ability to predict the flow conditions and the air entrainment in the sump is very important during the design process in order to improve the design and avoid the air entrainment to the pump. The physical laboratory study is a precious tool that helps to describe hydraulic phenomenon and predict very complicated flow conditions. However, it is common to use a scaled physical model in the laboratory due to economical and spatial demands. Due to hygienic reasons, water is used to imitate the wastewater in this stage of research.

3.1. Scale effects

A physical model is a geometrically reduced or sometimes enlarged reproduction of a real-world prototype [12], and is used as a research tool for finding the technically and economically optimal solution of engineering problems [9]. In free-surface flows, which this case is, gravity plays an important role and thus Froude similitude should be used in order to fulfil the geometric similarity of the water surface [9]. This similarity means that the Froude number, as shown in Eq. (1), is kept identical both in the model and the prototype.

$$\mathrm{Fr} = \left(\frac{\text{Inertial force}}{\textit{Gravity Force}} \right)^{0.5} = \frac{\mathrm{V}}{\left(gL\right)^{0.5}} \tag{1}$$

The entrainment of air bubbles by a plunging jet is governed by the surface tension and the flow turbulence, implying the use of Weber similitude and Reynolds similarity respectively. Thus, the air entrainment in the small model based upon Froude similitude could be affected, due to the underestimation of the flow turbulence and the overestimation of the surface tension. There are many countermeasures to minimize scale effects in Froude models, such as calibration, the replacement of fluid, the use of scale series and the use of limiting criteria concerning the force ratios [9, 11].

On the contrary, the numerical models represent the real problem with no need of scaling. Hereof, the idea arises to use the numerical simulation to predict the air entrainment in such complicated situations. But on the other hand, the simplifications in the numerical solution lead to some deviations between the model and the prototype. Therefor, there is a need to calibrate and assess the accuracy of the numerical simulation with experimental investigations.

3.2. Qualitative evaluation of the air entrainment

After Bin [6], the bubbles resulting from plunging liquid jet will be dispersed beneath the liquid surface and form two regions classified according to the size of the bubbles:

- The biphasic conical region containing bubbles that reach maximum depth where the buoyancy forces balance the momentum of the jet.
- The region of bigger rising bubble.

The prediction of the bubble size is difficult. In addition, the accurate calculation and measurement of the air flow rate that enters the water is very complicated. However, as already mentioned above, air entrainment of all amounts should be avoided, and consequently, it is irrelevant to measure and find the exact amount of air entrained to the sump, but rather to find the operation and flow conditions that led to air entrainment into the pump.

In this research, two methods are used to evaluate the air entrainment in the pumping station.

1. Measuring the dimension of the bubble cloud (Fig. 2) i.e. the region occupied with the bubbles, which represents a qualitative evaluation of the air entrainment in the sump.
2. Observing the air bubbles in the outlet pipe of the pump. This gives an indicator of the air entrainment to the pump, which is the most important one.

In this sense, a physical model that fulfils the demands of these methods is designed.

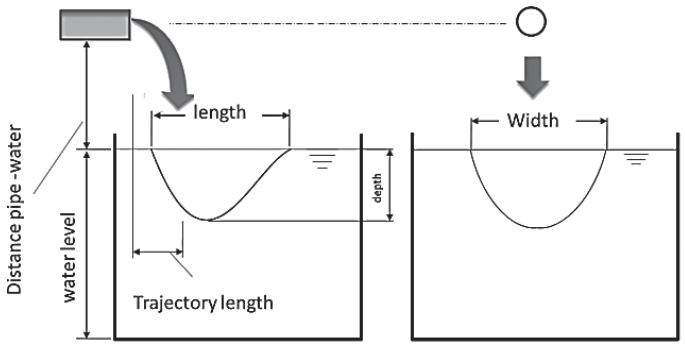

Fig. 2. Sketch of the ‘entrained bubble cloud’

3.3. The physical test model

The physical model is designed upon Froude similarity. The scale 1:3.2 is chosen to simulate a typical market standard sump of a 1600 mm diameter with a standard acrylic cylinder of 500 mm. The height of the model is 750 mm and the inflow pipes are mounted at a height of 450 mm above the bottom of the tank, reproducing the height of 1440 mm in original full-scale design.

A simplified model has been used to represent the most important features of the duplex circular wet pit pumping station. The Representative Model consists of: coupling systems, guide bars, pressure pipe and dummy pumps. The need of reference geometry implies the use of a simple tank with a flat floor, called the 'baseline geometry'. The inflow direction relative to the pumps centreline position as well as the water level can be changed in the model (Fig. 3).

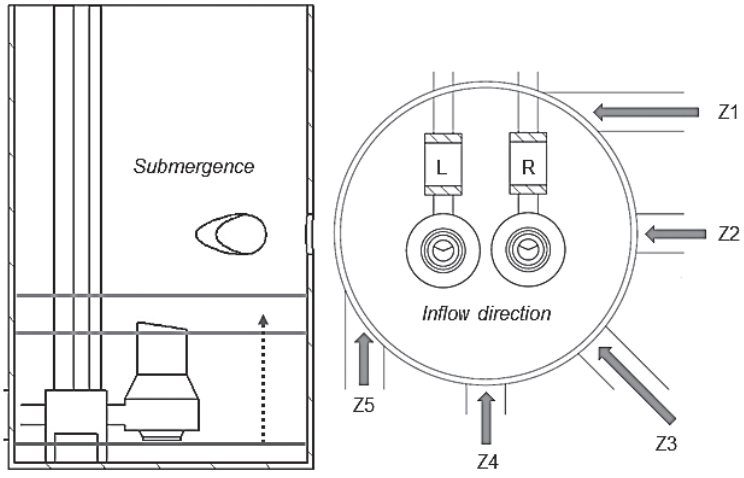

Fig. 3. The adaptable parameters of the model

The implemented test rig of the physical model is made of acrylic (Fig. 4) to enable the observation of the aerated region inside the sump and the bubbles entering the dummy pump at various operating conditions. It is possible to conduct the experiments in two working conditions:

1. Varied water level to reproduce pumping cycles.
2. Constant water level to enable the conduction of the test for constant inflow.

3.4. Numerical test model

There are many numerical simulation studies concerning the air entrainment, for example [4] presents 2D simulation the results of round vertical liquid jet plunging into bath with focus on bubbles size and the influence of the jet velocity using smoothed volume of flow technique [20]

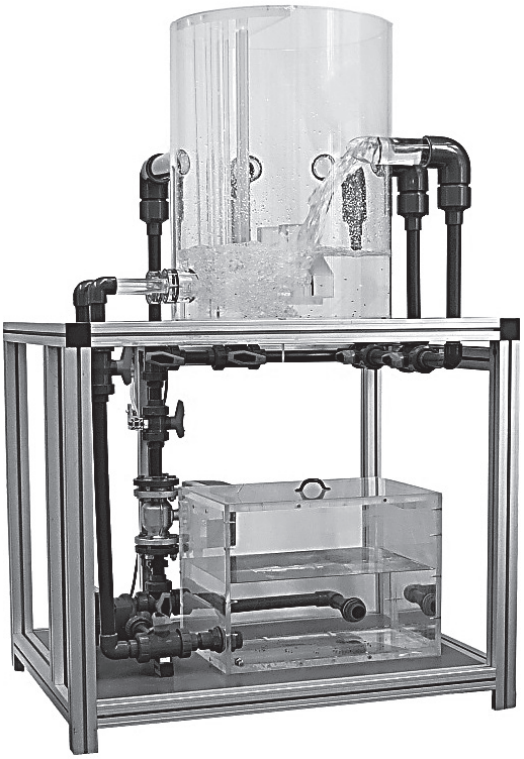

Fig. 4. Model test rig

studied the formation of the air cavities generated by translating plunging jet into a pool, whereas [5] researched the influence of the air entrainment on fibber transportation in the sump.

In our study, the Volume of Fluid (VOF) method was used to simulate the air entrainment and the air bubble formation. The water and the air are assumed to be incompressible Newtonian fluids. In this method, a phase q_A of the multiphase fluid consisting of the phases q_W (water) with the density ρ_W and q_A (air) with the density ρ_A is described by its volume fraction (α_A) in a computational cell. For α_A the following three states apply:

$\alpha_A = 0$, the cell is empty of the q_A phase,

$\alpha_A = 1$, the cell is full of the q_A phase,

$0 < \alpha_A < 1$, the cell contains the interface between the q_W and the q_A phase.

In the absence of sources of mass and momentum, the continuity equation for the volume fraction of the phase q_A is written as:

$$\frac{\partial}{\partial t}\left(\alpha_q \rho_A\right) + \nabla\left(\alpha_q \rho_A u\right) = 0 \tag{2}$$

Thereupon, the q_W phase volume fraction is computed from the relation: $\alpha_W + \alpha_A = 1$. The momentum equation depends on the volume fractions of the phases through the properties ρ and μ.

$$\frac{\partial(\rho\mathbf{u})}{\partial t} + \nabla(\rho\mathbf{u}\mathbf{u}) = -\nabla p + \nabla\left[\mu\left(\nabla\mathbf{u} + \nabla\mathbf{u}^T\right)\right] + \rho g + F \tag{3}$$

In this equation **u** is the velocity vector, ρ is the density, p is the pressure, g is acceleration of gravity and F is the equivalent volume force due to the surface tension.

A transport equation is solved for the water phase to model the surface between water and air in the absence of any inter-phase mass transfer:

$$\frac{\partial}{\partial t}(\alpha_w) + \nabla(\alpha_w u) = 0 \tag{4}$$

In this two-phase system, the volume fraction of the air phase is being tracked, the density in each cell is given by:

$$\rho = \alpha_A\rho_A + (1 - \alpha_A)\rho_W \tag{5}$$

The viscosity μ is computed in the same manner:

$$\mu = \alpha_A\mu_A + (1 - \alpha_A)\mu_W \tag{6}$$

Furthermore, k-e turbulence model was used with wall functions.

3.4.1. Computational domain and boundary conditions

Unsteady CFD calculations applying the CFD code ANSYS/Fluent were performed. Fig. 5 shows the 3D computational domain. It is discretised into 4.9 × 106 tetrahedral cells with max 3 mm length in each direction, and partitioned into 14 subdomains, every domain calculated with one processor. The assessment of the independence of the results on the computational grid was checked by further calculations, applying a finer grid to capture the smallest air bubbles, and the suitable mesh where selected, not presented here.

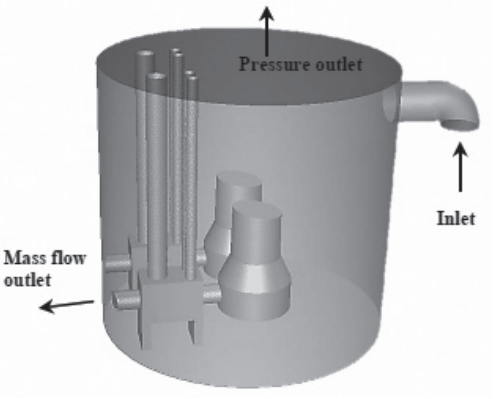

Fig. 5. Numerical setup

The calculations were made with the densities and viscosities of air and water at 15°C. The simulations were performed with a water-air surface tension set at 0.073 N/m. The PISO algorithm was used for pressure–velocity coupling. The interface between fluids was represented with Geometric Reconstruction Scheme. At the inlet, a velocity profile is specified for the velocity. The open top of the pit has a pressure outlet boundary condition, and the outlet of the simulation geometry has a mass flow boundary condition. With this combination, the water level in the pit remains constant. Computations were continued until the global residuals reached 10−5. During the unsteady calculation, an adaptive time-stepping method was used to ensure a Courant-Friedrichs-Levy number less than 1. At the initial time, the domain is filled up to a certain level with water. The remaining region consists of air.

4. Results and conclusions

The experimental investigations were systemically conducted by choosing an inflow direction and carrying out the experiments at various water levels and flow rates. During every experiment, the bubbles zone was monitored using video recording. Moreover, the acrylic outlet pipes of the dummy pumps were observed for air bubbles (Fig. 6). Depending on the records of the depth, the width and the length of the cloud were determined.

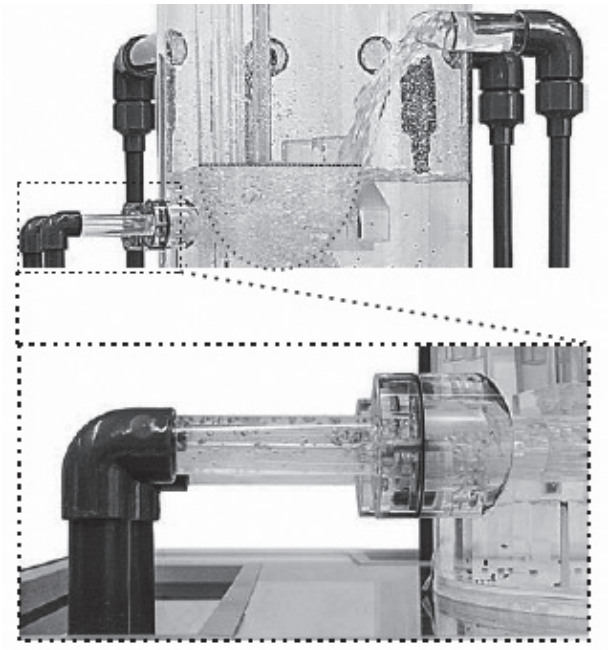

Fig. 6. Bubble cloud and the air entrainment to the pump

A series of computations was started with boundary conditions that represent the experimental flow conditions. The simulated time was 30 s. After that, a video was generated and the same procedure of the experimental investigation was applied, concerning the dimensions of the bubbled region (Fig. 7).

The air entrainment to the pump was analysed by checking the appearance of the air phase using a control surface positioned on the suction side of the pump. The number of the executed experimental test series was very large, as a result of the diversity of the working combinations for five chosen water levels (Fig. 8).

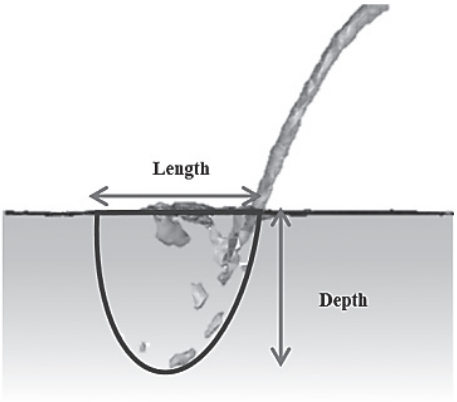

Fig. 7. Measured variables of the air entrainment

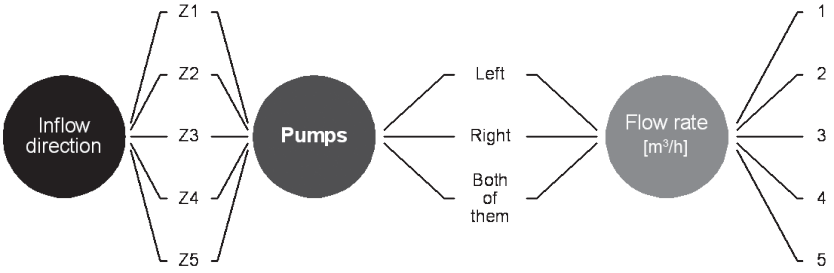

Fig. 8. Possible working combinations

Thus, only 8 cases were simulated in the numerical model, namely the inflow direction Z2 at two water level and four flow rates as shown in the Table 1.

Table 1

Summary of the numerical cases

Water level [m]	0.2	0.32
Flow Rate [m³/ h]	1	1
	2	2
	3	3
	4	4

Both experimental and numerical results are presented. The experimental observations were used to assess the impact of the inflow direction on the air entrainment to the pump and to validate the simulation results regarding the dimensions of the bubble cloud and the (yes/no) indicator of the air entrainment to the pump.

4.1. The minimum submergence required to avoid air entrainment

Fig. 9 shows the experimental results of the minimum submergence for all possible combinations of inflow direction, flow rate and the working pump, in addition to a schematic illustration of the inflow direction influences on the pumps inside the pit. The minimum submergence is the water level required to prevent air entrainment to the pumps, which means, in the experiments, if the water level beneath this submergence, bubbles appear in the outlet pipe.

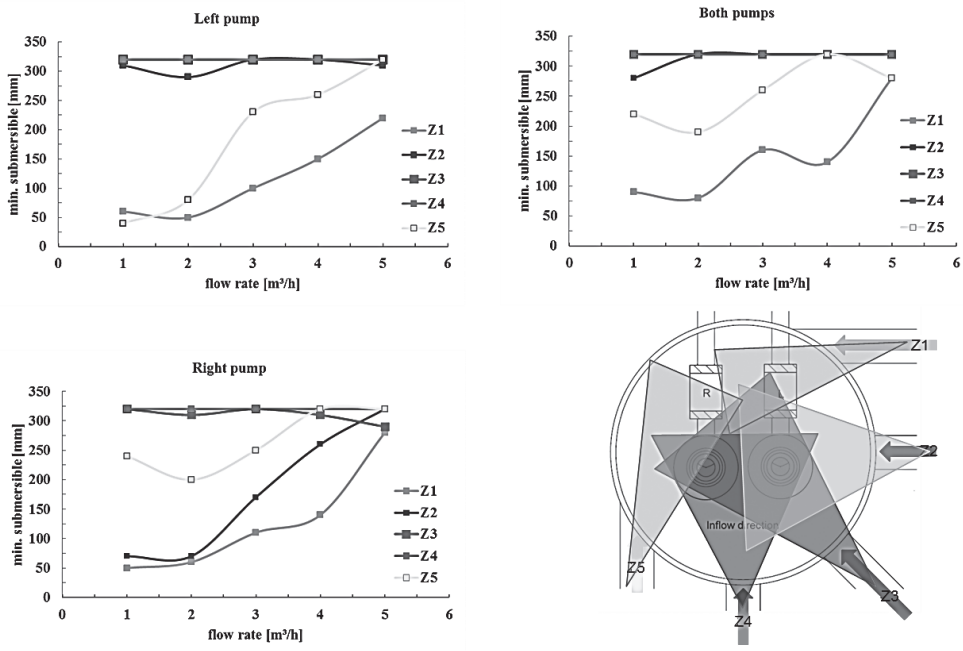

Fig. 9. Experimental results for minimum required submergence at different working combinations

The experimental results show that the flow directions Z3 and Z4 need the highest water level to prevent the air bubbles from reaching the pumps. Whereas it was very clear that both tangential directions produce suitable flow conditions inside the pumping station that minimize the amount of entrained air to both pumps.

Therefore, it can be concluded that the best inflow direction to the pump station concerning the air entrainment is the Z1 because it is associated with the lower water level.

4.2. Dimensions of the bubbles cloud

By determining the dimensions of the cloud, the average bubble size is considered. From Fig. 10, it can be seen that the simulation results and the experimental values are relatively in good agreement. The behaviour is captured and the results reveal that the model and the interface tracking are able to capture the bubble cloud generated from an impinging jet.

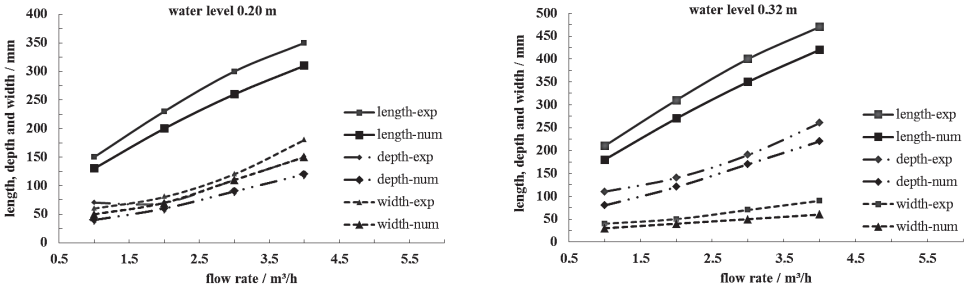

Fig. 10. Experimental and numerical dimensions of the bubbles cloud

The results show that the numerical model underestimates the phenomena. The deviation can be explained by the uncertainties of the numerical model and the inaccuracy of the measurements in the experimental setup.

At the inlet, the turbulence is neglected, which means that the jet instability and the free surface deformation are not sufficiently reproduced. The air entrainment is highly affected by the turbulence in the jet and the free surface of the receiving pool.

Furthermore, the measurements of the flow rate, the dimensions of the bubble zone as well as the water level contain some inaccuracy, leading to a mismatch between the boundary conditions in both setups and to deviations in the results.

4.3. Air entrainment to the pump

The air entrainment to the pump depends on the balance of various forces that act on the bubbles, depending on their volume, namely the buoyancy forces, the momentum of the moving bubbles and the effect of the flow induced from the working pump. Considering all the difficulty to capture small bubbles, the dimensions of the bubble cloud are underestimated. In this sense, it can be justified that the numerical model succeeded to predict the air entrainment to the pump in 5 of the 8 cases.

However, the calculations of the rest of the cases are planned, which will give a better indicator on the accurate of the numerical simulation.

5. Summary

The presented paper described the research of experimental and simulation investigations to assess the influence of inflow direction on air entrainment from a plunging water jet on a free surface of a wet pit pumping station. The experimental investigations conducted on the model of a wet pit pumping station show the influence of inflow direction and the water level on the performance of the station with respect to air entrainment. As a conclusion derived from the model test, the use of the tangential inflow direction can be suggested. The three-dimensional numerical model was applied to reproduce the experimental setup in order to predict the air entrainment and the flow characteristics at several flow conditions. The air entrainment was

qualitatively evaluated by defining the dimensions of the bubble cloud and observing the air bubbles entering the suction side of the pump. The numerical VOF model proved to give relatively acceptable results compared to the experimental data. The dimensions of the cloud in the numerical approach had the same behaviour of the experimental model, but with some underestimations. Assessing the use of CFD as tool in the scale series is planned as future works to define the scale effect on the air entrainment and evaluate the transferability of the model results to the original prototype.

References

[1] American National Standards Institute ANSI/HI 9.8, 2012, *American National Standard for Pump Intake Design*.

[2] Zhu Y., Oguz H.N., Prosperetti A., *On the mechanism of air entrainment by liquid jets at a free surface*, Journel of Fluid Mechanics, Vol. 401, 2000, 151–177.

[3] Kiger K.T., Duncan J.H., *Air-Entrainment Mechanisms in Plunging Jets and Breaking Waves*, Annual Review of Fluid Mechanics, Vol. 44, 2011, 563–596.

[4] Qu X.L. et al., *Characterization of plunging liquid jets: A combined experimental and numerical investigation*, International Journal of Multiphase Flow, 37, 2011, 722–731.

[5] Krepper E. et al., *Influence of air entrainment on the liquid flow field caused by a plunging jet and consequences for fibre deposition*, Nuclear Engineering and Design 241, 2011, 1047–1054.

[6] Bin A.K., *Gas entrainment by plunging liquid jets*, Chemical Engineering Science, Vol. 48, 1993, 3585–3630.

[7] Gülich J., *Kreiselpumpen: Handbuch für Entwicklung, Anlagenplanung und Betrieb: Ein Handbuch für Entwicklung, Anlagenplanung und Betrieb*, Springer, 2008.

[8] Chanson H. et al., *Similitude of Air Entrainment at Vertical Circular Plunging Jets*, Proceedings of ASME FEDSM'02, 2002.

[9] Heller V., *Scale effects in physical hydraulic engineering models*, Journal of Hydraulic Research, Vol. 49, No. 3, 2011, 293–306.

[10] Weismann D., Gutzeit T., *Kommunale Abwasser-pumpwerke*, Vulkan Verlag, 2006.

[11] Bollrich D., *Technische Hydromechanik. 2. spezielle Probleme*, Verl. für Bauwesen 1989.

[12] Kobus H., *Wasserbauliches Versuchswesen. DVWK Schriften 39. Spezielle Probleme*, Verl. Paul Parey 1984.

[13] Kawakita K. et. al., *Experimental study on the similarity of flow in pump sump models*, 26th IAHR Symposium on Hydraulic Machinery and Systems, 2012.

[14] Padamabhan M. et. al., *Scale Effects in Pump Sump Models*, Journal of Hydraulic Engineering, Vol. 110, 1984, 1540–1556.

[15] Chanson H., Aoki S., Hoque A., *Bubble entrainment and dispersion in plunging jet flows: freshwater versus seawater*, J Coastal Res, 22 (3), 2006, 664–677.

[16] Chanson H., *Turbulent air-water flows in hydraulic structures: dynamic similarity and scale effects*, Environ Fluid Mech, 9 (2), 2008, 125–142.

[17] Nakasone H., *Study of Aeration at Weirs and Cascades*, Journal of Environmental Engineering, Vol. 113, No. 1, 1987, 64–81.

[18] Yamagiwa K., Mashima T., Kadota S., Ohkawa A., *Effect of liquid properties on gas entrainment behavior in a plunging liquid jet aeration system using inclined nozzles*, Journal of Chemical Engineering of Japan, 26, No. 3, 1993, 333–336.
[19] Sande E. van der, Smith J.M., *Eintragen von Luft in eine Flussigkeit durch einen Wasserstrahl*, Chemie-Ing.-Techn. 44, Jahrg. 1972/Nr. 20.
[20] Brouilliot D., Lubin P., *Numerical simulations of air entrainment in a plunging jet of liquid*, Journal of Fluids and Structures Volume 43, November 2013, 428–440.

TECHNICAL TRANSACTIONS | CZASOPISMO TECHNICZNE
ENVIRONMENT ENGINEERING | ŚRODOWISKO
1-Ś/2016
DOI: 10.4467/2353737XCT.16.192.5941

MARYAM ALIHOSSEINI, PAUL UWE THAMSEN*

AN OVERVIEW OF SPH SIMULATION AND EXPERIMENTAL INVESTIGATION OF SEDIMENT FLOWS IN SEWER FLUSHING

PRZEGLĄD SYMULACJI SPH ORAZ BADAŃ EKSPERYMENTALNYCH NAD PRZEPŁYWEM OSADÓW W SPŁUKIWANIU ŚCIEKÓW

Abstract

This paper concerns the application of the Smoothed Particle Hydrodynamics (SPH) method for sewer hydraulics with a focus on free-surface flows and sediment flushing. SPH is the most popular mesh-free method and has been widely used in the field of fluid mechanics. Here, the previous studies in the last few years are summarized, which have investigated the application of the relatively new model for the simulation of solid transport, free-surface and multiphase flows.

Keywords: smoothed particle hydrodynamics, free-surface flows, sediment transport, flush cleaning

Streszczenie

Niniejszy artykuł dotyczy zastosowania metody cząstek rozmytych (ang. *Smoothed Particle Hydrodynamics* – SPH) dla hydraulicznych systemów kanalizacyjnych ze szczególnym uwzględnieniem przepływów powierzchni swobodnej oraz spłukiwania osadów. SPH stanowi najbardziej popularną metodę bezsiarkową, powszechnie stosowaną w dziedzinie mechaniki płynów. W niniejszej pracy zestawiono dotychczasowe badania przeprowadzone w ciągu ostatnich kilku lat, które dotyczyły zastosowania stosunkowo nowego modelu do symulacji transportu materiału stałego, przepływów powierzchni swobodnej oraz przepływów wielofazowych.

Słowa kluczowe: metoda cząstek rozmytych, przepływy powierzchni swobodnej, transport osadów, spłukiwanie

* M.Sc. Maryam Alihosseini, Prof. D.Sc. Ph.D. Eng. Paul Uwe Thamsen, Fluid System Dynamics, Department of Fluid Dynamics and Technical Acoustics, Technische Universität Berlin.

1. Introduction

Solids in sewage originating from precipitation, sanitary, commercial and industrial inputs deposit on the bottom of sewers and build sediments mostly during dry weather periods. Sewer sediment deposition represents a crucial aspect of the maintenance of sewer systems. Therefore, it is very important to avoid the accumulation of large amounts of sediments. Among different cleansing devices, flushing gates have been widely used to remove sediments periodically from sewers. The flushing gates require low maintenance and are cost-effective. In the last decades, many numerical and experimental investigations on the sediment flushing in sewers have been carried out. In some cases (e.g. sewer networks), the practical investigations could be complicated, expensive and time-consuming due to the complex phenomena. Furthermore, for the general design of flushing devices, it is necessary to understand the hydraulic principles of the flush wave. However, it is difficult to transfer the measurement results of one sewer to other sewers as well as to other cleaning devices [45]. Therefore, numerical methods have become an essential alternative to laboratory experiments for simulating several phenomena in the field of sewer networks. For many years, the free-surface flows have been simulated using Eulerian mesh-based methods. However, by dealing with highly deformable flows or complex geometries, creating a mesh can be difficult and expensive. Therefore, in the last years, the Lagrangian mesh-free methods have been widely used to simulate free-surface flows that are rapidly changing. Smoothed particle hydrodynamics (SPH) is a relatively new Lagrangian method developed by Gingolds and Monaghan [22] and Lucy [28] to solve astrophysical problems. The SPH method is the most popular mesh-free method and it is capable of dealing with problems concerning free surfaces, deformable boundary, moving interface, wave propagation and solid simulation. The following paper briefly describes the origins and the characteristics of solids in sewage, sediment transport in sewers, sediment flushing and the SPH method. Finally, the paper summarizes varied applications of the SPH method for simulating free-surface flows and sediment transport.

2. Solids in sewage

The solids in sewage come from different sources, in particular from wastewater and stormwater discharge. They vary from organic to inorganic materials. In sewer systems, it is important to know settle-able sediments, which could form bed deposits, such as faeces, food waste, hygiene items, paper, sand, stone, etc. They have settling velocities between 0.2 and 30 cm/s. However, it is not easy to determine the particle settling velocities accurately because of particle aggregation. There are some other particles of very small size or low density, which remain in suspension under normal flow conditions and do not have a very important influence on the hydraulic capacity of sewerage systems. Many studies have been carried out on characteristics of the sediments in sewers [3, 11, 34, 44, 55]. The non-cohesive materials are mostly characterized by their grain size distribution and the settling velocity [29]. Schlütter [46] categorized the solids according to their pollutants into fine faecal and other organic matter, large faecal and large organic matter (gross solids) and paper and rags

(sanitary litter). Ashley et al. [5] subdivided solids in sewers depending on where they are found, in four primary classes: coarse granular bed material widespread, mobile and fine-grained found in slack zones, organic pipe wall slimes and zoogleal biofilms around the mean flow level, and fine-grained mineral and organic material found in the combined sewer overflow (CSO) storage tank. Ashley and Verbanck [4] considered the solids as sanitary, separate (fine) stormwater solids and grit.

3. Sediment transport

The transport of sewage with its solids takes place in sewers. The solids make up only 1% of the total wastewater volume, but they affect the function and operation of the whole wastewater network. They are an essential part of the total pollution load of sewage. Their transportation to the wastewater treatment plant or other water bodies leads to high pollution challenges [19]. It has been required to investigate the sediment transport in sewers to control the pollution transport. The solids move by the flow of the fluid. Therefore, their transport is determined by hydraulic properties, such as viscosity and flow velocity of the fluid, and the characteristics of the solids, such as size and density. In sewers, the rapid change of the hydraulic conditions in time and space affects the sediment transport. Several studies investigated the complex processes of the sediment transport in sewers [4, 16, 19, 24, 25 and 46]. The bed shear stress is an important parameter to define the transport of solids. The mean bed shear stress for stationary and turbulent flow conditions in open channels is evaluated as [17]:

$$\tau_0 = \rho \frac{\lambda}{8} V_m^2 \tag{1}$$

where:

ρ – the water density,
λ – the resistance coefficient of the pipe friction,
V_m – the mean flow velocity,

In general, the solids may travel either in suspension or as bedload, depending on the size of the bed material particles and the flow conditions. The solids in bedload have different movement modes, depending on the value of the bed shear stress: rolling, jumping or sliding. When the value of the bed shear stress just exceeds the critical value for initiation of motion, the particles will be rolling and sliding, or both. When the bed shear stress increases more, the particles will be jumping. The suspended load includes solids that are in suspension because of turbulence and may settle down when flow conditions are insufficient (Fig. 1). Another mode of transport introduced by some researchers is wash load [52]. This mode is in suspension load and includes the proportion of suspended solids that remain in suspension in sufficient flow conditions and never settle down. The total sediment load is the sum of these three loads, which has been investigated by several researchers such as Yang [57] and van Rijn [53]. However, in natural conditions, it is not easy to distinguish between these phases.

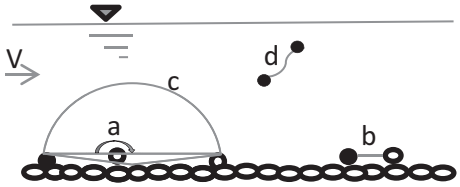

Fig. 1. Different modes of sediment transport: a – rolling, b – sliding, c – jumping, d – in suspension (graphic idea from Bollrich [9])

Another important parameter to describe the transport behavior of solids is the settling velocity, which is influenced by the flow conditions in the channel, such as turbulence, and the solids' characteristics, such as particle size and density. The process of sediment transport in sewage systems is very complex and the available data are insufficient. Furthermore, the laboratory experiments are not able to describe the underlying physics in detail [56]. Therefore, not only experimental investigations are carried out, but also several numerical methods are developed for modelling the sediment transport in sewer systems [19, 46].

4. Sediment flushing

In the last decades, great attention has been drawn to the sediment control in sewers. During periods of dry weather, by low flow velocities and prolonged duration times, the solids deposit on the bottom of sewers and build sediments [50]. Sediment deposition represents a crucial aspect of the maintenance of sewer systems. The accumulation of large amounts of sediments leads to various hydraulic and environmental problems in sewer networks, such as reduction of the design flow capacity and increase of the overflows in combined sewer systems, loss of hydraulic capacity, gas and corrosive acid production, odor problems and concentration of pollutants. There are different techniques for the removal of sediment deposits from sewer systems, based on the use of different mechanical and hydraulic devices [7, 13, 41]. Several studies have investigated the use of flushing devices and the scouring effects of flushing waves [8, 12, 42, 51].

Flushing gates have become very popular, because they are mostly self-controlled systems and a cost-effective solution to remove the sewer sediments. They are in-line flushing devices designed in order to produce flushing waves with high flow velocities and shear stresses that lead to re-suspend and transport the solids along sewers [12, 26]. The function of the flushing device is mostly divided into four general phases. First, the gate is closed. Second, water is stored by a closed gate in the vertical position. Third, the gate is opened, which lead to a fast discharge of the stored water generating the flushing waves. Finally, the flushing process starts. The transported solids can be collected downstream in special tanks or removed manually. The cleansing efficiency of flush waves is the most important parameter, which depends on flush volume, flush discharge rate, sewer slope and length, sewer flow rate, sewer

diameter and population density [41]. Experiments have proven that the solids could be re-suspended and transported not only with large flushing waves at high velocity, but also with small waves at low velocity [17].

5. Smoothed Particle Hydrodynamics

During the last decades, numerical models have become very popular, because they are cost-effective and can simulate the same size as the real case. The Lagrangian mesh- free methods have been widely used to simulate free-surface flows that are rapidly changing. Smoothed Particle Hydrodynamics (SPH) is a mesh-free method, which was developed to solve astrophysical problems [22, 28]. Furthermore, it was successfully used to simulate free-surface flows [38] and multi-phase flows [39]. In Lagrangian approaches, the particles are carrying physical properties, such as mass, momentum, density, pressure and velocity. In SPH, the system contains a large number of particles that move with the fluid, which means that the motion of the fluid is represented by the motion of the particles [14]. The mass and the number of particles are constant, so that continuity of mass is solved. The particles interact with each other, controlled by a smoothing function [26], and their properties can change with time [23]. A smoothing kernel $W(h, r)$, which is nonzero only for $r = |x - x_i| \leq 2h$; h = smoothing length and r = position vector; approximates field quantities at arbitrarily distributed discretization points and these points move with their local velocity. The smoothing kernel has compact support to limit the number of interacting particles and the width of this kernel represents the discretization length scale of SPH. Figure 2 shows the kernel-weighted influence of the neighborhood of each particle. The physical quantity of any particle can be obtained by summing the relevant properties of all particles, which lie within the range of the smoothing kernel $W(h, r)$. Spatial derivatives are calculated only from interactions with neighboring particles [1].

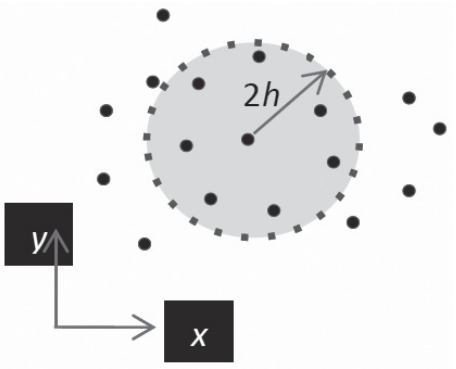

Fig. 2. The kernel-weighted influence of the neighbors of an SPH particle

In order to adapt the SPH method to fluid mechanics applications, the Navier-Stokes equations need to be solved. The Lagrangian form of the Navier-Stokes equations for a weakly compressible viscous fluid is transformed into a system of ordinary differential equations that are written as [31]:

$$\frac{D\rho}{Dt_i} = \sum_{j=1}^{N_i} m_j (u_j - u_i) \nabla_i W_{ij} \tag{2}$$

$$\frac{Du}{Dt_i} = -\sum_{j=1}^{N_i} m_j \left(\frac{p_i}{\rho_i^2} + \frac{p_j}{\rho_j^2} + \Pi_{ij} \right) \nabla_i W_{ij} + \sum_{j=1}^{N_i} \frac{m_j}{\rho_i \rho_j} \frac{4\mu_i \mu_j}{\mu_i + \mu_j} \frac{x_{ij} \nabla_i W_{ij}}{x_{ij}^2 + 0.01h^2} u_{ij} + g \tag{3}$$

where:

N_i – the summation is extended to the N_i points occupied by all neighbors within the compact support of the kernel function centered on the *i*th particle,
$x_{ij} = x_i - x_j$ – relative position vector,
u – particle velocity vector,
$u_{ij} = u_i - u_j$ – relative velocity vector,
g – gravitational acceleration vector,
ρ – density,
μ – dynamic viscosity,
m – mass,
p – pressure of the particle,
Π_{ij} – Monaghan artificial viscosity for the numerical stability of the method that is introduced as:

$$\Pi_{ij} = \begin{cases} -\alpha_M \dfrac{c_{si} + c_{sj}}{\rho_i + \rho_j} \dfrac{h u_{ij} x_{ij}}{x_{ij}^2 + 0.01h^2} & u_{ij} x_{ij} < 0 \\ \text{if} & \\ 0 & u_{ij} x_{ij} > 0 \end{cases} \tag{4}$$

where:

α_m – constant parameter,
c_s – speed of sound.

Each moving fluid element is followed in time. Therefore, SPH simulations need a large number of calculations that increase with the increasing resolution. To speed up the large SPH simulations, graphics processing units (GPUs) and parallel programming are required [36]. SPH is, in comparison to mesh-based methods, more expensive due to the high computational demand. However, SPH offers important advantages for simulating free-surface and multi-phase flows. Because of the Lagrangian nature of SPH, advection is treated exactly and tracking of the phase interface is very simple. SPH can specially treat complex geometry changes, such as fragmentation without any large preprocessing of a simulation [1]. More details about the methodology of SPH are provided by Monaghan [37, 40] and Liu and Liu [27].

6. SPH application for free-surface and sediment transport simulations

Free-surface flows in hydrodynamic are very important, but they are difficult to simulate due to the boundary conditions on a moving surface. In the last decades, the SPH method has been widely used to model free-surface flows [32, 38] and to simulate free-surface channels [20]. Monaghan [38] concluded that SPH can simulate free-surface flows without any difficulties. Furthermore, many researchers have investigated modelling of multiphase flows using SPH [14, 39] and only a few SPH studies have dealt with the transport of solid bodies driven by a free-surface [2]. The SPH modelling has also been used by many researchers to investigate waves and their breaking process [6, 15, 18, 40, 47, 48, 54]. There are some studies analyzing the simulation of sediment transport using SPH [30, 31, 56]. Some of the most interesting studies for our future work are briefly described in the following.

Amicarelli et al. [2] developed and validated a 3D SPH model for the transport of rigid solids in free-surface flows. This study has implemented fluid-body and solid-solid multiple coupling terms in the SPH equations for both the flow and the transported bodies. The numerical model is validated on a complex 3D experimental test case representing a dam break event. The comparison between validations and experimental, theoretical and other SPH numerical results showed that the SPH method is a reliable way to model the transport of rigid bodies in free-surface flows.

Burger and Rauch [10] introduced the fundamentals of SPH for use in pipe hydrodynamics. The Torricelli's law and Poleni's formel were chosen to test a 2D SPH model, which was implemented for pipe flow hydrodynamics. The results were realistic, but there was still the lack of a turbulence model for pipe hydraulics, which was under consideration. The authors foresee a huge potential of the SPH method in simulating sewer hydraulics, multiphase flow and pollution transport.

Fourtakas et al. [21] used the DualSPHysics code, an SPH solver, to simulate the sediment suspension and the shear layer induced by rapid flows resulting in scouring of the sediments in industrial tanks. The liquid and sediments were treated as compressible pseudo-Newtonian fluids. In this study, two yield criteria the Mohr-Coulomb and Drucker-Prager were used with the SPH formulation. The results of the two models were agreeable, but the DP method is preferred because the MC criterion did not predict the yield strength of the sediment resulting in larger viscosities. It was also concluded that the particle spacing can influence the results of the simulations.

Manenti et al. [30] investigated an application of the improved SPHERA code, an SPH solver, to simulate non-cohesive sediment flushing by bottom discharge of water from a tank. The comparison between the experimental results and the results of 2D and 3D numerical simulations of the sediment profile and water level according to the Shields erosion criterion showed an adequate degree of accuracy of the SPH method. However, the 2D model could reproduce the final eroded profile with higher precision than the 3D model.

Manenti et al. [31] developed an SPH model to simulate the coupled fluid-sediment dynamics induced by the rapid water discharge in an artificial reservoir. The liquid phase and the eroded granular particles are considered as weakly compressible fluids. The Mohr-Coulomb yielding criterion and the Shields criterion were implemented and compared for determining the onset of the bottom sediment motion induced by the hydrodynamic shear

stress. The comparison between the experimental and numerical slope profiles showed that the Shields approach is preferable for practical applications because it can represent the sediment dynamics better.

Meister et al. [33] investigated the application of the SPH method for several problems in urban water management. They simulated flume flows, sedimentation and transport processes and also aerated flows in wastewater treatment. Although the results of the study concluded that SPH can be a powerful method for channel flow simulations, some improvements are still needed to use SPH in the field of urban water management particularly due to the high computational demand. The investigation on the sediment flushing using a flushing gate confirmed that the SPH method is especially viable in this case, because the rapid deformation of free-surface flows can be modelled very well with the SPH method.

Mirmohammadi and Ketabdari [35] used the SPH method to simulate water and sandy sediment interaction around a marine pipeline as well as wave generation and propagation. The sediment was assumed as a non-Newtonian fluid and the Bingham model was used to simulate the sediments behavior. The results of the numerical model showed a good level of agreement with the results of inviscid wave propagation and damping empirical model. They concluded that the SPH method is a powerful tool to simulate the transport of sediments, although the sediment transport is a complex and long term phenomenon.

Razavitoosi et al. [43] proposed a two-dimensional SPH model to simulate the sediment transport caused by dam break over a movable bed. The fluid and sediment phases were described by particles as weakly compressible fluids. The fluid phase was modelled as a Newtonian fluid and the sediment phase as a non-Newtonian fluid using three alternative approaches of 'artificial viscosity', 'Bingham and Artificial viscosity' and 'Bingham and Cross'. The numerical results were compared with experimental results, showing that the combination of the Bingham model and the artificial viscosity has the most acceptable accuracy.

Sitzenfrei et al. [49] discussed three issues in scientific computing in urban water management involving the SPH method as an alternative to explore fluid flow phenomena. They mentioned that SPH has several advantages due to its Lagrangian nature that make it more applicable than grid-based CFD methods to hydrodynamic simulations in sewers, such as modelling of pollution transport and sewer solids. Despite the challenge of high computational demand for SPH simulations, which could be tackled using technologies like graphics processing units (GPUs), the authors foresee a huge potential of the method to be applied to simulate real world pipe networks in order to tackle the problem of pollution transport in drainage systems.

7. Conclusion

In this paper, an overview of the SPH simulation of free-surface flows and sediment transport has been illustrated. It is important to investigate the sediment transport in sewers in order to be able to predict the transport of pollutants. Several factors influence the efficiency of the flushing devices in sewer systems (e.g. channel geometry and total amount of sediments

and their characteristics). Therefore, it is very expensive and time-consuming to assess the efficiency of the cleaning operation with experimental investigations. The numerical methods allow overcoming these difficulties by reasonable simulation of the free-surface flows in channels and sediment transport. The SPH method can simulate very complex geometries, even in 3D. Many studies have been carried out on the SPH simulation of free-surface flows in coastal areas, rivers and artificial reservoirs, but only a few of these studies have investigated the modelling of free-surface channels and sediment flushing in sewers. These studies show satisfactory results. However, there is still a lack of knowdlege on SPH application in sewer management. It could be expected that, in a few years, SPH will be a powerful modelling tool for the simulation of flows and sediment transport in order to solve several problems related to sewer systems.

References

[1] Adami S., Hu X.Y., Adams N.A., *A transport-velocity formulation for smoothed particle hydrodynamics*, Journal of Computational Physics 241, 2013, 292–307.

[2] Amicarelli A., Albano R., Mirauda D., Agate G., Sole A., Guandalini R., *A Smoothed Particle Hydrodynamics model for 3D solid body transport in free surface flows*, Computers & Fluids 116, 2014, 205–228.

[3] Ashley R.M., Crabtree R.W., *Sediment origins, deposition and build-up in combined sewer systems*, Water Science and Technology, 25 (8) , 1992, 1–12.

[4] Ashley R.M., Verbanck M.A., *Mechanics of sewer sediment erosion and transport*, Journal of Hydraulic Research, 34 (6), 1996, 753–770.

[5] Ashley R.M., Bertrand-Krajewski J.L., Hvitved-Jacobsen T., Verbanck M., *Solids in Sewers: Characteristics, Effects and Control of Sewer Solids and Associated Pollutants*, Joint Committee on Urban Drainage, IWA Publishing, 2004.

[6] Aureli F., Dazzi S., Maranzoni A., Mignosa P., Vacondio R., *Experimental and numerical evaluation of the force due to the impact of a dam-break wave on a structure*, Advances in Water Resources, 76, 2015, 29–42.

[7] Bertrand-Krajewski J.L., *Sewer sediment management: some historical aspects of egg-shaped sewer and flushing tanks*, Water Science and Technology, 47 (4) , 2003, 109–122.

[8] Bertrand-Krajewski J.L., Campisano A., Creaco E., Modica C., *Experimental analysis of the Hydrass flushing gate and field validation of flush propagation modelling*, Water Science and Technology, 5 (2), IWA Publishing, 2005, 129–137.

[9] Bollrich G., Technische Hydromechanik, Band 2. Berlin, VEB Verlag für Bauwesen, 1989.

[10] Burger G., Rauch W., *Investigating Smoothed Particle Hydrodynamics in Sewer Hydraulics Modeling*, 12th International Conference on Urban Drainage, Porto Alegre/ Brazil, 11–16 September 2011.

[11] Butler D., Tedchanamoorthy S., Payne J.A., *Aspects of surface sediments characteristics on an urban catchment in London*, Water Science and Technology, 25 (8), 1992, 13–19.

[12] Campisano A., Creaco E., Modica C., *Experimental and numerical analysis of the scouring effects of flushing waves on sediment deposits*, Journal of Hydrology, 299, 2004, 324–334.

[13] Chebbo G., Laplace D., Bachoc A., Sanchez Y., Le Guennec B., *Technical solutions envisaged in managing solids in combined sewer networks*, Water Science and Technology, 33 (9) , 1996, 237–244.

[14] Chen Z., Zong Z., Liu M.B., Zou L., Li H.T., Shu C., *An SPH model for multiphase flows with complex interfaces and large density differences*, Journal of Computational Physics, 283, 2015, 169–188.

[15] Dao M.H., Xu H., Chan E.S., Tkalich P., *Numerical modelling of extreme waves by Smoothed Particle Hydrodynamics*, National Hazards and Earth System Sciences 11, 2011, 419–429.

[16] De Sutter R., Rushforth P., Tait S., Huygens M., Verhoeven R., Saul A., *Validation of existing bed load transport formulas using in-sewer sediment*, Journal of Hydraulic Engineering, ASCE, 129 (4), 2003, 325–333.

[17] Dettmar J., *Beitrag zur Verbesserung der Reinigung von Abwasserkanälen*, Ph.D. Thesis, Fakultät für Bauingenieurwesen der Rheinisch-Westfälischen Technischen Hochschule Aachen, 2005.

[18] Dominguez J.M., Suzuki T., Altomare C., Crespo A.J., Gomez-Gesteira M., *Hybridisation of a wave propagation model (SWASH) and a meshfree particle method (SPH) for real applications*, 3rd IAHR Europe Congress, Book of Proceedings, Porto – Portugal, 2014.

[19] Engelke P., Gießler M., Eckstädt H., *Modelling of Sediment Transport in Sewers*, 16th International Conference Transport and Sedimentation of Solid Particles, Rostock, Germany, 18–20 September 2013.

[20] Federico I., Marrone S., Colagrossi A., Aristodemo F., Antuono M., *Simulating 2D open-channel flows through an SPH model*, European Journal of Mechanics B/Fluids 34, 2012, 35–46.

[21] Fourtakas G., Rogers B.D., Laurence D.R., *Modelling sediment resuspension in industrial tanks using SPH*, La Houille Blanche, 2, 2013, 39–45.

[22] Gingold R.A., Monaghan J.J., *Smoothed particle hydrodynamics: Theory and application to non-spherical stars*, Monthly Notices of the Royal Astronomical Society, 181, 1977, 375–389.

[23] Gomez-Gesteira M., Rogers B.D., Dalrymple R.A., Crespo A.J.C., *State-of-the-art of classical SPH for free-surface Flows,* Journal of Hydraulic Research 48, Extra Issue, International Association of Hydraulic Engineering and Research, 2010, 6–27.

[24] Ghani A.Ab., *Sediment transport in sewers*, Ph.D. Thesis, University of Newcastle upon Tyne, Department of Civil Engineering, 1993.

[25] Graf W.H., *Hydraulics of sediment transport*, McGraw-Hill Book Company, New York 1971.

[26] Liu M.B., Liu G.R., Lam K.Y., *Constructing smoothing functions in smoothed particle hydrodynamics with applications*, Journal of Computational and Applied Mathematics, 155, 2003, 263–284.

[27] Liu G.R., Liu M.B., *Smoothed Particle Hydrodynamics: an Overview and Recent Developments*, Archives of Computational Methods in Engineering, 17, 2010, 25–76.

[28] Lucy L., *A numerical approach to the testing of fusion process*, Journal of Astronomical, 82, 1977, 1013–1024.
[29] Lucas-Aiguier E., Chebbo G., Bertrand-Krajewski J.L., Gagne B., Hedges P., *Analysis of the methods for determining the settling characteristics of sewage and stormwater solid*, Water Science and Technology, 37 (1), 1998, 53–60.
[30] Manenti S., Sibilla S., Gallati M., Agate G., Guandalini R., *3D SPH Simulation of non-Cohesive Sediment Flushing*, 6th International SPHERIC workshop, Hamburg, Germany, 2011.
[31] Manenti S., Sibilla S., Gallati M., Agate G., Guandalini R., *SPH Simulation of Sediment Flushing Induced by a Rapid Water Flow*, Journal of Hydraulic Engineering, 138 (3), 2012, 272–284.
[32] Maruzewski P., Oger G., Le Touzé D., Biddisccombe J., *High performance computing 3D SPH model: Sphere impacting the free-surface of water*, 3rd ERCOFTAC SPHERIC workshop on SPH applications, Lausanne, Switzerland, 2008.
[33] Meister M., Fleischhacker N., Rauch W., *Anwendung von Smoothed Particle Hydrodynamics in der Siedlungswasserwirtschaft*, Conference Aqua Urbanica, Innsbruck, Germany, 2015.
[34] Michaelbach S., *Origin, resuspension and settling characteristics of solids transported in combined Sewage*, Water Science and Technology, 31 (7), 1995, 69–76.
[35] Mirmohammadi A., Ketabdari M.J., *Numerical simulation of wave scouring beneath marine pipeline using smoothed particle hydrodynamics*, International Journal of Sediment Research, 26, 2011, 331–342.
[36] Mokos A., *Multi phase Modelling of Violent Hydrodynamics Using Smoothed Particle Hydrodynamics (SPH) on Graphics Processing Units (GPUs)*, Ph.D. Thesis, University of Manchester, 2013.
[37] Monaghan J.J., *Smoothed Particle Hydrodynamics*, *Annual Review of Astronomy and Astrophysics*, 30, 1992, 543–574.
[38] Monaghan J.J., *Simulating free surface flows with SPH*, Journal of Computational Physics, 110, 1994, 399–406.
[39] Monaghan J.J., Kocharyan A., *SPH simulation of multi-phase flow*, Computer Physics Communications, 87, 1995, 225–235.
[40] Monaghan J.J., *Smoothed particle hydrodynamics*, Reports on Progress in Physics, 68, 2005, 1703–59.
[41] Pisano W.C., Barsanti J., Joyce J., Sorensen H., *Sewer and tank sediment flushing: case studies*, US EPA National Risk Management Research Laboratory, Office of Research and Development, U.S. Environmental Protection Agency, Cincinnati, Ohio 45268, Report No. EPA/600/R-98/157, 1998.
[42] Pisano W.C., Queiroz C.S., *Automated sewer and drainage flushing systems in Cambridge, Massachusetts*, Journal of Hydraulic Engineering, 129 (4), 2003, 260–266.
[43] Razavitoosi S.L., Ayyoubzadeh S.A., Valizadeh A., *Two-phase SPH modelling of waves caused by dam break over a movable bed*, International Journal of Sediment Research, 29 (3), 2014, 344–356.
[44] Ristenpart E., *Sediment properties and their changes in a sewer*, Water Science and Technology, 31 (7), 1995, 77–84.

[45] Schaffner J., Oberlack M., Kirchheim N., *The application of numerical modeling (3-D) for the calculation of flush waves in sewer channels*, 6th International Conference on Urban Drainage Modelling, Dresden, Germany, 2004.

[46] Schlütter F., *Numerical Modelling of Sediment Transport in Combined Sewer Systems*, Ph.D. Thesis, Aalborg University, Department of Civil Engineering, 1999.

[47] Shao S.D., *Simulation of breaking wave by SPH method coupled with k-epsilon model*, Journal of Hydraulic Research, 44 (3), 2006, 338–349.

[48] Shao S.D., Lo E.Y.M., *Incompressible SPH method for simulating Newtonian and non-Newtonian flows with a free surface*, Advances in Water Resources, 26 (7), 2003, 787–800.

[49] Sitzenfrei R., Kleidorfer M., Meister M., Burger G., Ulrich C., Mair M., Rauch W., *Scientific Computing in Urban Water Management*, Computational Engineering, Springer International Publishing, Switzerland, 2014, 173–193.

[50] Thamsen P.U., Gerlach S., Höchel K., *Remarks on wastewater transport challenges for today and the future*, 16th International Conference Transport and Sedimentation of Solid Particles, Rostock, Germany, 18–20 September 2013.

[51] Todeschini S., Ciaponi C., Papiri S., *Experimental and numerical analysis of erosion and sediment transport of flushing waves*, 11th International Conference on Urban Drainage, Edinburgh, Scotland, UK, 2008.

[52] van Rijn L.C., *Sediment transport, part I: bed load transport*, Journal of Hydraulic Engineering, 110 (10), American Society of Civil Engineers, Reston, VA, USA, 1984, 1431–1456.

[53] van Rijn L.C., *Sediment transport, part II: suspended load transport*, Journal of Hydraulic Engineering, 110 (11), American Society of Civil Engineers, Reston, VA, USA, 1984, 1613–1641.

[54] Vaughan G.L., *Simulating Breaking Waves Using Smoothed Particle Hydrodynamics*, Ph.D. Thesis, University of Waikato, Hamilton, New Zealand, 2005.

[55] Verbanck M., *Sewer Sediment and its relation with the quality characteristics of combined sewer overflows*, Proceedings of the 2nd Wageningen Conference, 1989, 11.

[56] Vetsch D., *Numerical Simulation of Sediment Transport with Meshfree Methods*, Ph.D. Thesis, Mitteilungen 219, Versuchsanstalt für Wasserbau, Hydrologie und Glaziologie (VAW) der Eidgenössischen Technischen Hochschule Zürich, 2012.

[57] Yang C.T., *Unit Stream Power and Sediment Transport*, Journal of the Hydraulics Division, 98 (10), 1972, 1805–1826.

TECHNICAL TRANSACTIONS | CZASOPISMO TECHNICZNE
ENVIRONMENT ENGINEERING | ŚRODOWISKO
1-Ś/2016
DOI: 10.4467/2353737XCT.16.193.5942

JERZY CIEPLIŃSKI, STANISŁAW M. RYBICKI*

IMPACT OF DAILY FLOW TO MID-SIZE WWTP BIOREACTOR ON ELECTRIC ENERGY CONSUMPTION

WPŁYW ZMIENNOŚCI OBCIĄŻENIA REAKTORA BIOLOGICZNEGO W ŚREDNIEJ OCZYSZCZALNI ŚCIEKÓW NA ZUŻYCIE ENERGII

Abstract

The paper analyses the share of single SBR in the total energy consumption of the studied wastewater treatment plant. The analysis is based on a two sets of data measurements, gathered by an automated measuring installation and data archived manually by the plant's operator. Energy consumption was also analyzed with reference to the archive data of daily flows. The paper is based on data collected from November of 2015 to January of 2016. This is a continuation of an ongoing research.

Keywords: energy consumption, wastewater treatment plant, SBR

Streszczenie

W artykule zestawiono zużycie energii elektrycznej pojedynczego reaktora typu SBR w odniesieniu do całkowitego zużycia energii przez badaną oczyszczalnię ścieków. Porównania dokonano w oparciu o dwa zestawy danych: pomiary, zarejestrowane przez automatyczną instalację pomiarową oraz dane eksploatacyjne archiwizowane przez operatora oczyszczalni. Analizę zużycia energii odniesiono również do zarejestrowanych przepływów dobowych przez oczyszczalnię. Analizowane dane pochodzą z okresu od listopada 2015 do stycznia 2016 i stanowią kontynuację wcześniejszych badań.

Słowa kluczowe: zużycie energii, oczyszczalnia ścieków, SBR

* M.Sc. Eng. Jerzy Ciepliński, D.Sc. Eng. Stanisław M. Rybicki, Institute of Water Supply and Environmental Protection, Faculty of Environmental Engineering, Cracow University of Technology.

1. Introduction

This paper presents the continuation of measurements launched in May of 2014. Its focus is on a 3-month cold period (late autumn to mid-winter), during which the average daily temperature oscillated around 0 degree Celsius [1]. During the studied period, the observed average daily flows were lower than usual.

2. Basic information

2.1. Plant's description

The studied plant is located near Kraków, in Southern Poland. The plant consists of two parallel treatment lines of a SBR (Sequencing Batch Reactor) type [2, 3, 4] and one sludge stabilization chamber each [5]. The plant's capacity is 1250 m^3/day and its PE (Population Equivalent) equals to 14 950. However, due to incomplete municipal sewerage, the real daily flows usually are below 700 m^3/day. Daily flows during tests were even lower, but the operator is not switching the plant into one-train only in order to prevent the installation against freezing. That is why all of the four reactors were rotationally activated according to the scheme: SBRs 3 and 4 were on line all the time and the SBRs 1 and 2 were activated alternately. Therefore, during the entire studied period, 3 of 4 reactors were constantly operational.

The plant's main device list (1.5 kW of power and above) [6]:

- sludge truck discharge station 3.5 kW
- vertical sieve 1.5 kW
- stage 1 pumping station 4.7 kW (1+1 in reserve, working interchangeably)
- grit & grease removal 4.0 kW
- retention tank blowers 5.5 kW (1+1 in reserve, working interchangeably)
- stage 2 pumping station 7.5 kW (1+1 in reserve, working interchangeably)
- 2x2 SBRs (no 1.2 – older tech-line, no 3, 4 – newer tech-line):
  - 2x3 blowers 30.0 kW each (2x2+1 in reserve, working interchangeably)
  - 2x2 excess sludge pumps 5.5 kW each (1 pump per reactor)
  - 2x2 internal turbines 11.0/7.5 kW (2 gears) (1 turbine per reactor)
- 2x1 sludge stabilization chamber (1 chamber per 2 reactors):
  - 2x1 blower 11.0 kW each (1 blower per chamber)
  - 2x1 internal turbines 5.5 kW (1 turbine per chamber)
- stabilized sludge pump 2.2 kW
- centrifuge (sludge dewatering) 17.2 kW
- dewatered sludge auger 1.5 kW.

During the studied period, WWTP operated flawlessly and easily met the administrative requirements [7, 8].

2.2. Measuring grid components

The measuring grid consists of (main elements only):
- 1 central unit (notebook) with specialized software
- 1 signal converter
- 5 automated energy counters.

Software installed on the central unit controls the work of the installation. The notebook functions also as a data archive. The signal converter translates data from meters to a form acceptable by the computer. Automated counters measured total energy used by selected devices in 5 minutes intervals (current settings). Counters are installed on following devices:
- Blowers (D4, D5, D6)
- SBR internal mixing-aerating turbine (Tr4)
- Excess sludge pump (P11).

To measure the energy usage of one reactor, installation of meters on all devices directly connected with this reactor is needed – SBR internal turbine Tr4, excess sludge pump P11, and oxygen source. Because of reliability reasons, all three blowers are connected into one oxygen supply system for both reactors [9]. During measurements, only blower D5 supplied SBR4 with oxygen.

3. Data

This paper contains data from two sources: automated measurements provided by a measuring grid and plant's journal of the exploitation provided by WWTP's operator.

Data archived by the plant's operator have daily intervals, except Saturdays, Sundays and statutory holidays. After consultation with WWTP operator concerning the average daily flows and total energy consumption, it became clear that extrapolation of missing data with simple arithmetic average will be sufficient. Extrapolated flows and energy consumption are a bit lower than the recorded ones; however, during weekends, no additional wastewater is delivered by sludge trucks, hence smaller results are plausible. Please note that these averages were based on data received from an effluent meter; therefore, the total flow in the studied period was not extrapolated. Only missing daily flows are the result of extrapolation. The exact same situation was with WWTPs total energy consumption [10]. All vital data used for analyzes are presented in Tables 1, 2 and 3.

Data recorded by the installation was registered in 5-minute intervals and the single series covers one month. It was the last three series recorded with a 5-minute time-step before the grid's extension and recalibration in February.

The presented results are free of a small software error, which caused sudden stops in data archiving on the 26th day of each month [10]. The error was caused by an improper configuration of the maximum volume of ANSI file in Windows 7. The error was finally corrected in September of 2015, and since then, interruptions in the measurements have been incidental and caused by sporadic power outages. It should be noted that the WWTP is equipped with a diesel electric generator. The installed meters are resilient to energy spikes during switches in power supply between the main grid and the generator.

Table 1

SBR4 energy consumption compared to WWTP's total energy usage in November of 2015

Date	D5 [kWh]	Tr4 [kWh]	P11 [kWh]	SBR4 [kWh]	TEC [kWh]	SBR4 % of TEC	Dailyflow [m^3/day]
2015-11-02	142.57	94.91	0.28	237.76	1320	18.01	305
2015-11-03	145.91	86.49	0.53	232.93	1320	17.65	431
2015-11-04	148.80	87.40	0.27	236.47	1560	15.16	344
2015-11-05	149.66	96.15	0.56	246.36	1440	17.11	436
2015-11-06	147.08	88.66	0.61	236.35	1080	21.88	243
2015-11-07	86.03	86.89	0.34	173.26	1080	16.04	243
2015-11-08	114.10	87.94	0.34	202.37	1080	18.74	243
2015-11-09	117.38	84.62	1.33	203.33	1200	16.94	517
2015-11-10	150.39	77.12	0.92	228.43	1140	20.04	222
2015-11-11	143.39	87.77	0.33	231.49	1140	20.31	222
2015-11-12	140.97	81.99	0.45	223.40	1200	18.62	370
2015-11-13	136.55	82.92	0.53	220.00	1140	19.30	297
2015-11-14	114.38	76.20	0.55	191.13	1140	16.77	297
2015-11-15	99.64	91.19	0.00	190.83	1140	16.74	297
2015-11-16	102.16	77.81	0.54	180.51	1200	15.04	534
2015-11-17	107.97	80.97	0.53	189.48	1200	15.79	378
2015-11-18	141.76	92.77	0.26	234.80	1200	19.57	373
2015-11-19	89.63	78.39	0.74	168.75	1200	14.06	364
2015-11-20	127.66	85.25	1.01	213.92	1020	20.97	390
2015-11-21	105.70	84.43	0.56	190.68	1020	18.69	390
2015-11-22	71.65	87.15	0.27	159.07	1020	15.59	390
2015-11-23	81.00	88.31	0.26	169.57	1260	13.46	555
2015-11-24	94.24	72.08	2.07	168.39	1260	13.36	385
2015-11-25	86.52	93.20	0.51	180.23	1260	14.30	420
2015-11-26	79.93	85.10	0.70	165.74	1380	12.01	376
2015-11-27	77.18	82.66	0.95	160.79	1080	14.89	286
2015-11-28	82.60	88.48	0.28	171.37	1080	15.87	286
2015-11-29	52.40	88.45	0.28	141.13	1080	13.07	286
2015-11-30	114.24	111.84	0.27	226.34	1140	19.85	577
TOTAL	3251.48	2507.12	16.27	5774.87	34380	–	10456
MIN	52.40	72.08	0.00	141.13	1020	12.01	222
MAX	150.39	111.84	2.07	246.36	1560	21.88	577
Average	112.12	86.45	0.56	199.13	1186	16.89	361

Table 2

SBR4 energy consumption compared to WWTP's total energy usage in December of 2015

Date	D5 [kWh]	Tr4 [kWh]	P11 [kWh]	SBR4 [kWh]	TEC [kWh]	SBR4 % of TEC	Dailyflow [m^3/day]
2015-12-02	117.93	101.56	0.46	219.95	1200	18.33	396
2015-12-03	73.40	87.24	0.74	161.39	1260	12.81	388
2015-12-04	70.99	97.48	0.61	169.08	1040	16.26	299
2015-12-05	90.28	101.20	0.27	191.75	1040	18.44	299
2015-12-06	112.60	100.47	0.27	213.34	1040	20.51	299
2015-12-07	88.10	97.13	0.24	185.47	1020	18.18	502
2015-12-08	113.78	82.35	0.51	196.63	1020	19.28	409
2015-12-09	91.02	84.17	0.86	176.05	1440	12.23	506
2015-12-10	93.73	83.38	0.37	177.48	1320	13.45	423
2015-12-11	130.90	92.93	0.39	224.22	1240	18.08	274
2015-12-12	102.42	89.85	0.28	192.55	1240	15.53	274
2015-12-13	71.14	89.15	0.27	160.56	1240	12.95	274
2015-12-14	100.12	92.39	0.27	192.77	1500	12.85	481
2015-12-15	135.34	81.70	0.55	217.59	1320	16.48	355
2015-12-16	111.09	83.62	0.72	195.43	1260	15.51	504
2015-12-17	148.77	96.06	0.52	245.35	1380	17.78	502
2015-12-18	134.50	86.13	0.52	221.15	1320	16.75	329
2015-12-19	129.91	99.85	0.27	230.02	1320	17.43	329
2015-12-20	117.14	97.61	0.26	215.01	1320	16.29	329
2015-12-21	117.53	111.45	0.28	229.25	1320	17.37	504
2015-12-22	129.89	91.82	0.52	222.22	1260	17.64	493
2015-12-23	122.81	93.85	1.31	217.97	1296	16.82	262
2015-12-24	137.98	103.17	0.27	241.42	1296	18.63	262
2015-12-25	89.93	96.52	0.28	186.73	1296	14.41	262
2015-12-26	75.56	107.92	0.00	183.48	1296	14.16	262
2015-12-27	74.60	103.31	0.27	178.18	1296	13.75	262
2015-12-28	91.51	103.84	0.71	196.07	1200	16.34	330
2015-12-29	70.43	97.27	0.37	168.08	1260	13.34	395
2015-12-30	91.05	95.34	0.88	187.26	1260	14.86	335
2015-12-31	135.21	107.36	0.28	242.86	1275	19.05	243
TOTAL	3169.62	2856.12	13.54	6039.27	37575	–	10781
MIN	70.43	81.70	0.00	160.56	1020	12.23	243
MAX	148.77	111.45	1.31	245.35	1500	20.51	506
AV	105.65	95.20	0.45	201.31	1253	16.18	359

Table 3

SBR4 energy consumption compared to WWTP's total energy usage in January of 2016

Date	D5 [kWh]	Tr4 [kWh]	P11 [kWh]	SBR4 [kWh]	TEC [kWh]	SBR4 % of TEC	Dailyflow [m^3/day]
2016-01-01	73.87	104.41	0.27	178.54	1275	14.00	243
2016-01-02	48.40	105.74	0.00	154.15	1275	12.09	243
2016-01-03	38.11	104.25	0.00	142.36	1275	11.17	243
2016-01-04	78.17	103.31	0.27	181.75	2400	7.57	391
2016-01-05	111.26	106.71	1.15	219.12	1800	12.17	243
2016-01-06	48.07	93.01	0.39	141.47	1800	7.86	243
2016-01-07	104.57	101.35	0.41	206.32	1860	11.09	481
2016-01-08	130.03	92.47	0.80	223.29	1680	13.29	274
2016-01-09	88.00	97.70	0.40	186.10	1680	11.08	274
2016-01-10	95.02	99.99	0.40	195.41	1680	11.63	274
2016-01-11	109.16	108.00	0.39	217.54	1740	12.50	461
2016-01-12	141.73	96.07	0.81	238.62	1680	14.20	467
2016-01-13	103.04	71.47	0.41	174.91	1500	11.66	351
2016-01-14	100.95	84.36	2.08	187.39	1440	13.01	459
2016-01-15	94.11	90.28	0.85	185.25	1400	13.23	243
2016-01-16	95.07	91.27	0.47	186.80	1400	13.34	243
2016-01-17	97.35	91.72	0.47	189.54	1400	13.54	243
2016-01-18	71.22	87.89	0.47	159.58	1680	9.50	375
2016-01-19	108.06	79.77	0.95	188.78	1860	10.15	363
2016-01-20	51.97	86.86	0.48	139.31	1800	7.74	314
2016-01-21	92.17	83.27	0.94	176.38	1800	9.80	364
2016-01-22	33.18	89.60	0.87	123.66	1560	7.93	199
2016-01-23	62.64	90.12	0.46	153.22	1560	9.82	199
2016-01-24	42.32	87.17	0.47	129.96	1560	8.33	199
2016-01-25	84.00	95.66	0.56	180.22	1920	9.39	461
2016-01-26	95.36	83.01	0.91	179.29	1380	12.99	372
2016-01-27	77.03	79.78	1.30	158.11	1380	11.46	468
2016-01-28	60.71	86.61	0.46	147.78	1380	10.71	344
TOTAL	2335.53	2591.88	17.44	4944.85	45165	–	9032
MIN	33.18	71.47	0.00	123.66	1275	7.57	199
MAX	141.73	108.00	2.08	238.62	2400	14.20	481
AV	83.41	92.57	0.62	176.60	1613	11.12	323

The time of power source change for WWTP is far shorter than the grid's central unit battery life. Since the beginning of the measurements, only a handful Random Missing Records (RMR) was observed. The amount of RMR was so small that it could be considered negligible.

The acronym "TEC" used in all tables below stands for Total Energy Consumption.

The average flow in November was roughly 30% of the designed flow. Underflow conditions had no negative impact on effluent quality. However, in terms of energy efficiency, it is a very undesirable situation. On average, to process 1 m^3 of sewage, 3.28 kilowatt-hours (kWh) of energy was needed. It is more than it should be for flow above 100 m^3/day [11]. SBR4 had, on average, a 16.89% share in the Total Energy Consumption with the maximum value of almost 22%, which is about half of the share registered in May of 2015 [10]. A similar situation can also be observed in December and January.

Similar to November, in December, the average daily flow was also roughly 30% of the designed flow. The SBR4 share in TEC in December was also very similar to the previous month and was 16.18% with a maximum also below 22%. It can be said that, despite not operating in the designed conditions, the plant operated steadily.

The last data set was registered in January of 2016. Average daily flow was little lower than during the previous 2 months, and reached about 26% of the designed flow. In addition, the SBR4 share in TEC was a bit lower and was on average 11,12%, never reaching more than 14.20%. It is a result of putting more pressure onto the rest of the reactors by the plant's operator, which is clearly visible in the D5 column. A lower amount of sewage resulted in a lower amount of processed BOD, nitrogen and phosphorus compounds, thus a lower amount of air had to be supplied to the SBR4.As a result, in January, blower D5 used only 2335 kilowatt-hours. This is 919 kilowatt-hours less than in December and 916 kilowatt-hours less than in November. Since the D5 is one of the 2 main contributors of the SBR4 share in TEC, the lower share in January is not a surprise.

Table 4

SBR4 energy consumption compared to WWTP's total energy usage 3 moths summary

3 months:	D5 [kWh]	Tr4 [kWh]	P11 [kWh]	SBR4 [kWh]	TEC [kWh]	SBR4 [%] of TEC	Dailyflow [m^3/day]
TOTAL	8756.63	7955.11	47.25	16758.98	117120	–	30269
MIN	33.18	71.47	0.00	123.66	1020	7.57	199
MAX	150.39	111.84	2.08	246.36	2400	21.88	577
AV	100.65	91.44	0.54	192.63	1346	14.79	348

As can be seen in Table 4, the average daily flow for a three-month period was 348 m^3/day, which is as low as 28% of designed average flow. This resulted in an average of 3.87 kWh being needed for treatment of 1 cubic meter of wastewater. For all 3 months, the average energy usage for 1 m^3 of treated sewage was higher than expected based on design calculations. Such a situation appears to be unavoidable, even with highly efficient equipment installed. Design power shall match the designed flow; therefore, if the flow is lower than designed, the energy efficiency of the whole plant will be lower than expected. Countermeasures to improve energy efficiency during underflow conditions are limited.

One of the methods are Variable-Frequency Drives (VFDs) thanks to which it is possible to greatly reduces the amount of energy needed by a device by adjusting it with VFD to current operating conditions, but at least for now, most of the devices operating at WWTPs are not equipped with such drives due to their high cost. Usually, blowers or other high-energy units are powered by VFDs. The studied plant is one of such examples, with blowers equipped with VFDs. The rest of the devices are powered directly or with few operating modes and the inflexibility of these devices results in higher than normal energy usage per 1 m^3 of treated wastewater. Another solution in situations like the ones described is turning off a part of the treatment plant; usually it is one or more of few technological lines. This method is a drastic step because a complete shutdown of a technological line takes time; restarting a tech-line is even more problematic and it takes weeks before a bio-reactor can reach optimal operating parameters (active sludge composition, effluent quality etc.) [12, 13]; therefore, this solution is uncommon. The best solution to problem of WWTPs operating not efficiently due to too low daily flows is avoiding its occurrence with good coordination of the construction of the sewerage network and sewage treatment plants. This, however, is a hard goal to achieve. However, the energy efficiency of the plant will rise after the sewerage system is complete.

The two main contributors of SBR4 energy usage are blowers and the internal turbine. The amount of energy used by the sludge pump is almost negligible.

The average share of SBR4 in TEC was around15%, which may seem low, but there were also 2 more active reactors during the studied period. That means the SBR section of Wołowice WWTP is responsible of about 50% of the plant's TEC. SBR4 share in each month and as a 3-month average was shown in Fig. 1. The share varies in time, but only data collected across a few months can show how big this variation can get.

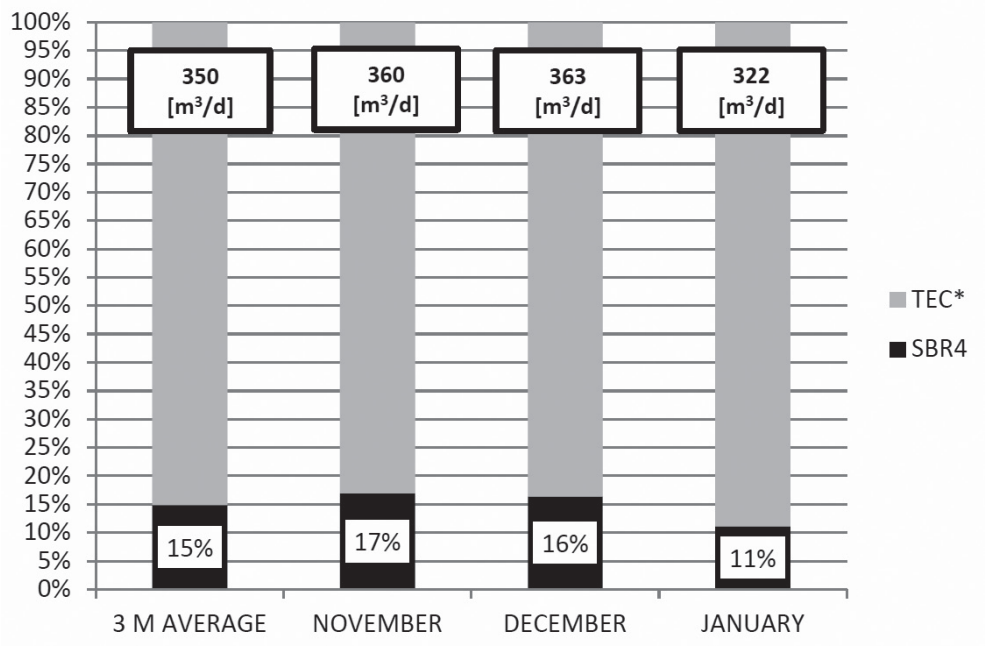

Fig. 1. SBR4 share in the Total Energy Consumption during the studied period

For example, there is a significant difference between May of 2015 (~30% of TEC) [9, 10] and any of the 3 discussed months ~15% of TEC). This difference may be caused by several factors. It could be caused by overall seasonal changes in WWTP performance or due to more sewage being directed to the rest of the reactors; also, the composition of wastewater affects the energy consumption. The factors that have the biggest influence on the variation of the SBR4 share in the plant's energy consumption are a subject of further research.

The collected data indicates weaker than expected correlation between DF and EC, especially in the case of individual reactors. This is a result of stronger than expected impact of varying Hydraulic Retention Times. The HRTs usually range from 0 to 30 hours in the case of the Wołowice plant. The exact influence of HRT on the correlation between DF and EC is hard to determine due to dynamic changes of HRT values; however, the mathematical description of it is under development.

4. Analysis

4.1. Correlation between the Total Energy Consumption and the daily flow

The best way to determine the influence of the Daily Flow (DF) on the energy consumption of the plant is calculating the correlation coefficient. In theory, the relation between DF and the energy usage seems to be directly proportional. A higher daily flow causes more wastewater to be treated, which leads to a longer work-time of the plant devices and therefore higher energy consumption.

The previous statement is definitely true for pumps and other devices involved in transporting and mixing of the wastewater. The situation is more complex for the blowers – higher flow may carry lower concentration of pollutants; therefore, the demand for oxygen can be lower during higher flow, which leads to a lower energy consumption by the blowers. Since the blowers are the main contributor to the TEC [14, 15], a higher flow with lower pollutant concentration may result in the same or even lower TEC than for smaller flows, but with higher concentration of BOD, N and P.

WWTPs, similar to the Wołowice plant, with retention tanks and based on the SBR technology, have one more significant factor influencing the relationship between the daily flow and the energy consumption – the retention time and/or the sewage distribution between reactors. It may take anywhere from a few hours to over a day for the portion of wastewater to reach the reactor(s). This means that the registered energy consumption for a given day never fully corresponds with the measured inflow from that day. It affects the TEC-DF correlation, but it affects the correlation between single SBR EC and the daily flow even more. The Wołowice plant does not have flow meters installed on each individual reactor. With 3–4 active reactors, it is hard to determine how much wastewater and from which days it is being processed on a given day by a given reactor. A method to determine the exact amount of sewage distributed between SBRs is currently being developed. Due to the presence of the retention tank, which normalizes the composition of wastewater, the developed method will not have to take into account the differences between the pollutant concentrations in different reactors. It can be safely assumed that differences in the sewage composition within a few-day period in different SBRs are minimal.

In Table 5, the calculations of the correlation coefficient between the energy consumption and the daily flow on a given day are shown. The results in Table 5 illustrate that the relationship between energy use and the daily flow in WWTP with retention tank and SBR is not straightforward.

Table 5

Correlation between the daily flow (DF) and SBR4 or WWTP-TEC energy consumption

	NOV 2015		DEC 2015		JAN 2016	
	SBR4-DF	TEC-DF	SBR4-DF	TEC-DF	SBR4-DF	TEC-DF
Correlation Coefficient	–0.04	0.29	–0.01	0.19	0.42	0.34

In November and December of 2015, there was no correlation between SBR4 energy usage and the daily flow. Some correlation can be observed globally, which indicates that, in fact, there is a relationship between the plant's total energy usage and the daily flow, but the influence of the daily flow variation seems to be insignificant. In January, however, the influence of daily flow is quite significant from the global point of view, but the most drastic change occurred for SBR4-DF. CC jumped from 0 to 0.42. The preliminary analyses of the sewage distribution between SBRs indicate that the causes of such a drastic change are retention times. In November and December, wastewater was kept longer in the retention tank before being transported to the reactors. In January, the retention times were lower than for the two previous months and this is reflected by the higher correlation between the energy consumption and the daily flow for both SBR4 and the entire plant. These results will be verified after the method for calculating sewage distribution between reactors will reach desired accuracy.

The relationship between the energy consumption and the flow can be observed in Fig. 2–7. It is rather consistent with the results of correlation coefficient calculations. Although, from Figures 2–7, it seems that the relationship is stronger than that expected from the values of correlation coefficient. The line for the TEC follows pattern of the daily flow, sometimes at once, sometimes with visible delay. Of course, there are periods when TEC seems to be completely unaffected by the DF. This supports the statement that the relationship between the energy consumption and the daily flow may be heavily influenced by the operating mode of the WWTP, with a significant role of the sewage retention time. The exact nature of this relationship will be closely investigated after more data is obtained.

4.2. Relationship between SBR4, or the Plant energy consumption, and the daily flow

Based on the obtained data, 2 diagrams for each month were created – one for changes in the Total Energy Consumption and the Daily Flow during the studied month; the second very similar, but with SBR4 energy consumption instead of the plant's total energy usage.

In both November and December of 2015, TEC and DF drew similar lines. Changes in TEC generally corresponded with changes in DF, at the same time or with some delay. Fig. 2 and 4 are consistent with CC values; however, a similarity between both lines indicates

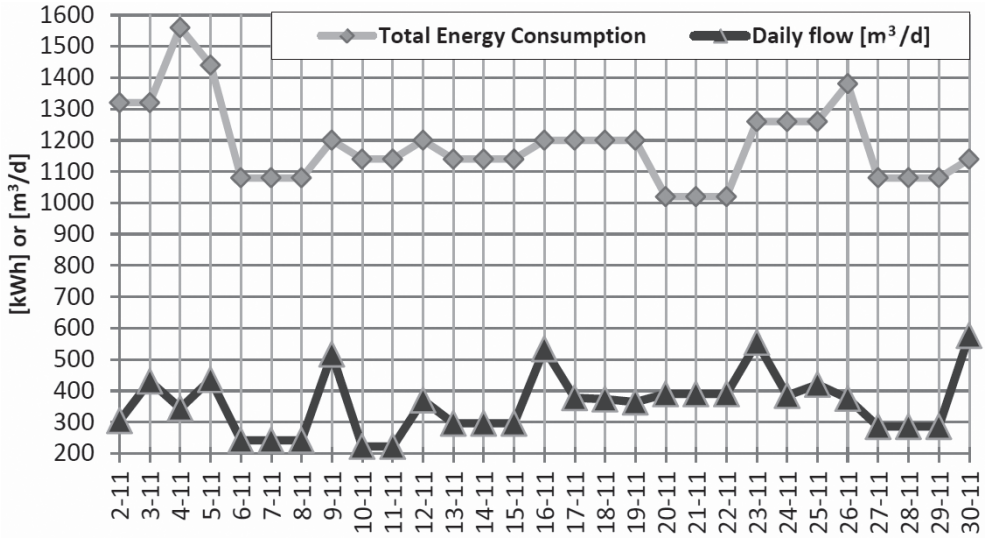

Fig. 2. Dependency between the Total Energy Consumption and the daily flow in November of 2015

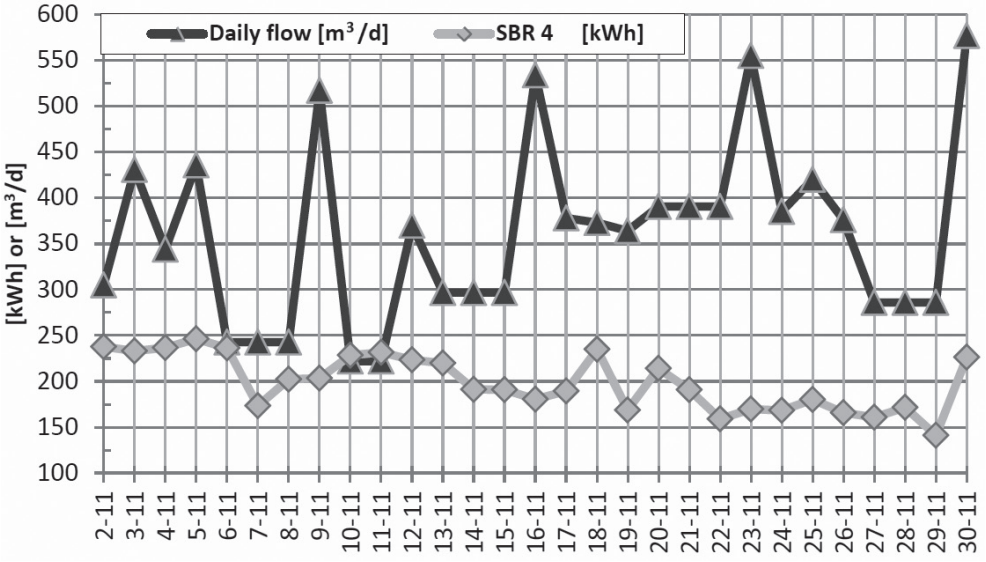

Fig. 3. Dependency between SBR4 Energy Consumption and the daily flow in November of 2015

a higher correlation between TEC and DF than the one presented in Table 5. Verification of the influence of the retention time on CC will be the next step in this area of research.

Ideally, a method of including dynamic retention times into calculations of TEC-DF correlation will be developed and will improve the accuracy of results.

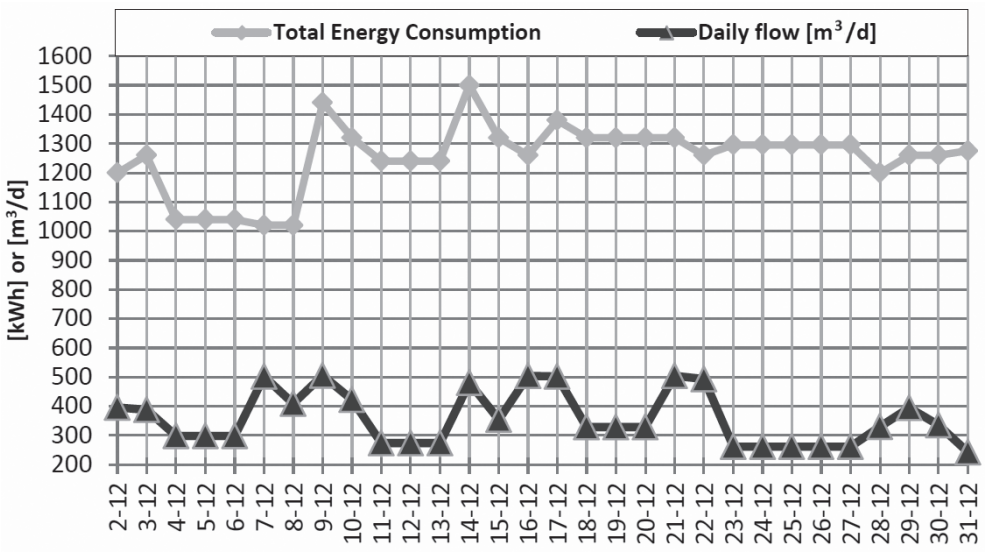

Fig. 4. Dependency between the Total Energy Consumption and the daily flow in December of 2015

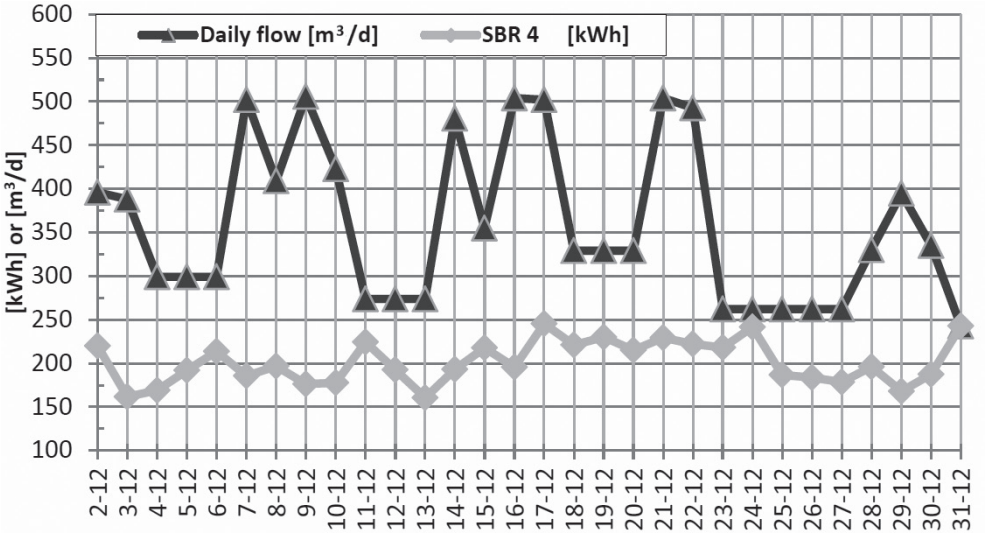

Fig. 5. Dependency between SBR4energy consumption and the daily flow in December of 2015

The diagrams for SBR4 energy usage in November and December of 2015 are consistent with the calculated correlations. This confirms that the retention times and sewage distribution between reactors had a significantly larger impact on the single reactor energy usage than the WWTP's daily flow.

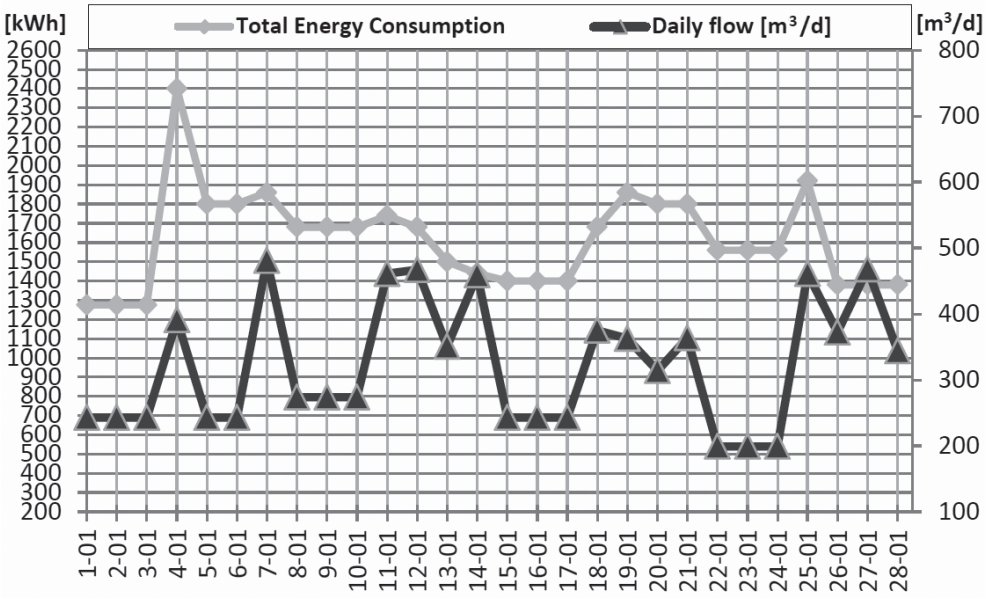

Fig. 6. Dependency between the Total Energy Consumption and the daily flow in January of 2016

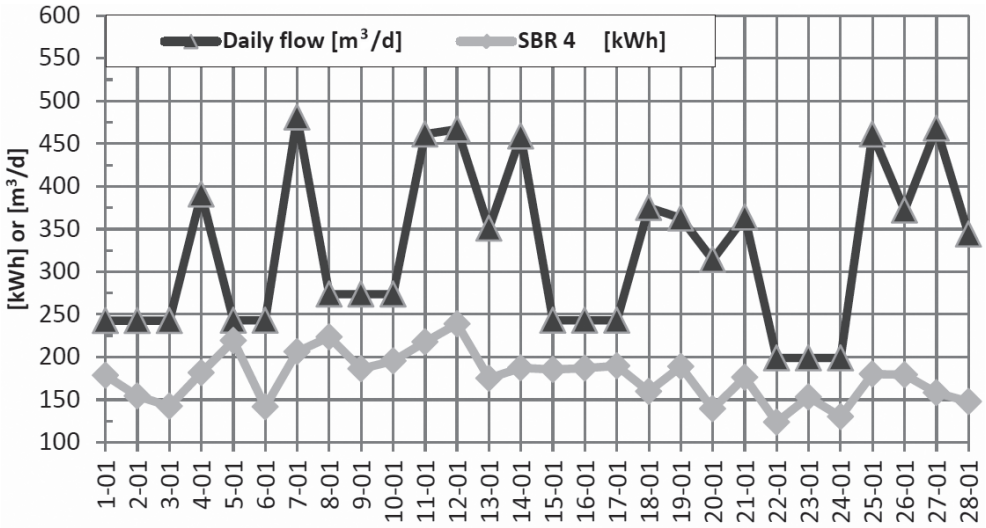

Fig. 7. Dependency between SBR4 Energy Consumption and the daily flow in January of 2016

The situation in January was different compared to the two previous months. The retention times of raw sewage were smaller. This is reflected by a higher correlation coefficient for the WWTP, but also for the SBR4, even despite the unequal distribution of the inflow between reactors.

All of the gathered data and observations that were made will be used in subsequent studies and will help in the determination of the exact nature of the relationship between the daily flow and the energy consumption at the Wołowice plant.

5. Conclusions

The impact of daily flows on WWTP's total energy consumptions had been observed and was consistent with previous measurements.

The impact of daily flows on single SBR energy consumptions had been observed during one of the three months of observation. This dependency will be monitored in future to determine the exact nature of this relationship.

Initial observations showed that a HRT impacts a plant's daily TEC. It is difficult to find a mathematical relationship between a HRT and a daily TEC, especially at longer HRTs. In such a case (e.g. when a HRT is longer than 15 hours), a wastewater flow value is 'counted' on the day of its discharge to the WWTP, while higher TEC is 'counted' on the next day. The relation is even harder to describe mathematically in the case of a single reactor due to the unequal sewage distribution between SBRs. This problem will be investigated more comprehensively in further steps of investigations.

The collected data had a reasonable quality, but there is still room for improvement. A tighter cooperation with plant's crew and plant cooperators (f. e. electricity supplier) in collecting data should result in even further improvement of the quality of gathered data.

The 5-minute interval for on-line energy consumption measurements is barely enough for more detailed analyses, thus it will be lowered to 1 minute.

The SBR4 average share in the total energy consumption stayed almost the same during the studied period. It is consistent with previous measurements. However, seasonal change (between May of 2015 and Nov'15-Jan'16) had been observed.

References

[1] IMGW elektroniczne roczniki meteorologiczne http://www.imgw.pl/klimat/ 20.04.2016.

[2] Jyotsnarani Jenaa,Ravindra Kumarb, Md Saifuddina, Anshuman Dixitb, Trupti Das, *Anoxic-aerobic SBR system for nitrate, phosphate and COD removal from high-strength wastewater and diversity study of microbial communities*, Biochemical Engineering Journal, Volume 105, Part A, 15 January 2016.

[3] Cintia C. Loboa, Nora C. Bertolaa, Edgardo M. Contrerasb, *Approximate expressions of a SBR for wastewater treatment: Comparison with numeric solutions and application to predict the biomass concentration in real cases*, Process Safety and Environmental Protection, Volume 100, March 2016.

[4] Zhan Wang, Ximing Zhang, Zhongya Zhu, Yadong Kong, Kui Gao, Wei Yao, *Influence of various operating conditions on cleaning efficiency in sequencing batch reactor*

(SBR) activated sludge process, Journal of the Taiwan Institute of Chemical Engineers, April 2016.

[5] Shugen Liua, Nanwen Zhua, Ping Ningb, Loretta Y. Lic, Xudong Gongc, *The one-stage autothermal thermophilic aerobic digestion for sewage sludge treatment: Effects of temperature on stabilization process and sludge properties*, Chemical Engineering Journal, Volume 197, 15 July 2012.

[6] Mucha Z., Mucha J., *Projekt budowlany: budowa oczyszczalni ścieków w Wołowicach*, Kraków 2008.

[7] SGS Polska Sp. z o.o. (laboratorium akredytowane), *Oczyszczalnia ścieków Wołowice gm. Czernichów: Wylot ścieków z oczyszczalni – próbka średnia dobowa*.

[8] Regulation of the Minister of Environment of 16 December 2014 on required parameters of treated wastewater and on substances that are particularly harmful to the aquatic environment.

[9] Ciepliński J., *Budowa pilotażowej instalacji pomiarowej do określenia rzeczywistego zużycia energii przez reaktor typu SBR w małej oczyszczalni ścieków*, Podstawy Biotechnologii Środowiskowej – trendy, badania, implementacje, Gliwice 2015.

[10] Ciepliński J., *Single SBR reactor's energy usage in comparison with total energy consumption of medium wastewater treatment plant*, http://suw.biblos.pk.edu.pl/resources/i5/i8/i7/i1/i9/r58719/CieplinskiJ_SingleSBR.pdf

[11] Heidrich Z., Ramocki W., *Energochłonność miejskich oczyszczalni ścieków*, Forum Eksploatatora wrzesień–październik 2009.

[12] Dante M., Fatone F., Pavan P., Cecch F, *Removal of nitrogen from the anaerobic supernatant of a co-digestion process: start-up of a sequencing batch reactors (SBR) adopting the nitrite route*, Journal of Biotechnology Volume 150, Supplement, November 2010.

[13] Dong Lia, Yufeng Lva, Huiping Zenga, Jie Zhanga, *Startup and long term operation of enhanced biological phosphorus removal in continuous-flow reactor with granules*, Bioresource Technology, Volume 212, July 2016.

[14] US EPA, *Innovative Energy Conservation Measures at Wastewater Treatment Facilities*, Sheboygan Regional WWTP, May 2012.

[15] US EPA Region 3 and PADEP, MatthewYonkin, PE, BCEE, CEM, *Energy Efficiency Roundtable (Energy Audits & Guaranteed Savings/Performance Contracts)*, May 2012.

TECHNICAL TRANSACTIONS | CZASOPISMO TECHNICZNE
ENVIRONMENT ENGINEERING | ŚRODOWISKO
1-Ś/2016
DOI: 10.4467/2353737XCT.16.194.5943

ANNE KÖNIG, YUKI SORGLER, MARTIN JEKEL*

ANAEROBIC BIOLOGICAL DEGRADATION OF CARBAMAZEPINE AT ENVIRONMENTAL CONCENTRATIONS

BIOLOGICZNY ROZKŁAD KARBAMAZEPINY W WARUNKACH BEZTLENOWYCH W STĘŻENIU WYSTĘPUJĄCYM W ŚRODOWISKU NATURALNYM

Abstract

A removal of the antiepileptic drug carbamazepine is frequently observed under anaerobic redox conditions at managed aquifer recharge sites. The biological influence on this effect is widely unknown and therefore it is the focus of this study. Anaerobic degradation batch tests and long-term soil column experiments, conducted within this study, suggest a removal of 2 to 50% induced by microbiological processes. Transformation products and their molecular structures are suggested – one of them is clearly identified as 10,11-dihydro-carbamazepine. This study provides a deeper understanding regarding the biotic reduction of carbamazepine.

Keywords: organic micropollutants, bank filtration, redox potential, reductive transformation

Streszczenie

Eliminacja leku padaczkowego karbamazepiny jest często obserwowana podczas sztucznego wzbogacania wód gruntowych w warunkach beztlenowych. W poniższym artykule przedstawiono badania dotyczące dotychczas niedostatecznie zrozumiałego wpływu faktorów biologicznych na te zjawisko. Przeprowadzone testy naczyniowe (testy batch) w warunkach beztlenowych i testy ciągłe z kolumnami piaskowymi pokazały znaczną eliminację karbamazepiny spowodowanej przez procesy mikrobiologiczne w wysokości 2 do 50%. W artykule zasugerowano produkty transformacji karbamazepiny i ich struktury molekularne – jednoznacznie zidentyfikowana zostala 10,11-dihydro-karbamezepina. Przedstawione badania umożliwiają lepsze zrozumienie biotycznego rozkładu karbamazepiny.

Słowa kluczowe: organiczne mikrozanieczyszczenia, filtracja brzegowa, potencjał redox, transformacja w warunkach redukcyjnych

* Dipl.-Ing. Anne König, Yuki Sorgler B.Sc., Prof. D.Sc. Ph.D. Martin Jekel, Chair of Water Quality Control, Department of Environmental Technology, Technische Universität Berlin.

1. Introduction

The antiepileptic drug carbamazepine (CBZ) – used to medicate epilepsy, trigeminal neuralgia and depressions – is released into the anthropogenic water cycle by treated wastewater [1, 2]. In the aquatic environment, several transformation processes, such as photooxidation, sorption, precipitation, biodegradation and redox processes occur, changing the initial concentration of organic micropollutants considerably. For carbamazepine, all these conversion processes are very limited and rather unlikely as reported in literature [2–4]. However, under anaerobic redox conditions (Fe^{3+}/Mn^{4+} reducing, SO_4^{2-} reducing) at bank filtration sites, a removal of CBZ was occasionally observed in the past [5, 6].

Although oxidative transformation pathways of carbamazepine are thoroughly described in literature [7, 8], the fate of carbamazepine under reductive conditions has hardly been investigated so far. With electrochemical experiments, Moses et al. [9] and Atkins et al. [10, 11] described the abiotic reduction of carbamazepine to dihydro-carbamazepine ((2H)-CBZ) (Table 1). Within the study by Koenig et al. [12] using catalytic hydrogenation – besides (2H)-CBZ – eight further transformation products (TPs) were found and identified by high resolution mass spectrometry. Thus, three of them were detected in the effluent of a biologically active column containing zero valent iron to simulate strongly reducing conditions [12].

Table 1

Carbamazepine and selected transformation products (TPs) during reduction; TPs were all determined abiotically by electrochemical reduction [9–12] and catalytic hydrogenation [12]

Carbamazepine $C_{15}H_{12}N_2O$ 236,1 g/mol Consumption 2012: 52 t MEC_{max}/PNEC: 2,4	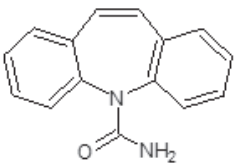	(2H)-CBZ[9-12] $C_{15}H_{14}N_2O$ 238,1 g/mol 10,11-dihydro-carbamazepine
(6H)-CBZa/b $C_{15}H_{18}N_2O$ 242,2 g/mol 1,2,3,4,4a,11a-hexahydro-5H-dibenzo[b,f]azepine-5-carboxamide	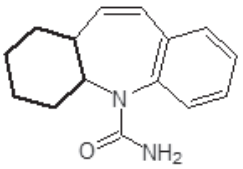	(8H)-CBZ[12] $C_{15}H_{20}N_2O$ 244,2 g/mol 1,2,3,4,4a,10,11,11a-octahydro-5*H*-dibenzo[*b*,*f*]azepine-5-carboxamide

In this study, the biological degradation of carbamazepine is investigated using an anaerobic long-term degradation test and lab scale soil columns, which characterize the fate of this compound more realistically. The study contributes to a deeper understanding of the biotically induced reductive transformation of the pharmaceutical carbamazepine, which possibly appears in the anaerobic subsoil at bank filtration sites.

2. Experimental

Anaerobic degradation tests were conducted by modifying the standard rule ISO 11734 [13]. The standard evaluates the "ultimate" anaerobic biodegradability of organic compounds in digested sludge. In triplicates, a test solution (100 mL) containing CBZ (c_0 = 11 µg/L or 8 mg/L CBZ), nutrients, reducing agent (Na_2S) and digested sludge from a waste water treatment plant in Berlin (Germany) was filled into serum bottles under nitrogen atmosphere and incubated at T = 35°C and pH = 7. After 90 days, the temperature was reduced to room temperature. Using a biodegradable organic carbon source (polyethylene glycole PEG 400, 100 mg/L), zero valent iron splints (ZVI; 5 g/L Fe^0) and external hydrogen (3 mL/bottle [14]), the redox potential was reduced. The hydrogen in the headspace was detected by gas chromatography using the GC-14A (Shimadzu, Japan carrier gas: nitrogen) equipped with a packed separation column (CTR I, 182.88 cm, carrier gas: nitrogen, Alltech GmbH, Germany).

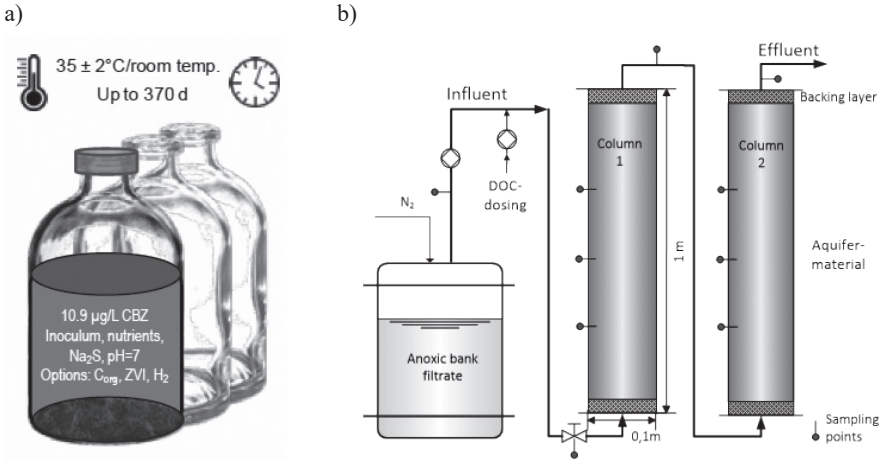

Fig. 1. Experimental setup of the anaerobic degradation batch test (a), scale 1:2 and soil the operated column system (b)

The three soil column systems used in this study consist of two columns in series (Perspex, length: 1 m; $Ø_{inner}$ = 0.09 m; porosity: 32%; pore volume: 7.8 L, residence time: 7.95 d), which are operated upflow with a flux of 250–350 mL/d for more than five years (Fig. 1). The columns are filled with natural aquifer material (grain size ≤ 2 mm) from a drinking water site in Berlin (Germany). The anoxic bank filtrate used for this long-term setup originates from a bank filtration site at lake Tegel in Berlin (Germany; depth: 25 m) and was obtained, transported and stored (at 11°C) gastight in stainless steel barrels. The initial DOC (Dissolved Organic Carbon) concentration (background 5 mg/L DOC; additional 0.5–30 mg/L DOC) was varied, in order to stimulate redox dependent microbiology. Samples from the soil columns were filtered by a 0.45 µm membrane filter (cellulose nitrate), stored in the dark at 6°C and analyzed for CBZ, (2H)-CBZ, DOC and total inorganic carbon (TIC),

pH, conductivity, nitrate, iron, manganese and sulfate within three days. Samples from the degradation tests were handled in the same way, if necessary diluted a hundredfold and analyzed only for CBZ, (2H)-CBZ.

DOC and TIC were measured by thermal oxidation using a Vario TOC cube device for DOC and a High TOC II device for TIC (both: Elementar, Germany). The redox potential was determined with a SenTix ORP electrode (WTW, Germany) and converted to the standard hydrogen electrode (DIN 38404). Nitrate was analyzed using the flow injection analysis system FIAstar 5000 from Foss Tecator (Sweden). Iron and manganese were detected by atomic absorption spectroscopy (AAS) depending on their concentration either with a graphite furnace AAS (GF-AAS, SpectrAA-400 Varian, Agilent Technologies, USA) or flame AAS (F-AAS, GBC 906AA; GBC, USA). Sulfate was determined by ion chromatography (DX 500, Dionex, USA), equipped with an AS11 separation column and a conductivity detector. Methane was analyzed by the gas chromatograph 5890 Series II (Hewlett Packard, USA), including a flame ionization detector and equipped with a aluminum sulfate column (30 m × 0,53 mm, Supelco, Sigma-Aldrich, USA).

CBZ and (2H)-CBZ (Sigma Aldrich, USA or Dr. Ehrensdorfer GmbH, Germany) as well as [$^{13}C_6$]-CBZ (Alsachim, France) were analyzed by a LC-MS-MS (TSQ Vantage; Thermo Fisher Scientific, USA) equipped with a Kinetex C18 (2.6 µ) or Luna C18 (3 µ) chromatography column (Phenomenex, USA). The chromatography was applied at a flow rate of 0.2 mL/min and a column temperature of 30 °C (IQL: 50 ng/L CBZ; 50 ng/L (2H)-CBZ). For lower concentrations from the column setup, an online extraction (IQL: 1 ng/L CBZ; 5 ng/L (2H)-CBZ) with a Hypersil Gold enrichment column followed by a Hypersil Gold Phenyl separation column (both Thermo Fisher Scientific (USA) was performed (IQL: 1 ng/L CBZ; 5 ng/L (2H)-CBZ). For both methods, a linear gradient of water (1% methanol, 0.1% formic acid) and methanol starting with 90:10 was chosen. To exclude matrix effects, the samples were spiked with [$^{2}H_8$]-CBZ (Alsachim, France) before analysis.

3. Results & Discussion

Due to the discharge of treated wastewater into the anthropogenic water cycle, carbamazepine (CBZ) is frequently detected in surface water, with average concentrations between 0.5 µg/L to 1.7 µg/L in urban areas [1, 15]. Therefore, biological processes involving low initial concentrations are the focus of the presented experiments.

3.1. Anaerobic degradation of carbamazepine

Standardized degradation tests allow the general comparison of the biological availability of different substrates under identical testing conditions. By modifying these test conditions, the removal effects are no longer fully comparable. Thus, the degradation may be optimized and a specific removal potential of an organic substrate can be determined.

The modified degradation test with CBZ as substrate is characterized by strongly reductive conditions due to the addition of either an organic carbon source (PEG 400), iron splints (ZVI, inducing anaerobic corrosion and hydrogen production) and hydrogen. The triplicates

were sampled over an experimental period up to 370 days. Within 12 days of incubation in all bottles, initial hydrogen concentrations ranging from 5 to 20 mmol/bottle were detected, depending on the testing variation (PEG 400, ZVI, H_2).

Hydrogen was present over the whole experiment and is partly converted to methane by anaerobic microbes, which can be concluded from methane measurements of a batch test at higher CBZ concentration (8 mg/L). A redox potential of –50 ± 40 mV, independent from the applied reductive agent, was detected throughout the experiment.

Figure 2 presents the c/c_0 ratio of CBZ (c_0 = 11 µg/L) in comparison to the formation of its reductive transformation product (2H)-CBZ over the experimental duration of 370 days. The CBZ concentration decreased slightly at all setup variations within the first 150 days, where the triplicates with ZVI showed the highest removal rate of 20% after 135 days.

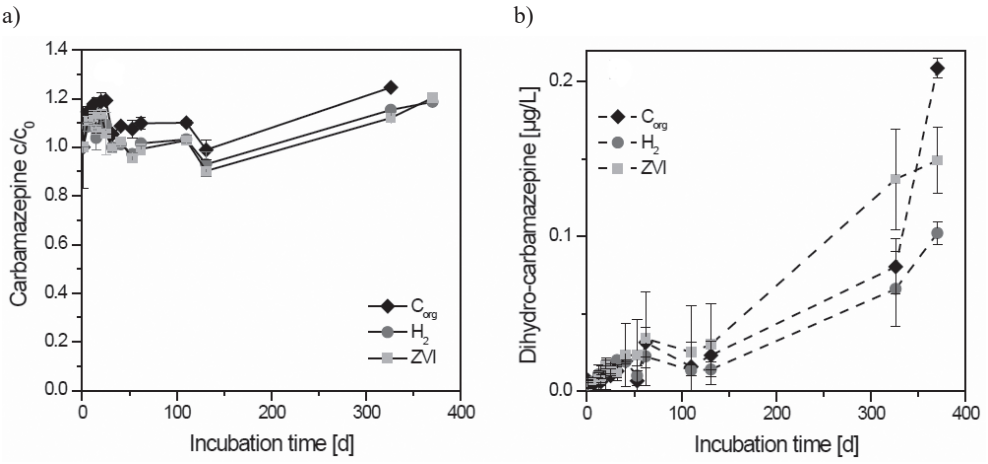

Fig. 2. Microbial degradation of carbamazepine (CBZ) within a modified test standard for anaerobic degradation (ISO 11734): c/c_0-ratio of CBZ (a) and (2H)-CBZ (Dihydro-CBZ) concentration (b); c_0(CBZ) = 10.9 ± 1.3 µg/L; experimental time: 360 days; The addition of zero valent iron (ZVI), external hydrogen or the organic carbon source varied the test conditions

Only after a long incubation time, a significant formation of (2H)-CBZ becomes obvious. After 370 days, up to 0.21 µg/L CBZ were transformed to (2H)-CBZ, representing two percent of the initial CBZ concentration. Several studies determined (2H)-CBZ as the main abiotically formed transformation product, either by electrochemical reduction or catalytic hydrogenation of CBZ [9–12].

However, this study demonstrates the biotic transformation of CBZ to (2H)-CBZ by adapted microbes. Long adaption times and the presence of hydrogen seem to be necessary. ZVI might enhance the reduction by additional hydrogen supply and providing a catalytic surface. Sterile duplicates (CBZ and ZVI) sampled on day 168 showed neither a change of the initial CBZ concentration nor a formation of (2H)-CBZ supporting the findings that the adapted microcosm is responsible for the fate of CBZ.

The other two test conditions (PEG 400 and external hydrogen) showed lower, but also clear conversion rates. With an organic carbon source, the adapted anaerobic bacteria were

capable to transform CBZ at environmental concentrations to (2H)-CBZ, which is especially remarkable, since biological degradation processes in the subsoil during bank filtration are mainly influenced by available DOC. In anaerobic aquifers, micro-milieus with strongly reductive conditions can evolve (e.g. in dead end pores of an aquifer) [16, 17] where the observed transformation of CBZ to (2H)-CBZ is conceivable.

The presented findings are supported by the results of the second batch test at a higher initial CBZ concentration of 8 mg/L. The test variations (ZVI, H_2, PEG 400) were equal to the test conditions described before. The highest conversion regarding both – CBZ removal and (2H)-CBZ formation – was observed in bottles with ZVI. Thus, at day 300 50% of the initial CBZ concentration was degraded, of which 20% is transformed to (2H)-CBZ (data not shown, publication in progress). Therefore, the conversion was more effective compared to the first batch test.

However, in both degradation tests under anaerobic conditions, the mass balance of CBZ could not be fully elucidated, implying that the reductive transformation of the compound might involve other, yet undetected TPs and degradation processes.

3.2. Fate of carbamazepine in soil columns

With regard to long hydraulic retention times of bank filtrate in the subsoil, an adapted microcosm is the key factor for the removal of organic micro pollutants. Saturated soil columns simulate relevant transformation processes at bank filtration sites – more or less – near natural. The soil column systems used in this study are operated for five years with anoxic bank filtrate from the lake Tegel in Berlin (Germany), which provides an initial CBZ concentration of 0.65 ± 0.14 µg/L. Due to the long operation time, ad- and desorption effects of CBZ with the column material are assumed to be balanced.

To stimulate microbial growth of redox specific microbes, the redox milieus were controlled by adding DOC to the column influent. Whereas in one column line no DOC was added resulting in anoxic redox conditions ($c/c_0(NO_3^-) \approx 0.3$; neither iron nor manganese release), in two lines the additional DOC was limited to 2 mg/L DOC for four years inducing iron and manganese reduction. Thus, increasing effluent concentrations of 113 ± 40 µg/L for manganese and 4140 ± 1280 µg/L for iron were observed. Both compounds originate from the column filling.

Strongly reducing conditions were then implemented for more than thirteen months by adding high amounts of DOC (30 mg/L). As a result, the iron and manganese concentration proceeded similar to the previously set redox range, and additionally, sulfate is reduced by 80% to 11.6 ± 17.9 mg/L. Small amounts of methane were detected (single measurement) in the effluent proving that the set redox conditions are in the sulfidogenic and partly methanogenic range.

Figure 3 compares the three experimental conditions regarding the fate of CBZ and the known reduced TP (2H)-CBZ. Whereas, at anoxic and iron/manganese reducing conditions neither a removal of CBZ nor a (2H)-CBZ formation were observed, under sulfidogenic conditions (2H)-CBZ is released in the effluent in the range of 30 ng/L, representing 5% of the initial CBZ concentration.

Under sulfate reducing conditions, the isomers (6H)-CBZa and (8H)-CBZ were found in the effluent of the soil columns. Both TPs belong to the reductive reaction pathway

presented by Koenig et al. (2015) [12] and represents the six- and eightfold hydrogenated CBZ molecule. The signal intensity is much lower within high-resolution mass spectrometry indicating very low concentrations. Since both TPs were not found in the anaerobic degradation batch tests, abiotic reduction of CBZ might also take place in the soil columns.

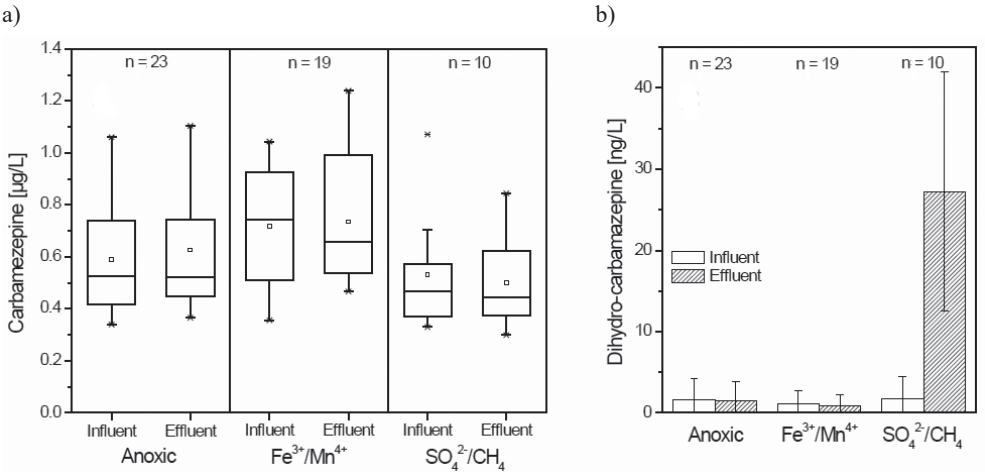

Fig. 3. Fate of carbamazepine (CBZ) and dihydro-CBZ ((2H)-CBZ) under different redox conditions in the soil column system: In- and effluent concentration of CBZ (a) and (2H)-CBZ (b) at anoxic, iron/manganese reducing and sulfogenic/methanogenic redox milieu

Since the c/c_0-ratio of CBZ in this redox milieu is with 0.94 close to 1.00 and the need of adsorption for the reductive transformation was proven for abiotic reduction processes [9–12], the detected (2H)-CBZ is possibly not formed from the CBZ of the current bank filtrate influent. It is rather generated from already adsorbed compound molecules on the column filling. To investigate this aspect, isotope labelled CBZ ($[^{13}C_6]$-CBZ) was introduced into the columns within tracer experiments. Besides the retardation factor for CBZ in the column system, the time shift until the $[^{13}C_6]$-(2H)-CBZ formation occurs can also be estimated.

Whereas conservative tracer experiments with KBr show residence times very close to the calculated residence time of 7.95 d, the injected isotope labelled CBZ interact with the soil material leading to a certain delay of the $[^{13}C_6]$-CBZ signal peak (Figure 4). Using the C_{peak}-method described by Schudel et al. (2002) [18], the specific retardation factor for CBZ is estimated with $R_d = 2.5$. In literature, the R_d values for CBZ during soil passage range from 2.3 to 3.3 [19, 20].

The tracer experiment with the isotope labelled CBZ is still running (04/2016). Remarkably, even after more than 60 days after $[^{13}C_6]$-CBZ-injection, no isotope labelled (2H)-CBZ was observed in the effluent, which indicates that either the injected load of $[^{13}C_6]$-CBZ was too low for the detection of the related transformation product or the necessary time shift for the transformation has not been reached yet. This implies that some isotope labelled CBZ must remain in the column system and be transformed very slowly to the reduced product.

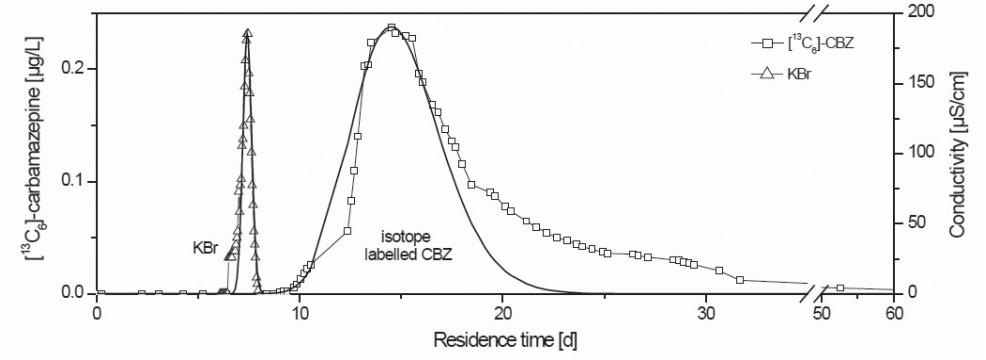

Fig. 4. Residence time peaks of two different tracer experiments with the conservative tracer potassium bromide (KBr, triangles) and the isotope labelled Carbamazepine (CBZ, squares); The respective model curves were determined by an analytical solution of the transport equation suggested by Schudel et al. (2002) [18] which considers advection and dispersion effects

4. Conclusion

The presented study focuses on the biological degradation of carbamazepine under reductive conditions occurring in anaerobic aquifers. In the conducted degradation tests as well as in the soil column experiments, the transformation of carbamazepine was successfully demonstrated at environmental concentrations. The compound was transformed in the range of 2–10% to dihydro-carbamazepine ((2H)-CBZ) in the anaerobic batch tests. The presence of hydrogen appears to be necessary. The microbial transformation of CBZ to (2H)-CBZ was confirmed in the near-natural soil column system at initial CBZ concentrations below 1 µg/L. Thus, under sulfidogenic and methanogenic redox conditions, besides (2H)-CBZ, two further TPs were found in the effluent of the columns. The results of this study show that an adapted microcosm is capable to transform CBZ under reducing conditions. (2H)-CBZ constitutes a central molecule not only in the abiotic – as already shown in literature – but also in the biotic reduction path of CBZ. The experiments imply that other unidentified TPs might be formed, since the mass balance of CBZ in the degradation tests is not closed at all. This aspect and the occurrence of identified TPs at bank filtration sites with anaerobic soil passage require further research and field studies.

Acknowledgement
The authors kindly thank Dipl.-Ing. Renata Mehrez for the fast and valuable translation of the English abstract into her native language.

References

[1] Zhang Y.J., Geissen S. U., Gal C., *Carbamazepine and diclofenac: Removal in wastewater treatment plants and occurrence in water bodies*, Chemosphere, 73, No. 8, 2008, 1151–1161.

[2] Jekel M., Dott W., Bergmann A., Dünnbier U., Gnirss R., Haist-Gulde B., Hamscher G., Letzel M., Licha T., Lyko S., Miehe U., Sacher F., Scheurer M., Schmidt C.K., Reemtsma T., Ruhl A.S., *Selection of organic process and source indicator substances for the anthropogenically influenced water cycle*, Chemosphere, 125, 2015, 155–167.

[3] Schramm C., Gans O., Uhl M., Grath J., Scharf S., Zieritz I., Kralik M., Scheidleder A., Humer F., *Carbamazepin und Koffein – potenzielle Screeningparameter für kommunale Verunreinigungen des Grundwassers?*, Umweltbundesamt GmbH, Wien 2006.

[4] Clara M., Strenn B., Kreuzinger N., *Carbamazepine as a possible anthropogenic marker in the aquatic environment: Investigations on the behaviour of carbamazepine in wastewater treatment and during groundwater infiltration*, Water Research, 38, No. 4, 2004, 947–954.

[5] Schmidt C.K., Lange F.T., Brauch H.J., *Characteristics and evaluation of natural attenuation processes for organic micropollutant removal during riverbank filtration*, Water Science & Technology: Water Supply, 7, No. 3, 2007, 1–7.

[6] Wiese B., Massmann G., Jekel M., Heberer T., Dünnbier U., Orlikowski D., Grützmacher G., *Removal kinetics of organic compounds and sum parameters under field conditions for managed aquifer recharge*, Water Research, 45, No. 16, 2011, 4939-4950.

[7] Ghauch A., Baydoun H., Dermesropian P., *Degradation of aqueous carbamazepine in ultrasonic/Fe0/H2O2 systems*, Chemical Engineering Journal, 172, No. 1, 2011, 18–27.

[8] Hübner U., Seiwert B., Reemtsma T., Jekel M., *Ozonation products of carbamazepine and their removal from secondary effluents by soil aquifer treatment – indications from column experiments*, Water Research, 49, 2014, 34-43.

[9] Moses G.S., Rao K.M., Rao N.S., Ramachandraiah A., *Electrochemical studies of carbamazepine*, Journal of the Indian Chemical Society, 72, No. 5, 1995, 333–337.

[10] Atkins S., Sevilla J.M., Blazquez M., Pineda T., Gonzalez-Rodriguez J., *Electrochemical behaviour of carbamazepine in acetonitrile and dimethylformamide using glassy carbon electrodes and microelectrodes*, Electroanalysis, 22, No. 24, 2010, 2961–2966.

[11] Atkins S., Gonzalez-Rodriguez J., Sevilla J.M., Blazquez M., Pineda T., Jimenez-Perez R., *Electrochemical reduction of carbamazepine in ethanol and water solutions using a glassy carbon electrode*, International Journal of Electrochemical Science, 8, No. 2, 2013, 2056–2068.

[12] König A., Weidauer C., Seiwert B., Reemtsma T., Unger T., Jekel M., *Reductive transformation of carbamazepine by abiotic and biotic processes*, Water Research, 101, 2016, 272–280.

[13] International Organization for Standardization (Editor), *Wasserbeschaffenheit – Bestimmung der vollständigen anaeroben biologischen Abbaubarkeit organischer Verbindungen im Faulschlamm – Verfahren durch Messung der Biogasproduktion*, EN ISO 11734:1998, DIN Deutsches Institut für Normung e.V., 1998.

[14] Zhu L., Lin H.-Z., Qi J.-Q., Xu X.-Y., Qi H.-Y., *Effect of H_2 on reductive transformation of p-ClNB in a combined ZVI-anaerobic sludge system*, Water Research, 46, No. 19, 2012, 6291–6299.

[15] Bergmann A., Fohrmann R., Weber F.-A., *Zusammenstellung von Monitoringdaten zu Umweltkonzentrationen von Arzneimitteln*, Umweltbundesamt, Deutschland 2010.

[16] Madigan T.M., Martinko J.M., Parker J., *Brock – Mikrobiologie*, Spektrum Akademischer Verlag, Heidelberg, Berlin 2003.

[17] Schulte-Ebbert U., Hollerung R., Willme U., Kaczmarczyk B., Bahrig B., Schöttler U., *Verhalten von anorganischen Spurenstoffen bei wechselnden Redoxverhältnissen im Grundwasser*, Dortmunder Beiträge zur Wasserforschung, I. f. W. GmbH (Editor), Vol. 43, Institut für Wasserforschung GmbH, Dortmund 1991.

[18] Schudel B., Biaggi D., Dervey T., Kozel R., Müller I., Ross J.H., Schindler U., *Einsatz künstlicher Tracer in der Hydrogeologie – Praxishilfe*, Berichte des BWG, Serie Geologie, Work group: Tracer der Schweizerischen Gesellschaft für Hydrogeologie SGH, Bern 2002.

[19] Zippel M., Hannappel S., Duscher K., Scheytt T., *Mathematische Simulation des Eintrages von Arzneimitteln aus Oberflächengewässern in das Grundwasser durch Uferfiltration*, Umweltforschungsplan des Bundesministerium des Umwelt, Naturschutz und Reaktorsicherheit, Umweltbundesamt (Editor), Dessau-Roßlau, 2010.

[20] Mersmann P., *Transport- und Sorptionsverhalten der Arzneimittelwirkstoffe Carbamazepin, Clofibrinsäure, Diclofenac, Ibuprofen und Propyphenazon in der wassergesättigten und -ungesättigten Zone*, dissertation, Institut für Angewandte Geowissenschaften der Technischen Universität Berlin, 2003.

TECHNICAL TRANSACTIONS | **CZASOPISMO TECHNICZNE**
ENVIRONMENT ENGINEERING | ŚRODOWISKO
1-Ś/2016

DOI: 10.4467/2353737XCT.16.195.5944

KRZYSZTOF W. KSIĄŻYŃSKI*

SIMPLE DESCRIPTION OF GROUNDWATER RECHARGE THROUGH THE VADOSE ZONE

PROSTY OPIS ZASILANIA WÓD PODZIEMNYCH PRZEZ STREFĘ AERACJI

A b s t r a c t

The paper presents the calculation rules for infiltration into the saturated zone using a simplified piston model. It has been indicated that recharge is the same as during free infiltration for unsaturated infiltration and that a new system of boundary conditions has been proposed for saturated infiltration and redistribution of moisture. The volumes of infiltration calculated for those cases have also been compared with the results obtained in a simulation based on the conductivity equation, showing convergence.

Keywords: groundwater recharge, piston model, supported infiltration, Richards equation

S t r e s z c z e n i e

W artykule przedstawiono zasady obliczeń infiltracji do strefy pełnego nasycenia z użyciem uproszczonego modelu tłokowego. Wskazano na niezmienność zasilania w stosunku do infiltracji swobodnej przy nienasyconym charakterze infiltracji i zaproponowano nowy układ warunków brzegowych przy charakterze nasyconym i przy redystrybucji wilgoci. Porównano również wielkości infiltracji wyliczone dla tych przypadków z wynikami uzyskiwanymi z symulacji opartej na równaniu przewodnictwa, wykazując zbieżność.

Słowa kluczowe: zasilanie wód podziemnych, model tłokowy, infiltracja podparta, równanie Richardsa

* Assoc. Prof. D.Sc. Ph.D. Eng. Krzysztof W. Książyński, Institute of Water Engineering and Water Management, Faculty of Environment Engineering, Cracow University of Technology.

List of symbols

$c(h_s)$ – capillary capacity (soil water capacity) [m^{-1}]
D_w – moisture diffusion coefficient [$m^2\ s^{-1}$]
H – water head [m]
H_k – water head on the limit of capillary height [m]
h_s – suction head [m]
h_g – water depth on the soil surface [m]
h_k – capillary height [m]
$k(\theta)$ – effective hydraulic conductivity of soil as the function of its moisture [$m\ s^{-1}$]
k_n – maximum hydraulic conductivity for wetting [$m\ s^{-1}$]
k_o – hydraulic conductivity [$m\ s^{-1}$]
m_a – thickness of vadose zone [m]
n – porosity of soil [$m^3\ m^{-3}$]
S – hydraulic gradient [m]
t – time [s]
v – seepage velocity [$m\ s^{-1}$]
v_e – evapotranspiration [$m\ s^{-1}$]
v_f – wetting front velocity [$m\ s^{-1}$]
v_g – ground absorbency [$m\ s^{-1}$]
v_k – seepage velocity in capillary zone [$m\ s^{-1}$]
v_r – surface recharge [$m\ s^{-1}$]
v_w – recharge on the groundwater table[$m\ s^{-1}$]
z – vertical coordinate [m]
z_i – wetting front coordinate [m]
z_k – coordinate of capillary zone [m]
θ – soil moisture [$m^3\ m^{-3}$]
θ_n – maximum moisture for wetting [$m^3\ m^{-3}$]
θ_r – moisture near the surface [$m^3\ m^{-3}$]
θ_w – residual moisture [$m^3\ m^{-3}$]

1. Introduction

Groundwater recharge usually occurs through the unsaturated zone, the so-called vadose zone. Infiltration of water from the surface results in complex changes in moisture within that zone, which determine the delay and equalization of groundwater recharge. Storage capacity of the saturated zone is low (which results from the low compressibility of water and the soil skeleton structure), thus the transformation of precipitation into groundwater outflow depends on the vadose zone storage capacity. In this situation, a correct description of the processes occurring within that zone is very significant in the cognitive aspect and facilitates an effective simulation of the entire transformation process.

This paper contains an attempt to describe the groundwater recharge changes using a general seepage equation and a simplified piston model. Both models have long been used

for describing motion within the vadose zone. However, the issue of feeding is relatively less identified in the piston model. A number of new factors have a significant effect on its course.

2. Support model assumptions

Repeated precipitation events, separated by rainless periods, result in an increase in soil moisture within the subsurface area of the vadose zone, dependent on the intensity and course of precipitation. Simultaneously, under the influence of gravity and capillary forces, the moisture redistribution process takes place. It takes place through propagation of high moisture deeper into the soil column, while for a certain period, sections with constant moisture gradients might occur, elongating at constant rates. Such phenomena are called "wetting fronts" and constitute the basis for simplified descriptions. It is the so-called "free infiltration". As far as groundwater recharge is concerned, reaching the saturated zone by those fronts is highly important and referred to as the "support".

When a wetting front reaches a closed capillary zone (fully saturated), distinct changes occur in the infiltration rate and saturation zone feeding. Both of these variables may be inhibited due to hydraulic slope limiting caused by new motion boundary conditions. This process is called supported infiltration, to differentiate it from free infiltration in which wetting fronts occur.

2.1. A model based on the general seepage equation

A generalization of the Darcy's formula, also valid for the vadose zone, is the Buckingham-Darcy equation, which has the following form for vertical motion (infiltration):

$$v = -k(\theta)\frac{\partial H}{\partial z} \tag{1}$$

Effective hydraulic conductivity of soil $k(\theta)$ is the function of its moisture [1], and in fully saturated conditions it has the value of hydraulic conductivity k_o. When the formula is inserted to the equation of continuity, the equation of motion is obtained:

$$\frac{\partial}{\partial z}\left[k(\theta)\frac{\partial H}{\partial z}\right] = \frac{\partial \theta}{\partial t} \tag{2}$$

It is a one-dimensional version of the Richards equation [5], giving a precise description of isothermal seepage for both saturation zones [6]. However, it cannot be solved directly, as it contains two unknowns – hydraulic head H and moisture θ. They are correlated through the soil-moisture retention characteristics, since $H = -z - h_s$ (z – vertical coordinate, h_s – suction head), thus the solution may be obtained by substituting moisture with that characteristics $\theta(h_s)$. As a result, a general seepage equation (conductivity equation) is obtained.

As for storativity (right side of equation 2), moisture θ must be treated as a composite function:

$$\frac{\partial \theta}{\partial t} \equiv \frac{\partial \theta}{\partial h_s}\frac{\partial h_s}{\partial t} \equiv \frac{\partial \theta}{\partial h_s}\frac{\partial (z-H)}{\partial t} \equiv -\frac{\partial \theta}{\partial h_s}\frac{\partial H}{\partial t} \equiv c(h_s)\frac{\partial H}{\partial t} \tag{3}$$

where $c(h_s) = -\partial\,\theta/\partial h_s$ is the capillary capacity (soil water capacity), which is actually a suction head h_s derivative of the soil-moisture retention characteristics. Such form of the retention section has been introduced by Richards [5]. The *c* parameter may be generalized for the saturation zone, where it corresponds to the specific storativity. In motion calculations for unconfined seepage, its value may be taken as zero. This way, the equation of motion takes the following form [2]:

$$\frac{\partial}{\partial z}\left[k(h_s)\frac{\partial H}{\partial z}\right] = c(h_s)\frac{\partial H}{\partial t} \tag{4}$$

An identical equation describes thermal conductivity, thus the formula presented above is referred to as the conductivity equation. Another name in use is the general seepage equation, since it describes motion in both saturation zones. Simulations performed using formula (4) are usually based on a discrete model. In this paper, they are used for verification of the piston model.

2.2. Simplified piston model [4]

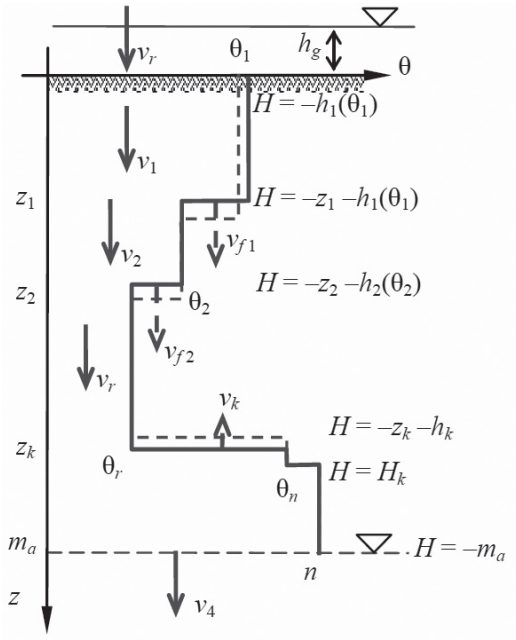

The piston model assumes invariability of vertical moisture redistribution behind the soil wetting front (piston motion). In the traditional model, front course is simplified to a local moisture increase from the initial value θ_{i+1} to the value of θ_i (Fig. 1) actually reached in a certain distance behind the front. The initial moisture must therefore be lower than the maximum saturation value θ_n – it is free infiltration. The infiltration rate is calculated depending on the recharge conditions on the surface.

Fig. 1. Scheme of vertical moisture redistribution in the piston model

Submerged infiltration occurs when surface recharge (v_r) is higher than ground absorbency (v_g). Moisture behind the front reaches the maximum moisture value θ_n for wetting, while infiltration rate results from the Darcy's formula and boundary conditions:

$$v_g = k_n \left(1 + \frac{h_g + h_k}{z_1} \right) \tag{5}$$

Saturated infiltration occurs when recharge is lower than ground absorbency, but higher than the maximum hydraulic conductivity for wetting (k_n). This situation is similar to submerged infiltration, the difference is the lack of surface submergence, while the infiltration rate corresponds to the recharge value:

$$v_r = \min \left[v_r ; k_n \left(1 + \frac{h_k}{z_1} \right) \right] \tag{6}$$

The second value, here described with the formula, corresponds to the limit of ground absorbency, above which surface submergence and submerged infiltration occur.

Unsaturated infiltration occurs when recharge is lower than maximum hydraulic conductivity for wetting. Moisture behind the front is constant and lower than the full saturation value, while the infiltration rate corresponds to the hydraulic slope with the value of 1 (due to constant moisture behind the front). The Buckingham-Darcy equation determines the dependence of these values:

$$v_r = k(\theta_2) \tag{7}$$

which allows to calculate the value of moisture behind the front.

Front velocity results from the water balance within the wetting front:

$$v_{fi} = \frac{v_i - v_{i+1}}{\theta_i - \theta_{i+1}} \tag{8}$$

The dependence is valid for each infiltration regime.

Moisture redistribution occurs when recharge is lower than it is necessary to maintain previous soil moisture, which means that it depends on its current effective hydraulic conductivity. Water outflow guaranteeing front propagation corresponds to unsaturated infiltration (equation 7) and is higher than surface recharge, as a result of which moisture behind the front gradually decreases. Moisture changes may be calculated on the basis of the column balance.

The piston model (PM) presented here has been thoroughly verified using available measurement data [4]. This model describes a version of the classic free infiltration in a simplified way, and cannot be used directly to describe supported infiltration. It is only

possible when several additional assumptions are made, which result from the analysis of the actual course of this process.

2.3. Capillary rise zone moisture

Below the unsaturated zone is the capillary rise zone, which has the height of h_k over the groundwater level (at the depth of m_a), in static conditions. Moisture of the permanent capillary zone corresponds to full saturation of soil pores ($\theta = n$), due to constant washing by vertical seepage. Moisture of a zone occurring sporadically after precipitation corresponds to the maximum saturation for wetting ($\theta = \theta_n$), which results from the presence of air entrapped in the smallest pores. Further wetting of this zone ($\theta > \theta_n$) is impossible due to hysteresis, which explains its name – closed capillary zone. In fact, as a result of diffusion of entrapped air, a certain moisture increase occurs, but it is very slow and not taken into account in this case.

Over the so-called closed capillary zone is the open zone, with moisture decreasing with the height, up to the level of residual moisture θ_w that depends on the history of the infiltration process. Assuming a rapid moisture change within the front in the PM leads to omitting this zone, which is followed by local errors in determining the rate and moisture. However, it has only a slight influence on the description of the course of groundwater recharge.

3. Capillary infiltration

The height of the capillary zone is determined by the recharge from the vadose zone, regardless of whether it is infiltration or the effect of the motion of the groundwater level. In the case of lack of recharge ($v_r = 0$), closed capillary zone is stabilized at the height of standard capillary rise h_k, which is at the level $z_k = m_a - h_k$, and being stable, it reaches full saturation moisture ($\theta = n$, Fig. 2). The flow through this zone causes changes in its height and its moisture.

Traditional solutions to this issue regard only the water level motion, with the assumption that no hysteresis occurs, which is particularly important with the so-called active capillary rise. It occurs when the level rises, as a result of which the capillary zone shortens and negative hydraulic slope is generated. It allows the upper boundary of the closed capillary zone to rise following the groundwater level. However, the outflow to the vadose zone may occur only when the moisture gradient exceeds the value of gravitational slope. Such a situation may occur locally near the soil surface as a result of strong evapotranspiration (section 9). Below, only moisture redistribution may occur, causing a slow decrease in the capillary zone recharge, until static state ($v_k = 0$) is reached. Consequently, considering this situation is practically insignificant.

A passive rise occurs with positive slope within the rise zone, which is when the groundwater level drops, or when a groundwater recharge occurs Fig. 2, $v_r > 0$). The capillary rise zone gradually extends ($z_k < m_a - h_k$) until hydraulic slope necessary to maintain flow continuity appears. The rate of rise of the z_k level is determined by the balance, so it depends on recharge intensity.

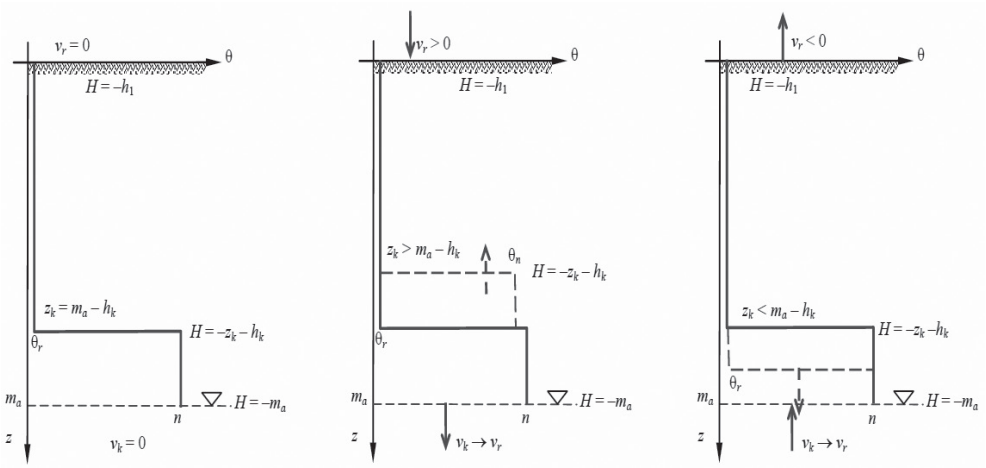

capillary zone in balance passive rise active rise

Fig. 2. Schemes of changes in the range of the capillary rise zone

Calculating the rate of outflow from the capillary zone in short-term rain infiltration conditions requires taking hysteresis into account, which leads to the formation of a new layer with the moisture value of θ_n over the stationary zone with the moisture value *n*. The traditional solution known from hydraulic engineering assumes stability of infiltration, which is connected with the loss of moisture diversification (also over h_k $\theta = n$). Such a situation occurs when the groundwater level drops, as the rise zone extends at the cost of the fully saturated zone.

In the case of non-steady infiltration, with a stabilized groundwater level, this solution is not correct. Assuming that the stationary capillary zone is stable, which implies that it is fully saturated and has the height of h_k, while a new moisture value $\theta_n < n$ (Fig. 2) appears above it, the following equation of flow continuity in zones with variable moisture:

$$v_k = k_n \frac{-z_k - h_k - H_k}{m_a - h_k - z_k} = k_o \frac{H_k + m_a}{h_k} \tag{9}$$

may be used to calculate the value of hydraulic head H_k at the boundary of different effective conductivity zones ($H_k < 0$, as it is below the soil level):

$$v_k = k_o \frac{H_k + m_a}{h_k} \quad \rightarrow \quad H_k = h_k \frac{v_k}{k_o} - m_a \tag{10}$$

Substituting to the equation of continuity will give:

$$v_k = k_n \frac{-H_k - z_k - h_k}{m_a - z_k - h_k} = k_n \frac{-h_k \frac{v_k}{k_o} + m_a - z_k - h_k}{m_a - z_k - h_k} = k_n \left(1 - \frac{v_k}{k_o} \frac{h_k}{m_a - z_k - h_k}\right) \tag{11}$$

The equation may be used to derive a formula of the rate of infiltration through the rise zone:

$$v_k = k_n \frac{m_a - z_k - h_k}{m_a - z_k - h_k + h_k \frac{k_n}{k_o}} = k_n \left(1 - \frac{h_k}{\frac{k_o}{k_n}\left[m_a - z_k - h_k\right] + h_k}\right) \cong \tag{12}$$

$$\cong k_n \left(1 - \frac{h_k}{2\left(m_a - z_k\right) - h_k}\right)$$

In the flow equilibrium conditions, i.e. when $v_k = v_r$, the wetting front stabilizes at the level:

$$\boxed{z_k \cong m_a - \frac{h_k}{2}\left(1 + \frac{k_n}{k_n - v_w}\right)} \tag{13}$$

The capillary zone is forming gradually as a result of the lack of equilibrium of water balance – limited outflow through the current zone height is lower than the recharge. Consequently, the process is asymptotic, with decreasing rate, until the equilibrium is reached. However, as a result of the recharge decrease, the balance of the capillary zone will be negative. It causes a lowering of the upper boundary of the zone, again asymptotically towards the new equilibrium. Thus, the equilibrium is actually never reached. For small values of the average yearly or seasonal feeding, the height of the stable capillary zone is only slightly different from the height of rise h_k.

When flow is prolonged, a slow increase in the soil moisture and conductivity mentioned above occurs, which causes gradual increase of its absorbency, until the hydraulic conductivity value k_o is reached.

4. Submerged infiltration

This infiltration regime occurs when recharge exceeds the value of ground absorbency ($v_r > v_g$, $h_g \geq 0$), irrespective of the range of the capillary rise zone ($z_k >$, = or < $m_a - h_k$). In case of rapid runoff, the depth of water on the surface remains around zero ($h_g \cong 0$, Fig. 3).

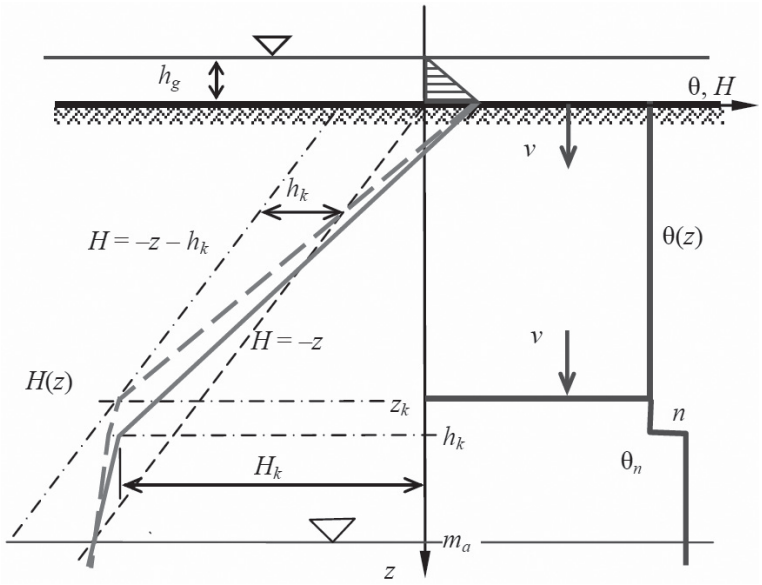

Fig. 3. Scheme of moisture θ and hydraulic head H changes in the piston model, during submerged supported infiltration

4.1. Infiltration rate compensation

The common zone formed after support, with the moisture value equal to full saturation for wetting θ_n lies above the stable part of the capillary rise zone with the moisture value equal to effective porosity n (Fig. 3). Due to the saturation inertia resulting from hysteresis, retention related to this moisture difference is filled extremely slowly. Consequently, quick rate compensation ($v_n \to v_k$) occurs within these zones, which also have different conductivity values:

$$k_n \frac{h_g - H_k}{m_a - h_k} = k_o \frac{H_k + m_a}{h_k} \tag{14}$$

Therefore, the hydraulic head at the boundary of the zones will be:

$$H_k = \frac{k_n\, h_k\, h_g - k_o\, m_a \left(m_a - h_k\right)}{k_n\, h_k + k_o \left(m_a - h_k\right)} \tag{15}$$

which determines the limit ground absorbency:

$$\boxed{v_g = k_n \frac{h_g + m_a}{m_a - h_k + \dfrac{k_n}{k_o} h_k} \cong k_n \left(1 + \frac{2\, h_g + h_k}{2\, m_a - h_k}\right)} \tag{16}$$

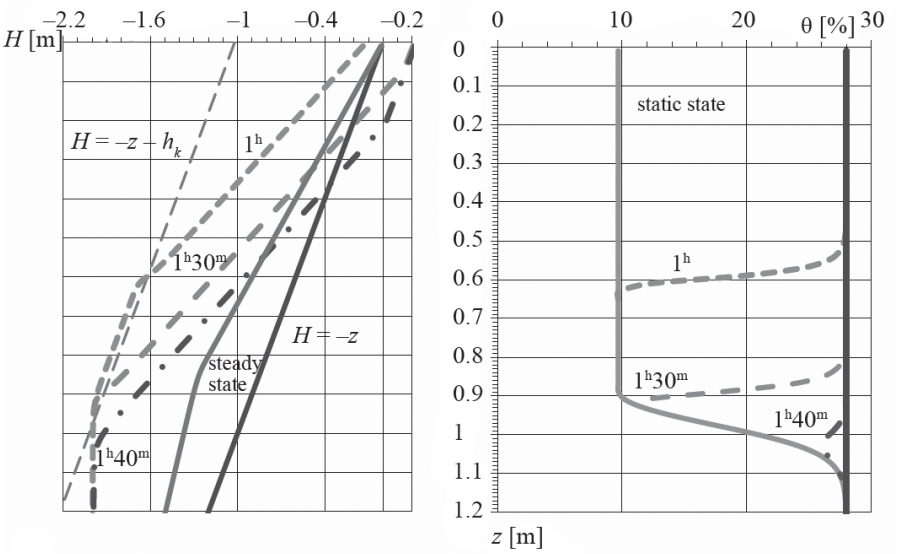

Fig. 4. Changes of moisture θ and hydraulic head *H* in submerged conditions, after support (discrete imulation)

For free infiltration, absorbency is described by formula (5), so after support, its value decreases, while the runoff value increases. The decrease of absorbency also leads to the occurrence of lower values of hydraulic slope in both capillary zones. In Fig. 4, the blue line indicates the value of hydraulic head with constant moisture value θ_n in a column, while the grey line – with moisture increasing from θ_n to n (within the stable capillary zone). Proper recharge values may be calculated using formula (16).

4.2. Submerged supported infiltration process

In the initial phase of infiltration within the zone after the wetting front, the traditional model of submerged infiltration (formula 5) is applicable. The flow within the residual zone and within the capillary rise zone has the same course as in unsaturated infiltration. Runoff occurs due to the fact that precipitation intensity exceeds ground absorbency.

When both zones reach each other, i.e. $z_1 = z_k$ (Fig. 3), the infiltration zone becomes the capillary rise zone and the infiltration rate drops to the absorbency value (formula 16). Because retention is impossible, runoff recharge increases rapidly and almost stabilizes (provided that groundwater level remains unchanged). Over time, as air diffuses from the smallest soil pores, a slow increase of the infiltration rate occurs, towards the value of hydraulic conductivity ($v_g \rightarrow k_o$), but precipitations are never so long. It causes a proper slow decrease of runoff recharge.

5. Supported saturated infiltration

This infiltration regime appears when the recharge value exceeds the maximum value of effective hydraulic conductivity for wetting, but falls within the range of ground absorbency ($k_n < v < v_g$), irrespective of the range of the capillary rise zone ($z_k >$, = or < $m_a - h_k$). In such conditions, pressure guaranteeing full saturation is generated on the surface, but runoff does not occur ($-h_k \le h_g < 0$, Fig. 5).

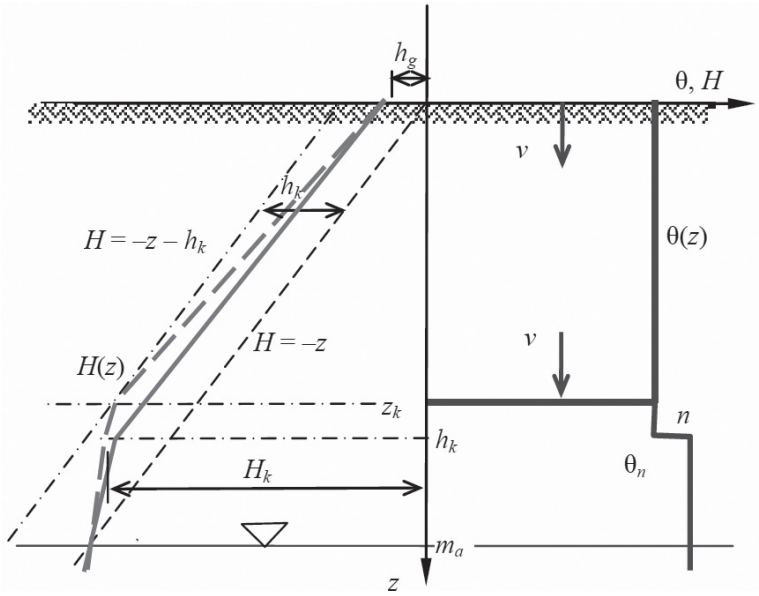

Fig. 5. Scheme of moisture θ and hydraulic head H changes in the piston model, during supported saturated infiltration

When support occurs, the infiltration zone and the capillary rise zone merge (Fig. 6), so the situation is similar to that observed during submerged infiltration. However, in this case, the boundary condition on the surface is the recharge value v_r. Rate compensation within these two zones with different conductivities leads to the following equation:

$$v_r = v = v_k \quad \rightarrow \quad v_r = k_n \frac{h_g - H_k}{m_a - h_k} = k_o \frac{H_k + m_a}{h_k} \tag{17}$$

that may be used for determining the hydraulic head at the zones boundary:

$$H_k = h_k \frac{v_r}{k_o} - m_a < 0 \tag{18}$$

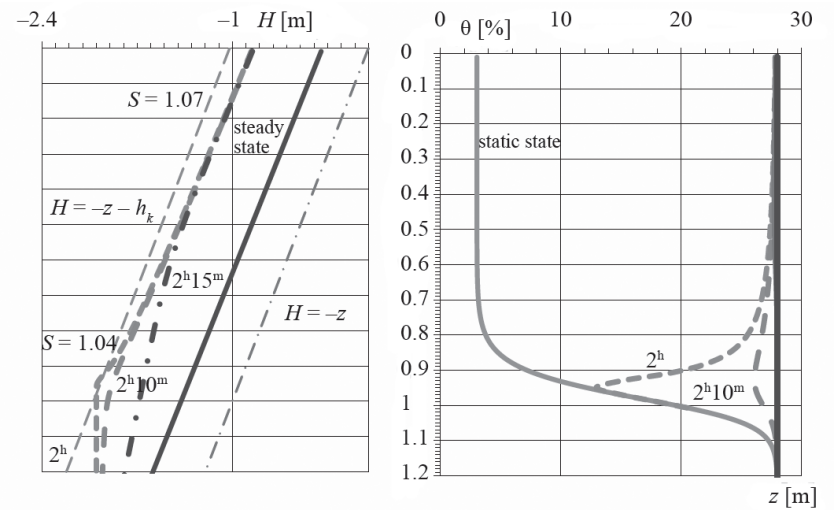

Fig. 6. Changes of moisture θ and hydraulic head H in supported saturated infiltration (discrete simulation)

as well as the equation to be satisfied by the rate of seepage:

$$v_r = k_n \frac{h_g + m_a - h_k \dfrac{v_r}{k_o}}{m_a - h_k} \quad \rightarrow \quad v_r = k_n \frac{h_g + m_a}{m_a - h_k + \dfrac{k_n}{k_o} h_k} \tag{19}$$

5.1. Pressure head on the surface

The previous equation may be used to determine the value of pressure head on the surface that is generated as a result of precipitation with the intensify of v_r:

$$\begin{aligned} h_g &= \frac{v_r}{k_n}\left(m_a - h_k + h_k \frac{k_n}{k_o}\right) - m_a = m_a\left(\frac{v_r}{k_n} - 1\right) - h_k\left(\frac{v_r}{k_n} - \frac{v_r}{k_o}\right) \cong \\ &\cong m_a\left(\frac{v_r}{k_n} - 1\right) - \frac{h_k}{2}\frac{v_r}{k_n} < 0 \end{aligned} \tag{20}$$

The pressure head value should not be higher than 0, as otherwise a proper layer of water would have to accumulate on the surface. Negative values, indicating suction head, cannot be lower than h_k, because the moisture value would drop below θ_n. In particular for recharge $v_r = k_n$, the suction head on the surface will be $h_g \cong -1/2 h_k$.

5.2. Ground absorbency v_g

Ground absorbency corresponds to $h_g = 0$ and is the **maximum value of recharge for this regime** (when it is higher, submerged infiltration takes place). A proper equation for submerged infiltration (formula 16) may be used, with the said value h_g inserted:

$$v_g = k_n \frac{m_a}{m_a - h_k + h_k \frac{k_n}{k_o}} \cong k_n \left(1 + \frac{h_k}{2\, m_a - h_k}\right) \tag{21}$$

Therefore, ground absorbency also decreases in this case. When feeding is very intensive, it can lead to submergence of infiltration.

5.3. Supported saturated infiltration process

In the initial phase of infiltration behind the wetting front, the traditional model of saturated infiltration may be used (formula 6). The flow within the residual zone and the capillary rise zone has the same course as in unsaturated infiltration. When both zones reach each other ($z_1 = z_k$), the slope within the capillary rise zone increases rapidly (no retention), and the rate of infiltration in the entire column reaches the value of surface recharge. Actually, because of the open capillary zone, this process takes place until the zone is fully saturated, which takes several minutes (Fig. 6). It is related with the increase of the hydraulic head on the surface h_g (formula 20). If recharge intensity exceeds the absorbency value reduced as a result of the support (formula 21), this value will be positive and surface submergence will occur. Thus, submerged infiltration will take place, with intensity lower than the recharge.

Prolonged saturated infiltration causes a gradual removal of air entrapped in soil pores, with moisture increase until reaching the porosity value n. It leads to the increase of effective hydraulic conductivity of ground, and also its absorbency to the value of hydraulic conductivity k_o, similarly as during submerged infiltration.

6. Unsaturated infiltration

In the initial phase of infiltration behind the wetting front, the traditional model of unsaturated infiltration is applicable (free infiltration, formula 7). In the shrinking residual zone (with the initial moisture value), the seepage rate is calculated in the same way on the basis of residual moisture θ_w.

Water in capillaries remains under the influence of gravity and surface tension, so after the support of unsaturated infiltration the rate remains unchanged and unit slope is maintained ($v = k(\theta)$, Fig. 7). Only within the capillary zone does a new balance appear, with slope resulting from the new recharge value (section 3), for effective hydraulic conductivity during wetting $k_n = k(\theta_n)$.

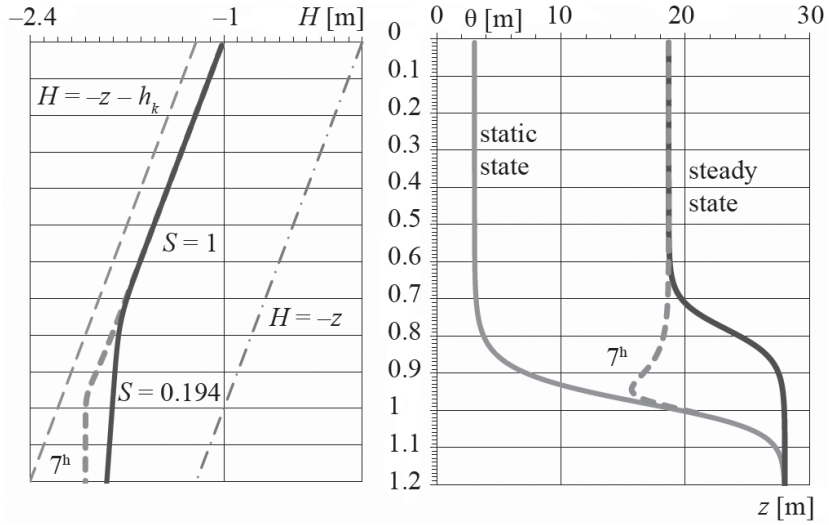

Fig. 7. Changes of moisture θ and hydraulic head H in supported unsaturated infiltration (discrete simulation)

In the model with the sharp wetting front, moisture within the front is constant until the moment of support: θ_w = const, $v = k(\theta_w)$. Actually, the moisture value increases gradually downwards the column, until reaching θ_n, along the section defined by the steepness of soil characteristics and the recharge value. The height of such open capillary zone changes similarly as in the case of a closed zone (Fig. 7). Accordingly, support does not change the rate of flow, but only moisture distribution.

7. Residual infiltration

Residual infiltration is the infiltration between the last front z_1 and the capillary zone z_k. The moisture within this zone is the result of moisture redistribution in periods between precipitations. In this process, due to negative column balance, water slowly flows out of the vadose zone. When a new wetting front occurs during precipitation with intensity that guarantees positive balance ($v_r > k(\theta_r)$), redistribution is ceased because the flow to the residual zone compensates the outflow.

As it has been confirmed by the analysis of the actual course of the process, the slope within the column with constant residual moisture remains equal to 1, which is determined by constant suction head and invariability of moisture change trend. A similar process occurs in free infiltration, so just as in that case, the rate of infiltration corresponds with the effective hydraulic conductivity at a given moisture level $v = k(\theta_w)$. Consequently, it is the efficiency of the capillary zone recharge, or the other way round – the formula may be used in order to determine the moisture level within the residual zone, for a given recharge value, before the occurrence of a new wetting front.

8. Moisture redistribution

Moisture redistribution consists in the outflow of water from larger capillaries in the top part of the column and infiltration to its lower parts. As a result, the flow within the capillaries has the character of the flow supplied on the length, reaching the full efficiency at the end of the column, which is when $z = z_k$. When the recharge does not compensate the outflow to the capillary zone, the slope increases along with the depth, from the value corresponding to the current surface recharge to the value corresponding to the outflow. Within the capillary zone, the slope decreases along with the increase of conductivity at a given level, so that the maximum slope level occurs at the upper boundary of the open capillary zone. As a result, the suction head within the vadose zone drops only slightly, while the moisture value slightly increases downwards the column (Fig. 7), with a small departure from the assumptions of the piston model. That increase accelerates only within the open capillary zone.

In the piston model, vadose zone moisture θ_w is determined on the basis of its balance (to the depth of z_k), while the rate of the capillary zone recharge is calculated as in the case of free infiltration, which is on the basis of the moisture retention characteristics $v_k = k(\theta_w)$. The depth of the front z_k should be calculated on the basis of the rate of infiltration to the capillary rise zone, as described in section 3. Such a method of calculation gives results that are quite consistent with the actual values (Fig. 8), which is not provided by the free infiltration model (traditional).

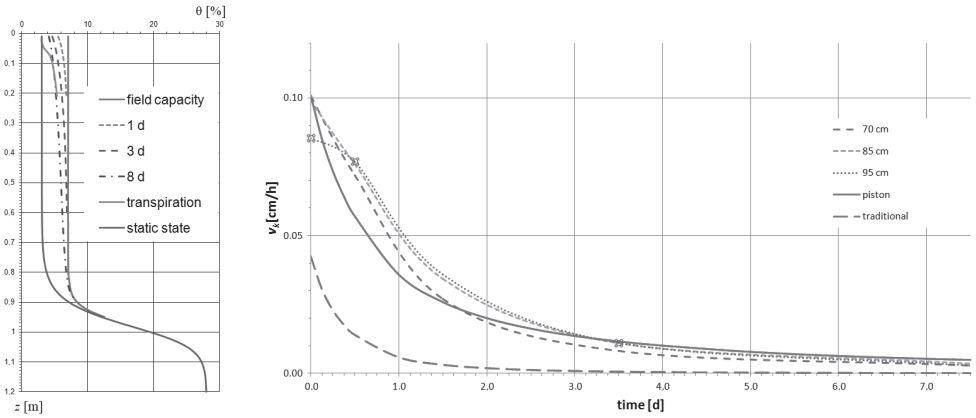

Fig. 8. Changes of the rate of the capillary zone recharge in moisture redistribution conditions for piston model and discrete simulation

9. Groundwater evaporation

Precipitation events appear periodically, while in times between them, moisture is constantly determined by redistribution. It occurs in the area above the first wetting front, or after its disappearance – above the residual zone. Thus, water outflow through the surface

may occur above the first front z_1, or above the range of the residual zone (z_k). Outflow intensity corresponds to the current evapotranspiration v_e (i.e. $v_r = -v_e < 0$). The consequence of evaporation is the decrease in the moisture level. Thus, it is a process in which hysteresis occurs, just as in the case of moisture redistribution.

According to the Buckingham-Darcy equation, infiltration may be described as the sum of moisture diffusion and gravity flow:

$$v = -k(\theta)\frac{\mathrm{d}(-h_s - z)}{\mathrm{d}z} = D_w(\theta)\frac{\mathrm{d}\theta}{\mathrm{d}z} + k(\theta) \tag{22}$$

where $D_w(\theta)$ denotes the moisture diffusion coefficient. Water outflow towards the surface requires negative slope (upwards), and such situation is possible only when the suction head drop exceeds 100%, which is when a very large moisture decrease occurs, possible only within the several-centimeter thick sub-surface layer (Fig. 8, light blue line). Intensive drying of this layer causes an increase of its thermal insulation properties, which quickly impedes further evaporation. Only plants, thanks to their root systems, are capable of acquiring water from the quite extensive rhizosphere, for a certain time maintaining the outflow of moisture to the atmosphere. However, when boundary moisture level is exceeded within this layer, transpiration is also impeded [3]. With such moisture values, the water outflow is very small, so redistribution decays as well.

The piston model, being simplified, does not allow to include such local changes, determining only the average moisture value within the adhesion zone. While calculating the moisture value behind the wetting front – $\theta = k(v_r)$, it should be taken into account that input value for conductivity characteristics can be only positive ($v_r > 0$), so this restriction must be included in the identification of the infiltration regime.

10. Conclusions

As it may be concluded on the basis of the examples presented above, the course of the support process is quite complex and difficult to reflect using a simple solution of the general seepage equation, because it requires using an advanced program. The issue of hysteresis in different directions of moisture changes and at variable moisture values within the saturated zone should be taken into account in calculations. The results obtained using the simplified model, based on several standard analytical formulas, are sufficient in practical purposes. Despite significant schematization, they allow to estimate major values occurring after the support, such as the recharge level, capillary zone height, size of effective precipitation (runoff recharge), etc.

The article proposes a simple method for calculating the capillary rise in the presence of recharge from the vadose zone and hysteresis of moisture. It also analyzes the impact of support on the infiltration and presents the necessary modifications to the calculation using the principles of piston model.

References

[1] Brooks R.H., Corey A.T., *Properties of porous media affecting fluid flow*, J. Irrigation and Drainage Div. ASCE ‘66/IR2, 61–88.
[2] Kaluarachchi J.J., Parker J.C., *Effects of hysteresis with air entrapment on flow in the unsaturated zone*, Water Resour. Res. 23, 10, 1987, 1967–1976.
[3] Książyński K.W., *Calculation of actual evapotranspiration on vegetation-covered soils*, Technical Transactions, 1-Ś/2015, 53–60.
[4] Książyński K.W., *Tłokowy model filtracji w strefie niepełnego nasycenia* (*Piston model of seepage in the vadose zone*), Monografia 353, Seria Inżynieria Środowiska, Wyd. PK, Kraków 2007, 188.
[5] Richards L.A., *Capillary conduction of liquids through porous media*, Physics, 1, November 1931, 318–333.
[6] Swartzendruber D., Clague F.R., *An inclusive infiltration equation for downward water entry into soil*, Water Resour. Res., 25, 4, 1989, 619–626.

TECHNICAL TRANSACTIONS | CZASOPISMO TECHNICZNE
ENVIRONMENT ENGINEERING | ŚRODOWISKO
1-Ś/2016
DOI: 10.4467/2353737XCT.16.196.5945

DOMINIKA ŁOMIŃSKA*

HUMIC SUBSTANCES AS BY-PRODUCT PRECURSORS GENERATED DURING OXIDATION AND DISINFECTION – REVIEW OF THE LITERATURE

SUBSTANCJE HUMUSOWE JAKO PREKURSORZY UBOCZNYCH PRODUKTÓW UTLENIANIA I DEZYNFEKCJI – PRZEGLĄD LITERATURY

Abstract

Humic substances (HS), including soluble fulvic acids (FA), are commonly occurring pollutants, particularly in surface waters. HS were considered as substances, which are harmless for humans until now. They were mainly removed from the water because of turbidity, color and as a source of odor. HS in the process oxidation and disinfection are precursors of carcinogenic and mutagenic substances. Because of this, an analysis has been conducted, discussing their construction, properties and methods used of their disposal.

Keywords: humic substances, fulvic acids, water treatment, wastewater treatment

Streszczenie

Do powszechnie występujących zanieczyszczeń, szczególnie wód powierzchniowych należą substancje humusowe (SH), w tym rozpuszczalne kwasy fulwowe (KF). SH dotychczas uważane były za substancje zupełnie nieszkodliwe dla człowieka, a usuwane były z wody głównie ze względu na mętność, barwę oraz jako źródło przykrego zapachu. W procesach utleniania oraz dezynfekcji SH są prekursorami substancji kancerogennych oraz mutagennych. Ze względu na ten fakt przeprowadzono analizę studialną ich budowy oraz właściwości, a także stosowanych metod ich unieszkodliwiania.

Słowa kluczowe: substancje humusowe, kwasy fulwowe, uzdatnianie wody, oczyszczanie ścieków

* M.Sc. Eng. Dominika Łomińska, Institute of Water Supply and Environmental Protection, Department of Environmental Engineering, Cracow University of Technology.

1. Introduction

Along with an increasing number of people and their standard of living, the demand for water also increases, which is a natural environment for the occurrence of many substances and living organisms. It is worth noting that, in water, there are a lot of pathogenic organisms, such as: viruses, bacteria, fungi and their mold spores, protozoan cysts and worm eggs, which are parasites that live in the human digestive tract. The occurrence of the above-mentioned pathogens can lead to many diseases and even death. Disinfection can be used to destroy or inactivate them and prevent their redevelopment in the water supply system. Physical methods of disinfection of water can include: cooking, pasteurization of water, ultrasound orultraviolet radiation [1].

The relatively new, but also costly physical method, is disinfection by means of thermal techniques. Compared with the chlorination method, it is much less effective in preventing the formation and development of bacterial environments [2].

Chemical methods are used much more often. They are based on adding strong oxidizing agents to water, such as: chlorine, chlorine dioxide, sodium hypochlorite, chloramines and ozone less bromine or iodine. These substances react with the compounds present in water, leading to the creation of new compounds, which are known as disinfection by-products (DBP) [1].

Water treatment leads to the removal the majority of impurities. Purified water should meet the rigorous standards of both international – European Directive and national – Regulation of the Minister of Health. Humic substances, including soluble fulvic acids, are commonly occurring pollutants, particularly in surface waters.

2. Characteristics of humic substances

Humic substances exist in soils, rivers and lakes. They are usually aromatic and acidic in nature [3]. These substances are formed by humification, i.e. the microbiological decomposition of plant and animal residues, such as lignin, proteins, pectins, polysaccharides, and tannins [4]. They are biogenic, heterogeneous substances, belonging to organic compounds [5]. HS are commonly known as the most widespread and ubiquitous components, which belong to natural organic matter (NOM) [6].

According Górniak, humic acids (HA) constitute up to 70% of the soil's organic matter, and up to 80% soluble organic carbon. HA has an unspecified structure [7]. These substances can be formed "in situ" in "aquatic ecosystems, but mostly are supplied from soil drainage areas [8].

Their color depends on their origin, concentrations and pH of the solution; it may change from yellow to dark brown. The molecular weight of HS ranges from a few hundred to a few thousand Daltons [9]. Humic substances are natural macromolecules commonly found in the aquatic environment, soil, sludge etc. [8]. Humic acids occur in a dissolved, colloidal form, small dispersion connection with suspensions or in the form of very small particles. As it was mentioned, these substances are commonly found on the surface of the Earth. Typically, their concentration in the rivers can be about 6 mg/l, while in the water marsh, even above

18 mg/l. HS represent between 50% and 75% of the total organic carbon contained in the surface waters [10, 11]. Fulvic and humic acids are the largest group present in the aquatic environment. Natural organic matter sediments and seawater contains 10–80% humic substances [10, 11].

In a pure state, humic substances are natural pollution, harmless to humans, but as a result of the oxidation and disinfection processes, they undergo chemical changes and form carcinogenic and mutagenic products. It is worth mentioning that the content of HS in drinking water is not normalized [12].

According Li et al. [13] who extracted humic acids from digested sludge by alkaline treatment and ultrafiltration, humic acids (HA) were the major constituent of humic substances in digested sludge, and most of the humic acids had molecular weights higher than 50 kDa [13].

Although the structure of humic substances was studied for about 200 years and has yet to be recognized, there are many models of their structure [10].

Figure 1 shows a model structure of humic acids by Stevenson.

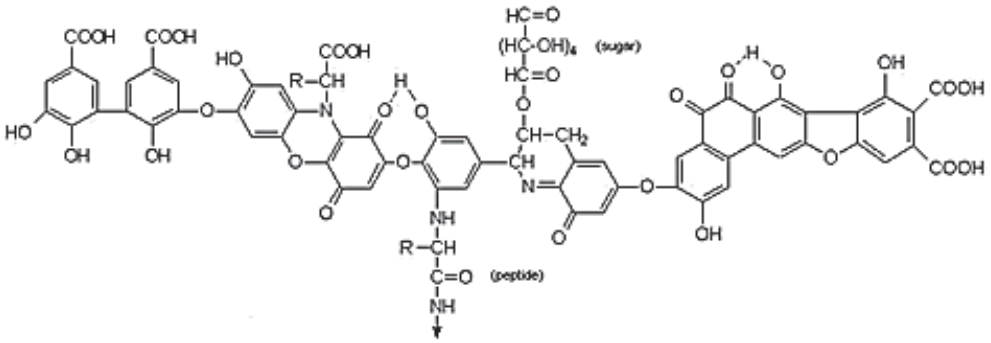

Fig. 1. Model structure of humic acid by Stevenson (1982)

Figure 2 shows a model structure of fulvic acid by Buffle.

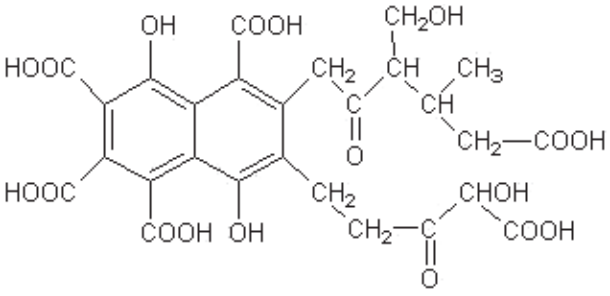

Fig. 2. Model structure of humic acid by Buffle [14]

One of the methods characterizing the construction of humic substances is the absorption analysis of infrared radiation. The absorption of the selected wavelength is suitable for the specific structural elements. For example, absorption bands of 3500–3000 nm are attributed to the amine groups and hydroxyl, which tend to form hydrogen bonds; the range of 3000–2800 nm is attributed to bonding between carbon and hydrogen in the methyl and methylene groups; 1500 nm – a carboxyl group and a secondary amine; 1430 nm – OH group in phenols; 1680–1650 nm aldehydes, ketones, and carboxylic acids as well as double bonds in the carbon chain aliphatic and aromatic rings [15].

According to most authors, HS are long-chain molecules, forming coils with elements of aromatic and aliphatic. However, in aqueous solutions, they create spherical forms [15].

Humic substances can be classified according to their solubility as: humic acids (HA), fulvic acids (FA), hymatomelanic acids and humin. Humic acids dissolve in an alkaline solution and precipitate in strongly acidic conditions (pH < 2). Fulvic acids dissolve in both alkaline and acid solution, while humin remains insoluble in acids and alkalis. Hymatomelanic acids (ulmine) dissolve in ethanol [9, 10].

Currently, the removal dissolved organic matter (DOM) from water includes coagulation, adsorption, nano-filtration (NF) and biological methods [16–17]. The most frequently used method mentioned above is adsorption [16–19]. Linnik and Vasilchuk [21], in their research, investigated the role of HS in the complexation and detoxification of heavy metals in Dnieper Reservoirs. The results of research showed that humic substances are the main component of dissolved organic matter (DOM) in Ukrainian rivers. The concentration of fulvic acids was 20–40 times higher than humic acids. Humic substances, and more specifically fulvic acids, preferentially bind heavy metals (HM). The content of metals bound into complexes with DOM depends on the season and reaches 70–100% of the total dissolved forms. The maximum content of HS is usually observed in spring, owing to the high water season [21].

3. Humic substances as by-product precursors of oxidation and disinfection

Fulvic acids were considered as harmless substances for humans and were removed from water mainly because of turbidity, color and as a source of odor.

The studies conducted in 1974 [22] showed that humic substances are precursors of carcinogenic and mutagenic compounds produced during oxidation and disinfection processes.

These substances are formed depending on the composition of the disinfectant and purified water. HS include substances such as: trihalomethanes (THM), haloacetic acids (HAA), halogeno-nitriles, halogeno ketones, trichlorophenol, trichlorobenzenes, hydroxi-furanes and others. This is the reason why humic substances should be investigated in the environment and eliminated from the water before sending it to treatment plants [22]. Trihalomethanes (THM) are the largest group of compounds generated during the chlorination of natural organic substances, such as HS [23]. The amount of trihalomethanes formed during the water chlorination process is affected by factors such as: temperature, pH, chlorine dose and duration of chlorination as well as the concentration of total organic carbon (TOC). The speed of their formation depends on the type of organic substances [24]. These compounds belong to the halogen derivatives of hydrocarbons. They have the general molecular formula CHX,

where X is atom fluorine, chlorine, bromine or iodine. The best-known representatives of trihhalomethanes are: chloroform ($CHCl_3$), bromoform ($CHBr_3$) dibromochloromethane ($CHClBr_2$) bromodichloromethane ($CHCl_2Br$) [25].

Table 1 shows the acceptable concentration of THM in drinking water recommended by the World Health Organization (WHO) (1998) [26].

Table 1

Allowable concentration of THM in drinking water recommended by the World Health Organization (WHO) [26]

Substance	Concentration [μg/l]
Chloroform	200
Dichlorobromomethane	60
Dibromochloromethane	100
Bromoform	100

According to the data provided by the WHO, the risk of death from cancer caused by trihalomethanes is 1/100-1/1000 of the risk of death caused by bacteria present in the not disinfected water. There are ongoing studies on the effects of chlorine on the mass occurrence of various diseases, such as: heart attacks, cancer of the bowel and bladder, or the gradual loss of memory or arteriosclerosis. Because of the universality of disinfecting water with chlorine, these studies are difficult because, in highly developed countries practically, it is impossible to find people who were not exposed to chlorine for a long time. Another important issue is the intensity of the smell and taste of chlorine. According to the Regulation of the Minister of Health, the only criterion for setting forth the issue of taste and smell of water is to determine whether it is acceptable by the consumer, which, according to Komusińska [27], is debatable because it is hard to determine if this legal criterion is met. It is precisely this factor and more specifically the high concentration that has a significant impact on the negative opinion of Poles about water coming from the water supply. According to the author, the aroma of chlorine is so strong that even 10% content of it leads the users to conclude that the water is distasteful [27].

Table 2 shows the chemical requirements for the trihalomethanes, which should correspond to the water on the basis of the Regulation of the Minister of Health from 2015.

The permissible concentration of THM in water intended for human consumption is subject to certain requirements and should be closely monitored. This is due to the mutagenic and carcinogenic influence of THM on living organisms. According to the Minister of Health of 13 November 2015 [27] regarding the quality of water intended for human consumption, the total value sum of THM concentration should not exceed 100 μg/l. This is due to the fact that the elevated levels of these substances lead to an increasing number of diseases – human tumor of the digestive system, urinary system and the number of increased risk of miscarriage in pregnant women. The most dangerous parameter listed in Table 3 THM is dibromochloromethane [25].

Table 2

Chemical requirements for the trihalomethanes, which should correspond to the water (Regu – lation of the Minister of Health of 13 November 2015 regarding the quality of water intended for human consumption, 7 Pos. 1989) [28]

Parameters	Maximum allowable concentration	Unit
Σ THM: trichloromethane, bromodichloromethane dibromochloromethane tribromomethane	100	[µg/l]
Σ THM – value is the sum of the concentrations of: trichloromethanes, bromodichloromethanes, dibromochloromethanes, tribromomethanes.		

Table 3 shows the allowable concentration of THM in drinking water in selected countries in the world.

Table 3

Allowable concentration of THM in drinking water in selected countries in the world [23]

Country	THM	$CHCl_3$	Unit
Australia	250	–	[µg/l]
China	–	60	
France	–	30	
Japan*	100	60	
Korea	100	–	
Taiwan	100	–	
USA	80	–	
Poland	100	–	
WHO**	–	200	

* $CHCl_2Br$ 30 µg/l, $CHClBr_2$ 100 µg/l, $CHBr_3$ 90 µg/l

** $CHCl_2Br$ 60 µg/l, $CHClBr_2$ 100 µg/l, $CHBr_3$ 100 µg/l

Based on the above data table, it can be seen that the strictest standards for the concentration of THM in drinking water are in the USA (80 µg/l). In Poland, the allowable concentration is 100 µg/l and it corresponds to the requirements of the European Union. It is worth noting that the allowable concentration of THM in Australia is rather high at 250 µg/l.

Table 4 shows the index value THM quality of drinking water in Krakow in 2011 in four Water Treatment Plants: Raba, Rudawa, Dłubnia and Bielany.

Table 4

The indicator values THM quality of drinking water in Krakow in 2011 [27]

Indicator water quality	Unit	Water Treatment Plant				Regulation of the Minister of Health (2007 with amendments 2010)
		Raba	Rudawa	Dłubnia	Bielany	
Σ THM	µg/l	18	< 0.3	< 0.3	9.4	150 (100)

Based on the above table, it can be seen that the value of the concentration indicator THM in drinking water at the Water Treatment Plant Raba was 18 µg/l, at Bielany 9.4 µg/l, while in Rudawa and Dłubnia, it was below 0.3 µg/l. The values of these concentrations comply with the applicable legal requirements.

Haloacetit acids (HAA) are mainly formed during the chlorination of water with chlorine gas. These are organic substances that are present in water; they are largely known as humic substances, referred to as HAA precursors [29]. Haloacetic acids are another group of dangerous compounds. Haloacetic acids include acids, such as: bromoacetic acid, trichloroacetic acid, monochloroacetic and dichloroacetic [23]. The last two are the precursors of THM in water distribution networks [24].

Table 5 shows the permitted concentration for the sum of five haloacetic acids established by the United States Environmental Protection Agency (US EPA).

Table 5

Concentration limits for the sum of five haloacetic acids established by the United States Environmental Protection Agency (US EPA) [30]

Type of haloacetic acid	The concentration limit of the sum of five acids	Unit
MCAA	60	mg/m^3
DCAA		
TCAA		
MBAA		
DBAA		

MCAA – monochloroacetic acid,
DCAA – dichloroacetic acid,
TCAA – trichloroacetic acid,
MBAA – monobromoacetic acid,
DBAA – dibromoacetic acid.

The United States Environmental Protection Agency (US EPA) has established a permissible value as a sum of the concentrations of five HAA, i.e. MCAA, DCAA, TCAA, MBA, equal to 60 mg/m^3. Due to the fact that haloacetic acids are carcinogens and dangerous for humans, a reduction to 30 mg/m^3 is expected.

WHO guidelines for drinking water quality recommend limits of dichloroacetic acid to 50 mg/m^3 and trichloroacetic acid to 100 mg/m^3. While the Regulation Minister of Health of 20 April 2010 defines the conditions to be met by water for drinking and domestic purposes, it refers only to a single acid – monochloroacetic. The maximum concentration may be 30 mg/m^3 [30].

Research conducted by Anielak, Grzegorczuk and Schmidt [24] has shown that by oxidizing natural substances, which are safe for the environment, aliphatic and aromatic compounds with different values of MAC and LD50 are obtained, testifying to the toxicity of oxidation products. It was observed that, with increasing doses of the oxidant (NaOCl and H_2O_2), there were increases in the amount of organic oxidation products, including flavoring substances. During the oxidation of fulvic acids chlorite (I), sodium formed trichloromethane, or the main representative of THM [24]. It is widely believed that active chlorine compounds are formed in processes of oxidation of water with chlorine gas or compounds thereof. Therefore, ozone treatment, UV disinfection and primarily the use of safe oxidants and disinfectants are recommended [24].

Uyguner et al. [31], in their researches, tried to explain the relationship between formation potential (THMFP) and physicochemical properties of humic substances, UV-visible absorbance, fluorescence in emission and synchronous scan modes, and NMR spectra were measured for several aquatic fulvic and humic acids. For comparison, they examined soil fulvic acids using the same methods. Based on the tested methods, it was found that none of the results of analysis provided a good correlation with the THMFP values reported for the HS studied. According the authors, this means that earlier correlations between THMFP and color, size, or aromatic content as measured by different UV wavelengths do not hold for all types of aquatic humic substances [31–32].

4. The importance of humic substances for humans and other living organisms

Humic substances, like most of the compounds present in the environment have positive as well as negative effects on the processes of water purification.

HS due to the high content of functional groups and a high resistance to the biodegradation play an important role in aquatic and land environments. The occurrence of FA in groundwater may lead to the formation of soluble complexes KF – Fe and and K-Mn, which contributes to obstructing disposal of the water removal of iron and manganese [12]. Based on numerous studies, demonstrated a directly proportional relationship between the amount of generated THM and organic carbon content, so humic substances too. Highlighted the fact that this problem is particularly important during the chlorination of surface waters without forgetting the groundwater [12]. Miller, Randtke and Hathaway [12] conducted studies during which determined the potential to create already mentioned THM compounds in 50 different samples of groundwater. Groundwater contained organic carbon in quantities of 0.21–3.31 gCl_2/m^3.

It was found that during the process of purification underground water contaminated of various types of humus compounds, the chlorine can be dosed after removing THM precursors. This is particularly important as humic acids are the precursors of THM [12].

The role of humic substances present in the soil is closely linked with the stability of sorption processes of soil [33]. High content of humic substances in water restricts the access of light and leads to a reduction quantity of available micronutrients and in the result this helps to reduce the productivity of ecosystems [34].

Age occurrence of HS in some soils may be several thousand years. This is particularly important because of the negative character of their functional groups may promote accumulation heavy metals in aqueous environment and the formation of complex compounds.

Interesting research were conducted by Navarrete et al. [35] HS are very good fertilizers and it was confirmed that in the presence of FA mineral ions are more evenly distributed in the leaves and flowers of vegetable. However it is worth noting that autoradiography small ions such as sodium was possible only in the absence of FA, it can be understood as HS showed evident selective qualities regarding toxic ions such as chromates or mentioned sodium. Moreover authors notes that so many curative properties that are attributed to FA deserve a closer look to them and a serious investigation [35, 36].

According Świderska-Bróż [37] the largest complexes of humic acids with copper and lead is formed at a pH of 5–8. It is necessary to remove them from water treatment process, due to their adsorption properties of such organic compounds as: pesticides, polychlorinated biphenyls (PCBs) and phthalates [37, 38].

5. Disposal methods of humic substances

In order to effectively remove the by-products of oxidation and disinfection, their precursors have to be first removed. Water treatment, in which there are humic substances, requires the use of suitable unit processes, such as coagulation, filtration, adsorption on activated carbon, chemical oxidation, chemical precipitation or ion exchange and membrane processes. The most commonly used adsorbents for the purification of drinking water are activated carbons [34, 39–41].

According Dojlido and Taboryska [42], two methods can be used for the determination of humic substances: extraction-spectrophotometric method and the measurement of organic carbon. The extraction–spectrophotometric method consists of extracting humic substances amyl alcohol in an acid environment and then converting them to a solution of sodium hydroxide. It can be seen that the intensity of the alkaline aqueous layer is proportional to the concentration of humic substances. The second method involves the binding of humic substances on anionic cellulose at a neutral pH. Subsequently, HS is eluted with a solution of sodium hydroxide. Then, after acidification and removal of inorganic, carbon is indicated by the dissolved organic carbon (DOC) [42].

Humic substances are characterized by a high resistance to biodegradation. The new direction of research project fri. “Used archea and unconventional sources of carbon in the process of municipal wastewater treatment” [43] showed that fulvic acids inhibit the process

of municipal wastewater treatment with activated sludge. As a result of bioaugmentation sludge, archea increased its activity and biodegradation resulted in fulvic acids. The efficiency of the process during the three days of observation was small and amounted to 21%. It must be concluded that it was not the result of sorption on the surface of activated sludge. In the presence of fulvic acids, the release of nitrogen occurred from the activated sludge; therefore, we should say that the FA adversely affect the denitrification process. Based on the research of molecular (PCR and RT-PCR), which formed part of the project, it has been shown that in the settlement, which was bioaugmentation, the archea created a stable population that was able to develop [43].

6. Summary

Humic substances, like most of the compounds present in the environment, have positive as well as negative effects on the removal of organic pollutants. The role of humic substances present in the soil is closely linked with the stability of sorption processes of soil [33].

HS as natural organic acids constitute an organic carbon source for plants, microorganisms, and play an important role in the biogenic cycle; they participate in biochemical and nutrients. According to Ukrainian researchers, major contribution to the humic substances is represented by FA, the content of which may 81–95% of the total of HS [44, 45].

Along with a high content of humic substances in water, there is limited access to light, leading to the reduction of the quantity of available micronutrients, which contributes to reduced productivity of ecosystems [34].

In order to effectively remove by-products of oxidation and disinfection, their precursors have to be first removed. Water treatment, which includes humic substances, requires the use of suitable unit processes, which include: coagulation, filtration, adsorption on activated carbon, chemical oxidation, chemical precipitation or ion exchange and membrane processes. The most commonly used adsorbent for the purification of drinking water are activated carbons [34, 39–41].

To sum up, humic substances have a negative influence on living organisms and have the ability to transport metals and other pollutants. The analysis has shown that HA penetrate to the surface water and become precursors of oxidation and disinfection by-products at treatment plants. So, this is the reason why they should be removed from water directed to Water Treatment Plants.

This is particularly important due to the fact that, according to the World Health Organization (WHO), “up to 80% of all diseases of modern civilization are related to the quality of drinking water” [46].

References

[1] Dojlido J., *Uboczne produkty dezynfekcji wody*, Polskie Zrzeszenie Inżynierów i Techników Sanitarnych, Warszawa 2002, 7–12.

[2] Kłos L., *Jakość wody pitnej w Polsce*, Acta Universitatis Lodziensis Folia Oeconomica, Vol. 313 (2), 2015, 195–205.

[3] Reija E.K., Jörg H.L., Jaakko A.P., *Natural organic matter (NOM) removal and structural changes in the bacterial community during artificial groundwater recharge with humic lake water*, Water Research, Vol. 41 (12), 2007, 2715–2725.

[4] Dojlido J., *Chemia wód powierzchniowych*, Wyd. Ekonomia i Środowisko, Białystok 1995.

[5] Stevenson F.J., *Humus Chemistry*, John Wiley & Sons, New York 1982.

[6] Senesi N., *Humic Substances as Natural Nanoparticles Ubiquitous in the Environ ment*, Molecular Environmental Soil Science at the Interfaces in the Earth's Critical Zone, Springer Berlin Heidelberg, 2010, 249–250.

[7] Górniak A., *Znaczenie kwasów humusowych jako czynnika wpływającego na funkcjonowanie fitoplanktonu*, Bibl. Monit. Środ., Łódź 1998, 125–134.

[8] Górniak A., *Substancje humusowe i ich rola w funkcjonowaniu ekosystemów słodkowodnych*, Dysertacja Uniwersytetu Warszawskiego, Białystok 1996, 448.

[9] Noel E., Palmer Ray von Wandruszka, *Dynamic light scattering measurements of particle size development in aqueous humic materials*, Fresenius J Anal Chem, Vol. 371, 2001, 951–954.

[10] Anielak A.M., *Wysokoefektywne metody oczyszczania wody*, PWN, Warszawa 2015, 28–32.

[11] Anielak A.M., Majewski A., *Physico-chemical Properties of Fulvic Acids Environmental Engineering studies. Polish research on the way to the EU*, Lublin 2003, 421–429.

[12] Świderska-Bróż M., *Związki azotowe i humusowe : uciążliwe domieszki wód podziemnych*, Vol. 45 (1), 1992, 15–20.

[13] Li H., Li Y., Zou S., Li C., *Extracting humic acids from digested sludge by alkaline treatment and ultrafiltration*, J Mater Cycles Waste Manag, Vol. 16 (1), 2014, 93–100.

[14] Charakterystyka swoistych związków próchnicznych (online) homepage: http://karnet.up.wroc.pl/~weber/kwasy1.htm (date of access: 2016-04-25).

[15] Anielak A.M., Jaworska E., Pitrus K., *Wybrane substancje organiczne występujące w wodach powierzchniowych, będące prekursorami UPUD*, Technologia Wody, Vol. 18 (4), 2012, 33–38.

[16] Wang J., Zhoua Y., Li A., Xu L., Xu L., *Adsorption of Humic Substances by Macro Weakly Basic Ionexchange Resin and Their Effects on Removal of Cu^{2+} and Pb^{2+*}*, Chinese Journal of Polymer Science, Vol. 28 (3), 2010, 427−435.

[17] Liping, Riemsdijk W., Koopal L., Hiemstra T., *Adsorption of Humic Substances on Goethite: Comparison between Humic Acids and Fulvic Acids*, Environmental Science & Technology, Vol. 40 (24), 2006, 7494–7500.

[18] Weng Y.H., Li K.C., Chaung-Hsieh L.H., Huang C.P., *Removal of humic substances (HS) from water by electro-microfiltration (EMF)*, Water Research, Vol. 40 (9), 2006, 1783–1794.

[19] Kilduff J., Karanfil T., Weber Jr. W., *Competitive Interactions among Components of Humic Acids in Granular Activated Carbon Adsorption Systems: Effects of Solution Chemistry*, Environmental Science& Technology, Vol. 30 (4), 1996, 1344–1351.

[20] Karanfil T., Kilduff J., Schlautman M., Weber Jr. J., *Adsorption of Organic Macromolecules by Granular Activated Carbon. 1. Influence of Molecular Properties Under Anoxic Solution Conditions*, Environmental Science & Technology, Vol. 30 (7), 1996, 2187–2194.

[21] Linnik P.N., Vasilchuk T.A., *Role of humic substances in the complexation and Detoxification of heavy metals: case study of the Dnieper Reservoirs*, Nato Science Series IV: Earth and Environmental Sciences. Use of Humic Substances to Remediate Polluted Environments: From Theory to Practice. Complexing interactions of humic substances with heavy metals and radionuclides and their remedial implementation, 2005, 135–154.

[22] Świderska R., Anielak A.M., *The significance of electrokinetic potential in the adsorption process of humic substances*, Rocznik Ochrona Środowiska, Vol. 6, 2004, 31–49.

[23] Anielak A.M., *Uboczne produkty procesu utleniania i dezynfekcji*, Technologia Wody, Vol. 20 (6), 2012, 24–27.

[24] Anielak A.M., Grzegorczuk M., Schmidt R., *Wpływ chlorków na powstawanie substancji chloroorganicznych w procesie utleniania kwasów fulwowych*, Przemysł Chemiczny, Vol. 87 (5), 2008, 404–407.

[25] Skowron P., Małuch I., *Trwałe związki organiczne zanieczyszczające środowisko przyrodnicze i żywność*, Projekt „Kształcenie kadr dla innowacyjnej gospodarki opartej na wiedzy w zakresie agrochemii, chemii i ochrony środowiska" (Inno-AgroChemOś), 44–46, (online) homepage: http://iaco.mirocms.pl/files/download/277/Trwale-zwiazki--organiczne.pdf (date of access: 2016-04-25).

[26] Wytyczne WHO dotyczące jakości wody do picia. Wydanie drugie. Tom 1. Zalecenia PZiTS, Warszawa 1998.

[27] Komusińska J., *Raport na temat stanu gospodarki wodnej w Polsce: jakość wody pitnej*, Vol. (1), 2012.

[28] Rozporządzenie Ministra Zdrowia z dnia 13 listopada 2015 r. w sprawie jakości wody przeznaczonej do spożycia przez ludzi, poz. 1989.

[29] Dojlido J., *Uboczne produkty dezynfekcji wody*, Polskie Zrzeszenie Inżynierów i Techników Sanitarnych, Vol. 9, Warszawa 2002, 59–68.

[30] Kowalska M., Dudziak M., Bohdziewicz J., *Biodegradacja kwasów halogenooctowych w bioreaktorze z poliamidową, enzymatyczną membraną ultrafiltracyjną*, Inżynieria i Ochrona Środowiska, Vol. 14 (3), 2011, 257–266.

[31] Uyguner C.S., Hellriegel C., Otto W., Larive C.K., *Characterization of humic substances: Implications for trihalomethane formation*, Anal Bioanal Chem, Vol. 378 (6), 2004, 1579–1586.

[32] Cardoza L., Almeida K., Carr A., Graham D., Larive C., *Trends in Analitycal Chemistry*, Vol. 22, 2003, 766–775.

[33] Kučerík J., Bursáková P., Průšová A., Grebíková L., Schaumann G., *Hydration of humic and fulvic acids studied by DSC*, J. Therm Anal Calorim, Vol. 110, 2012, 451–459.

[34] Grzegorczuk-Nowacka M., *Adsorpcja kwasów fulwowych z wodnych roztworów*, praca doktorska, Politechnika Krakowska, Kraków 2012, 15–37.

[35] Navarrete J.M., Urbina V.M., Martnez T., Cabrera L., *Autoradiography of mineral ions in green leaves and flowers, absorbed with and without synthetic fulvic acids*, Journal of Radioanalytical and Nuclear Chemistry, Vol. 263 (3), 2005, 779–781.
[36] Navarrete J.M., Urbina V.M., Martnez T., Cabrera1 L., *Role of fulvic acids for transporting and fixing phosphate and iron ions in bean plants by radiotracer technique*, Radioanal. Nucl. Chem., Vol. 259 (2), 2004, 311–314.
[37] Świderska R., *Wpływ wybranych obciążników na koagulację w procesie uzdatniania wody*, praca doktorska, Politechnika Lubelska, Lublin 2000.
[38] Pempkowiak J., Obarska-Pempkowiak H., Gajewska M., Ruta D., *Oczyszczone ścieki źródłem kwasów humusowych w wodach powierzchniowych*, Przemysł Chemiczny, Vol. 87 (5), 2008, 542–545.
[39] Bolto B., Dixon D., Eldridge R., *Ion exchange for the removal on natural organic matter by ion exchange*, Water Research, Vol. 36, 2002, 5057–5065.
[40] Bolto B., Dixon D., Eldridge R., *Ion exchange for the removal on natural organic matter*, Reactive and Functional Polymers, Vol. 60, 2004, 171–182.
[41] Lin C.F., Lin T.Y., Hao O.J., *Effects of humic substances on UF performance*, Water Research, Vol. 34 (4), 2000, 1097–1106.
[42] Dojlido J., Taboryska B., *Substancje humusowe*, Uboczne produkty dezynfekcji wody. Polskie Zrzeszenie Inżynierów i Techników Sanitarnych, Warszawa 2002, 173–178.
[43] Anielak A.M., Polus M., Łomińska D., Żaba T., *Biodegradacja kwasów fulwowych z wykorzystaniem osadu czynnego wzbogaconego archeanami*, Przemysł Chemiczny, Vol. 95 (1), 2016, 110–113.
[44] Linnik P.N., Ivanechko Ya. S., Linnik R.P., Zhezherya V.A., *Humic Substances in Surface Waters of the Ukraine*, Russian Journal of General Chemistry, Vol. 83 (13), 2013, 2715–2730.
[45] Linnik P.N., Ivanechko Ya. S., Linnik R.P., Zhezhery V.A., *Systematic Features in the Study of Humic Substances in Natural Surface Waters*, Journal of Water Chemistry and Technology, Vol. 35 (6), 2013, 295–304.
[46] Berelski T., Forowicz K., *Woda po polsku*, „Rzeczpospolita", 24.04.2002.

TECHNICAL TRANSACTIONS | CZASOPISMO TECHNICZNE
ENVIRONMENT ENGINEERING | ŚRODOWISKO
1-Ś/2016
DOI: 10.4467/2353737XCT.16.197.5946

AGNIESZKA MAKARA*, ZYGMUNT KOWALSKI**, KATARZYNA FELA*, AGNIESZKA GENEROWICZ***

UTILIZATION OF ANIMAL BLOOD PLASMA AS EXAMPLE OF USING CLEANER TECHNOLOGIES METHODOLOGY

UTYLIZACJA PLAZMY KRWI ZWIERZĘCEJ JAKO PRZYKŁAD STOSOWANIA METOD CZYSTSZEJ PRODUKCJI

Abstract

Dried animal blood plasma, which is offered to the market as a feed product, should meet appropriate standards of quality and epidemiological safety. That is why blood drawing, its transportation, storage and processing must be performed with absolute observance of the principles of hygiene and sanitation. The paper discusses the possibilities of application of techniques used in the food industry for the pretreatment of animal blood plasma to ensure a high quality of the final product. Both the proper treatment of this by-product from the animal's production as well as its recycling and re-use as a feed or food additives are examples of practical use of cleaner production methods.

Keywords: *blood plasma, pre-treatment, bacteria amount reduction, anticoagulation, blood stabilization, cleaner production*

Streszczenie

Suszona plazma krwi zwierzęcej, aby mogła być oferowana na rynku jako produkt paszowy, powinna spełniać odpowiednie standardy jakości oraz bezpieczeństwa epidemiologicznego. Dlatego ważne jest właściwe pobranie surowca, jego transport i magazynowanie oraz obróbka przy bezwzględnym przestrzeganiu zasad higieniczno-sanitarnych. W artykule omówiono możliwości aplikacyjne technik stosowanych w przemyśle spożywczym do obróbki wstępnej plazmy krwi zwierzęcej w celu zapewnienia wysokiej jakości produktu finalnego. Zarówno odpowiednie przetwarzanie tego produktu ubocznego z produkcji zwierzęcej jego recykling, jak i wtórne zużycie do produkcji pasz czy dodatków do żywności jest przykładem zastosowania w praktyce metod czystszej produkcji.

Słowa kluczowe: *plazma krwi, obróbka wstępna, redukcja flory bakteryjnej, antykoagulacja, stabilizacja krwi, czystsze produkcje*

* Ph.D. Eng. Agnieszka Makara, Ph.D. Eng. Katarzyna Fela, Institute of Inorganic Chemistry and Technology, Faculty of Chemical Engineering and Technology, Cracow University of Technology.
** Prof. Ph.D. Eng. Zygmunt Kowalski, Mineral and Energy Economy Research Institute, Polish Academy of Sciences.
*** Prof. Ph.D. Eng. Agnieszka Generowicz, Institute of Water Supply and Environmental Protection, Faculty of Environmental Engineering, Cracow University of Technology.

1. Introduction

Cleaner production includes pollution production, reduction at source, recovery of materials end energy, with or without proper processing of waste or byproducts and their recycling [1]. The proposed methods of management and processing of blood plasma are examples of recycling and reuse of this valuable product. Recycling and re-use of blood plasma is possible only in this case if sampling and treatment of animal blood and its processing into blood plasma [2].

Spray-dried blood plasma is a rich source of nutrients. It may therefore be used as a feed component in feeding monogastric animals. The dried pork plasma is a powder ranging in color from cream to pale yellow; it is dry, odorless, with specific density of 0.60–0.65 kg/dm^3 and a moisture content of 6–9%. It is readily dissolved in water (88%) [3–5]. A commercial product should contain min. 70% of protein and other components should be present in the following maximum amounts: fat – 2.0%, fibers – 0.3%, Na – 6.0% K – 0.6%, Ca – 0.15% P – 0.15% Cl – 3.0% Fe – 50 ppm, while the amount of ash obtained from the sample material should not exceed 14.0%. In addition, the plasma should have very low content of heavy metals and bacteria, especially from the group of the *E. coli* and *Salmonella*. Pb concentration limit is 0.3 mg/kg, for Cd – 0.05 mg/kg, Hg – 0.02 mg/kg, As – 0.2 mg/kg) [6–8]. The major protein fractions of the blood fraction are: albumin (approx. 50%), α-globulins (15%), β-globulins (15%) and γ-globulin, which include valuable immunoglobulins (15%) naturally stimulating the functioning of the immune system of animals. Typical composition of plasma proteins is as follows [%]: alanine – 3.8; arginine – 4.2; aspartic acid – 7.1; cysteine – 2.5; glutamic acid – 10.6; glycine – 2.7; histidine – 2.5; isoleucine – 2.6; leucine – 7.0; lysine – 6.1; methionine – 0.6; phenylalanine – 4.1; proline – 11.5; serine 4.2; threonine – 4.3; Tryptophan – 1.2; tyrosine – 3.3; valine – 4.8 [5, 9].

Drying of the animal plasma solution requires specific, properly selected process parameters to maintain its functional and biological values. Too aggressive treatment could in fact harm the quality of the finished product. Thus, the process is carried out by spray drying of plasma solution in a drying chamber through which hot air flows at the same time, causing a rapid evaporation of water droplets (mist), which then turn into powder particles falling to the bottom. Drying under such conditions allows using of high temperatures at a short contact time to minimize protein denaturation and to preserve the biological function of the plasma [10, 11].

Modification of the above-described method is spraying drying using a fluidized bed. In this case, drying is carried out as follows: the plasma solution is sprayed on a bed of small balls made of polycarbonate or dextrose, suspended in a stream of warm air. The balls were coated with a thin film of plasma solution; the applied layer immediately evaporates water. The balls rub against each other's surfaces, causing the abrasion of the applied material and increase in its bulk density. The beads are supported by a wire mesh through which dried powder is poured. Using of this method is preferred for economic reasons [5].

In order to commercial the product – dried porcine plasma, blood collected at slaughter must be subjected to stabilization with anticoagulants to prevent the clotting process, and then separated into plasma and material morphogenesis (blood cells). The resulting solution of plasma is treated further using processes of initial concentration, sterilization, and reduction of the mineral's content and discoloration. The use of all these operations should

ensure compliance with the requirements of the quality parameters of the product and meet the microbiological criteria to guarantee the safety of animal health, food products of animal origin and the environment [12, 13].

In the paper, we discussed the possibilities of application of techniques used in the food industry, for the pretreatment of animal blood plasma to ensure the high quality of the final product. Both the proper treatment of this by-product from the animal's production as well as its recycling and re-use as a feed or food additives is are examples of practical use of cleaner production methods.

2. Initial concentration

Blood plasma is an animal protein aqueous solution (8%) and mineral component (1%). The dry weight is about 9%. Thus, the main component of the plasma forming unwanted ballast in the production of dried plasma is water that must be removed. Its quantity is approx. 91%. Due to the protein denaturation occurring at an elevated temperature with the use of the simplest methods, concentration of the solution by heating and evaporation of water is not possible. Therefore, two leading techniques of initial plasma concentration are usually used: ultra-filtration and evaporation processes carried out under vacuum.

3. Minimization of the bacterial flora in the raw material and centrifugation products

Animal blood and blood products are highly microbiologically sensitive materials and can be easily contaminated. Therefore, both during slaughter and further processing of blood, the highest standards of hygiene must be maintained. However, when the raw material does not meet the microbiological purity, it becomes necessary to use special techniques to reduce microbial growth. The most common methods of sterilization are thermal processes, which, in this case, due to the specific properties of the blood and its derivatives (high temperature sensitivity), are practically not used. It is therefore necessary to use more technologically advanced processes, such as e.g. bactofugation or membrane techniques [14] and radiation [15]. Other proposals include sterilization of a porcine plasma solution using a bactericidal preparation based on nanosilver and dry plasma sterilization by irradiation in an electron accelerator.

Radiation techniques

For the sterilization, ionizing radiation, i.e. gamma radiation (γ), accelerated electrons (e-), and sometimes X-rays, causing the electrically neutral atoms and molecules, changes in electric charges or ionization, are used. Depending on the dose of radiation and the conditions in which this process takes place, inter alia temperature and oxygen, radiation in food preservation technology can be used:

- sterilization of food; large doses from 10 kGy to 50 kGy;
- extension of the storage stability of food products; middle dose, from 1 to 10 kGy;
- increase the stability of certain agricultural products, the prevention of parasitic diseases and food poisoning; small doses to 1 kGy.

Global standards for the use of techniques of radiation for food irradiation are defined by the Food Codex Commission FAO and WHO [15].

Radiation techniques allowing for the preservation of various kinds of food products are mainly used in the United States [16]. In the European Union and in other European countries, legal restrictions and a lack of experience in the application of these techniques mean that they are used to a lesser extent. In the EU, there are two Directives on the use of radiation techniques. The first unifies the law on the use of irradiation in the Member States [17], while the second establishes a positive list of foods that may be irradiated [18]. In the above-mentioned European directives, as foods authorized for treatment with radiation, these only include dried aromatic herbs, spices and vegetable seasonings. The maximum overall average absorbed radiation dose for these products is defined as 10 kGy. In Poland, all issues related to radiation preservation of foods are regulated by the Regulation of the Minister of Health of 15 January 2003. Under this regulation, the country can irradiate: onions, garlic, fresh and dried mushrooms, potatoes, dry spices, dried vegetables and pork plasma.

In addition to the formal and legal conditions, wider application of radiation techniques for sterilization of food is difficult, due to the high costs of preparing such an installation and problems associated with the necessity of cooperation with the specialized agencies of Atomic Energy and the difficulties of disposing spent radioactive element. In addition, in order for the development of such technology to be profitable, sterilization should be subjected to approximately 200–300 t of product per day, which in Polish conditions /rather low production capacity of poultry plants/ is not easy [16].

Tests of powdered plasma sterilization by irradiation with high-energy electrons at a dose of 2 × 10 kGy were conducted on the accelerator Electronics 10/10 at the Institute of Nuclear Chemistry and Technology at the Department of Chemistry and Radiation Technology in Warsaw. Their results confirmed the usefulness of methods for removing bacterial flora from the product, regardless of the size of the batch of exposed material. The material used in the tests was powdered plasma obtained in the experimental installation of Meat Plant Duda-Bis, and it did not meet the microbiological standards. Total number of bacteria exceeded 108, and the content of bacteria *E. Coli* group was at 5×10^3. Plasma sterilization under these conditions resulted in the total removal of the bacterial flora plasma.

The processes of the application importance used for the preservation of food, water sterilization, disinfection of production rooms, apparatus or technical equipment may also include ultraviolet light, ultrasound or microwaves. However, none of these techniques used in the laboratory tests – the irradiation of UV light in the so-called ultrasonic washer and microwave reactor Plazmatronika – gave positive results. On the contrary, in many cases, in the samples, elevated bacterial count was not observed. The time of exposure to radiation of sterilized material was limited by rising temperatures and the possibility of denaturation of proteins. It appears that the used exposure times are insufficient to achieve the desired effects, and the increased temperature favors the development of microflora.

Bactofugation

Bactofugation is the process of separating microbial cells from the liquid by centrifugation. The principle of the process is using the difference in the density of bacterial cells and the liquid itself. The distribution is made on disc drum centrifuges with s special design. Since the density of microbial cells is increased compared to the density of liquid plasma phase, they behave in the spaces between the discs analogously to the behavior of particulate matter in the sedimentation centrifuges. Bacterial concentrate flows toward the outer circumference of the drum, whereas the stream of liquid free of microorganisms is directed to the axis of rotation. The effectiveness of the separation of microbial cells from the stream dosed to the centrifuge plasma depends on the continuous discharge of the concentrate fraction bacterial outside. The increase in cell concentration in the outer part of drum can block the inflow of new particles, which can lead to contamination of the new batch of plasma [14, 19].

Membrane techniques

Membrane techniques [20] allow separating with different sizes of particles on the specially prepared filtration membranes. It is necessary to select such a membrane to separate undesirable substances, while at the same time not reducing the content of the essential components of the medium, thereby changing its physic-chemical properties. Removal of bacteria from liquid products is carried out using microfiltration membranes.

In work [12], the use of membranes TAMI Industries with the separation limits 1.4 μm; 0.45 μm; 0.07 μm; and 300 kD to eliminate the bacterial flora from pig's blood plasma was described in detail. The research results indicate that the target micro-plasma unit should work on the membranes with the separation limit 1.4 μm, enabling to obtain a satisfactory level of bacteria reduction in the raw material. The membrane retains almost the entire bacterial microflora and the filtrate does not indicate the presence of bacteria from group *E. Coli* and is fully permeable to proteins and mineral salts, the component responsible for the quality of plasma. Other membranes have a much greater efficiency of removal of bacteria, but the process of their use is accompanied by significant losses of proteins, increasing with decreasing separation limits of membranes. In the case of a 0.45 μm membrane, these losses are ~20%, while for membranes of 0.07 μm and 300 kD, they are close to 90%.

Bactericidal preparations

The use of bactericidal preparations to reduce the level of microorganisms in pig plasma is determined mainly by their composition. The addition of any substance is not such as to cause changes in the properties of the raw material, or limit its use.

The results of tests available on the market with an innovative formulation containing silver particles with bactericidal, fungicidal and deodorant properties for sterilization porcine plasma are presented below. The chemical composition of the preparation is as follows [%]: silver – 0.2; polyvinyl alcohol – 2.5; water – 97.3. The formulation is a colorless liquid with a slight odor and acid pH range of 6–9. The test were conducted with concentrate containing 2000 mg/L Ag, which, before the introduction into the plasma samples, was diluted with water to a concentration of about 100 mg/L Ag. Nanosilver solution was dispensed into the sterilized samples so as to obtain any suitable concentration of silver ions, and then left for

48 hours in sterile, sealed containers. After this time, microbiological analyzes specifying the total number of bacteria (OLB) and the number of bacteria *E. Coli* group in preparations were carried out. The results are presented in Table 1.

Table 1

Bactericidal effect of formulation obtained on the basis of silver nanoparticles, the level of bacteria in animal blood drawn

Test	Ag content [ppm]	Number of bacteria from the group *E. Coli*	Total number of bacteria
1	0	1×10^6	$> 10^8$
2	2	3×10^5	$> 10^8$
3	5	3×10^5	$> 10^8$
4	10	2×10^2	$> 10^8$
Limit	–	0	$< 1 \cdot 10^4$

The presented results demonstrate the unsuitability of this type of formulation for sterilization. It was observed that with an increase of silver ions, the number of *E. Coli* bacteria in the samples decreases; however, in each case, the standard requirements are not met. There were no positive results for the reduction in the level of total bacteria. Operation of preparations based on silver in the pig plasma sterilization process is not possible most likely due to interaction of silver ions with sulfur compounds contained in the feed and the unsuitable pH for formulation, causing its deactivation.

4. Decrease of mineral substances in the blood

An important role in the blood-collecting is played by its stability made in order to prevent coagulation. The process is realized by dosing a coagulant solution into the blood drawn from the aorta of a slaughtered animal, whose function is:

– decrease of the possibility of rapid development of bacterial flora,
– decrease of the possibility of the occurrence of the process of blood hemolysis,
– elimination of the blood clotting process.

The most commonly used as coagulants are sodium citrate citric acid, a mixture of phosphates (22% Na_2HPO_4, 22% $Na_4P_2O_7$, 16% $Na_2H_2P_2O_7$ and 40% NaCl), aqueous solutions of heparin and oxalate, oxalate, sodium or potassium hydroxide, the disodium salt of ethylene-diamine-tetra-acetic acid, proteolytic enzymes. The addition of most of these formulations in the blood increases the concentration of minerals in the liquid part of plasma blood. To maintain the quality standards of dried plasma, these substances must be removed. Most often, ultrafiltration is used for this purpose [14].

5. Discoloring of blood plasma

Blood pork plasma may contain impurities resulting from the improper treatment of both blood and plasma itself. Due to the improper treatment of blood, its hemolysis is possible. This means that plasma obtained by centrifugation will contain too much the particles of hemoglobin, causing its color to differ in comparison to the market standards. If the contamination of plasma with hemoglobin occurred during the blood fractionation, the selection of process parameters and operating parameters of the centrifugation is significant. They must take into account both the product quality and the process efficiency. From the practical point of view, there is no possibility of a complete separation of the blood. The increase in the yield of plasma results in the penetration of hemoglobin into liquid plasma, causing the deterioration of its color or transparency, and vice versa – decrease of the plasma outflow is associated with the improvement of its quality, but it drastically reduces the quantity of the obtained product. This has negative influence on the economics of the process. Theoretically, it is possible to further purify the obtained plasma in the second, additional centrifuge; however, incurred costs of operation increased the cost of the overall process, making it unprofitable.

The available techniques of plasma discoloring can be divided into two main groups. The first is the mechanical separation of the particles, causing coloration or turbidity of the plasma fraction. These are plasma centrifugation and filtration, including membrane filtration [20, 21]. The second group used the chemical methods [22], changing the characteristics of the particles so as not to affect the quality of the product [23, 24]. The usefulness of all these methods for the discoloration of plasma is described below.

Membrane techniques

Membrane filtration [19] is one of the most common methods for the purification of liquids and it usually helps to seperate fine impurities that are in them. Therefore, it seemed promising to use membrane to discoloration of plasma solutions.

Below are described the results of tests carried out with:

- the microfiltration membranes made by TAMI Industries with 0,14 μm separation limit;
- ceramic membranes of UNIPEKTIN (TiO_2 membrane in a cover made from Al_2O_3) with separation limits of Section 0.1;
- 0.075 and 0,05μm and membrane disc type M37GR40PP, M37FS40PP, M37FSM045PP offering the possibility of the discoloration of plasma and to obtain clear solutions, but at the expense of almost a total loss of the protein, which disqualifies membrane processes for the discoloration plasma.

Filtration

In addition, the application of filtration techniques, using a candle and disc, turns out to be useless. Filtration of raw plasma using them does not bring satisfactory results because the color of the solution does not change. Furthermore, the process complicated by drastically due to reducing of the process flow through the filtration partition, even to its complete stop.

The use of ion exchangers was pointless. Preliminary tests carried out using various types of ion exchange resins available on the market have not given the desired results; the degree of discoloration of the plasma was negligible.

Chemical methods

To reduce the dark characteristic color of hemoglobin, hydrogen peroxide bleaching can be used. Tests carried out with the use of H_2O_2 confirmed the usefulness of this solution for discoloring liquid plasma. Optimization of the process on a laboratory scale allowed to choose process parameters, i.e. temperature, pH and process time. The transfer of the process into a quarter-scale did not cause deterioration of the quality of the obtained solution.

The developed plasma discoloration procedure is as follows: plasma solution (pH 7.5–8.5) is alkalized slowly with a 4M solution of NaOH to obtain pH 13. Next, at the bottom of the reactor, hydrogen peroxide is introduced with concentration of 10% H_2O_2 in the amount of 1 vol. of H_2O_2 solution into 50 vol. of plasma solution. The system is left for 6 hours at 3°C and mixed extemporaneously so as not to cause foaming of the solution. After completion of the plasma, discoloring is made also with 2.5% HCl adjustment of pH to 7.

Comparison of the characteristics of crude and bleached plasma is reported in Table 2. Discolored plasma had a 1.36% lower protein content and 0.87 higher salts content. These results are not satisfactory.

Table 2

Analyses of blood plasma before and after discoloring process (quarter-technique scale)

Raw material	Color	pH	Content [%]		
			protein	water	salts
Raw plasma	Dark pink	6.90	5.97	91.53	0.66
Discolored plasma	Tea color	7.04	4.61	92.64	1.53

6. Summary

Proper treatment of blood, by-product from the animal's production, its processing into high quality of blood plasma, recycling and re-use of dried blood plasma as a feed or food additives, is an example of the practical use of cleaner production methods.

Production of dried pig's blood plasma with quality corresponding to the proper standards requires using (before the drying process) additional operations to improve its quality. In many cases, these are the methods of physical separation, whose task is to eliminate undesirable components of plasma; therefore, they are rarely chemical methods. This pre-treatment may often be used in techniques known and used in the food industry.

Due to the characteristic for proteins, the possibility of their denaturation under the influence of physical (temperature, pressure, ultrasonic) and chemical factors (heavy metal salts, acids, bases, urea, certain organic solvents, detergent) resulting in loss of their biological activities as well as the usefulness of each of the used methods, have to be verified. In the case of developing the techniques already used in other technologies, their procedures require modification and optimization of parameters.

To maintain quality standards of dried plasma, mineral substances must be removed. Most often, ultrafiltration is used for this purpose. Tests carried out with hydrogen peroxide bleaching confirmed the usefulness of this solution for discoloring of liquid plasma. Membrane filtration seemed promising to use membrane to discoloration of plasma solutions.

References

[1] Kowalski Z., Kulczycka J., *Cleaner production as a basic element for the sustainable development strategy*, Polish Journal of Chemical Technology, Vol. 6 (4), 2004, 35–40.

[2] Kowalski Z., Krupa-Żuczek K., *A model of the meat waste management*, Polish Journal of Chemical Technology, Vol. 9 (4), 2007, 91–97.

[3] Ockerman H.W., Hansen C.L., *Animal By-Product Processing & Utilization*, CRC Press LLC, 2000.

[4] Konopka M., Kowalski Z., Fela K., Klamecka A., Cholewa J., *Otrzymywanie plazmy metodą wirowania krwi – charakterystyka procesu*, Czasopismo Techniczne, 1-Ch/2007, 67–74.

[5] Kowalski Z., Makara A., Banach M., *Technologia produkcji plazmy krwi i hemoglobiny*, Chemik, Vol. 65, 2011, 466–475.

[6] PN-64/A-85701 Krew zwierząt rzeźnych i jej pochodne.

[7] PN-83/A-82054 Mięso i przetwory mięsne. Badania bakteriologiczne.

[8] Rozporządzenie Ministra Rolnictwa i Rozwoju Wsi w sprawie wykazu materiałów paszowych pochodzących z tkanek zwierząt, które mogą być stosowane w żywieniu zwierząt gospodarskich z dnia 2003-09-12 (Dz.U. 2003 r. Nr 165, poz. 1605).

[9] Rozporządzenie Ministra Rolnictwa i Rozwoju Wsi w sprawie wymagań weterynaryjnych przy produkcji i dla produktów mięsnych oraz innych produktów pochodzenia zwierzęcego umieszczanych na rynku z dnia 2004-06-29 (Dz.U. 2004 r. Nr 160, poz. 1673).

[10] Borg B.S., Campbell J.M., Russel L.E., Rodríguez C., Ródenas J., *Evaluation of the chemical and biological characteristics of spray-dried plasma protein collected from various locations around the world*, Proc. Am. Assoc. Swine Vet., Vol. 33, 2002, 97–100.

[11] Bosi P., Casini L., Finamore A., Cremokolini C., Merialdi G., Trevisi P., Nobili F., Mengheri E., *Spray-dried plasma improves growth performance and reduces inflammatory status of weaned pigs challenged with enterotoxigenic Escherichia coli K88*, J. Anim. Sci., Vol. 82, 2004, 764–1772.

[12] Silva V.D.M., Silvestre M.P.C., *Functional properties of bovine blood plasma intended for use as a functional ingredient in human food*, LWT – Food Science and Technology, Vol. 36 (7), 2003, 709–718.

[13] DeRouchey J.M., Tokach M.D., Nelssen J.L., Goodband R.D., Dritz S.S., Woodworth J.C., James B.W., Webster M.J., Hastad C.W., *Evaluation of methods to reduce bacteria concentrations in spray-dried animal plasma and its effects on nursery pig performance*, J. Anim. Sci., Vol. 82, 2004, 250–261.

[14] Konopka M., Kowalski Z., Cholewa J., Bajcer T., *Baktofugacja i technika membranowa używana do redukcji poziomu mikroflory w plazmie krwi*, Czasopismo Techniczne, 1-Ch/2007, 59–65.

[15] Codex Alimentarius, Code of practice for radiation processing of food (CAC/RCP 19-1979), (online) homepage: http://www.fao.org/fao-who-codexalimentarius/sh-proxy/en/?lnk=1&url=https%253A%252F%252Fworkspace.fao.org%252Fsites%252Fcodex%252FStandards%252FCAC%2BRCP%2B19-1979%252FCXP_019e.pdf

[16] Schmidt C.F., Nank W.K., Lechovich R.V., *Radiation Sterilization of Food*, Food Science, Vol. 27 (1), 1962, 77–84.

[17] Dyrektywa Unii Europejskiej, Directive 1999/2/EC.

[18] Dyrektywa Unii Europejskiej, Directive 1999/3/EC.

[19] Zander L., Zander Z., *Baktofugacja*, UWM Olsztyn, 2004, (online) homepage: http://www.uwm. edu.pl /kiap/dydaktyka/Baktofugacja.pdf

[20] Narębska A., *Membrany i membranowe techniki rozdziału*, Wydawnictwo UMK, Toruń 1997.

[21] Jankowska P., Lenik E., *Zatężanie i odbarwianie plazmy na drodze ultrafiltracji*, Materiały Firmy Duda-Bis. Sosnowiec, Luty 2006 (praca niepublikowana).

[22] Moure F., Rendueles M., Diaz M., *Coupling process for plasma protein fractionation using ethanol precipitation and ion exchange chromatography*, Meat Science, Vol. 64, 2003, 391–398.

[23] Bidwell E., *The Purification of Antihaemophilic Globulin from Animal Plasma*, British Journal of Hematology, Vol. 1 (4), 1955, 386–389.

[24] Chang-Kee Hyun, Heuyn-Kil Shin, *Utilization of bovine blood plasma proteins for the production of angiotensin I converting enzyme inhibitory peptides*, Process Biochemistry, Vol. 36 (1–2), 2000, 65–71.

TECHNICAL TRANSACTIONS | CZASOPISMO TECHNICZNE
ENVIRONMENT ENGINEERING | ŚRODOWISKO
1-Ś/2016
DOI: 10.4467/2353737XCT.16.198.5947

ANNA MŁYŃSKA, MICHAŁ ZIELINA*

EXPERIMENTAL RESEARCH ON THE IMPACT OF DIFFERENT HARDNESS WATERS ON THEIR CONTAMINATION BY PROTECTIVE CEMENT MORTAR LININGS AFTER PIPE RENOVATION

BADANIA EKSPERYMENTALNE WPŁYWU WÓD O ODMIENNEJ TWARDOŚCI NA ICH ZANIECZYSZCZANIE PRZEZ OCHRONNE WYKŁADZINY CEMENTOWE PO RENOWACJI PRZEWODÓW

Abstract

The paper presents laboratory experiments on the influence of different hardness water samples collected from the municipal water supply system on the intensification of leaching pollutants from the internal cement mortar pipe lining to drinking water. The paper presents the analysis of water quality indices, such as pH, aluminum and selected heavy metals concentrations after contacting with cement coatings.

Keywords: water hardness, renovation, cement mortar lining, water pipes

Streszczenie

W artykule przestawiono wyniki badań laboratoryjnych opisujących wpływ wód pobranych z miejskiej sieci wodociągowej, charakteryzujących się odmiennymi twardościami, na stopień przenikania do nich zanieczyszczeń z wewnętrznych powłok cementowych. Niniejsze opracowanie obejmuje analizę wskaźników jakości wody, takich jak pH, stężenie glinu oraz stężenie wybranych metali ciężkich na skutek jej kontaktu z powłokami cementowymi.

Słowa kluczowe: twardość wody, renowacja, wykładzina cementowa, przewody wodociągowe

* M.Sc. Eng. Anna Młyńska, Assoc. Prof. D.Sc. Eng. Michał Zielina, Institute of Water Supply and Environmental Protection, Faculty of Environmental Engineering, Cracow University of Technology.

1. Introduction

Corrosion of old iron or steel pipes in distribution systems contributes to many different problems. Corrosion products accumulated on the inner surface of water pipelines cause the reduction of the hydraulic capacity, increase of water flow resistance and thus, increase of water supply system operation costs. Additionally, corrosion products have a negative impact on the potable water quality. Deterioration of the water quality is mainly related to leaching of iron compounds from corroded metal pipes to the water. As a consequence, the color of the water becomes red and brown and the water turbidity increases. The corroded pipes influence the consumption of dissolved disinfectants, dissolved oxygen and intensive microbiological growth [1–4].

In order to protect the inner surface of water pipes against corrosion, many different methods are used, among which are trenchless technologies. The most commonly used trenchless method is cement coating by spraying, which was invented in 1930 [5, 6]. In opposite to other techniques, cement mortar lining protects pipes against corrosion not only by a mechanical separation of metal pipe from the water, but also by chemical protection. Cement mortar creates a high-alkaline environment, which strongly reduces corrosion process [7].

Considering the fact that the natural cements consist of many different components, mainly calcium, silicon, aluminum, iron, magnesium, sulfur, sodium, potassium compounds and also particularly dangerous trace chemical elements, such as arsenic, cadmium, chromium, lead, copper, nickel or zinc [8, 9], it is very important to analyze the impact of cement mortar lining on the water quality. Numerous performed studies show that, in a short period after applying cement coatings, the deterioration of some water quality parameters can be observed, especially an increase in water pH values and alkalinity [10–13] and also the growth of some chemical elements concentrations, mainly aluminum, calcium and chromium [10, 13, 14]. The level of water contamination by cement coating soon after renovation depends on the type of used cement [14, 15] and also on the quality of transported water. The hardness of water contacting with cement coating seems to be an important parameter for leaching of pollutants from the cement mortar. In comparison to the hard waters, soft waters are characterized by a low carbonate and bicarbonate content, and thus, soft waters are aggressive to calcium hydroxide, the main cement mortar component, which is visibly leached out from fresh cement mortar lining. Aggressive soft waters can also attack calcium silicate, which leads to the formation of silica gels and thus, to the reduction of the mechanical strength of cement coating. As a result of leaching out calcium from cement mortar lining, the value of pH cement coating decreases, water pH increases and the danger of leaching out the toxic metals from protective cement coating to water is greater [16, 17].

Given the above, it seemed to be important to analyze the influence of water hardness on polluting the water transported in distribution system by fresh protective inner cement coating. Two kinds of water samples, characterized by relatively high and relatively low hardness, were collected from outflows of two different Cracow water treatment plants for laboratory tests. The experiments were conducted under static conditions, using two test stands constructed for the purpose of this research. Numerous water quality parameters were tested during the experiments. However, only some of them, such as pH, aluminum, chromium, lead and cadmium concentrations, are analyzed in this paper. The results indicate which types of water are more exposed to contamination by leaching out the pollutants from cement mortar coating and show importance of water hardness parameter for process intensification.

2. Material and methods

Two identical test stands presented in Figure 1 were used in the experiments. The main element of both test stands was a steel pipe with internal cement mortar coating (Fig. 2).

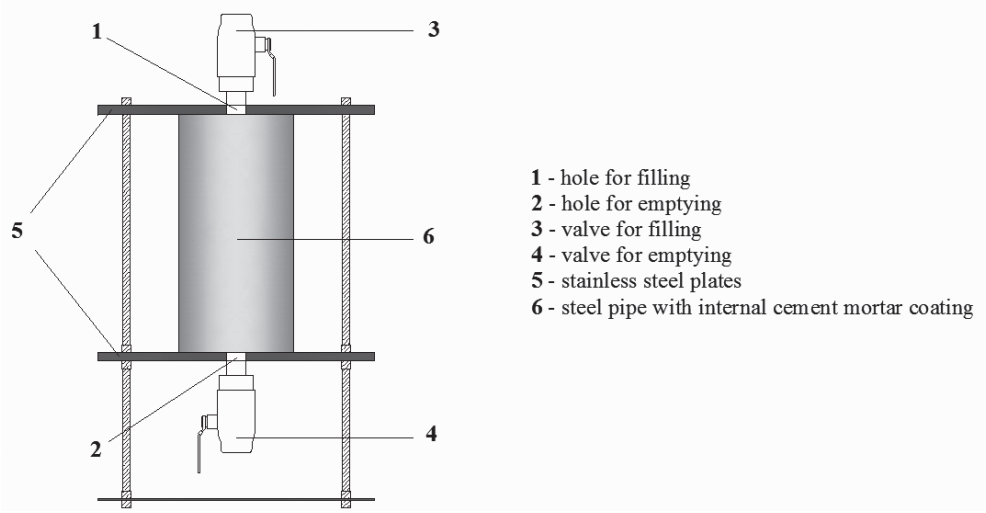

Fig. 1. The scheme of test stand for static research (Source: own elaboration)

Fig. 2. Steel pipes with internal cement coating (Source: author's photo)

The length of water pipes with the nominal diameter of 80 mm was 25.0 cm. The thickness of cement mortar coating was 0.7 cm and was made by mixing Portland Cement 42.5R manufactured by CEMEX with quartz sand in a ratio of 1 to 1 and with water, maintaining 0.35 water-cement ratio. Cement mortar lining process was made manually with 24 hours cure time. After this time, pipes interiors were filled with water samples collected from

outflow of two different Cracow water treatment plants. The first one was filled with hard water (293.0 mg $CaCO_3/dm^3$) and the second one was filled with soft water (130.0 mg $CaCO_3/dm^3$). Both water samples remained in contact with cement coatings for the same periods of time, which were determined based on the Dutch Standard (EA NEN 7375:2004) [18] and Polish Standard (PN-EN 14944-3:2008) [19]. Water samples contacting with cement mortar were replaced by raw water after the following periods: 0.25, 1, 2.25, 5, 6, 9, 13, 16, 33, 36, 52 and 56 days. All replaced water samples were collected and tested. Water quality indices like pH, alkalinity, aluminum, chromium, calcium, cadmium and lead concentrations were tested for samples collected during experiments. According to the Dutch Standard EA NEN 7375:2004 [18] and based on experimental measurements, the cumulative leaching aluminum and chromium from cement mortar lining to water was counted and presented in this paper.

3. Results

Figure 3 presents pH changes of both collected raw water samples contacting with cement mortar linings. The pH of both (soft and hard) raw water samples before contacting with cement mortar linings has reached 7.7. Soon after the contact of both water samples with cement mortar linings, the significant increase of pH was observed. The pH has reached 11.7 in both cases, exceeding maximum allowable value for drinking water, determined by the Polish Ministry of Health Regulation (pH = 6.5-9.5) [20] and also by U.S. EPA Secondary Drinking Water Standards (pH = 6.5-8.5) [21]. It was probably caused by intensive leaching of calcium alkali from cement mortar to water. For the first 13 days of contacting time, pH of both kinds of water samples was slightly rising up, reaching similar values, but not exceeding 12. After this time, a rapid decrease of hard water pH was observed, whereas pH of soft water was still kept at around 12. The decrease of hard water was still continued and reached 8.3 value after about 60 days of contact time, whereas decrees of pH of soft water was noticed after 36 days, finally reaching 10.3 after about 60 days of contact time. This research clearly shows that soft waters are more exposed to the maintaining a high level of pH values for a longer period of time than hard waters.

Figure 4 shows the increase of cumulative leaching aluminum for hard and soft waters contacting with cement mortar lining. The amounts of leached aluminum to both: hard and soft waters were initially almost the same. However, over time, the amount of leached aluminum for soft water was larger than for hard water. After the third day of the experiment, the difference between leaching of aluminum to soft and hard waters started to increase. After 52 days of contact time, leaching of aluminum to both types of tested waters almost stopped. Summarizing the above, for very short period after renovation it is expected to observe a similar leaching of aluminum independently on water hardness. However, leaching of aluminum from the cement mortar contacting with hard water decreases much quicker over time than contacting with a soft water.

In turn, as it was expected, the analysis of chromium concentration for tested waters shows that the amounts of leached chromium from cement mortar lining to both: hard and soft waters were much smaller than amounts of leached aluminum (Fig. 5). Initially, soon

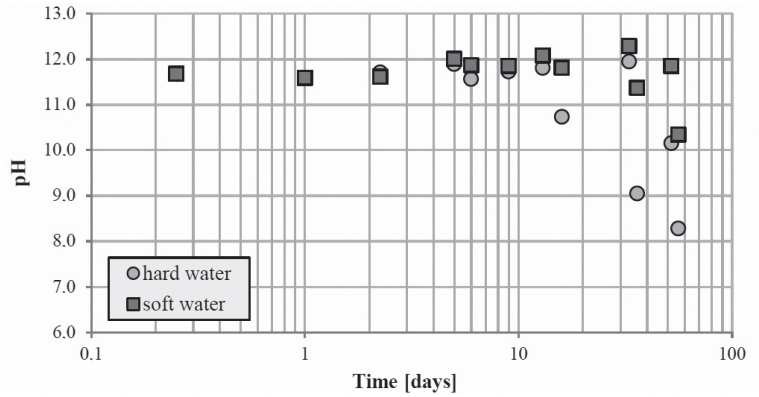

Fig. 3. Noted pH values of hard water and soft water in contact with cement mortar lining (Source: own elaboration)

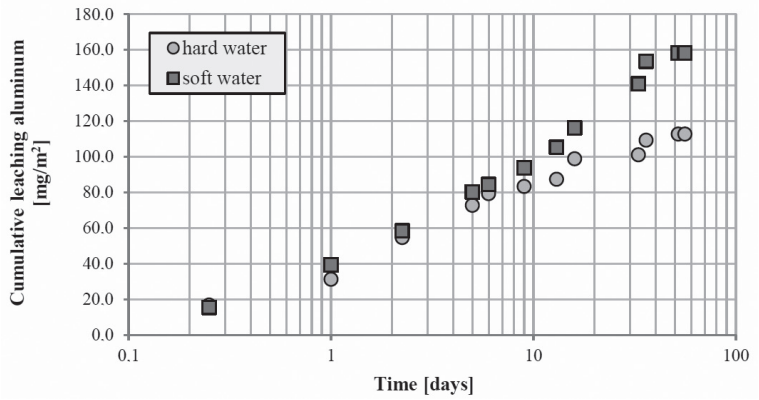

Fig. 4. Cumulative leaching aluminum from cement mortar lining to hard water and soft water (Source: own elaboration)

after lining, leaching of chromium from cement mortar to soft water was a few times higher than to hard water. However, over time, intensification of chromium leaching to soft water became quite similar to the leaching intensification of chromium to hard water. After 33 days of the study, it was noted that leaching of chromium to the hard water almost stopped. In the case of soft water, leaching process after 52 days was ceased.

Based on the obtained results concerning to the leaching aluminum and chromium from cement mortar lining to the water, it can be concluded that generally soft water in comparison to hard water is more exposed to the pollution by these chemical elements.

In the conducted experimental research, the measurements of the concentration of heavy metals, which are particularly harmful for drinking water quality, such as lead and cadmium, were also performed. The obtained research results indicate that there is no risk of water contamination caused by the leaching these toxic metals from cement mortar lining to both

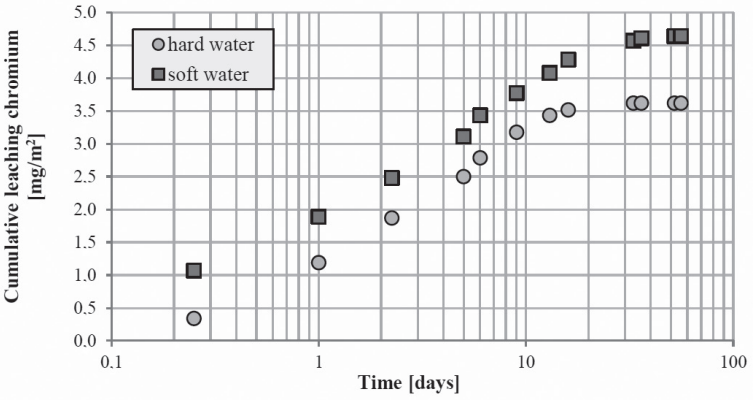

Fig. 5. Cumulative leaching chromium from cement mortar lining to hard water and soft water (Source: own elaboration)

tested waters. In all collected water samples, noted concentration of lead and cadmium was below detection. Lead concentration in all water samples was less than 0.002 mg/dm^3 (limitation value in drinking water regulated by [20] and [21] is 0.010 mg/dm^3) and cadmium concentration in all water samples was less than 0.00045 mg/dm^3 (limitation value for drinking water regulated by [20] and [21] is 0.005 mg/dm^3).

4. Conclusions

Cement mortar lining belongs to the widely used trenchless pipe rehabilitation technologies. This technique provides highly effective protection against corrosion, improves a technical conditions of the pipelines and their hydraulic parameters and also prevents against the secondary pollutants. Since cement includes many different compounds, controlling potential leaching of pollutants from fresh cement mortar to drinking water in short period after cementing is important.

The obtained research results indicate the influence of different hardness waters on pollutant leaching from fresh cement coatings. For both soft and hard waters, a significant increase of pH was observed. pH raised up to about 11.7. However, high pH values were maintained longer in the case of soft water than in the case of hard water.

Intensification of aluminum leaching from cement mortar contacting with both kinds of waters initially, soon after coating was very similar. However, in the case of soft water, a fairly high intensification was maintained much longer than in the case of hard water.

Intensification of chromium leaching was initially, soon after lining, a few times higher for soft water than for hard water. However, during the rest of the experiment, the intensification of chromium leaching was almost the same for both kinds of waters and decreased over time.

The conducted experimental research also showed that the risk of water contamination by lead or cadmium leached from cement mortar is negligible.

The experimental research confirmed that the water quality transported through water pipes within a short period after renovation by cement coating influences the degree of water contamination. It can be supposed that generally water pipelines transported soft water are more exposed to the contamination by leaching cement mortar compounds than hard water, especially aluminum and calcium ions. Thus, the probability of deterioration water quality delivered to the consumers and also the reduction of mechanical strength of protective coating as a consequence of leaching of its compounds is greater.

References

[1] McNeill L.S., Edwards M., *Iron pipe corrosion in distribution systems*, Journal AWWA, 93 (7), 2001, 88–100.

[2] Sarin P., Snoeyink V.L., Bebee J., Jim K.K., Beckett M.A., Kriven W.M., Clement J.A., *Iron release from corroded iron pipes in drinking water distribution systems: effect of dissolved oxygen*, Water Research, 38 (5), 2004, 1259–1269.

[3] Beimeng Q.I., Chongwei C., Yixing Y., *Effects of iron bacteria on cast iron pipe corrosion and water quality in water distribution systems*, International Journal of Electrochemical Science, 10, 2015, 545–558.

[4] Slavíčková K., Grünwald A., Šťastný B., *Monitoring of the corrosion of pipes used for drinking water treatment and supply*, Civil Engineering and Architecture, 1 (3), 2013, 61–65.

[5] Deb A., Hasit Y.J., Schoser H.M., Snyder J.K., Loganathan G.V., Khambhammettu P., *Decision support system for distribution system piping renewal*, AwwaRF and AWWA, 2002.

[6] Damodaran N., Pratt J., Cromwell J., Lazo J., David E., Raucher R., Herrick Ch., Rambo E., Deb A., Snyder J., *Customer acceptance of water main structural reliability*, AwwaRF, 2005.

[7] Kirmeyer G.J., Friedman M., Clement J., Sandvig A., Noran P.F., Martel K.D., Smith D., LeChevallier M., Volk Ch., Antoun E., Hiltebrand D., Dyksen J., Cushing R., *Guidance manual for maintaining distribution system water quality*, AwwaRF and AWWA, 2000.

[8] Bye G.C., *Portland cement: Composition, production and properties*, Thomas Telford Publishing, London 1999.

[9] Le Corre N., *Analysis of the major elements in cement by ICP*, Materiały firmy Jobin Yvon.

[10] Deb A., McCammon S.B., Snyder J., Dietrich A., *Impacts of lining materials on water quality*, Water Research Foundation, Denver 2010.

[11] Donaldson B.M., Whelton A.J., *Water quality implications of culvert repair options: cementitious and polyurea spray-on liners*, Virginia Center for Transportation Innovation and Research, Final Report, Virginia 2012.

[12] Whelton A.J., Salehi M., Tabor M., Donaldson B., Estaba J., *Impact of infrastructure coating materials on storm–water quality: Review and experimental study*, Journal of Environmental Engineering, Vol. 139, No. 5, 2013, 746–756.

[13] Clark D.D., *Water quality, aesthetic and corrosion inhibitor implications of newly installed cement mortar lining used to rehabilitate drinking water pipelines,* Master's Thesis, Virginia Polytechnic Institute and State University, Blacksburg 2009.
[14] Zielina M., Dąbrowski W., Radziszewska-Zielina E., *Cement mortar lining as a potential source of water contamination*, World Academy of Science, Engineering and Technology, Vol. 8, No. 10, 2014, 636–639.
[15] Meland I.S., *Durability of mortar linings in ductile iron pipes*, 8th International Conference on Durability of Building Materials and Components, Vancouver 1999.
[16] Bonds R.W., *Cement-mortar linings for ductile iron pipe*, Ductile Iron Pipe Research Association (DIPRA), report DIP-CML/3-05/3,5M, Alabama, USA 2005.
[17] Hall S.C., *Corrosion protection provided by mortar lining in large diameter water pipelines after many years of service*, Pipelines 2013, 100–112.
[18] EA NEN 7375:2004, Leaching characteristics of moulded or monolithic building and waste materials/Determination of leaching of inorganic components with the diffusion test – "The tank test", Netherlands Normalisation Institute Standard, April 2005.
[19] PN-EN 14944-3:2008, Wpływ wyrobów cementowych na wodę przeznaczoną do spożycia przez ludzi – Metody badań – Część 3: Migracja substancji z produkowanych fabrycznie wyrobów cementowych, Luty 2008.
[20] Rozporządzenie Ministra Zdrowia z dnia 29 marca 2007 roku w sprawie jakości wody przeznaczonej do spożycia przez ludzi (Dz.U. 2007, nr 61 poz. 417).
[21] United States Environmental Protection Agency (U.S. EPA), Secondary drinking water standards.

TECHNICAL TRANSACTIONS | CZASOPISMO TECHNICZNE
ENVIRONMENT ENGINEERING | ŚRODOWISKO
1-Ś/2016
DOI: 10.4467/2353737XCT.16.199.5948

JAROSŁAW MÜLLER*

ENERGY EFFICIENCY IMPROVEMENT OF THE REFRIGERATION CYCLE USING AN INTERNAL HEAT EXCHANGER

POPRAWA EFEKTYWNOŚCI ENERGETYCZNEJ OBIEGU ZIĘBNICZEGO POPRZEZ ZASTOSOWANIE DOZIĘBIACZA

Abstract

A refrigeration cycle modified using an Internal Heat Exchanger is presented. For different refrigerants, the net effect of using an IHX is either positive or negative due to refrigerant properties and working conditions. Wet refrigerant vapor at the inlet of IHX improves the cycle in various aspects. The evaporator performance is much better when not superheating the vapor. A "pure" effect of subcooling the refrigerant liquid at the inlet of the expansion valve results in an increased specific heat of evaporation. For zeotropic mixtures, increased subcooling results in lowering the evaporating temperature without lowering the pressure in the evaporator. The EER value can be improved for some refrigerants and for specific working conditions. Theoretical and experimental evaluations of this concept are presented. Commonly used refrigerants were evaluated theoretically and tested in a 10 kW (cooling capacity) test rig. R22 and R407C were analyzed.

Keywords: efficiency, refrigeration cycle, internal heat exchanger, refrigerant mixtures

Streszczenie

W artykule przedstawiono obieg ziębniczy zmodyfikowany przez dodanie doziębiacza. Efekt końcowy zastosowania doziębiacza jest różny w zależności od użytych ziębników oraz warunków pracy. Wprowadzenie pary mokrej do doziębiacza skutkuje wieloma pozytywnymi efektami. Praca parowacza jest efektywniejsza, jeżeli nie służy on do przegrzewania pary ziębnika, doziębienie cieczy przed zaworem rozprężnym skutkuje zwiększeniem właściwego ciepła parowania. Dla mieszanin zeotropowych obserwuje się obniżenie temperatury parowania bez obniżania ciśnienia parowania. Zwiększenie wartości wskaźnika EER może być uzyskane przez odpowiedni dobór ziębników oraz parametrów pracy obiegu. Przedstawiono również wyniki badań eksperymentalnych dla powszechnie używanych ziębników na stanowisku o wydajności ziębniczej 10 kW.

Słowa kluczowe: twardość wody, renowacja, wykładzina cementowa, przewody wodociągowe

* Ph.D. Eng. Jarosław Muller, Faculty of Environmental Engineering, Cracov University of Technology.

Nomenclature

c_p – specific heat capacity at constant pressure [kJ/kgK]
c_v – specific heat capacity at constant volume [kJ/kgK]
EER – Energy Efficiency of Refrigeration
h_{rp} – specific heat of evaporation [kJ/kg]
q_o – specific enthalpy of evaporation [kJ/kg]
U – heat transfer coefficient [W/m^{2}K]
l_t – specific compressor work [kJ/kg]
m – mass flow rate [kg/s]
p – pressure [MPa]
P – power [kW]
t – temperature [°C]
T – temperature [K]
κ – isentropic coefficient = cp/cv
υ – specific volume
x – vapor quality

Subscripts
k – condenser
o – evaporator
c – liquid
p – vapor
av – average
co – subcooling

1. Introduction

In literature, many authors presented the application of Internal Heat Exchanger as a way of improving the efficiency of refrigeration systems. Kruse [1] suggests the use of IHX in domestic refrigerators using flammable refrigerants, and an extensive set of refrigerants was discussed by Domanski et al. [2]. Angelino and Invernizzi [3] make a theoretical assessment of organic refrigerants. They define the "molecular complexity factor" dependent on the vapor specific heat capacity and prove that, for fluids with complex molecular particles, IHX may be necessary to obtain proper energy efficiency of the heat pump. McLinden [4] presents an analysis of refrigerating cycles with IHX using a semi-theoretical model and concludes that fluids with high vapor heat capacity may achieve high efficiency. Domanski et al. [5] presents a simulation of pure refrigerants in cycles with an IHX, and Jung et al. [6] give a theoretical analysis of pure refrigerants with an IHX suggesting that some of the fluids can be used as mixture components. Huelle [7] presents an analysis of the IHX impact on the energy demand for refrigeration machinery, and Vakil [8] presents a general analysis of applying fluid subcooling by vapor superheating for pure and mixed zeotropic refrigerants. Lavrenchenko et al. [9] compare refrigerant cycles with mixtures. Cycles that are modified by subcooling

in the condenser, superheating in the evaporator, IHX with wet and superheated vapor and energy efficiencies, are compared. Klein et al. [10] perform a theoretical analysis of IHX for new refrigerants and investigate the pressure drop impact on the exchanger performance.

In every application, a big disadvantage is noted: the excessive superheating of the vapor entering the compressor that leads to extra compressor work and reduces energy efficiency. The reason is that isentropes, which represent the compression process, increase the slope with superheating of the vapor.

2. Internal heat exchanger

In a typical refrigerating cycle consisting of four basic elements (evaporator, compressor, condenser and expansion valve – Fig. 1a), one of the disadvantages is the isenthalpic expansion process during which the refrigerant partially evaporates (3–4). Thus, the phase-change process in the evaporator suffers due to increased vapor quality at the evaporator inlet. Increased refrigerant subcooling at the condenser outlet "moves" state (4) of the refrigerant to the left (4′) – Fig. 2, increasing the specific heat of evaporation. Refrigerant subcooling is also very important for the proper operation of some of the refrigerating or air-conditioning machinery. In some installations, the refrigerant flows from the condenser to an expansion valve over a long distance, which can cause partial evaporation due to the pressure drop when the refrigerant leaves the condenser in a saturated state.

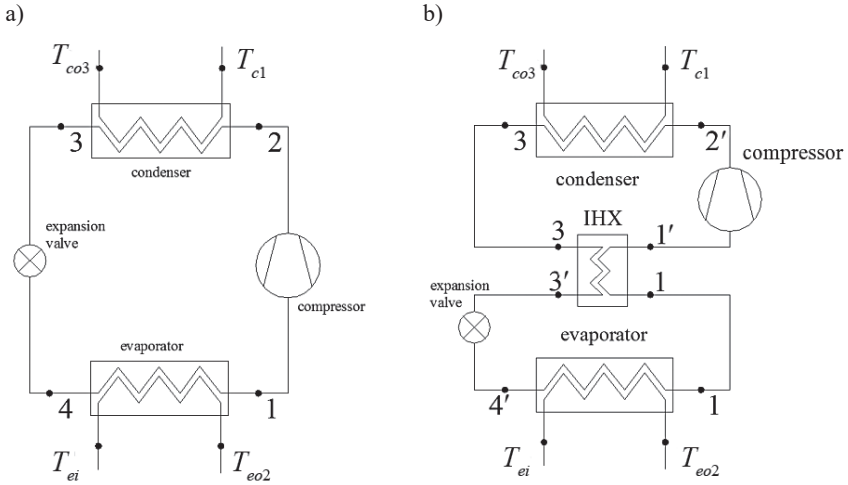

Fig. 1. Refrigerant cycle: a) without an IHX, b) with an IHX

There are several ways to obtain liquid subcooling. Some of them are: increasing the heat exchange area of condenser, increasing condensing pressure, additional external heat exchangers, mechanical subcooling (refrigeration cycle with evaporator-subcooler heat exchanger) etc.

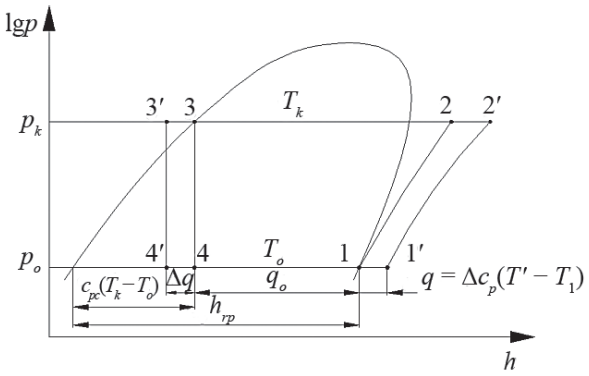

Fig. 2. Refrigerant state points and values used in calculations (Domanski et al. [2])

One of the solutions to the problem is a very the well-known internal heat exchanger (IHX), which subcools liquid refrigerant using cold vapor at the outlet of the evaporator (Fig. 1b). The heat transferred from liquid to the vapor causes superheating of the vapor entering the compressor and prevents the refrigerant liquid droplets from entering the compressor. Extensive vapor superheating is one of the great disadvantages of such a solution. For almost every refrigerant, compressor work increases with increased vapor superheat at the entrance to the compressor. This is caused by the slope of isentropes, which increases with the vapor superheating. Energy efficiency of the cycle, calculated as:

$$\mathrm{EER} = \frac{q_o}{l_t} \tag{1}$$

can increase or decrease, depending on the refrigerant used in the cycle. The heat exchange in the IHX reduces the irreversibility in the expansion process. Energy efficiency will increase only when the proportional increase of specific latent heat in the evaporator is larger than the corresponding specific work increase of the compressor:

$$\frac{\Delta q}{q_o} > \frac{\Delta l_t}{l_t} \tag{2}$$

Domanski et al. [2] compared the performance of cycles with and without the IHX using the same corresponding saturation temperatures in the evaporator and the condenser:

$$\mathrm{EER}' = \frac{q_o + \Delta q}{l_t + \Delta l_t} = \mathrm{EER}\,\frac{1 + \Delta q / q_o}{1 + \Delta l_t / l_t} \approx \mathrm{EER}\left(1 + \frac{\Delta q}{q_o} - \frac{\Delta l_t}{l_t}\right) \tag{3}$$

The formula in brackets must be larger than 1 if the system is to benefit from using the IHX. For obvious reasons, $\Delta q/q_o$ is always greater than 0 and $\Delta l_t/l_t$ is also positive. After some simplification, the specific enthalpy increase in the evaporator can be described as:

$$q_o = h_{rp} - \overline{c}_{p,c}(t_k - t_o)$$

where:

$$\overline{c}_{p,c} = \frac{1}{t_k - t_o}\int_{t_o}^{t_k} c_{p,c}\,dt$$

Enthalpy change in the evaporator Δq is equal to the amount of heat exchanged between high-pressure liquid and low pressure vapor:

$$\Delta q = \overline{c}_{p,p}(t_{1'} - t_1) \tag{4}$$

where:

$$\overline{c}_{p,p} = \frac{1}{t_{1'} - t_1}\int_{t_1}^{t_{1'}} c_{p,p}\,dt \tag{5}$$

Compressor specific work can be described by an equation of isentropic work of the ideal gas at constant heat capacity:

$$l_t = \frac{\kappa}{\kappa - 1} P_1 \upsilon_1 \left[1 - \left(\frac{P_2}{P_1}\right)^{\frac{\kappa-1}{\kappa}}\right] \tag{6}$$

and

$$l_t' = \frac{\kappa}{\kappa - 1} P_1 \upsilon_{1'} \left[1 - \left(\frac{P_2}{P_1}\right)^{\frac{\kappa-1}{\kappa}}\right] \tag{7}$$

From the above equations, one can derive:

$$\begin{aligned}\frac{\mathrm{EER}'}{\mathrm{EER}} &= \frac{1 + [\overline{c}_{p,p}(t_{1'} - t_1)]/[h_{r,p} - \overline{c}_{p,c}(t_k - t_o)]}{1 + (\upsilon_{1'} - \upsilon_1)/\upsilon_1} = \\ &= \frac{1 + (t_{1'} - t_1)/[h_{r,p}/\overline{c}_{p,p} - (t_k - t_o)\overline{c}_{p,c}/\overline{c}_{p,p}]}{1 + B_p(t_{1'} - t_1)}\end{aligned} \tag{8}$$

The above ratio will be greater than 1 when:

$$\frac{1}{h_{r,p} / \overline{c}_{p,p} - (t_k - t_o)\overline{c}_{p,c} / \overline{c}_{p,p}} > B_p \tag{9}$$

where:

$$B_p = \frac{\upsilon_{1'} - \upsilon_1}{\upsilon_1 (t_{1'} - t_1)} \tag{10}$$

is the average coefficient of thermal expansion (Domanski et al. [2]) Equation (9) shows that EER improvement will occur only if

h_(r, p)/c¯_(p, p) and B decrease and (t_k-t_o) c¯_(p, c)/c¯_(p, p) increases

The ratio between vapor and liquid heat capacity plays a significant role when there are large temperature differences between evaporation and condensation. Equations (9) and (10) can be presented in a form of function:

$$F(t_o, t_k, t_{1'} p_o(t_o)) = \frac{1}{\dfrac{h_p(p_o)}{\overline{c}_{pp}(t_o, t_{1'})} - (t_k - t_o) \cdot \dfrac{\overline{c}_{pc}(t_k, t_o)}{\overline{c}_{pp}(t_o, t_{1'})}} - \frac{\upsilon_{1'}(t_o, t_{1'}) - \upsilon_1(t_o)}{\upsilon_1(t_o) \cdot (t_{1'} - t_o)} > 0 \tag{11}$$

The calculations were made using Refprop (Gallager et al. [11])

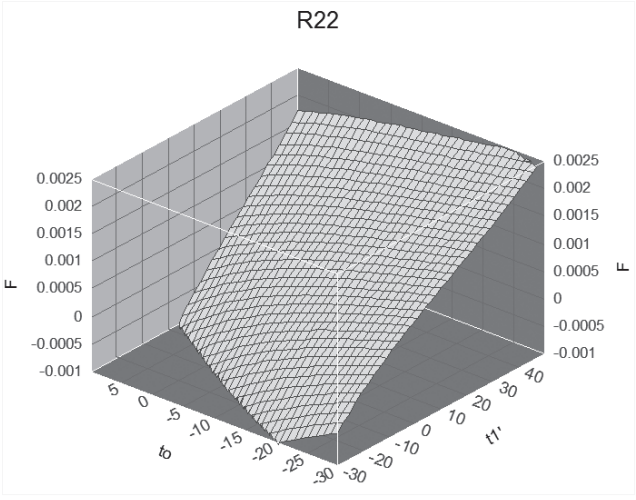

Fig. 3. Function $F(t_o, t_{1'})$ values for R22

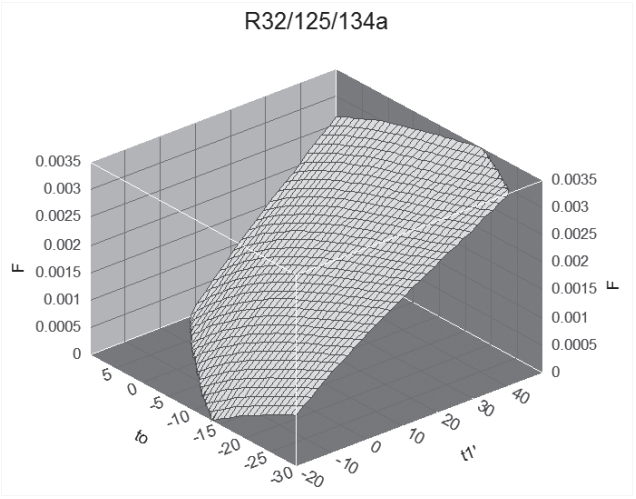

Fig. 4. Function $F(t_o, t_{1'})$ values for R407C

Figures 3 and 4 present the values of function $F(t_o, t_{1'})$ for two refrigerants. The refrigerants selected for tests were evaluated theoretically and experimentally, and presented by Maczek et al. [12, 13].

As one can notice, the value of function F for the mixture is greater than "0", which means that for such conditions of evaporation temperature to and superheating temperature $t_{1'}$ using the IHX is of interest.

3. Wet vapor entering IHX

As mentioned above, the use of the IHX has one disadvantage: excessive superheating of the vapor entering the compressor. If we analyze wet vapor entering the IHX (point 1 in Fig. 2 moved to the left) and saturated vapor entering the compressor (point 1′ on Fig. 2 on the saturated line), we obtain different situation with all advantages of the IHX without superheating of the vapor.

For zeotropic mixtures (Fig. 5), the process of subcooling the liquid using wet vapor in the IHX causes several differences in comparison to the cycle with no IHX and with the IHX using superheated vapor.

The evaporation process is shifted to the left from 4-1 to 4′-1′, where lower temperatures of the evaporator inlet can be noted. Obtaining lower temperatures for pure refrigerants can be achieved only by lowering the evaporating pressure, which is always energy inefficient. Fig. 6 shows the calculation results of the IHX impact on the average evaporation temperature for different evaporation pressures for R407C.

Experimental data show a slight improvement of the energy efficiency of the refrigeration cycle. The change of the cycle was obtained by moving the remote sensor bulb of the

thermostatic expansion valve (which is usually set for slight superheating of the vapor) onto the pipe downstream the IHX.

Fig. 7 Shows some of the results of the test for evaporation temperature p_o = 0.58 MPa with wet vapor at the IHX inlet.

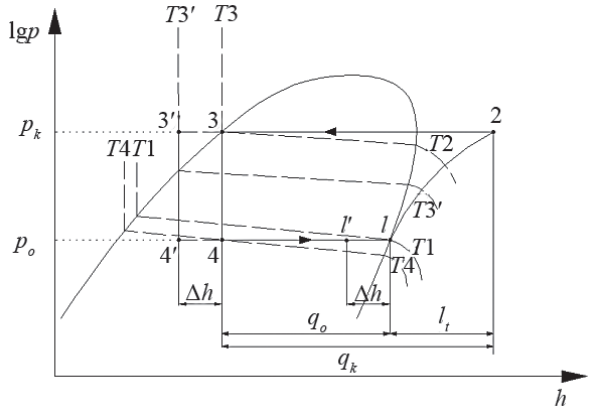

Fig. 5. Refrigerant cycle for zeotropic mixtures with IHX

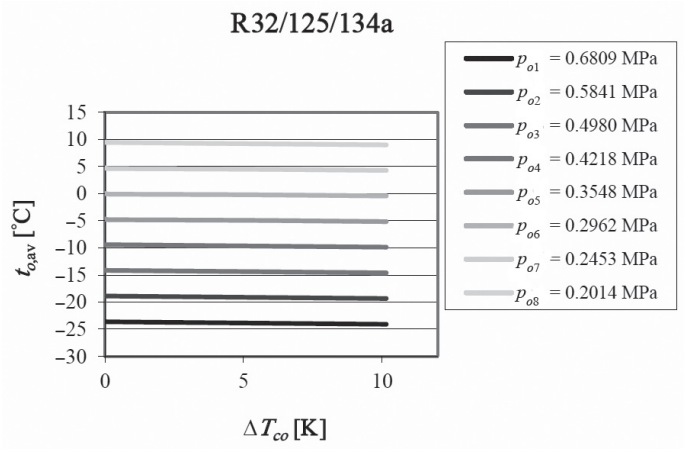

Fig. 6. Average evaporation temperature as a function of refrigerant subcooling at the IHX exit ($p_{o1} \div p_{o8}$ – evaporation pressure)

Also, a relative change of EERrel [%] was calculated from the experimental data as:

$$EER_{rel} = 100 \cdot (EER' - EER)/EER$$

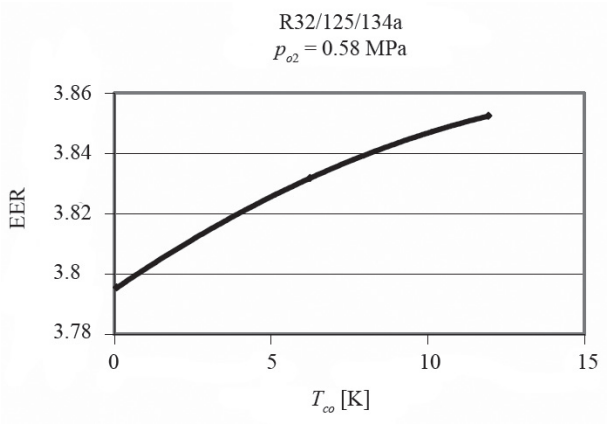

Fig. 7. Energy efficiency as a function of refrigerant subcooling at the IHX exit

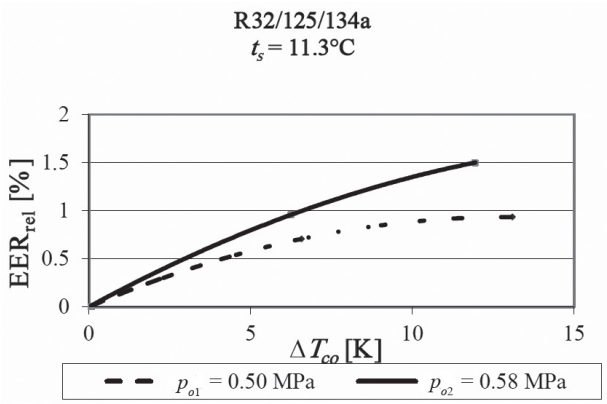

Fig. 8. Relative EER change as a function of refrigerant subcooling at the IHX exit for the same compressor suction temperature t_s = 11.3°C

4. Conclusions

The internal heat exchanger can be effectively applied in the refrigerant cycle using zeotropic refrigerant mixtures. The calculations made for R22 and R407C show that IHX is always improving the EER for the cycle with the refrigerant mixture, while there is no improvement in EER in the cycle using R22 with the low evaporation temperature. The experimental tests show a slight EER improvement for R407C with the use of wet vapor in the IHX.

Moreover, the performance of the evaporator is better when there is no superheating of the vapor. The end part of the heat exchange area can be more effectively used. A slightly superheated vapor at the inlet of the compressor is accepted, otherwise a too high discharge temperature is observed, together with an increase of the specific work of the compressor. The positive effect of refrigerant subcooling at the inlet of the expansion valve is the increased specific heat of the evaporation. Subcooling the liquid leaving the condenser results in lowering the average evaporating temperature without lowering the pressure in the evaporator – for zeotropic mixtures with temperature glide during the phase change.

References

[1] Kruse H., *Energy savings when using hydrocarbon as refrigerant*, International CFC and Halon Alternatives Conference, Washington, DC, USA, 1995.

[2] Domanski P.A. et al., *Evaluation of suction-line/liquid-line heat exchange in the refrigeration cycle*, Int. J. Refrig., Vol. 17, 1994.

[3] Angelino G., Invernizzi C., *General method for the thermodynamic evaluation of heat pump working fluids*, Int. J. Refrig., Vol. 11, 1988.

[4] McLinden M.O., *Optimum refrigerants for non-ideal cycles: an analysis employing corresponding states*, Proc. ASHRAE – Purdue CFC & IIR – Purdue Refrigeration Conferences, W Lafayette, IN, 1990.

[5] Domanski P.A., Didion D.A, Mulroy W.J., Parise J., *A simulation model and study of hydrocarbon refrigerants for residential heat pump systems*, Proceedings Int. Conference New Applications of Natural Working Fluids in Refrigeration and Air Conditioning, IIR, Commission B2, Hannover, Germany 1994.

[6] Jung D., Kim Ch., Hwangbo H. Ji. H., *Effect of suction line heat exchangers on the performance of various HCFC22 alternatives*, International Conference on Ozone Protection Technologies, Washington, DC (USA), 1996.

[7] Huelle Z.R., *Wpływ ukształtowania obiegu chłodniczego na zapotrzebowanie energii urządzeń chłodniczych* (The refrigerant cycle configuration impact on the energy consumption), Konferencja Naukowo-Techniczna: Współczesne Problemy Techniki Chłodniczej, Kraków 1999.

[8] Vakil B.H., *Thermodynamics of heat exchange in refrigeration cycles with non-azeotropic mixtures. Part II, Suctionline heat exchange and evaporative cooling of capillary*, Proceedings XVI Int. Congress of Refrigeration Paris, France, International Institute of Refrigeration, Commission B1, 1983.

[9] Lavrenchenko G., Khmelnuk M., Tikhonova E., *Thermodynamical aspects of using mixtures of substances in refrigerating machines*, CFC's The Day After. Refr. Sci. and Tech. Proceedings Commissions B1, B2, E1, E2, Padova 1994.

[10] Klein S.A., Reindtl D.T., Brownell K., *Refrigeration system performance using liquid-suction heat exchangers*, Int. J. Refrig., 23, 2000.

[11] Gallager J., McLinden M., Morrison G., Huber M., *NIST Thermodynamic Properties of Refrigerants and Refrigerant Mixtures Database. (REFPROP 8.0)*, National Institute of Standards and Technology, Gaithersburg, MD, 2007.

[12] Maczek K., Müller J., Wojtas K., Domański P., *Ternary zeotropic mixture with CO_2 component for R-22 heat pump application. Clima 2000/Brussels 1997a*, World Congress.

[13] Maczek K., Wojtas K., Müller J., *Ternary mixture as R22 replacement in heat pumps*, IIF-IIR – Commissions E2 with E1 and B2, Linz, Austria 1997b.

TECHNICAL TRANSACTIONS | CZASOPISMO TECHNICZNE
ENVIRONMENT ENGINEERING | ŚRODOWISKO
1-Ś/2016
DOI: 10.4467/2353737XCT.16.200.5949

PAWEŁ OPALIŃSKI, KRZYSZTOF RADZICKI*, STEPHANE BONELLI**

NUMERICAL MODELLING OF COUPLED HEAT AND WATER TRANSPORT ON EMBANKMENT DAM IN KOZLOWA GORA

MODELOWANIE SPRZĘŻONEGO TRANSPORTU CIEPŁA I WODY W ZAPORZE ZIEMNEJ W KOZŁOWEJ GÓRZE

Abstract

The paper discusses the use of the thermo-hydraulic numerical model to verify the hypothesis of subsoil seepage and erosion development in a section of the Kozłówa Góra dam. This dam is provided with an innovative and advanced system for quasi-3D thermal monitoring of seepage and erosion, which was used for temperature measurements. The herein reported analysis of the measurements showed high applicability of the thermal monitoring method in determining the severity of erosion and seepage processes using numerical modelling.

Keywords: earth dam, thermal monitoring, numerical modelling

Streszczenie

W artykule przedstawiono wykorzystanie termo-hydraulicznego modelu numerycznego w celu weryfikacji hipotezy o rozwoju procesów filtracyjno-erozyjnych w podłożu w jednym z przekrojów zapory Kozłowa Góra. Zapora ta posiada innowacyjny, zaawansowany, system termomonitoringu quasi 3D procesów filtracyjno-erozyjnych, który został wykorzystany do realizacji pomiarów temperatury. Przedstawiona w niniejszym artykule analiza pomiarów wykazała dużą przydatność metody termomonitoringu w określaniu stopnia nasilenia procesów filtracyjno-erozyjnych z zastosowaniem modelowania numerycznego.

Słowa kluczowe: zapora ziemna, termomonitoring, modelowanie numeryczne

* M.Sc. Eng. Paweł Opaliński, Ph.D. Eng., Krzysztof Radzicki, Institute of Water Engineering and Management, Faculty of Environmental Engineering, Cracow University of Technology.

** Ph.D. Stephane Bonelli, Hydraulic Structures and Hydrology, National Research Institute of Science and Technology for Environment and Agriculture.

1. Introduction

Thermal monitoring methods are currently recommended and considered the most promising for the detection and evaluation of seepage and erosion phenomena in earth dams [3, 7, 8]. Changes in the thermal field caused by seepage and leakage through the dam body or foundation allow for the assessment of the intensity of these processes as well as an indirect analysis of the erosion processes.

The Kozłowa Góra earth dam on Świerklaniecki reservoir, an important flood protection and Upper Silesia regional water supply asset, has been provided with Poland's first modern and innovative thermal monitoring system [16], also designed as a field R&D laboratory for seepage/erosion thermal monitoring method development. The Kozłowa Góra earth dam is owned by Górnośląskiego Przedsiębiorstwa Wodociągowego S.A., a regional water company.

At the dam, several seepage/erosion phenomena have been observed. In the 2010 flood, a piece of downstream slope lost stability at the perimeter ditch. The observations, research and analyses, including those defined in the dam condition's evaluation, suggest two development mechanism of seepage and erosion in the dam body and foundation. The first is leaking in the upper part of the inclined clay core and development of a privileged seepage path towards the downstream toe in the dam's main static body. The other is erosion in the dam foundation related to the sheet piles' under-depth and/or leakage. These hypotheses are widely described in chapter 4.

Thermometric measurements at the Kozłowa Góra main dam have been taken since 2014. Due to the relatively low water level at that time, the first hypothesis could not be verified, and this article reports an analysis of the second hypothesis by the thermal monitoring method.

Thermal monitoring offers a wide array of temperature measurement analysis tools [8, 15]. They also include thermal-hydraulic numerical models of the test object. Such a model of transient heat and water transfer was developed for piezometric cross section No. 6 of the dam. This cross-section is located in the area of the 2010 ditch slope failure. To define the model's boundary conditions, a series of upstream and downstream slope temperature measurements was used, taken at different heights on both slopes of the dam, and upper and lower water levels. The period from the 24th of May to the 4th August 2015 was modelled.

2. The Kozłowa Góra Dam

The Kozłowa Góra main dam was made of locally available material. It is a class II, 6 m high dam, built in 1933 and 1939 as a temporary facility for military purposes, i.e. flooding the downstream areas. In line with the reservoir's intended purpose, the technical requirements for permanent damming hydro-engineering structures were ignored in the dam's construction. Material for the embankments was not properly sorted, and the embankment density was neither proper nor controlled in the earthworks [5, 9, 17]. The dam body is made of sandstone and limestone fragments, sand and silt sand. The waterproof

element is the inclined pre-quaternary clay core, 0.70 m thick at base and 0.18 m at the top (altitude 279.19 m OSL). Seepage in the foundation under the dam is limited by a wooden sheet pile set at the toe of the upstream slope. It connects to the inclined clay core, forming a 600 m long waterproof element. The clay core is protected by 1.60 m thick gravel layer. The upstream slope is protected by 30–35 cm thick stone block paving laid on cement mortar (Fig. 1).

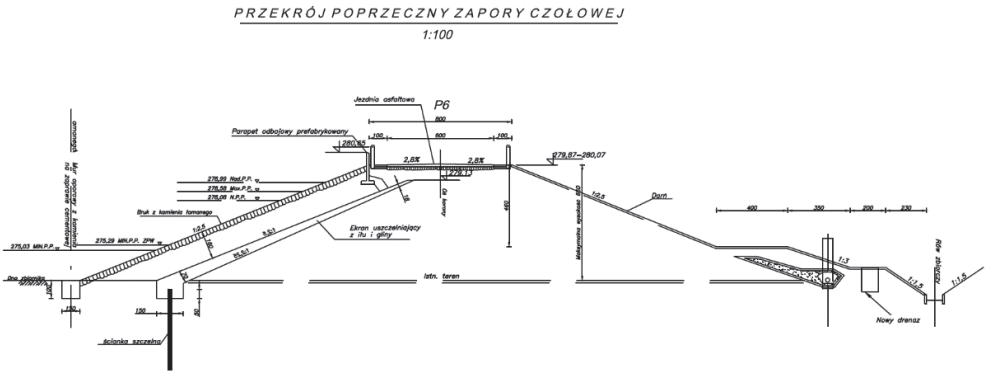

Fig. 1. Typical cross-section of the Kozłowa Góra frontal dam body

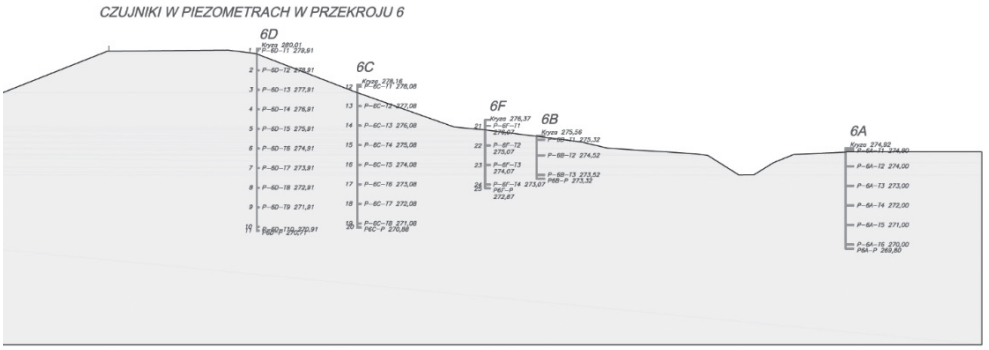

Fig. 2. Fragment of the Kozłowa Góra dam's downstream side cross-section with thermal sensors installed in piezometers

The downstream slope is planted with grass and divided by two 4.0 m × 2.0 m benches. Frontal dam seepage water is drained through ceramic drains in aggregate surround of three-layer gravel filter set in the downstream slope toe. Water from the drains flows to an open ditch running at 6 m distance from the drainage axis. On the upstream side, the crest is protected with sill made of prefabricated reinforced concrete slabs, combined with the tight pre-quaternary clay core. There is an asphalt-paved road on the damn crest [9, 17].

The thermal monitoring system for the Kozłowa Góra dam was designed by Krzysztof Radzicki from Cracow University of Technology and developed by Neostrain Sp. z o.o. This fully automatic system of quasi-3D monitoring (continuous over the length of the dam and extended in chosen piezometric cross-sections) was described in detail by Radzicki et. al [16]. Temperature sensors in piezometric cross-sections, the measurements from which are discussed here, are mounted along the entire length of each piezometer at 1 meter intervals (Fig. 2), thus enabling measurements of vertical temperature profiles in the dam body. On the upstream and downstream slopes of each instrumented piezometric cross-section, numerous temperature sensors are mounted for measuring external thermal loads.

3. Thermal monitoring of earth dams

Thermal monitoring is used to detect and assess seepage and erosion processes on the basis of analysis of temperature measurements in earth dams. The methodology is intensely developed by some major research centers in the world, and in Poland by the Institute of Water Engineering and Management at the Cracow University of Technology.

Thermal methods of analysis of water flow in the ground are based on the relation in the heat and liquid transfer processes, which are coupled. These relations are described by the energy conservation equation. At zero water velocity, only heat is transferred, which is a relatively slow process. However, even only a change of soil moisture due to even minimal leakage causes local changes in the thermal front transition rate and disturbs the local isotherm pattern [4, 11]. In the event of the liquid's movement, heat is also transported with the mass of water also. This process is called advection and is predominant over conduction. Heat and water (seepage, leakage) penetrate the facility's body and cause significant disturbance in the temperature field; the greater the disturbance, the higher the seepage rate.

As a result, the body temperature measurements and their analysis allow to identify leaks and to monitor seepage processes. Since the erosion process changes the structure and values of soil parameters, it affects the values and directions of water flow vectors in the seepage area, and, consequently, influences the soil medium temperature field. Each type of erosion process causes characteristic disturbances of the hydro-thermal field, allowing its thermal monitoring exploration [4, 13, 14]. In summary, the thermal monitoring method enables the detection and analysis of the seepage and erosion processes. As an example, Fig. 3 shows the numerical analysis of the impact of the development of erosion processes, such as suffosion, on the thermal field in the dam section, at the same thermal and hydraulic loads. It can be seen that the effect of water temperature from reservoir on the thermal field inside the dam's body is predominant where the hydraulic gradient is the largest, and the impact increases with the development of erosion processes.

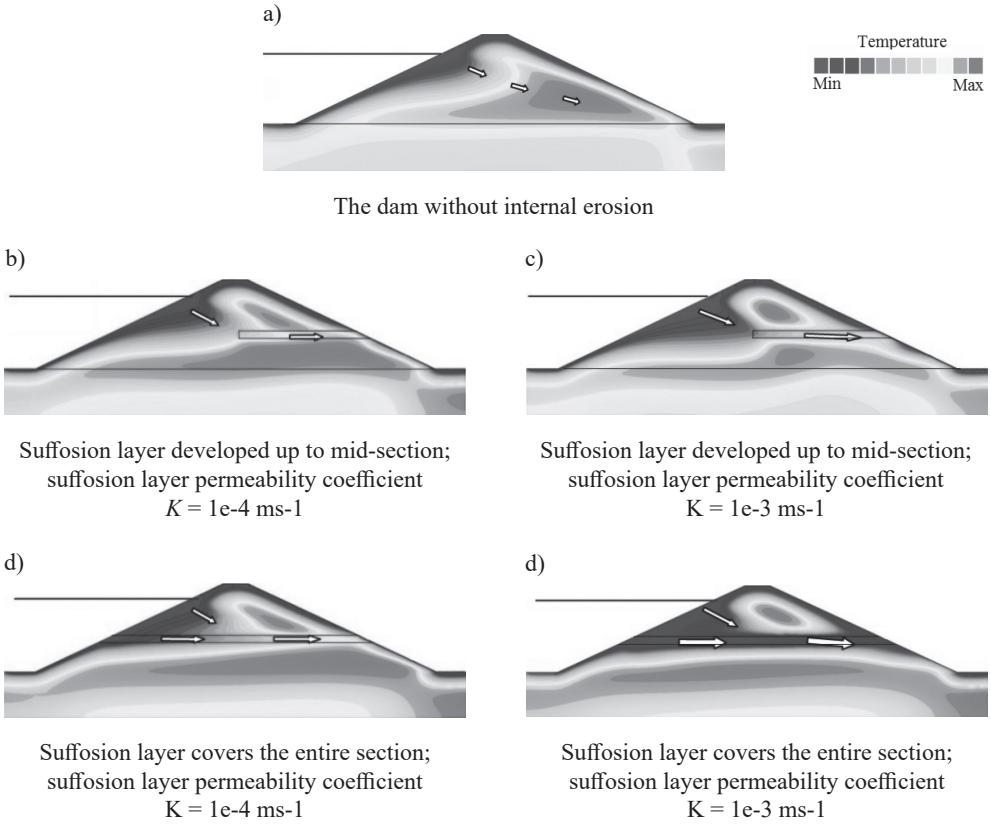

Fig. 3. Thermal fields of an earth dam cross-section at the same point in time for various suffosion layer lengths and the layer's permeability coefficient (Radzicki, Bonelli, 2012) [14]

4. Hypothetical seepage/erosion mechanisms in earth dam body and foundation

As mentioned in the introduction, a number of seepage/ erosion phenomena have been monitored on the main dam. The multi-year monitoring shows that one of the areas where significantly intense erosion and seepage processes have been observed is the section between and around piezometric cross-sections 6 and 7, of total width ca. 200 m. Benchmarks located on the facility crest within this region showed subsidence therein by ca. 2 cm in the last 20 years, including an increase in its intensity between 1995 and 1998, when the settlement amounted to 1 cm. In addition, over a few hundred meters of the downstream bench along the dam's right side, the bench crest has lowered by several tens of centimeters. Soil compaction probing carried out from the bench on the downstream side of the dam showed that, at the seepage curve level in the bench embankment, the soil compaction in most of the holes was described as loose and very loose in a ca. 0.3 to 0.6 m thick layer. Beneath, in the foundation under the bench, the soil is mid-compacted [19]. In the zone of piezometric cross-sections 6 and 7, some voids and cracks were observed in the stone paving on the upstream slope

that could indicate the locations of enhanced seepage penetration into the body. In addition, relatively large rates of delivery from drainage wells and moisture on the downstream bench surface were observed in this zone. Variability analyses of the position of piezometric levels in the frontal dam, in particular at the reservoir water level increase during the 2010 flood, indicate in several dam sections, including this piezometric cross-section 6, a likely unsealing of the clay core in its top part [9, 17, 18]. Two hypotheses were defined of the mechanism of the seepage/erosion processes in the main dam body, under the assumption that the may be concurrent. The first hypothesis, substantiated with observations of the relationship of changes in the piezometric levels relative to the reservoir level, and with geo-engineering tests of the dam body, assumes that the clay core in its upper part above elevation 277.80 m OSL does not provide an effective anti-seepage protection, as evidenced by the piezometric water levels measurements, whereby at the reservoir's damming above the aforementioned value, the pressure very considerable increases. In addition, the upper part of the core is above the freezing zone. Freezing of waterproof elements of earth dams made of clays affects the emergence of horizontal fractures and a potential significant increase in the rate of seepage. Many years of impoundment, prior to 2006 above elevation of 277.80 m OSL could result in the development of a privileged seepage path between the upper porous part of the core towards the bottom toe in the facility body. The other hypothesis assumes the development of suffosion processes in the dam's tertiary foundation resulting from the sheet piles' underdepth and/or leaks. The sheet piles' partition in the river valley most likely has not reached the impervious formations in the valley bottom and is suspended in the Pleistocene complex of sandy-gravel formations filling the river valley. This applies particularly to the right part of the dam (piezometric cross-sections 4-4 to 7-7). Also doubtful may seem the tightness of the wooden sheet piles itself, set in the foundation, after more than 70-years of operation.

The low damming level maintained at the dam in 2014 prevented the first hypothesis' verification and analysis by the thermal method. In contrast, a multi-scenario analysis of the second hypothesis was possible and included permeability coefficient estimate in the lower and saturated part of the embankment and in the foundation, the results of which are shown in the following two sections hereof.

5. Matching the numerical model of dam's thermo-hydraulic cross-section to measurements

Mapped in the numerical model was the frontal main cross-section 6-6. For the modelling, a FeFlow model was used, whose accuracy and calibration in this regard has been verified by numerous applications and checks against models and physical objects [6]. A numerical model of the cross-section was developed, under the assumption of transient heat transfer and variable water levels on the upstream side, based on actual multi-point temperature measurements on the upstream and downstream slopes, and water level measurements in the reservoir. In the next step, by applying the back-analysis method, (1) the dam body and foundation permeability coefficients were matched to reference-literature parameters pre-established for the soil types identified by way of geo-engineering tests, (2) the seepage window opening under the wooden sheet piles was determined. While fitting the model,

the best correlation was sought of the modelled piezometric level and, in particular, of the modelled vertical thermal profiles measured in piezometers for cross-section 6 in the analyzed period, with actual measurements. Fig. 4 shows a comparison of the actual and modelled temperatures in the vertical profiles in piezometers 6C and 6D. The mean error between the data obtained from thermal monitoring and modelling amounted to 0.66°C for piezometer 6D and 0.46°C for piezometer 6C. The maximum error for piezometric pressures was 0.18 m for piezometer 6D and 0.10 m for piezometer 6C. Finally, the modelling allowed to determine the permeability coefficient for the foundation as 1e-5 m-1s, and the seepage window opening under the sheet piles as 0.3 m.

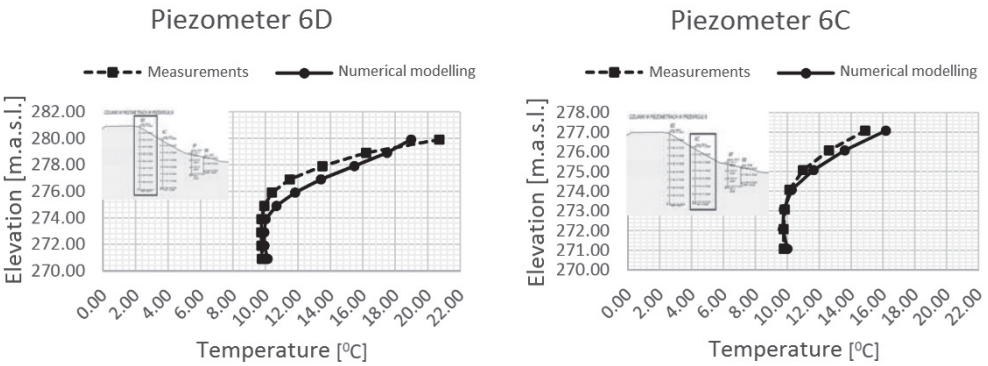

Fig. 4. Vertical thermal profiles in piezometers 6D and 6C for data obtained from the numerical model and data from thermal monitoring of the Kozłowa Góra dam on 30 June 2014

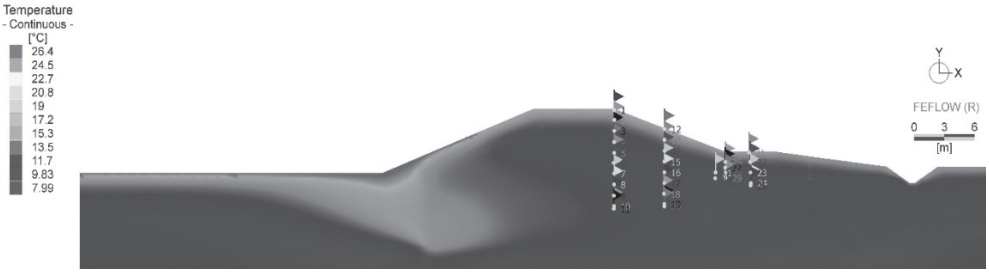

Fig. 5. Thermal field of Kozłowa Góra dam cross-section 6-6 modelled for 30 June 2014

The obtained data do not completely rule out the occurrence of suffosion erosion processes in the dam foundation, but they ruled out the existence of severe erosion or a zone of particularly privileged flow and locally severe erosion. Hypothetical impact of the emergence of such a zone on temperature measurements is presented in section 6.

6. Modelling the hypothesis of seepage/erosion processes occurrence in the foundation

This section describes the hypothetical impact of a privileged flow zone with deteriorated soil parameters on the temperature field in cross-section 6-6, if such a zone existed in the foundation. In relation to the calibrated numerical model described in section 5, the permeability coefficient in the foundation was increased by an order of magnitude, i.e. to k = 1e-4 m-1s. There was a seepage opening between sheet piles and impermeable tertiary foundation layer as in the previous case. Fig. 6 shows the modelled vertical temperature profiles in piezometers 6C and 6DZ with actual measurements. A significant increase in the difference between modeled and the actual temperatures is evident from elevation of 275.50 m OSL downwards, increasing with depth in relation to the results

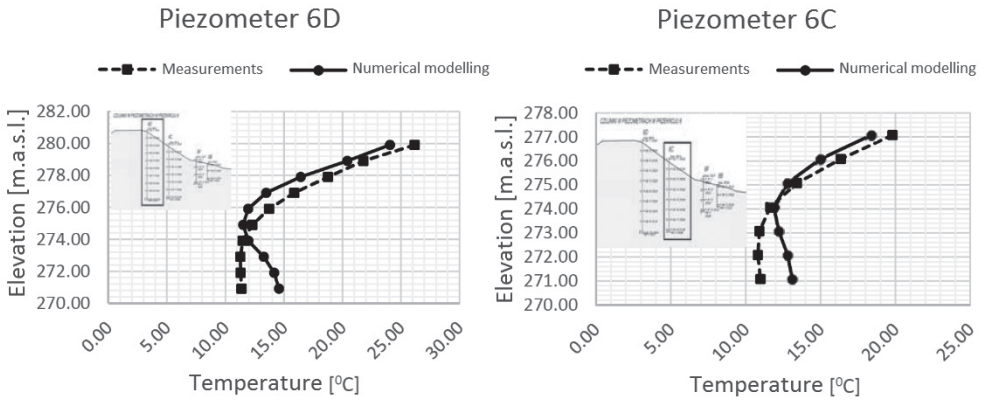

Fig. 6. Thermal profiles in piezometers 6D and 6C for data obtained from the numerical model and data from thermal monitoring of the Kozłowa Góra dam on 4 August 2014

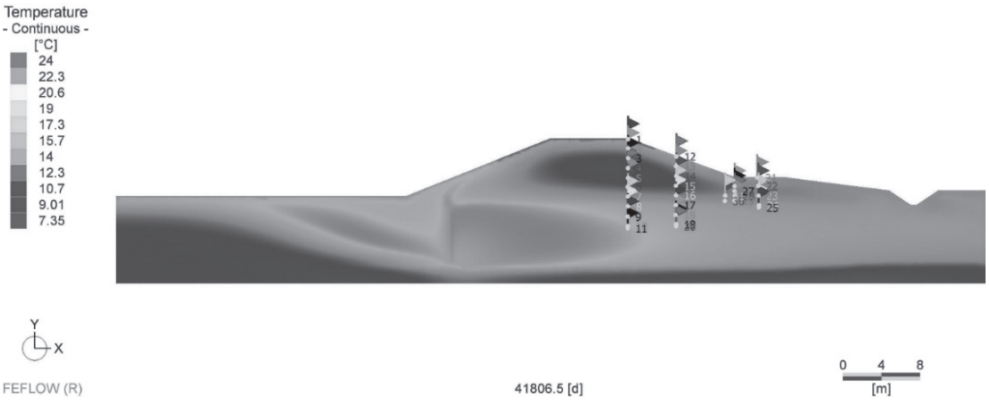

Fig. 7. Thermal field of Kozłowa Góra dam cross-section 6-6 modelled for 4 August 2014

shown in Fig. 4. Such a thermal anomaly would result from the modelled, hypothetical zone of privileged flow, and consequently the increased advective heat transfer towards the downstream side.

7. Summary and conclusions

Based on the temperature measurements at the Kozłowa Góra dam and thermal-hydraulic numerical modelling, the hypothesis of potentially intensified seepage/erosion processes in the dam foundation was verified and rejected. The seepage opening between sheet piles and the impermeable tertiary foundation layer was also confirmed, which, however, does not result in significant intensification of seepage/erosion processes in the dam foundation as far as the present case is considered. The modelling confirms the thermal method's high sensitivity to seepage rate changes, which enables detailed analysis of the seepage field and accurate adjustment of the soil permeability coefficient using the back-analysis method. Unfortunately, due to the low reservoir water levels in the analyzed period, the hypothesis of fractured upper part of the core could not be analyzed by the thermal method.

Thermal monitoring methods, together with advanced data analysis, are well suitable for the analysis of complex problems of water seepage through earth dams. The Kozłowa Góra dam is provided with an advanced thermal monitoring system that allows a wide range of analyses, the results of which will be presented in future papers. However, the application of that particular method in view of cross-sectional analysis with an already existing piezometric cross-section does not require a permanent system of temperature measurement system at the dam. In addition, installing temperature sensors, e.g. rented for several months (length of the period depends on, inter alia, the size of the dam and its body and foundation soil parameters) would be sufficient.

References

[1] DHI-WASY Software, *Finite Element Subsurface Flow & Transport Simulation System*, White Papers FeFlow 6.

[2] Hellstron G., Mattsson H., Lundstrom T., *Research Report on Internal Erosion in Earth dams, A literature survey of the phenomenon and the prospect to model it numerically*, 2008.

[3] Fry J.J., *How to Prevent Embankments from Internal Erosion Failure?*, International symposium on dams for a changing world, 5 czerwca, Kyoto, Japonia, 2012, 6.

[4] Johansson S., *Seepage Monitoring in Earth dams*, Doctoral Thesis, February, 1997.

[5] Geoprojekt, *Dokumentacja geologiczno-inżynierska dla zabezpieczenia zapory ziemnej w Kozłowej Górze*, Gdańsk 1965.

[6] Guidoux C., *Developpement et validation d'un systeme de detection et de localization par fibres optiques de zones de fuite dans digues en terre*, Doctoral Thesis, December 2007.

[7] ICOLD, *Internal Erosion of Existing Dams, Levees and Dikes, and Their Foundation*, Bulletin, No. 164, Volume 1: Internal erosion processes and engineering assessment, 2013, 151.
[8] ICOLD, *Internal Erosion of Existing Dams, Levees and Dikes, and Their Foundation*, Draft of Bulletin, No. 164, Volume 2: Investigations, testing, monitoring and detection, remediation and case histories, marzec 2014.
[9] OTKZ, *Zapora Kozłowa Góra, ocena stanu technicznego i bezpieczeństwa budowli hydrotechnicznych w roku 2013*, Warszawa 2013.
[10] Radzicki K., *Badania filtracji w ziemnych budowlach piętrzących metodami termodetekcji*, Gospodarka Wodna, nr 5, 2005, 372–376.
[11] Radzicki K., *Analyse retard des mesures de températures dans les digues avec application à la détection de fuites*, PhD rapport, AgroParisTech, Paris 2009, 175.
[12] Radzicki K., *Identyfikacja procesów erozyjnych w ziemnych obiektach hydrotechnicznych metodami termodetekcji*, Referat przygotowany na sympozjum naukowo-techniczne Hydrotechnika XII, Ustroń, maj 2010.
[13] Radzicki K., Bonelli S., *A possibility to identify piping erosion in earth hydraulic works using thermal monitoring*, 8h ICOLD European Club Symposium, 22–25 September, Austria, 2010, 618–623.
[14] Radzicki K., Bonelli S., *Monitoring of the suffosion process development using thermal analysis performed with IRFTA model*. 6th ICSE, 2012, 593–600.
[15] Radzicki K., *The Thermal Monitoring Method – A Quality Change in the Monitoring of Seepage and Erosion Processes in Dikes and Earth Dams*, Modern monitoring solutions of dams and dikes, Vietnam, 2014, 33–41.
[16] Radzicki K., Siudy A., Stoliński M., *An innovative 3d system for thermal monitoring of seepage and erosion processes and an example of its use for upgrading the monitoring system at the Kozłowa Góra dam in Poland*, ICOLD 25th Congress, 2015, 16.
[17] Strzelecki T. et al., *Kompleksowa ocena stanu technicznego zapory czołowej zbiornika retencyjnego Kozłowa Góra*, Politechnika Wrocławska, Wrocław 2010.
[18] Szczęsny J., Dembski B., *Opinia rzeczoznawców o stanie zapory Kozłowa Góra na rzece Brynnicy*, przegląd 2001, 2002, Kraków 2002.
[19] Zakład Prac Geologicznych KILAR, *Dokumentacja geotechniczna, Zapora czołowa zbiornika wodnego „Kozłowa Góra" – badania gruntów rodzimych podłoża oraz nasypów wbudowanych w korpus obiektu*, Tychy 2006.

TECHNICAL TRANSACTIONS | **CZASOPISMO TECHNICZNE**
ENVIRONMENT ENGINEERING | ŚRODOWISKO
1-Ś/2016

DOI: 10.4467/2353737XCT.16.201.5950

AGATA PAWŁOWSKA-SALACH*, MICHAŁ ZIELINA**,
ALEKSANDRA POLOK-KOWALSKA***

ANALYSIS OF A WEDGE-WIRE SCREEN'S WORK

ANALIZA PRACY GŁOWICY SZCZELINOWEJ

Abstract

The article presents the results of numerical calculations performed in a computer software. The simulations concern water flow through an intake screen. This kind of screen can be used in surface water intakes. Thanks to the small inlet velocities and a small mesh size, the screen does not pose a threat to ichthyofauna.

Keywords: water intake, water intake screen, ichthyofauna

Streszczenie

W artykule zamieszczono wyniki obliczeń numerycznych wykonanych w oprogramowaniu komputerowym. Symulacje dotyczyły przepływu wody przez szczelinową głowice. Tego typu głowica znajduje zastosowanie w ujęciach wody powierzchniowej. Dzięki małym prędkościom wlotowym oraz małym otworom szczelin głowica nie stwarza zagrożenia dla ichtiofauny.

Słowa kluczowe: ujęcie wody, głowica, ichtiofauna

* M.Sc. Ph.D. Agata Pawłowska-Salach, student, Institute of Water Supply and Environmental Protection, Faculty of Environmental Engineering, Cracow University of Technology.

** Ph.D. Eng. Michał Zielina, Institute of Water Supply and Environmental Protection, Faculty of Environmental Engineering, Cracow University of Technology.

*** Ph.D. Eng. Aleksandra Polok-Kowalska, POL-EKO-APARATURA Sp. J.

1. Introduction

Human intervention, including regulation of rivers and streams, construction of water intakes and dams, poses a threat to ichthyofauna. Depending on the type of construction, there are various types of dangers for ichthyofauna. An example of such a threat can be a disruption of river continuum as well as danger for fish and fry connected with getting into hazardous parts of the water intake installation.

As a result of the intensive investigations into the phenomenon of upstream fish migration and fish passage restoration, today, there are defined details on the dimensioning and design of functioning upstream fish passes available. It is undisputed that upstream fish passes contribute substantially to a sustainable protection of the ecosystem [2].

Despite the high awareness of the necessity to ensure migration up the river, the issue of downstream fish migration receives little attention. A major threat to the migrating fish is posed by hydroelectric power plant's water intakes. Nevertheless, water intakes supplying drinking water are also a problem.

The degree of negative impact of water intake on the ichthyofauna depends on the number, size, arrangement of ichthyofauna and swimming ability of individuals, as well as the water velocity, inflow into the intake and depth at which the intake is installed. Other important factors are the type and size of water intake and the mesh size of a screen [1].

In order to protect fish and fry from entrainment, special devices known as physical barriers are installed in water intakes. These are the intakes equipped with special screens. The screens can have different shapes. A cylindrical wedge-wire screen is taken into account in this study. Inside the wedge-wire part of the screen, there is a deflector installed. The aim of the deflector is to equalize the velocity distribution on the surface. It is obtained thanks to different sizes of slots.

2. Wedge-wire screen

One of the materials that the screen can be made of is wedge-wire. It is a commonly used material in modern water intake screens. In this type of screen, the broad side of the bars forms the screen surface that faces the flow, so that the bars become smaller in the flow direction, while the clear spacing widens in the wedge-shape.

This type of screens significantly reduces the risk of injuries to fish as the small clear spacing of the bars and the position of the broad side of the triangular shaped cross-section against the approach flow forms a very smooth surface [2].

Another important aspect is the water intake position in the watercourse. In order to reduce the normal flow velocity, the screens are set at an angle to the watercourse flow. The established flow is parallel to the screen in order to guide fish past the screen. If screens are oriented normally (90 degrees) to the channel flow, the fish tend to hold in front of the screens or are impinged on the screen. In either case, the fish are not directed to the bypass entrance [3].

The flow approaching the fish screens can be characterized in a vector format. The channel velocity Vc can be broken into an approach velocity component Va, which is normal to the screen face, and a sweeping velocity component Vs, which is parallel to the screen face. The component oriented normally to the screen face Va, is the part of the channel velocity that draws fish and debris to the screen surface. The component parallel to the screen face Vs is the part of the channel velocity that directs fish and debris along the screen [3].

Thus, it can be said that approach velocity is a determining parameter in terms of ichthyofauna protection in water intakes. According to [3], when the screen is equipped with a flushing system preventing clogging, the approach velocity measured 76 mm (3 inches) from the screen is lower than 0.12 m/s and is safe for fry and 0.24 m/s for fish.

Apart from the approach velocity, the inlet velocity measured in the screen's slots is an important parameter. According to USA guidelines [3], this velocity should be lower than 0.15 m/s to be safe for ichthyofauna.

3. Method

In order to check the work of the water intake screen and to analyze the velocity distribution, the Solid Works Flow Simulation computer software was used. The software provides computational fluid dynamics (CFD) simulation, which is a simulation technique that mathematically simulates fluid flow and heat transfer.

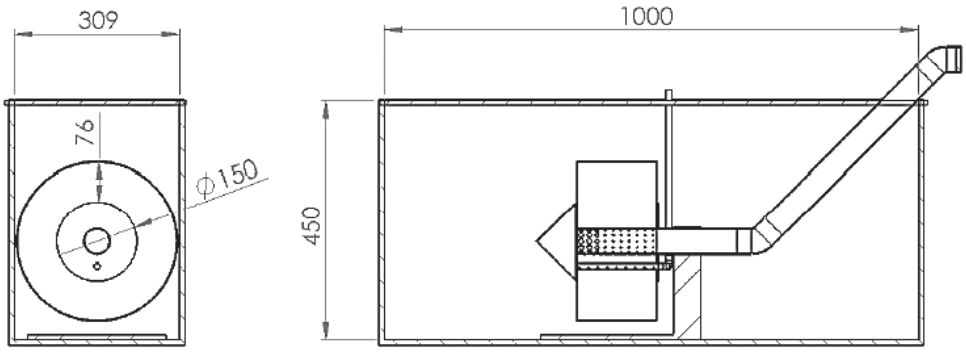

Fig. 1. Dimensions of the model

The dimensions of the analyzed water intake screen are presented in the Fig. 1. The screen's diameter equals to 150 mm. Inside, there is a deflector installed. At 76 mm from the screen, the velocity measurements were performed. It was assumed that the screen is installed in a tank under atmospheric pressure of 101325 Pa. The outflow from the screen equals to 5 kg/s ≈ 432 m^3/d.

4. Results

Thanks to the performed simulations, the velocity distribution during water flow through the screen was found and it is presented in Fig. 2.

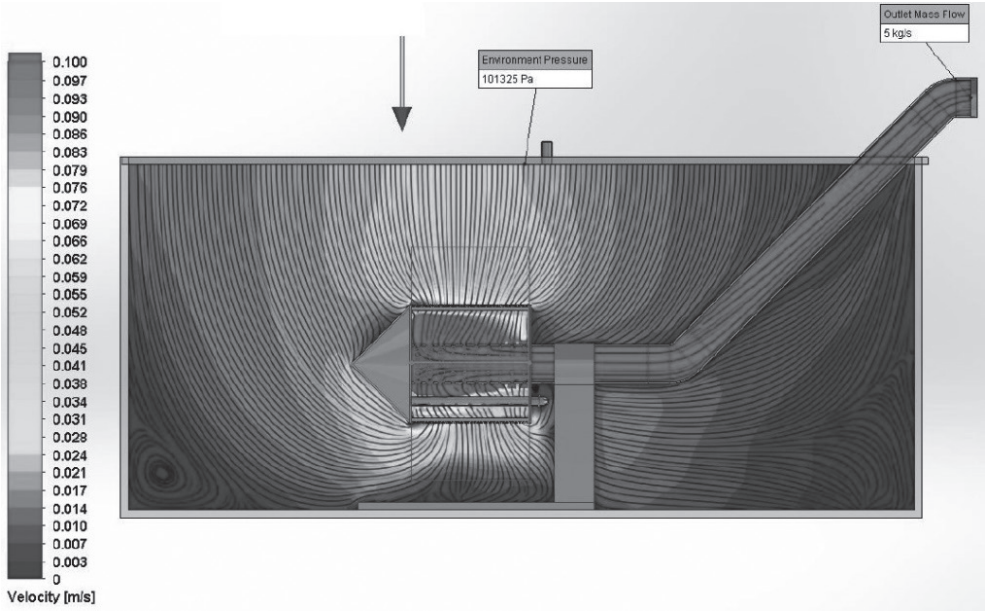

Fig. 2. Velocity distribution

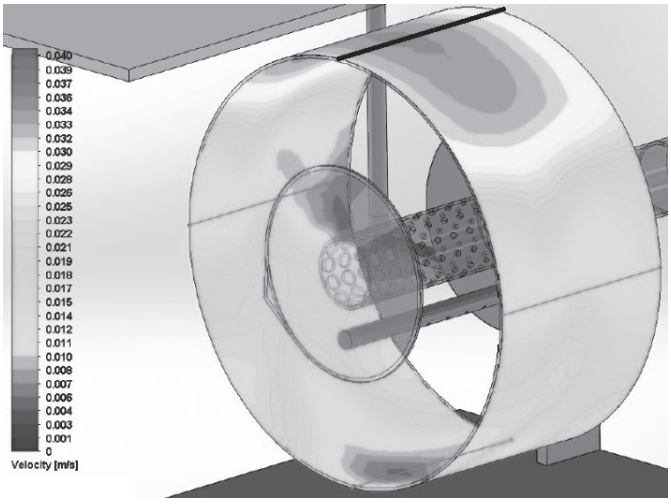

Fig. 3. Velocity distribution within 76 mm (3 inches) from the surface of the intake screen

As mentioned before, the key parameter in terms of ichthyofauna protection is the velocity within 76 mm (3 inches) from the surface of the intake screen. This velocity distribution is shown in the Fig. 3.

It can be seen that the maximum values of velocity appear above the water intake screen surface. A more precise distribution of velocities within 76 mm from the upper surface (along line marked in the Fig. 3) is shown in the diagram in the Fig. 4.

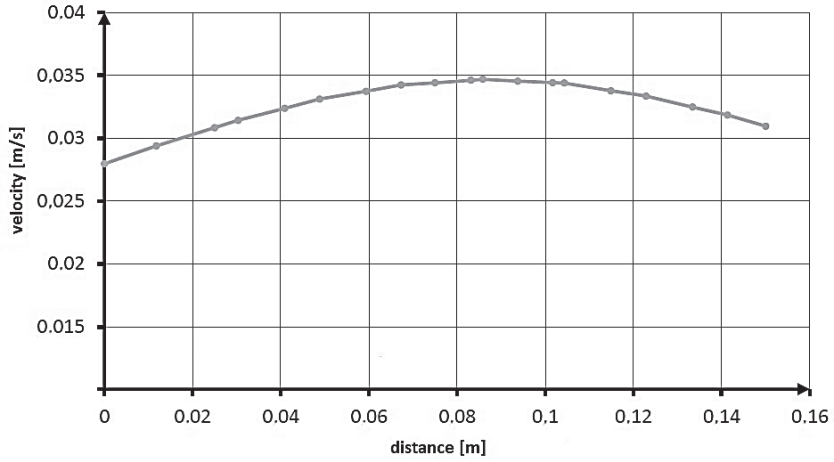

Fig. 4. The velocity distribution within 76 mm (3 inches) from the upper surface of the intake screen

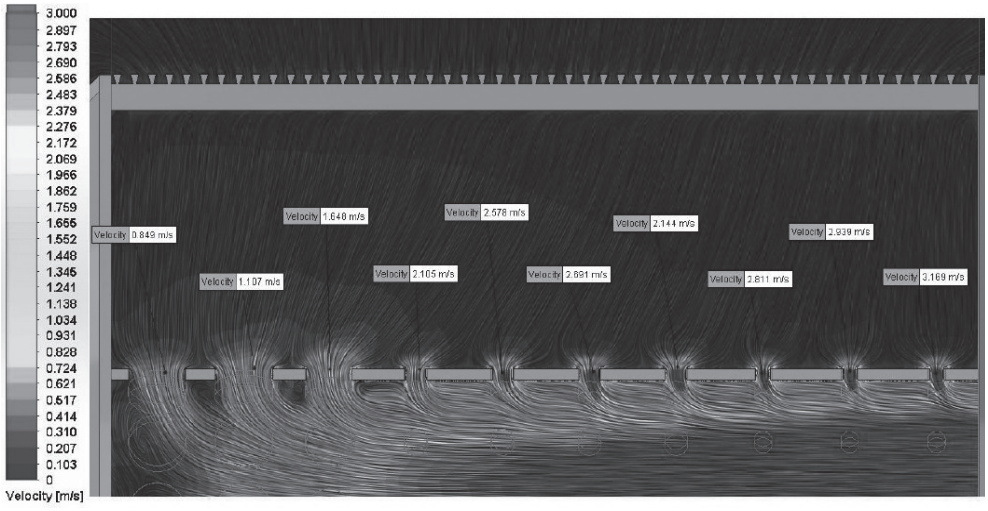

Fig. 5. The velocity distribution in the deflector's slots

According to Fig. 2 and Fig. 3, it can be said that the velocity within 76 mm from the surface of the screens, at each point, is lower than 0.035 m/s. The crucial velocity value that may pose a threat to fry is 0.12 m/s. Thus, it can be concluded that the analyzed water intake screen should not threaten ichthyofauna. What is more, such a small difference in velocities is favorable for a water intake screen. A huge difference could lead to uneven work as well as clogging of some parts of the screen.

A steady velocity distribution on the screen's surface is obtained thanks to the use of the deflector. The velocity distribution inside the deflector's different sized slots is presented in Fig. 5.

5. Summary

The used computer software seems to be a good tool for analyzing the cylindrical wedge-wire screen's work. Numerical simulations allow to obtain qualitative and quantitative results of the examined issues. Thanks to the performed simulation, it was possible to determine the velocity distribution inside the water intake screen and around it. It is an essential issue in designing water intake screens protecting fish and fry.

The analyzed wedge-wire screen seems to be safe in terms of ichthyofauna protection. Thanks to a steady velocity distribution on the surface, exploitation problems can be minimized.

References

[1] Freshwater Intake End-of-Pipe *Fish Screen Guideline*, Department of Fisheries and Oceans, Ottawa, Ontario, Canada, 1995.

[2] *Fish Protection Technologies and Downstream Fishways: Dimensioning, Design, Effectiveness Inspection*, Deutsche Vereinigung für Wasserwirtschaft, Abwasser und Abfall e.V.German Association for Water, Wastewater and Waste, DWA – Topics, Deutschland, 2005.

[3] *Fish Protection at Water Diversions. A Guide for Planning and Designing Fish Exclusion Facilities*, Department of the Interior Bureau of Reclamation Denver, Colorado, USA, 2006.

TECHNICAL TRANSACTIONS | CZASOPISMO TECHNICZNE
ENVIRONMENT ENGINEERING | ŚRODOWISKO
1-Ś/2016
DOI: 10.4467/2353737XCT.16.203.5952

PIOTR REZKA, WOJCIECH BALCERZAK*

OCCURRENCE OF ANTIBIOTICS IN THE ENVIRONMENT

WYSTĘPOWANIE ANTYBIOTYKÓW W ŚRODOWISKU

Abstract

Antibiotics are the most commonly used group of pharmaceuticals used in human and animal treatment. The main sources are hospital and household sewage and waste from animal production. The paper is a review of the literature confirming the prevalence of antibiotics in wastewater influents and effluents, natural waters, sludge and sediments. Studies conducted around the world confirm that there is a risk of antibiotic accumulation in soil and their infiltration to drinking water despite advanced methods of water purification. The concentrations of several substances found in surface water samples exceed the levels considered as safe for the studied aquatic organisms several hundred times, which indicates a real threat to their lives.

Keywords: antibiotics, wastewater, surface water, sludge

Streszczenie

Antybiotyki są najczęstszą grupą farmaceutyków stosowanych w leczeniu ludzi i zwierząt. Głównymi źródłami tych leków są ścieki szpitalne, ścieki bytowo-gospodarcze i ścieki z produkcji zwierzęcej. W artykule dokonano przeglądu literatury potwierdzającej powszechną obecność antybiotyków w ściekach doprowadzanych do oczyszczalni, ściekach oczyszczonych, wodach naturalnych oraz osadach ściekowych i dennych. Analizy wykonane na świecie potwierdzają także ryzyko magazynowania się antybiotyków w glebie i przenikania do wody przeznaczonej do picia pomimo zaawansowanych metod uzdatniania. W przypadku kilku substancji, stężenia w wodach powierzchniowych przekraczały kilkaset razy poziomy uznawane za bezpieczne dla badanych organizmów wodnych, co wskazuje na realne zagrożenie dla ich życia.

Słowa kluczowe: antybiotyki, ścieki, wody powierzchniowe, osady

* M.Sc. Eng. Piotr Rezka, Assoc. Prof. D.Sc. Ph.D. Wojciech Balcerzak, Institute of Water Supply and Environmental Protection, Faculty of Environmental Engineering, Cracow University of Technology.

1. Introduction

The consumption of pharmaceuticals in human and animal (veterinary) therapies has been steadily increasing for many years, while the issues of their occurrence and impact on the environment (aquatic and terrestrial) have been the subjects of worldwide research for only two decades. Nowadays, more and more research centers conduct research on the prevalence of pharmaceuticals in the natural environment, which seems to confirm the opinions on pharmaceuticals as a growing threat to the environment and animals. The most commonly used and prevalent group of pharmaceuticals, found in environmental samples in the largest quantities, are undoubtedly antibiotics [39]. Despite a more difficult access to this group of drugs (which are issued only on prescription) than in the case of anti-inflammatory drugs and painkillers, antibiotics are among the most abused drugs. In the case of many ailments with which patients go to the GP (general practitioner), therapy without antibiotics could be successful. However, some doctors still consider antibiotics as the only effective (and perhaps also the easiest) form of therapy of diseases caused by bacteria. This is despite the calls for reducing the excessive use of antibiotics, which affects the emergence of antibiotic resistance in patients, and which is a growing problem worldwide. Resistance to antibiotics is caused by both the correct application of the drug, as well as taking higher doses than prescribed or abandonment of therapy before its completion [4]. This applies to human as well as animal therapy. The bacteria carrying antibiotic resistance genes (ARGs) infiltrate the aquatic environment with sewage from urban treatment plants and livestock production, where the transmission of ARGs occurs between different bacterial species [14]. The prevalence and fate of these bacteria is currently relatively poorly understood. Due to the fact that ARGs are sometimes not completely eliminated during water purification processes [40] and they may be present in drinking water, we should focus on the source of the problem, which is the excessive antibiotic therapy of humans and animals. This paper is emphasizing the problem of antibiotic prevalence in wastewater and the environment.

2. Characteristics of selected antibiotics

Antibiotics are natural, semisynthetic or synthetic substances that act selectively on the cell structure (bactericidal) or the metabolism of microorganisms by inhibiting their growth and cell division (bacteriostatic). Antibiotics are produced by bacteria, actinomycetes, imperfect fungi (fungi imperfecti), rarely by basidiomycetes, lichens, green plants and animal cells [41]. The first discovered antibiotic in history was penicillin, found by Alexander Fleming in 1928. The structure of penicillin G, among other selected antibiotics, is presented in Fig. 1.

Since then, thousands of natural antibiotics were discovered, of which only a small portion may be used for the treatment of humans and animals due to their side effects. Side effects are divided into three basic groups: toxic (to kidney, liver or bone marrow), allergic reactions and dysbacteriosis (imbalance of body's bacterial flora). The consequences of dysbacteriosis are dangerous when microorganisms resistant to antibiotics appear in place of the natural bacterial flora, e.g. staphylococcus, which can even lead to death.

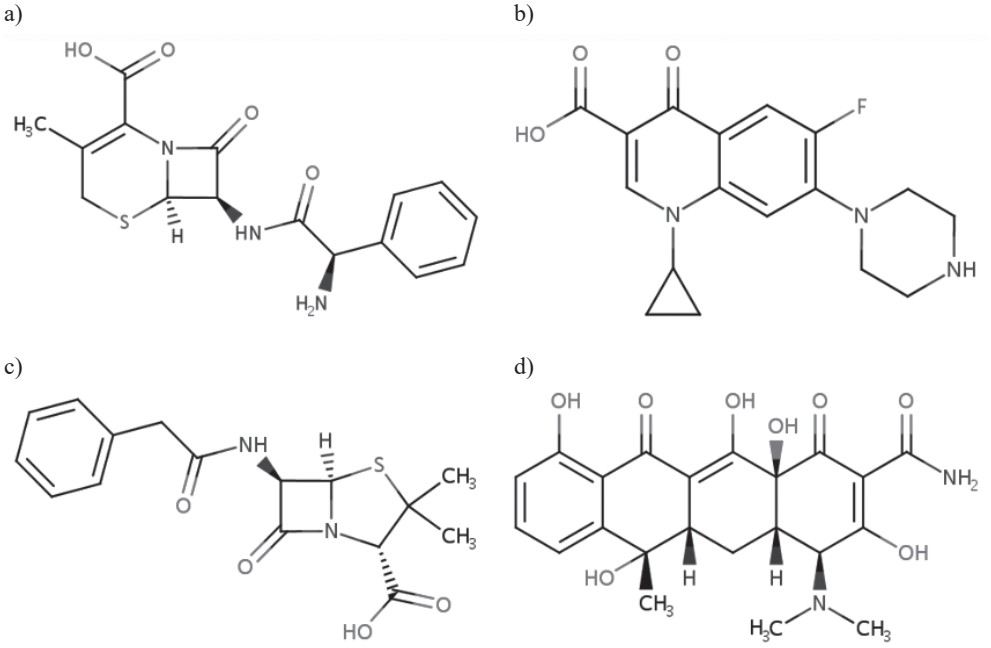

Fig. 1. Structures of selected antibiotics: a) Cephalexin, b) Ciprofloxacin, c) Penicillin G, d) Tetracycline [10]

For this reason, antibiotic therapy should be conducted only under the doctor's supervision and not exceed the recommended and prescribed doses. Table 1 contains the basic characteristics of commonly used antibiotics, which were detected in environmental samples (Table 2).

Table 1

Characteristics of selected antibiotics [10]

Compound	Formula	Molecular mass [g/mol]	CAS	Half-life
Amoxicillin	$C_{16}H_{19}N_3O_5S$	365.404	26787-78-0	1 h
Ampicillin	$C_{16}H_{19}N_3O_4S$	349.405	69-53-4	1 h
Azithromycin	$C_{38}H_{72}N_2O_{12}$	748.985	83905-01-5	68 h
Cefaclor	$C_{15}H_{14}ClN_3O_4S$	367.807	53994-73-3	0.6–0.9 h
Cephalexin	$C_{16}H_{17}N_3O_4S$	347.389	15686-71-2	1 h
Chlortetracycline	$C_{22}H_{23}ClN_2O_8$	478.88	57-62-5	6–9 h
Ciprofloxacin	$C_{17}H_{18}FN_3O_3$	331.342	85721-33-1	4 h
Clarithromycin	$C_{38}H_{69}NO_{13}$	747.953	81103-11-9	3–4 h
Clindamycin	$C_{18}H_{33}ClN_2O_5S$	424.983	18323-44-9	2–3 h

Continue Table 1

Compound	Formula	Molecular mass [g/mol]	CAS	Half-life
Cloxacillin	$C_{19}H_{18}ClN_3O_5S$	435.881	61-72-3	0.5–1 h
Doxycycline	$C_{22}H_{24}N_2O_8$	444.435	564-25-0	18–22 h
Enrofloxacin	$C_{19}H_{22}FN_3O_3$	359.4	93106-60-6	1.5–6 h
Erythromycin	$C_{37}H_{67}NO_{13}$	733.927	114-07-8	0.8–3 h
Lincomycin	$C_{18}H_{34}N_2O_6S$	406.537	154-21-2	4.5–6.5 h
Lomefloxacin	$C_{17}H_{19}F_2N_3O_3$	351.348	98079-51-7	8 h
Norfloxacin	$C_{16}H_{18}FN_3O_3$	319.331	70458-96-7	3–4 h
Ofloxacin	$C_{18}H_{20}FN_3O_4$	361.368	82419-36-1	9 h
Oxytetracycline	$C_{22}H_{24}N_2O_9$	460.434	79-57-2	6–8 h
Penicillin G	$C_{16}H_{18}N_2O_4S$	334.39	61-33-6	0.4–0.9 h
Penicillin V	$C_{16}H_{18}N_2O_5S$	350.39	87-08-1	0.5–0.7 h
Roxithromycin	$C_{41}H_{76}N_2O_{15}$	837.047	80214-83-1	12 h
Sulfadiazine	$C_{10}H_{10}N_4O_2S$	250.277	68-35-9	–
Sulfadimethoxine	$C_{12}H_{14}N_4O_4S$	310.329	122-11-2	–
Sulfamerazine	$C_{11}H_{12}N_4O_2S$	264.304	127-79-7	–
Sulfamethazine	$C_{12}H_{14}N_4O_2S$	278.33	57-68-1	–
Sulfamethizole	$C_9H_{10}N_4O_2S_2$	270.331	144-82-1	3–8 h
Sulfamethoxazole	$C_{10}H_{11}N_3O_3S$	253.278	723-46-6	10 h
Sulfathiazole	$C_9H_9N_3O_2S_2$	255.317	72-14-0	–
Tetracycline	$C_{22}H_{24}N_2O_8$	444.435	60-54-8	6–12 h
Trimethoprim	$C_{14}H_{18}N_4O_3$	290.318	738-70-5	8–11 h
Tylosin	$C_{46}H_{77}NO_{17}$	916.10	1401-69-0	–

3. Occurrence of antibiotics

Figure 2 shows the sources and routes of antibiotic contamination of aquatic and terrestrial environments. Unlike cytostatic drugs [2], the main sources of antibiotic pollution are not be only hospital and household sewage, but also, in an equally high degree, the wastewater from farms and animal production. In most cases, today's animal production is inherently associated with antibiotic therapy and often its main purpose is not so much a fight with possible animal diseases, but to accelerate their growth and ultimately increase production [26]. Hospital wastewater is also one of the main sources of pollution, especially if not pretreated before discharge to the municipal treatment plant. Concentrations of antibiotics in such waste can reach high values (10 000 ng/l cephalexin and 15 000 ng/l ciprofloxacin) [38]. However, the dominant sources of antibiotics are domestic sewage because the majority of infections requiring antibiotics is treated in-home after a visit to the clinic.

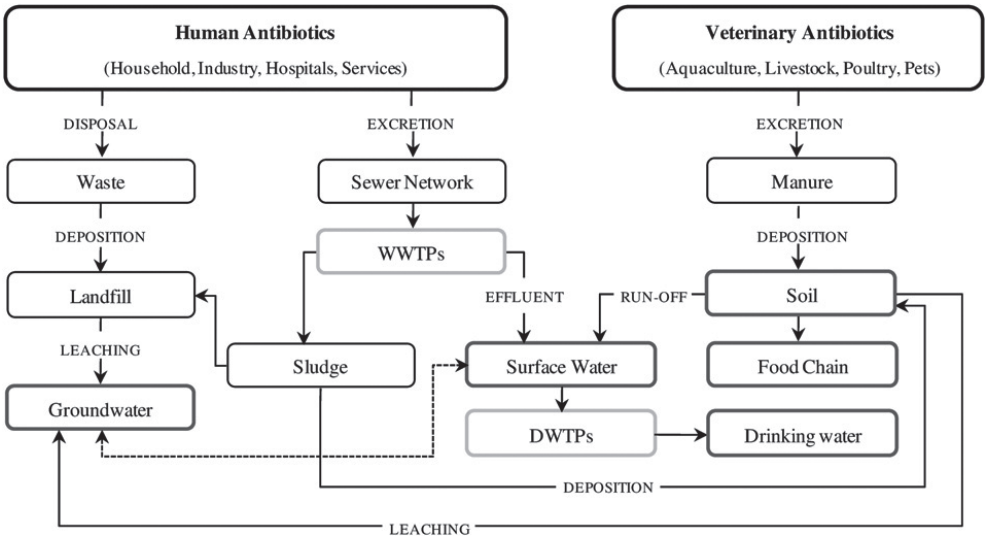

Fig. 2. Origin and principal contamination routes of human and veterinary antibiotics [13]

Excessive prescribing of antibiotics by GPs when it is not absolutely necessary, affects the growth of consumption and, consequently, increases the emissions of antibiotics to municipal treatment plants. Discontinuation of therapy before the scheduled end may cause only a partial elimination of pathogens from the body, while supporting the development of resistance to the antibiotic. Increased resistance to antibiotics poses not only a risk of creating bacterial strains completely resistant to the prescribed therapy, but also the use of increased doses of antibiotics (risk of dysbacteriosis) and the use of subsequent antibiotics when there are no health improvements. It is not surprising that, in the case of some municipal influent samples, the concentrations of antibiotics are higher than in the hospital wastewater (cephalexin 64 000 ng/l, penicillin V 13 800 ng/l, sulfamethoxazole 3000 ng/l, 4300 ng/l trimethoprim) [38].

Ineffective treatment of wastewater containing antibiotics results in their constant emission to effluent receivers. This is confirmed by the analysis of effluents, showing low to very high concentrations of antibiotics in the discharged wastewater effluent (ciprofloxacin 2,050 ng/l [20], ofloxacin 991 ng/l [19], sulfamethoxazole 2,000 ng/l [12], tylosine 3400 ng/l [38]). The result of pharmaceutical emission into the aquatic environment is its contamination and the risk of further migration of pollutants. Table 2 shows a summary of the analysis results showing the presence of antibiotics in the wastewater influents, wastewater effluents, surface and groundwater as well sludge and bottom sediments.

Not only the aquatic environment is being contaminated, as soils are being contaminated as well. One of the possibilities of sewage sludge management is its use in agriculture, which also creates certain risks. Particular attention should be payed to the risk of soil contamination as a result of this kind of sludge usage. Soil contamination can also occur as a result of leaching the residues of antibiotics by precipitation from landfills from animal production. There are known cases of significant antibiotic pollution of soil where the concentrations are higher than in sewage sludge (clarithromycin 67 μg/kg, ciprofloxacin 6–52 μg/kg, tetracycline 450–900 μg/kg) [17].

Table 2

Concentrations (min-max or max) of antibiotics in environmental samples

Compound	Influent (ng/l)	Effluent (ng/l)	Sludge µg/kg	Surface water (ng/l)	Groundwater (ng/l)	Sediments µg/kg
Amoxicillin	18-6940 [19],[38],[43]	30-50[19],[38]		200[38]		
Ampicillin	1805[24]	498[24]				
Azithromycin	98-711 [19],[42]	88-728 [19],[42]	146-599 [42]	2.1-569 [23],[33],[34],[42]	0.5-0.7 [33]	26.8-265 [11]
Cefaclor	6150[38]	1800[38]		200[38]		
Cephalexin	20-64000 [19],[38],[42]	10-1800 [19],[38],[42]		23-100 [38],[42]		
Chlor-tetracycline	0.14-970 [9],[19],[38]	0.3-250 [9],[19],[38]		2.6-68870[15],[17], [18],[32],[33],[38]	58-47444 [15],[33]	698.3[15]
Ciprofloxacin	0.82-1100 [6],[9],[16],[17], [19],[24],[38],[43]	0.4-2050 [9],[19],[16], [20],[24],[43]	2.09[43]	1.3-9660 [3],[11],[8],[15],[20],[32],[33], [34],[35],[38],[43]	0.28-40 [15],[20],[33]	6-2119 [15],[35],[37]
Clarithromycin	17.8-6524 [9],[19],[43]	3.5-621 [9],[12],[19],[43]	156[43]	0.89-2330[11],[12], [17],[23],[33],[34],[43]	0.5-0.7[33]	0.96-3.8 [11],[23]
Clindamycin	5.16-1870 [28],[38]	6.69-952 [28],[38]	2-80.6 [28],[29]	10-1000 [3],[38]		
Cloxacillin	15-4600 [19],[38]	700[38]				
Doxycycline	210-2480 [19],[38]	13.1-915 [7],[19],[38]		5.6-400 [7],[32],[33],[38]	2.7-64.2[33]	
Enrofloxacin	40[38]	2[38]		3.3-978.8 [15],[18],[32],[33],[38]	24.1-182.2 [15],[33]	82.1[15]
Erythromycin	15.5-10000 [6],[9],[16],[19],[21], [24],[43]	20-6000 [9],[12],[16],[19], [21],[43]	185[43]	0.78-3847 [6],[8],[12],[15],[17],[23], [33],[34],[43]	2.3-377.8[33]	2-26.7 [15],[23]
Lincomycin	15.2-1467 [6],[24],[28],[38]	3.92-300 [28],[38]	0.85-174 [28],[29]	19-21100 [6],[17],[38]		
Lomefloxacin				1.1-13.1[32],[33]	2.2-2.3[33]	
Norfloxacin	11.1-964 [6],[9],[19],[38],[42]	0.3-527 [9],[17],[19],[38],[42]	160-370 [42]	6.9-1150[8],[15],[17], [31],[32],[33],[35],[38],[42]	4.5-47.1 [15],[33]	6.8-801 [15],[35]
Ofloxacin	15.7-5560 [6],[7],[9],[19],[42],[43]	0.2-991 [7],[9],[19],[42],[43]	3.4-214 [42],[43]	0.65-11734.6 [6],[7],[8],[15],[31],[32] [33][34],[35],[42],[43]	1.9-382.2 [15],[33]	2.7-370.6 [15],[35],[37]
Oxytetracycline	0.2-350 [6],[9],[19],[38]	0.1-70[9],[38]		1.23-361107 [11],[15],[18],[32],[33],[38],[43]	4.1-1364.7 [15],[33]	162673[15]
Penicillin G	10[38]	300[38]		250[38]		
Penicillin V	160-13800 [19],[38]	80-2000[19],[38]		10[38]		
Roxithromycin	4.3-1500 [9],[19],[38],[42]	2.8-1000 [9],[12],[19],[38],[42]	14-87[42]	2-2251.6 [6],[12],[15],[17],[33],[38],[42]	2.9-146.2 [15],[33]	2581.8[15]

Continue Table 2

Compound	Influent (ng/l)	Effluent (ng/l)	Sludge µg/kg	Surface water (ng/l)	Groundwater (ng/l)	Sediments µg/kg
Sulfadiazine	0.14-5150 [7],[9],[19],[24]	15.3-194 [9],[19],[24]		1.3-4130 [7],[15],[17],[32],[33]	9.6-46.3 [15],[33]	5.6[15]
Sulfadimethoxine	0.2-460[9],[19]	0.02-2.1[9]		1.1-80[18],[32]		
Sulfamerazine	0.4-1530[9],[19]	3,6[9]		4.5-11.0[15],[33]	0.6-7.0[33]	5.7[15]
Sulfamethazine	1.1-4010 [6],[7],[9],[16],[19]	0.5-6.2[9]		0.7-580.4 [6],[7],[15],[18],[32],[33]	0.4-240 [12],[17],[33]	2.2[15]
Sulfamethizole	0.6-7.3[9]	0.3-1.2[9]				
Sulfamethoxazole	0.4-7910 [6],[7],[9],[16],[19],[21], [24],[28],[38],[43]	0.3-2000 [1],[7],[9],[12],[16], [19],[20],[21],[24], [27],[28],[38],[43],	31[28]	0.2-6000 [3],[6],[7],[8],[12],[15],[17],[18], [20],[21],[23],[31],[32],[3 3],[34], [35],[36],[38],[43]	0.1-1110 [12],[15],[17],[20], [21],[22],[33],[35]	2.4[15]
Sulfathiazole	0.8-10570 [9],[19],[38]	0.4-600 [9],[19],[38]		3.7-123 [38],[15],[33],[18]	1.4[33]	1.7[15]
Tetracycline	0.1-1300 [6],[9],[16],[19],[38]	0.09-850 [9],[16],[19],[38]		7.2-25537 [3],[38],[15],[33],[18],[32]	6-1082 [15],[17],[33]	6.5-16799 [15],[35]
Trimethoprim	0.14-6800 [6],[9],[16],[19],[21] [24],[28],[30],[38]	0.7-3050 [9],[12],[16],[19],[20] [21],[24],[27],[28],[38]	6.7-7.4 [29]	0.1-1808 [3],[6],[8],[12],[15],[17],[18], [20],[21],[23],[31],[33],[34], [35],[36],[38]	1.4-18 [15],[20],[21],[33]	1.6-87.55 [15],[22],[35]
Tylosin	44-60[6],[38]	3400[38]		9-187[6],[15],[17],[38]		11.2[15]

Unlike other types of pharmaceuticals and similar to estrogen [25], some antibiotics have negative effects on aquatic organisms at relatively low concentrations. PNEC (Predicted No Effect Concentration) estimated for ciprofloxacin, ofloxacin, sulfamethoxazole and tetracycline are respectively 5, 11.3, 27 and 90 ng/l [15]. It means that, in the analyzed natural water samples, concentrations of antibiotics significantly exceeded (220x for sulfamethoxazole, 280 for tetracycline, 1900x for ciprofloxacin) the level estimated as safe for the tested organisms. Regarding the concern for the environment and aquatic organisms that live in it, we should not allow the continuous emission of antibiotics into the environment.

The presence of antibiotics in the source water for the water purification plants poses a risk of exposure to consumers of drinking water. Even very low levels of antibiotics consumed with the water can have a negative impact on the human body and its natural bacterial flora. In addition, it should be kept in mind that a low dose of antibiotic will not be able to eliminate pathogens from the body, and at the same time can support the formation of resistance to antibiotics. Unfortunately, antibiotics infiltrate into the water intended for human consumption, as it was confirmed by analysis - 0.2 ng/l clarithromycin, 5 and 13.8 ng/l erythromycin, 19.8 ng/L trimethoprim [5] and 12.7, 13.7 [5] and 66 ng/l sulfamethoxazole [17].

4. Conclusions

Antibiotics are commonly found in the environment, which is the result not only of excessive consumption of pharmaceuticals in health care, but also their use in animal production to increase productivity. The data from Table 2 shows that antibiotics have the potential to pollute almost every part of the aquatic environment – surface waters, groundwater, bottom sediments. The first step to protect the environment should be preventive measures to reduce the use of antibiotics or possibly withdraw them from use if they are not absolutely necessary. It seems crucial to point out that agriculture is a big contributor to antibiotic pollution of the natural environment and withdrawing from excessive use of antibiotics in farms would be beneficial not only for the environment, but also for consumers of the produced meat.

Next, hospital wastewater should be initially pretreated, with particular focus put on the elimination and degradation of antibiotics before their discharge to municipal treatment plants. Another source of antibiotics, the household sewage, is a problem far more difficult to solve. Reducing consumption of antibiotics in households requires a greater awareness of primary care physicians and choosing the therapy without the use of antibiotics. The sewage system for households is incomparably more diffused than in the case of hospitals – hospital waste produced by all patients can be collected and purified. For residential development, such a possibility does not exist. The only possibilities of elimination of antibiotics from household sewage are efficient and effective processes used in municipal wastewater treatment plants.

Unfortunately, not all antibiotics are effectively eliminated from the wastewaters, thus environmental pollution occurs. Antibiotics present in surface waters, being the effluent receivers, seep into groundwater, accumulate in the sediments, and in some cases, they penetrate into the drinking water. In these cases, there is a risk of unconscious antibiotic consumption at very low doses, which may lead to the formation of resistance to the consumed antibiotic. We should make every effort to decrease the emission of antibiotics into the environment, for example by improving the efficiency of municipal wastewater treatment processes.

Although it seems natural to focus primarily on providing the highest purity and quality of drinking water, it should not be our only goal. Ignoring the problem of antibiotic pollution of the environment, especially water, can have serious consequences, such as the development of resistance of pathogenic bacteria and wide transfer of resistance genes between different types of bacteria. The emergence of strains of pathogenic bacteria resistant to most or at least some of the antibiotics used in therapy poses a very serious threat to human life and health.

References

[1] Alidina M., Hoppe-Jones C., Yoon M., Hamadeh A.F., Li D., Drewes J.E., *The occurrence of emerging trace organic chemicals in wastewater effluents in Saudi Arabia*, Science of the Total Environment, Vol. 478, 2014, 152–162.

[2] Balcerzak W., Rezka P., *Occurrence of anti-cancer drugs in the aquatic environment and efficiency of their removal – the selected issues*, Technical Transactions, vol. 1-Ś/2014, 11–18.

[3] Batt A.L., Bruce I.B., Aga D.S., *Evaluating the vulnerability of surface waters to antibiotic contamination from varying wastewater treatment plant discharges*, Environmental Pollution, Vol. 142, 2006, 295–302.
[4] Bergeron S., Boopathy R., Nathaniel R., Corbin A., LaFleur G., *Presence of antibiotic resistant bacteria and antibiotic resistance genes in raw source water and treated drinking water*, International Biodeterioration& Biodegradation, Vol. 102, 2015, 370–374.
[5] Białk-Bielińska A., Kumirska J., Borecka M., Caban M., Paszkiewicz M., Pazdro K., Stepnowski P., *Selected analytical challenges in the determination of pharmaceuticals in drinking/marine waters and soil/sediment*, Journal of Pharmaceutical and Biomedical Analysis, Vol. 121, 2016, 271–296.
[6] Chang X., Meyer M.T., Liu X., Zhao Q., Chen H., Chen J., Qiu Z., Yang L., Cao J., Shu W., *Determination of antibiotics in sewage from hospitals, nursery and slaughter house, wastewater treatment plant and source water in Chongqing region of Three Gorge Reservoir in China*, Environmental Pollution, Vol. 158, 2010, 1444–1450.
[7] Deng W., Li N., Zheng H., Lin H., *Occurrence and risk assessment of antibiotics in river water in Hong Kong*, Ecotoxicology and Environmental Safety, Vol. 125, 2016, 121–127.
[8] Dinh Q.T., Alliot F., Moreau-Guigon E., Eurin J., Chevreuil M., Labadie P., *Measurement of trace levels of antibiotics in river water using on-line enrichment and triple-quadrupole LC-MS/MS*, Talanta, Vol. 85, 2011, 1238–1245.
[9] Dong H., Yuan X., Wang W., Qiang Z., *Occurrence and removal of antibiotics in ecological and conventional wastewater treatment processes: A field study*, Journal of Environmental Management, Vol. 178, 2016, 11–19.
[10] Drugbank database (http://www.drugbank.ca) – online 25.05.2016.
[11] Feitosa-Felizzola J., Chiron S., *Occurrence and distribution of selected antibiotics in a small Mediterranean stream (Arc River, Southern France)*, Journal of Hydrology, Vol. 364, 2009, 50–57.
[12] Hirsch R., Ternes T., Haberer K., Kratz K.-L., *Occurrence of antibiotics in the aquatic environment*, Science of the Total Environment, Vol. 225, 1999, 109–118.
[13] Homem V., Santos L., *Degradation and removal methods of antibiotics from aqueous matrices – A review*, Journal of Environmental Management, Vol. 92, 2011, 2304–2347.
[14] Jiang L., Hu X., Xu T., Zhang H., Sheng D., Yin D., *Prevalence of antibiotic resistance genes and their relationship with antibiotics in the Huangpu River and the drinking water sources, Shanghai, China*, Science of the Total Environment, Vol. 458-460, 2013, 267–272.
[15] Jiang Y., Li M., Guo C., An D., Xu J., Zhang Y., Xi B., *Distribution and ecological risk of antibiotics in a typical effluent-receiving river (Wangyang River) in north China*, Chemosphere, Vol. 112, 2014, 267–274.
[16] Karthikeyan K.G., Meyer M.T., *Occurrence of antibiotics in wastewater treatment facilities in Wisconsin, USA*, Science of the Total Environment, Vol. 361, 2006, 196–207.
[17] Kemper N., *Veterinary antibiotics in the aquatic and terrestrial environment*, Ecological Indicators, Vol. 8, 2008, 1–13.
[18] Kim Y., Lee K.-B., Choi K., *Effect of runoff discharge on the environmental levels of 13 veterinary antibiotics: A case study of Han River and Kyangahn Stream,*

South Korea, Marine Pollution Bulletin, 2016, in press (http://dx.doi.org/10.1016/j.marpolbul.2016.03.011).

[19] Le-Minh N., Khan S.J., Drewes J.E., Stuetz R.M., *Fate of antibiotics during municipal water recycling treatment processes*, Water Research, Vol. 44, 2010, 4295–4323.

[20] Li W.C., *Occurrence, sources, and fate of pharmaceuticals in aquatic environment and soil*, Environmental Pollution, Vol. 187, 2014, 193–201.

[21] Luo Y., Guo W., Ngo H.H., Nghiem L.D., Hai F.I., Zhang J., Liang S., Wang X.C., *A review on the occurrence of micropollutants in the aquatic environment and their fate and removal during wastewater treatment*, Science of the Total Environment, Vol. 473–475, 2014, 619–641.

[22] Matongo S., Birungi G., Moodley B., Ndungu P., *Pharmaceutical residues in water and sediment of Msunduzi River, KwaZulu-Natal, South Africa*, Chemosphere, Vol. 134, 2015, 133–140.

[23] Moreno-Gonzalez R., Rodriguez-Mozaz S., Gros M., Barcelo D., Leon V.M., *Seasonal distribution of pharmaceuticals in marine water and sediment from a mediterranean coastal lagoon (SE Spain)*, Environmental Research, Vol. 138, 2015, 326–344.

[24] Papageorgiou M., Kosma C., Lambropoulou D., *Seasonal occurrence, removal, mass loading and environmental risk assessment of 55 pharmaceuticals and personal care products in a municipal wastewater treatment plant in Central Greece*, Science of the Total Environment, Vol. 543, 2016, 547–569.

[25] Rezka P., Balcerzak W., Kryłów M., *Occurrence of synthetic and natural estrogenic hormones in the aquatic environment*, Technical Transactions, vol. 3-Ś/2015, 47–54.

[26] Ronquillo M.G., Hernandez J.C.A., *Antibiotic and synthetic growth promoters in animal diets: Review of impact and analytical methods*, Food Control, 2016, 1–13, in press (http://dx.doi.org/10.1016/j.foodcont.2016.03.001).

[27] Salveson A., Rauch-Williams T., Dickenson E., Drewes J., Drury D., McAvoy D., Snyder S., *Trace organic compound indicator removal during conventional wastewater treatment*, IWA, Alexandria 2012.

[28] Subedi B., Balakrishna K., Sinha R.K., Yamashita N., Balasubramanian V.G., Kannan K., *Mass loading and removal of pharmaceutical and personal care products, including psychoactive and illicit drugs and artificial sweeteners, in five sewage treatment plants in India*, Journal of Environmental Chemical Engineering, Vol. 3, 2015, 2882–2891.

[29] Subedi B., Lee S., Moon H.-B., Kannan K., *Emission of artificial sweeteners, select pharmaceuticals, and personal care products through sewage sludge from wastewater treatment plants in Korea*, Environment International, Vol. 68, 2014, 33–40.

[30] Sui Q., Huang J., Deng S., Yu G., Fan Q., *Occurrence and removal of pharmaceuticals, caffeine and DEET in wastewater treatment plants of Beijing, China*, Water Research, Vol. 44, 2010, 417–426.

[31] Tamtam F., Mercier F., Le Bot B., Eurin Joelle, Dinh Q.T., Clement M.,Chevreuil M., *Occurrence and fate of antibiotics in the Seine River in various hydrological conditions*, Science of the Total Environment, Vol. 393, 2008, 84–95.

[32] Tang J., Shi T., Wu X., Cao H., Li X., Hua R., Tang F., Yue Y., *The occurrence and distribution of antibiotics in Lake Chaohu, China: Seasonal variations, potential source and risk assessment*, Chemosphere, Vol. 122, 2015, 154–161.

[33] Tong L., Huang S., Wang Y., Liu H., Li M., *Occurrence of antibiotics in the aquatic environment of Jianghan Plain, central China*, Science of the Total Environment, Vol. 497–498, 2014, 180–187.
[34] Valcarcel Y., Gonzalez Alonso S., Rodriguez-Gil J.L., Gil A., Catala M., *Detection of pharmaceutically active compounds in the rivers and tap water of the Madrid Region (Spain) and potential ecotoxicological risk*, Chemosphere, Vol. 84, 2011, 1336–1348.
[35] Vazquez-Roig P., Andreu V., Blasco C., Pico Y., *Risk assessment on the presence of pharmaceuticals in sediments, soils and waters of the Pego-Oliva Marshlands (Valencia, eastern Spain)*, Science of the Total Environment, Vol. 440, 2012, 24–32.
[36] Vazquez-Roig P., Blasco C., Pico Y., *Advances in the analysis of legal and illegal drugs in the aquatic environment*, Trends in Analytical Chemistry, Vol. 50, 2013, 65–77.
[37] Vazquez-Roig P., Segarra R., Blasco C., Andreu V., Pico Y., *Determination of pharmaceuticals in soils and sediments by pressurized liquid extraction and liquid chromatography tandem mass spectrometry*, Journal of Chromatography A, Vol. 1217, 2010, 2471–2483.
[38] Watkinson A.J., Murby E.J., Kolpin D.W., Constanzo S.D., *The occurrence of antibiotics in an urban watershed: From wastewater to drinking water*, Science of the Total Environment, Vol. 407, 2009, 2711–2723.
[39] Węgrzyn A., Machura M., Żabczyński S., *Możliwości usuwania środków cieniujących ze ścieków*, Ochrona Środowiska, Vol. 37 (1), 2015, 55–63.
[40] Xu L., Ouyang W., Qian Y., Su C., Su J., Chen H., *High-throughput profiling of antibiotics resistance genes in drinking water treatment plants and distribution systems*, Environmental Pollution, Vol. 213, 2016, 119–126.
[41] Zejc A., Gorczyca M., *Chemia leków*, PZWL, Warsaw 2009.
[42] Zhang H., Liu P., Feng Y., Yang F., *Fate of antibiotics during wastewater treatment and antibiotic distribution in the effluent receiving waters of the Yellow Sea, northern China*, Marine Pollution Bulletin, Vol. 73, 2013, 282–290.
[43] Zuccato E., Castiglioni S., Bagnati R., Melis M., Fanelli R., *Source, occurrence and fate of antibiotics in the Italian aquatic environment*, Journal of Hazardous Materials, Vol. 179, 2010, 1042–1048.

TECHNICAL TRANSACTIONS | CZASOPISMO TECHNICZNE
ENVIRONMENT ENGINEERING | ŚRODOWISKO
1-Ś/2016
DOI: 10.4467/2353737XCT.16.204.5953

PIOTR REZKA, WOJCIECH BALCERZAK*

OCCURRENCE OF ANTIDEPRESSANTS – FROM WASTEWATER TO DRINKING WATER

WYSTĘPOWANIE LEKÓW PRZECIWDEPRESYJNYCH – ZE ŚCIEKÓW DO WODY UZDATNIONEJ

Abstract

The article's subject is the presence of antidepressants in the wastewater and aquatic environment. The basic characteristics of selected antidepressants were presented. A review of the literature on the occurrence of these compounds in sewage influents and effluents, surface waters and sludge was made. As a general rule, drinking water should be free of any organic, especially pharmaceutical, contaminants. But according to data, the presence of antidepressants in source water for water purification plants poses a threat to their penetration to the water supply system and, eventually, to consumers of water intended for human consumption.

Keywords: *Selective Serotonin Reuptake Inhibitors, SSRI, wastewater, surface water, drinking water, sewage sludge*

Streszczenie

W artykule omówiono zagadnienie występowania leków przeciwdepresyjnych w ściekach i środowisku wodnym. Dokonano przeglądu literatury dotyczącej występowania tych związków w ściekach surowych i oczyszczonych oraz wodach powierzchniowych, a także w osadach z oczyszczalni. Jak wynika z danych literaturowych, obecność antydepresantów w wodzie surowej ujmowanej przez stacje uzdatniania wody stwarza realne zagrożenie dla systemów wodociągowych, a w następstwie dla odbiorców wody przeznaczonej do spożycia.

Słowa kluczowe: *selektywne inhibitory zwrotnego wychwytu serotoniny, ścieki, wody powierzchniowe, wody, woda do picia, osady ściekowe*

* M.Sc. Eng. Piotr Rezka, Assoc. Prof. D.Sc. Ph.D. Wojciech Balcerzak, Institute of Water Supply and Environmental Protection, Faculty of Environmental Engineering, Cracow University of Technology.

1. Introduction

The subject of pharmaceuticals and their presence in the wastewater or the environment has become one of the most analyzed problems over the years. Despite the passing years since the first mention of drug pollution of the aquatic environment, treatment technologies that can completely eliminate the issue of their emissions still have not been implemented. On the one hand, the difficulty lies in the variability of the composition of the wastewater supplied to the treatment plant and various properties of the impurities in them, such as low adsorbability and biodegradability of cytostatic drugs [5]. On the other hand, economic considerations are the ones that restrict the implementation of advanced and modern methods of wastewater treatment, which will most likely entail a significant increase in the costs and an increase in the prices of sewage management. Insufficient elimination and degradation of pharmaceutical pollutants during wastewater treatment poses a risk of emission of these substances into the aquatic environment. One group of pharmaceuticals widely used in medicine is antidepressants. They are found in the environmental samples in one of the largest quantities (8%) out of all the detected pharmaceuticals [49].

2. Characteristics of antidepressants

Drugs for depression are a type of psychotropic drugs, which are substances that affect the mental processes of humans that refer to, among other things, affecting mood, sedation, stimulation, thinking and behavior [53]. Most antidepressants in use are Selective Serotonin Reuptake Inhibitors (SSRIs), which act to regulate the levels of serotonin, which is a neurotransmitter (a chemical compound of transmitting signals between neurons). Antidepressants are used to treat depression, anxiety, panic disorder, eating disorder, obsessive compulsive disorder and social phobia [11]. The most commonly used antidepressants and fluoxetine metabolite norfluoxetine as well as their basic characteristics (e.g. Chemical Abstracts Service (CAS) number and half-life) are presented in Table 1.

3. Occurrence of antidepressants

Antidepressant pharmaceuticals are typical anthropogenic pollutants because those are not the type of substances naturally occurring in the environment. For this reason, the main sources of these drugs in wastewater and natural waters are households and hospitals. Fig. 1 presents the sources and paths of emission of pharmaceutical impurities in the environment. Hospital wastewater has a much higher concentration range of antidepressants, but in their case, there is a possibility for pre-treatment prior to their transport to the treatment plant. In the case of municipal wastewater produced by people in their homes, there is no possibility for pre-treatment. Metabolized, or in the form of primary, antidepressants are transported via a sewer system to municipal wastewater treatment plants, where they should be removed from the wastewater during treatment processes.

Table 1

Characteristics of selected antidepressants [13]

Name	Formula	Molecular mass [g/mol]	CAS No.	Half-life
Amitriptyline	$C_{20}H_{23}N$	277.4	50-48-6	10–50 h
Bupropion	$C_{13}H_{18}ClNO$	239.7	34841-39-9	24 h
Citalopram	$C_{20}H_{21}FN_2O$	324.4	59729-33-8	35 h
Dosulepin	$C_{19}H_{21}NS$	295.4	113-53-1	14–54 h
Fluoxetine	$C_{17}H_{18}F_3NO$	309.3	54910-89-3	1–6 d
Fluvoxamine	$C_{15}H_{21}F_3N_2O_2$	318.3	54739-18-3	15.6 h
Norfluoxetine(m)	$C_{16}H_{16}F_3NO$	295.3	126924-38-7	4–16 d
Nortriptyline	$C_{19}H_{21}N$	263.4	72-69-5	16–90 h
Paroxetine	$C_{19}H_{20}FNO_3$	329.4	61869-08-7	21–24 h
Risperidone	$C_{23}H_{27}FN_4O_2$	410.5	106266-06-2	20–24 h
Sertraline	$C_{17}H_{17}Cl_2N$	306.2	79617-96-2	25–26 h
Venlafaxine	$C_{17}H_{27}NO_2$	277.4	93413-69-5	5 h

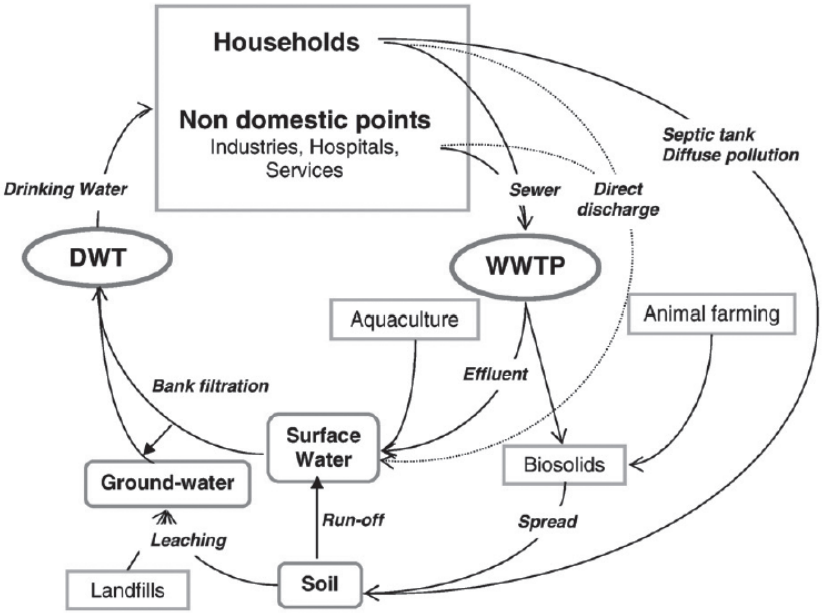

Fig. 1. Potential sources of pharmaceuticals in aquatic environment [32]

Table 2

Concentrations (min-max or mean) of detected antidepressants

Compound	Influent (ng/l)	Effluent (ng/l)	Surface water (ng/l)
Amitriptyline	341-5143[24] 106-2092[33] 35.8-1055.5[4] 3100[48] 659[3] 138[28]	53-357[24] 18.2-243.0[4] 66-207[33] 140[48] 129.8[3] 83[47] 71[28]	0.5-72[33] 1.0-2.0[20] 29.5[3]
Bupropion	17.1-378[41] 74[35]	28-4300[50] 7.3-264[41] 57[35]	–
Citalopram	27-180[19] 35.1-170[41] 99.2-213.6[38] 650.0[14] 236[28] 180[35] 4.0[52]	21-520[50] 104-404[41] 30-120[19] 82.8-95.6[38] 173[28] 120[35] 53.0[14] 5.0[52]	40-8000[16] 0.5-219[37] 4-206[30] 26-160[44] 3-120[1] 2-95[35] 40-90[36] 4-17[18] 3.4-11.5[27]
Dosulepin	17.2-673.3[4] 227.6[3]	3.1-125.1[4] 57.2[3]	0.5-32[33] 9.7[3]
Fluoxetine	17-3645[34] 4.9-175.9[4] 20-91[30] 105.8-157.4[38] 8.0-30.0[42] 1.1-18.7[45] 3.1-3.5[27] 0.4-2.4[46] 540[48] 86.1[3] 51.0[14] 26[22] 24[35] 18.0[28] 18.0[29]	19-929[10] 11-76[50] 50-99[31] 40-73[7] 5.6-44.9[4] 0.6-8.4[45] 2.0-3.7[27] 0.12-1.3[46] 240[48] 29.3[3] 26.0[14] 16[22] 14[29] 11.0[28] 1.7[25] 8[35]	4-141[30] 0.6-66.1[15] 8.0-44.0[1] 0.5-43.2[37] 12.0-20.0[36] 5.8-14[33] 3.2-5.5[18] 1.0-2.0[20] 0.42-1.3[27] 12.0[26] 9.0[3] 3.0[22]
Fluvoxamine	0.4-3.9[46] 0.8-1.7[45] 5.2[28]	0.49-0.8[45] 0.15-0.8[46] 3.4[28]	0.5-4.6[37] 0.5-0.8[45]

Continue Table 2

Compound	Influent (ng/l)	Effluent (ng/l)	Surface water (ng/l)
Norfluoxetine(m)	3.4-118.0[4] 1.8-4.2[27] 62.8[3] 13[35] 12.0[48] 11.0[30] 9.1[28]	1.1-20.2[4] 1.7-1.8[27] 13.2[3] 10.0[48] 7.4[28] 1.0[35]	0.5-13.6[37] 1.2-1.3[27] 0.83-1.0[36] 4.0[30] 3.5[33]
Nortriptyline	6.9-185.8[4] 114.1[3] 18.0[28]	0.9-53.8[4] 32.9[3] 11.0[28]	0.8-19[33] 6.8[3]
Paroxetine	14-32228[34] 137.9-186.4[38] 45-105[39] 2.9-12.9[45] 4.6-5.3[27] 16.0[48] 9.1[35] 8.0[28]	60-240[39] 1.0-11.7[45] 4.3-5.2[27] 1141[10] 81.1[38] 13.0[7] 5.6[28] 7.0[48] 2.3[35]	2.1-3.0[36] 1.3-3.0[27] 0.5-5.8[37] 0.6-1.4[45] 90[51]
Risperidone	364[47]	154[47]	–
Sertraline	31.6-114[41] 14.0-34.0[30] 7-27[19] 6.0-6.1[27] 8.4-19.8[45] 100.4[38] 49[35] 20.0[28]	15.7-88.3[41] 57-87[7] 3-6[19] 3.7-14.6[45] 5.1-5.8[27] 12.0[28] 9.0[35]	0.5-37.5[37] 33-49[36] 6.0-17.0[30] 0.84-2.4[27] 11.0[23]
Venlafaxine	40-980[21] 120-800[19] 169-609[41] 28.8-446.1[4] 121-529[42] 1343[28] 403[47] 352.7[14] 260[35] 249[3]	12-5500[50] 120-1110[19] 60-550[21] 209-553[41] 21.4-285.1[4] 1087[28] 365[47] 220.3[14] 220[35] 187.5[3]	100-1003[44] 0.8-250[18] 1-202[2] 11-180[35] 1.1-85[33] 35.1[3]

However, the efficiency of antidepressant removal in municipal sewage treatment plants is not high enough. Despite the relatively high efficiency of paroxetine elimination (over 90%), most anti-depression drugs are eliminated in an average degree: more than 25% for

venlafaxine, 40–90% for fluoxetine, 60–80% for amitriptyline; also in the case of metabolite norfluoxetine, 40–50% is eliminated [4, 24, 48]. It should be taken into consideration that, in some wastewater treatment plants, the removal efficiencies can be drastically lower.

Insufficient efficiency of processes used in wastewater treatment poses a risk of the emission of pharmaceuticals into the recipient rivers, which was confirmed by the analysis results by Baker and Kasprzyk-Hordern, showing an increase in the concentration of the analyzed antidepressants in water samples collected from rivers upstream and downstream from the point of effluent discharge [4]. Some substances (fluoxetine and its metabolite) were present only in downstream samples taken after effluent discharge (lack of detection in upstream samples). In most cases, the increase in the concentration range of a few to several ng/l, whereas the sample obtained in the vicinity of one of the treatment plants showed significant increases in the concentration of dosulepin (increase from 1.7 to 32.2 ng/l), venlafaxine (3.6 to 47.3 ng/l) and amitriptyline (4.9 to 71.0 ng/l). Table 2 presents a wide review of analysis results that confirm the presence of antidepressants in raw and treated wastewater and surface waters.

Regular emission of pharmaceuticals from wastewater treatment plants into rivers results in the contamination of water and exposure of aquatic organisms to these substances and their potential storage in the tissues of fish. Studies conducted in the USA on fish living in an effluent-impacted river showed the presence of fluoxetine, norfluoxetine, paroxetine and sertraline in the meat, brain and liver of the fish in quantities of 0.1–10 mg/kg [9]. Antidepressants in the fish meat have also been detected in Canada, where the analysis showed 0.14–1.02 mg/kg of fluoxetine, 0.15–1.08 mg/kg norfluoxetine and 0.48–0.58 mg/kg paroxetine [12]. Consumption of contaminated fish by humans may pose a risk to their health, especially in the case of allergy to the drug. In addition, the potential impact of even low concentrations of antidepressants on the human body should not be underestimated. These results allow to presume that frequent consumption of fish caught in effluent-impacted rivers is at least risky from the human health point of view.

The tendency to the accumulation of the organic contamination in sediments and soils poses a risk of contamination in agricultural use of sludge produced in the wastewater treatment plants. In addition, antidepressants that are present in surface waters can accumulate in sediments, which is confirmed by the analysis of sludge from wastewater treatment showing (per kg dry weight) concentrations of fluoxetine 170 ng/kg [17]; amitriptyline 263–583 μg/kg, citalopram 95–1381 μg/kg, fluoxetine 34–152 μg/kg, norfluoxetine 8.9–60 μg/kg, nortriptyline 22–61 μg/kg, paroxetine 11–70 μg/kg, sertraline 203–528 μg/kg and venlafaxine 289–499 μg/kg [28]; fluoxetine and venlafaxine less than 90 μg/kg [14]; bupropion 7.07–46.2 μg/kg, citalopram 131–429 μg/kg, sertraline 788–1993 μg/kg and venlafaxine 66.6–162 μg/kg [41]. The use of sludge of such quality in agriculture could result in soil pollution, which in combination with the possible migration of antidepressants from surface water, may result in their presence in groundwater, like in United States – 56 ng/l of fluoxetine in groundwater [6].

4. Antidepressants in drinking water

The presence of pharmaceuticals in surface and groundwater sources of raw water for drinking water treatment pose a risk of these compounds penetrating to water intended for human consumption. The use of advanced methods of purifying water should result in the

total removal of pharmaceutical impurities. However, an analysis of the finished water shows possible exposure to the effects of antidepressant for drinking water recipients. In the Polish capital, Warsaw, citalopram (1.5 ng/l) and venlafaxine (0.5–1.9 ng/l) were detected in tap water [18]; in USA, risperidone 0.34 ng/l in finished water (Snyder 2008) and fluoxetine 0.64 ng/l with norfluoxetine 0.77 ng/l in tap water (Benotti et al. 2009); in France amitriptyline 1.4 ng/l [43] and in Spain venlafaxine 9 ng/l also in tap water [44].

5. Conclusions

Extensive review of the literature confirms that the pharmaceuticals used, among others, to treat depression commonly occur in the aquatic environment. High, in some cases, concentrations of these compounds in the raw sewage indicate that these drugs are frequently prescribed. The effectiveness of the removal of these compounds during wastewater treatment is not satisfactory due to their continuous emission into the aqueous environment, especially recipient rivers. In addition, a clear tendency to accumulate in sludge and sediments means that using sludge from wastewater treatment in agriculture can pose a risk of soil pollution. This kind of sludge management should be approached with caution and thermal treatment seems advisable prior to using sludge for agricultural purposes.

Quoted analysis results of drinking water confirm that the phenomenon of antidepressant penetration to water intended for human consumption is not the domain of the underdeveloped countries or countries with low-advanced technologies for water treatment. As of today, it has not been clearly confirmed that the consumption of water containing low or very low amounts of antidepressants can affect the organisms of humans, especially people who are allergic to specific pharmaceuticals. Perhaps, there will be no serious allergic reaction, but there can be other unwanted side effects from the continuous supply of allergens. The best solution seems to be further work on the development of new or an improvement of the existing wastewater treatment technology, so that there is no pharmaceuticals emission into the aquatic environment.

References

[1] Alonso S.G., Catala M., Maroto R.R., Rodriguez J.L.G., Miguel A.G., Valvarcel Y., *Pollution by psychoactive pharmaceuticals in the rivers of Madrid metropolitan area (Spain)*, Environment International, Vol. 36, 2010, 195–201.

[2] Arlos M.J., Bragg L.M., Parker W.J., Servos M.R., *Distribution of selected antiandrogens and pharmaceuticals in a highly impacted watershed*, Water Research, Vol. 72, 2015, 40–50.

[3] Baker D.R., Kasprzyk-Hordern B., *Multi-residue analysis of drugs of abuse in wastewater and surface water by solid-phase extraction and liquid chromatography-positive electrospray ionization tandem mass spectrometry*, Journal of Chromatography A, Vol. 1218, 2011, 1620–1631.

[4] Baker D.R., Kasprzyk-Hordern B., *Spatial and temporal occurrence of pharmaceuticals and illicit drugs in the aqueous environment and during wastewater treatment: New developments*, Science of the Total Environment, Vol. 454-455, 2013, 442–456.

[5] Balcerzak W., Rezka P., *Occurrence of anti–cancer drugs in the aquatic environment and efficiency of their removal – the selected issues*, Technical Transactions, vol. 1–Ś/2014, 11–18.

[6] Barnes K.K., Kolpin D.W., Furlong E.T., Zaugg S.D., Meyer M.T., Barber L.B., *A national reconnaissance of pharmaceuticals and other organic wastewater contaminants in the United States-I) Groundwater*, Science of the Total Environment, Vol. 402, 2008, 192–200.

[7] Batt A.L., Kostich M.S., Lazorchak J.M., *Analysis of ecologically relevant pharmaceuticals in wastewater and surface water using selective solid-phase extraction and UPLC/MS/MS*, Analytical Chemistry, Vol. 80, 2008, 5021–5030.

[8] Benotti M.J., Trenholm R.A., Vanderford B.J., Holady J.C., Stanford B.D., Snyder S.A., *Pharmaceuticals and endocrine disrupting compunds in U.S. drinking water*, Environmental Science and Technology, Vol. 43, 2009, 597–603.

[9] Brooks B.W., Chambliss C.K., Stanley J.K., Ramirez A., Banks K.E., Johnson R.D., Lewis R.J., *Determination of select antidepressants in fish from an effluent-dominated stream*, Environmental Toxicology and Chemistry, Vol. 24, 2005, 464–469.

[10] Bueno M.J.M., Aguera A., Gomez M.J., Hernando M.D., Reyes J.F.G., Alba A.R.F., *Application of liquid chromatography/quadrupole-linear ion trap mass spectrometry and time-of-flight mass spectrometry to the determination of pharmaceuticals and related contaminants in wastewater*, Analytical Chemistry, Vol. 79, 2007, 9372–84.

[11] Caracciolo A.B., Topp E., Grenni P., *Pharmaceuticals in the environment: Biodegradation and effects on natural microbial communities. A review*, Journal of Pharmaceutical and Biomedical Analysis, Vol. 106, 2015, 25–36.

[12] Chu S., Metcalfe C.D., *Analysis of paroxetine, fluoxetine and norfluoxetine in fish tissues using pressurized liquid extraction, mixed mode solid phase extraction cleanup and liquid chromatography-tandem mass spectrometry*, Journal of Chromatography A, Vol. 1163, 2007, 112–118.

[13] Drugbank database (http://www.drugbank.ca) – online 27.04.2016.

[14] Evans S.E., Davies P., Lubben A., Kasprzyk-Hordern B., *Determination of chiral pharmaceuticals and illicit drugs in wastewater and sludge using microwave assisted extraction, solid-phase extraction and chiral liquid chromatography coupled with tandem mass spectrometry*, Analytica Chimica Acta, Vol. 882, 2015, 112–126.

[15] Fernandez C., Gonzalez-Doncel M., Pro J., Carbonell G., Tarazona J.V., *Occurrence of pharmaceutically active compounds in surface waters of the Henares-Jarama-Tajo river system (Madrid, Spain) and a potential risk characterization*, Science of the Total Environment, Vol. 408, 2010, 543–551.

[16] Fick J., Soderstrom H., Lindberg R.H., Phan C., Tysklind M., Larsson D.G.J., *Contamination of surface ground and drinking water from pharmaceutical production*, Environmental Toxicology and Chemistry, Vol. 28, 2009, 2522–2527.

[17] Gardner M., Jones V., Comber S., Scrimshaw M.D., Coello-Garcia T., Cartmell E., Lester J., Ellor B., *Performance of UK wastewater treatment works with respect to trace contaminants*, Science of the Total Environment, Vol. 456-457, 2013, 359–369.

[18] Giebułtowicz J., Nałęcz-Jawecki G., *Occurrence of antidepressant residues in the sewage-impacted Vistula and Utrata rivers and in tap water in Warsaw (Poland)*, Ecotoxicology and Environmental Safety, Vol. 104, 2014, 103–109.

[19] Golovko O., Kumar V., Fedorova G., Randak T., Grabic R., *Seasonal changes in antibiotics, antidepressants/psychiatric drugs, antihistamines and lipid regulators in a wastewater treatment plant*, Chemosphere, Vol. 111, 2014, 418–426.

[20] Gonzalez-Rey M., Tapie N., Le Menach K., Devier M.-H., Budzinski H., Bebianno M.J., *Occurrence of pharmaceutical compounds and pesticides in aquatic systems*, Marine Pollution Bulletin, Vol. 96 (1–2), 2015, 384–400.

[21] Gracia-Lor E., Sancho J.V., Serrano R., Hernandez F., *Occurrence and removal of pharmaceuticals in wastewater treatment plants at the Spanish Mediterranean area of Valencia*, Chemosphere, Vol. 87, 2012, 453–462.

[22] Gros M., Petrovic M., Barcelo D., *Tracing pharmaceutical residues of different therapeutic classes in environmental waters by using liquid chromatography/ quadrupole-linear ion trap mass spectrometry and automated library searching*, Analytical Chemistry, Vol. 81, 2009, 898–912.

[23] Huerta-Fontela M., Galceran M.T., Ventura F., *Occurrence and removal of pharmaceuticals and hormones through drinking water treatment*, Water Research, Vol. 45, 2011, 1432–1442.

[24] Kasprzyk-Hordern B., Dinsdale R.M., Guwy A.J., *The removal of pharmaceuticals, personal care products, endocrine disruptors and illicit drugs during wastewater treatment and its impacts on the quality of receiving waters*, Water Research, Vol. 43, 2009, 363–380.

[25] Kim S.D., Cho J., Kim I.S., Vanderford B.J., Snyder S.A., *Occurrence and removal of pharmaceuticals and endocrine disruptors in South Korean surface, drinking and waste waters*, Water Research, Vol. 41, 2007, 1013–1021.

[26] Kolpin D.W., Furlong E.T., Meyer M.T., Thurman E.M., Zaugg S.D., Barber L.B., Buxton H.T., *Pharmaceuticals, hormones and other organic wastewater contaminants in US streams, 1999–2000: a national reconnaissance*, Environmental Science and Technology, Vol. 36, 2002, 1202–1211.

[27] Lajeunesse A., Gagnon C., Sauve S., *Determination of basic antidepressants and their N-desmethyl metabolites in raw sewage and wastewater using solid-phase extraction and liquid chromatography-tandem mass spectrometry*, Analytical Chemistry, Vol. 80, 2008, 5325–5333.

[28] Lajuenesse A., Smyth S.A., Barclay K., Sauve S., Gagnon C., *Distribution of antidepressant residues in wastewater and biosolids following different treatment processes by municipal wastewater treatment plants in Canada*, Water Research, Vol. 46, 2012, 5600–5612.

[29] MacLeod S.L., Sudhir P., Wong C.S., *Stereoisomer analysis of wastewater-derived β-blockers, selective serotonin re-uptake inhibitors and salbutamol by high-performance liquid chromatography-tandem mass spectrometry*, Journal of Chromatography A, Vol. 1170, 2007, 23–33.

[30] Metcalfe C.D., Chu S., Judt C., Li H., Ken D.O., Servos M.R., Andrews D.M., *Antidepressants and their metabolites in municipal wastewater and downstream exposure in an urban watershed*, Environmental Toxicology and Chemistry, Vol. 29, 2010, 79–89.

[31] Metcalfe C.D., Miao X.S., Koenig B.G., Struger J., *Distribution of acidic and neutral drugs in surface waters near sewage treatment plants in the lower Great Lakes, Canada*, Environmental Toxicology and Chemistry, Vol. 22, 2003, 2881–2889.

[32] Mompelat S., Le Bot B., Thomas O., *Occurrence and fate of pharmaceutical products and by-products, from resource to drinking water*, Environment International, Vol. 35, 2009, 803–814.

[33] Petrie B., Barden R., Kasprzyk-Hordern B., *A review on emerging contaminants in wastewaters and the environment: Current knowledge, understudied areas and recommendations for future monitoring*, Water Research, Vol. 72, 2015, 3–27.

[34] Salgado R., Marques R., Noronha J.P., Mexia J.T., Carvalho G., Oehmen A., Reis M.A.M., *Assessing the diurnal variability of pharmaceutical and personal care products in a full-scale activated sludge plant*, Environmental Pollution, Vol. 159, 2011, 2359–2367.

[35] Schlusener M.P., Hardenbicker P., Nilson E., Schulz M., Viergutz C., Ternes T.A., *Occurrence of venlafaxine, other antidepressants and selected metabolites in the Rhine catchment in the face of climate change*, Environmental Pollution, Vol. 196, 2015, 247–256.

[36] Schultz M.M., Furlong E.T., *Trace analysis of antidepressant pharmaceuticals and their select degradates in aquatic matrixes by LC/ESI/MS/MS*, Analytical Chemistry, Vol. 80, 2008, 1756–1762.

[37] Schultz M.M., Furlong E.T., Kolpin D.W., Werner S.L., Schoenfuss H.L., Barber L.B., Blazer V.S., Norris D.O., Vajda A.M., *Antidepressant pharmaceuticals in two U.S. effluent-impacted streams: occurrence and fate in water and sediment and selective uptake in fish neural tissue*, Environmental Science and Technology, Vol. 44, 2010, 1918–1925.

[38] Silva L.J.G., Pereira A.M.P.T., Meisel L.M., Lino C.M., Pena A., *A one-year follow-up analysis of antidepressants in Portuguese wastewaters: Occurrence and fate, seasonal influence and risk assessment*, Science of the Total Environment, Vol. 490, 2014, 279–287.

[39] Sousa M.A., Goncalves C., Cunha E., Hajslova J., Alpendurada M.F., *Cleanup strategies and advantages in the determination of several therapeutic classes of pharmaceuticals in wastewater samples by SPE-LC-MS/MS*, Analytical and Bioanalytical Chemistry, Vol. 399, 2011, 807–822.

[40] Snyder S.A., *Occurrence, treatment and toxicological relevance of EDCs and pharmaceuticals in water*, Ozone: Science & Engineering Vol. 30, 2008, 65–69.

[41] Subedi B., Kannan K., *Occurrence and fate of select psychoactive pharmaceuticals and antihypertensives in two wastewater treatment plants in New York State, USA*, Science of the Total Environment, Vol. 514, 2015, 273–280.

[42] Tarcomnicu I., van Nuijs A.L.N., Simons W., Bervoets L., Blust R., Jorens P.G., Neels H., Covaci A., *Simultaneous determination of 15 top-prescribed pharmaceuticals and their metabolites in influent wastewater by reversed-phase liquid chromatography coupled to tandem mass spectrometry*, Talanta, Vol. 83, 2011, 795–803.

[43] Togola A., Budzinski H., *Multi-residue analysis of pharmaceutical compounds in aqueous samples*, Journal of Chromatography A, Vol. 1177, 2008, 150–158.

[44] Valcarcel Y., Alonso S.G., Rodriguez-Gil J.L., Gil A., Catala M., *Detection of pharmaceutically active compounds in the rivers and tap water of the Madrid*

Region (Spain) and potential ecotoxicological risk, Chemosphere, Vol. 84, 2011, 1336–1348.

[45] Vasskog T., Anderssen T., Pedersen-Bjergaard S., Kallenborn R., Jensen E., *Occurrence of selective serotonin reuptake inhibitors in sewage and receiving waters at Spitsbergen and in Norway*, Journal of Chromatography A, Vol. 1185, 2008, 194–205.

[46] Vasskog T., Berger U., Samuelsen P.J., Kallenborn R., Jensen R., *Selective serotonin reuptake inhibitors in sewage influents and effluents from TromsØ, Norway*, Journal of Chromatography A, Vol. 1115, 2006, 187–195.

[47] Vergeynst L., Haeck A., De Wispelaere P., Van Langenhove H., Demeestere K., *Multi-residue analysis of pharmaceuticals in wastewater by liquid chromatography-magnetic sector mass spectrometry: Method quality assessment and application in a Belgian case study*, Chemosphere, Vol. 119, 2015, S2–S8.

[48] Verlicchi P., Al. Aukidy M., Zambello E., *Occurrence of pharmaceutical compounds in urban wastewater: Removal, mass load and environmental risk after a secondary treatment-A review*, Science of the Total Environment, Vol. 429, 2012, 123–155.

[49] Węgrzyn A., Machura M., Żabczyk S., *Possibilities for Removal of Contrast Agents from Wastewater*, Ochrona Srodowiska, Vol. 37(1), 2015, 55–63.

[50] Writer J.H., Ferrer I., Barber L.B., Thurman E.M., *Widespread occurrence of neuro-active pharmaceuticals and metabolites in 24 Minnesota rivers and wastewaters*, Science of the Total Environment, Vol. 461–462, 2013, 519–527.

[51] Wu C., Witter J.D., Spongberg A.L., Czajkowski K.P., *Occurrence of selected pharmaceuticals in an agricultural landscape, western Lake Erie basin*, Water Research, Vol. 43, 2009, 3407–3416.

[52] Yuan S., Jiang X., Xia X., Zhang H., Zheng S., *Detection, occurrence and fate of 22 psychiatric pharmaceuticals in psychiatric hospital and municipal wastewater treatment plants in Beijing*, Chemosphere, Vol. 90, 2013, 2520–2525.

[53] Zejc A., Gorczyca M., *Chemia Leków*, Warszawa, PZWL, 2009.

TECHNICAL TRANSACTIONS | **CZASOPISMO TECHNICZNE**
ENVIRONMENT ENGINEERING | ŚRODOWISKO
1-Ś/2016

DOI: 10.4467/2353737XCT.16.205.5954

ANNA WASSILKOWSKA, ANNA CZAPLICKA, MICHAŁ POLUS*

IMAGING OF AQUATIC ORGANISMS USING VARIABLE-PRESSURE SEM

OBRAZOWANIE ORGANIZMÓW WODNYCH ZA POMOCĄ SEM ZE ZMIENNĄ PRÓŻNIĄ

Abstract

Examples of the use of a scanning electron microscope (SEM) to study organic matter in variable vacuum (VP) were presented. The organisms growing in water (e.g. *Chironomidae*), carried by water/wastewater (e.g. *Protozoa*, *Amoebozoa*) or inhabiting reservoirs (e.g. *Algae*), were investigated. The results indicate a good agreement between the predictions in source literature and the actual imaging quality in our VP-SEM experiments.

Keywords: scanning electron microscope, biological material, preparation

Streszczenie

Przedstawiono przykłady wykorzystania skaningowego mikroskopu elektronowego (SEM) do badań materii organicznej w warunkach zmiennej próżni (VP). Próbkami były organizmy rozwijające się w wodzie (np. *Chironomidae*), niesione przez wodę/ścieki (np. *Protozoa, Amoebozoa*), zasiedlające zbiorniki (np. *Algae*). Wyniki obrazowania uzyskane w naszych eksperymentach z użyciem VP-SEM wskazują zgodność z danymi literaturowymi.

Słowa kluczowe: elektronowy mikroskop skaningowy, materiał biologiczny, preparatyka

* Ph.D. Eng. Anna Wassilkowska, Ph.D. Eng. Anna Czaplicka, Ph.D. Nat. Michał Polus, Institute of Water Supply and Environmental Protection, Faculty of Environmental Engineering, Cracow University of Technology.

1. Introduction

The use of scanning electron microscope (SEM) in studies of biological, moist and wet samples requires its right settings of imaging conditions. Traditional SEMs operate with vacuums in the range of 10^{-3}–10^{-5} Pa, so naturally moist samples become dried out in a SEM chamber environment and lose important morphological features. Another serious problem is that the sample had to be electrically conductive in order to prevent charging under electron beam bombardment (electron beam accelerating voltage of 0.3–30 kV). There are only two options for biological sample studies [1, 2]: either modifying the environment inside the microscope column or stabilizing the specimens to make them sufficiently robust to withstand the SEM imaging conditions. Fig. 1 shows a diagram of preliminary preparation steps of biological sample for the SEM.

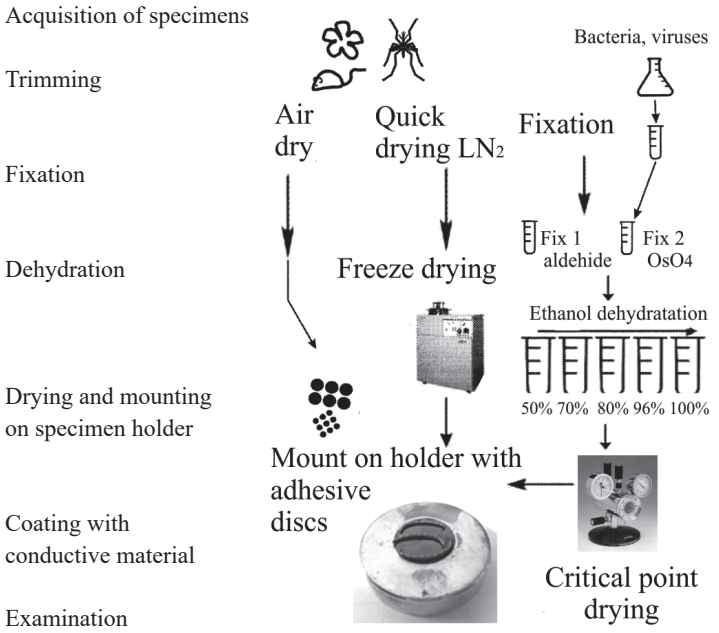

Fig. 1. Preparation methods of biological material for the SEM (according to [3, 4])

In ref. [1], there are numerous sample preparation principles suggested, concerning various impact stages: trimming, fixation, dehydration and different approaches to drying specimen, and final coating. However, structural damage and artifacts can occur prior to any microscopy analysis. It can happen that the end product is quite different from the original specimen. Thus, the design of *ab-initio* preparation protocols remains an empirical process around the sample concerned [1, 4].

Current SEMs are versatile in being able to operate in elevated gas pressure and low voltage, combined with sample cooling, together with specialized electron detectors

(to explore the high-pressure SE signals) etc. [5–11]. That gives new opportunities for examining specimens, which otherwise would be difficult to examine. The new environmental SEM generation (ESEM) permits also "*in-situ* experiments", i.e. the closest replication of the conditions associated with the problem under consideration [12].

The goal of the present work was to examine aquatic organisms exhibiting different humidity and dispersion in a variable-pressure scanning electron microscope (VP-SEM). A common fundamental step in sample preparation was the incorporation of the wet material on a conductive carbon substrate. This is a double side adhesive disk, used to support the sample on a standard flat specimen holder (Fig. 1). Then, samples were air-dried for varying periods of time. Some of them were vapor-deposited from the top with a thin gold layer. The incompletely dried samples were inserted in VP-mode without any coating. The capabilities of Peltier cooling device were used where necessary [11].

2. The specimens investigated

2.1. *Chironomidae*

Diptera is one of the major insect orders which is of great importance in terms of the environment. The *Chironomidae* are a family of nematoceran flies, class *Insecta*, order *Diptera*, suborder *Nematocera*, with a global distribution. It is characterized by high species diversity and is the major and very important component of zoobenthos in all freshwater ecosystems. *Chironomidae* may be a predator, algae eater, filter feeder, parasite or commensal of other invertebrates. It happens that *larvae* are predominant in the leaves and stems of aquatic plants. They are relatively rare in the semi-aqueous environment or in the seas [13]. The insect develops via complete metamorphosis from egg to adult, including larval stages and pupa.

A big role in bioindication of aquatic environment, e.g. in typology and biomonitoring of lakes, bioavailability and bioaccumulation of metals, is played by the *Chironomidae* larva (Fig. 2). Based on the quantitative and qualitative occurrence of particular *Chironomidae* species, the quality of the aquatic environment, its fertility and acidity can be evaluated [13, 16–23]. Due to the contamination of aquatic environment, the *Chironomidae* larva is susceptible to deformities of mouthparts (such as the asymmetry of the teeth or their displacement, the absence, addition or exacerbation of teeth or reducing the tooth surface), but also the changes in the DNA (there have been cases of changes in the structure and number of chromosomes) [24–27].

For research purposes, the larvae of species *Chironomus riparius* and *Glyptotendipes glaucus* were grown in the laboratory. The breeding aquatic environment consisted of 1 kg pure fine quartz sand (120–250 μm), to which a 1 g diet and 1 liter dechlorinated tap water was added. The culture medium was prepared two weeks in advance and placed in an aquarium under aeration. Next, the *Chironomidae* footbridge eggs were transferred from the natural water Reservoir Goczałkowice and inserted gently in aquarium under the water table surface. The larvae hatching from the eggs were fed with a suspension of fish food in dechlorinated water in concentration of 4 g/l. After the predetermined time (*Chironomidae* species have

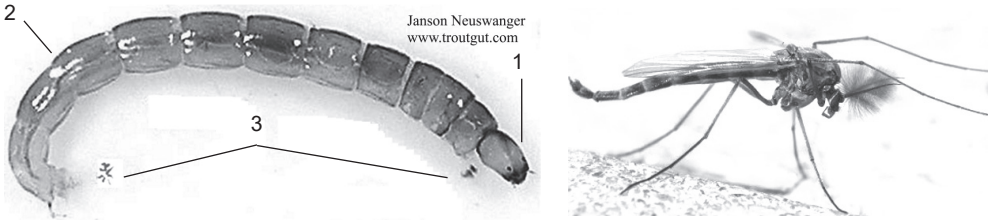

Fig. 2. Images of *Chironomidae* larva (left) and imago (right): 1 – capsule-like head distinct from the thorax; 2 – elongated body with distinct segments; 3 – two pairs of prolegs [14, 15]

different lengths of a life cycle, from a few days up to a year and even longer), the larva were collected by sieving the sediment through 1 mm mesh. The fished out individuals were further rinsed: first in tap water, than for 5 min. in deionized water, than for 10 min. in 0.001M of EDTA solution and finally, again for 5 minutes in deionized water. After the complete sequence of washing, specimens were preserved in formalin or alcohol.

Selected *Chironomidae* larvae, pupal exuvium and an imago were preserved from laboratory growth for SEM imaging. After few days of air-drying on a carbon tape, larvae were coated with conductive gold layer for high-vacuum SEM. Instead, pupal exuvium and an imago were dropped wet on a carbon tape of a specimen holder after rinsing, than put directly in a specimen chamber for VP-SEM.

2.2. Activated sludge

Activated sludge is a complex biological material, produced during sewage and wastewater treatments [28]. The granules (flocks) of activated sludge consist of various microorganisms, such as heterotrophic bacteria, algae, flagellate and amoebas [29, 30]. The quantitative relationship between bacteria, protozoa and some eumetazoa present in the flocks indicates the current condition of activated sludge. For VP-SEM, specimens were collected from an aeration tank of a sewage treatment plant. Single drops of sludge were air-dried on carbon discs direct on a specimen holder.

2.3. Protozoan intestinal parasites

Protozoan intestinal parasites are single cell microorganisms that cause infection of the gastrointestinal tract of humans and animals through the consumption of potable water containing live cysts/oocysts or through the contact with infected carriers (excrements) [31]. The most dangerous for humans are small intracellular parasites of epithelial cells of the gastrointestinal and respiratory tracts, which belong to vertebrates species *Cryptosporidium parvum* and *C. hominis* (phylum *Apicomplexa*, class *Coccidea*, order *Eucoccidiorida*, family *Cryptosporidiidae*, genus *Cryptosporidium*) or to flagellate species *Giardia intestinalis* (= *G. lamblia*, = *G. duodenalis*) [32–35]. In fluorescence light microscope, *Cryptosporidium* oocyst looks like a slightly oval object with a diameter about 5 μm, while *Giardia* cyst exhibit clearly elliptical shape with a typical width to length size approximately 8 to10 μm.

The differences in the size of individual oocyst yield maximum 1–2 μm regardless of the type of species. The wall of infective oocysts has typical thickness about 0.5 μm; it is multi-layered and resistant to mechanical forces and physicochemical factors. Inside the cysts, there are four sporozoites (with visible nuclei) and residual body; the visualization of them require special staining techniques for fluorescent microscope or different interference contrast microscopy [36, 37].

Due to the emission of huge amounts of oocysts from the host (up to several million oocysts per gram of feces) and the significant resistance to environmental factors (including traditional methods of water treatment that cannot destroy those parasites), oocysts are extremely widespread in surface waters and soil. The small dimensions of the invasive forms of the protozoa allow them to pass through some filters used in water treatment plants. The biology and epidemiology of waterborne outbreaks caused by parasitic protozoa, e.g. cryptosporidiosis, giardiasis or toxoplasmosis, are well documented in scientific literature [38, 39]. On the other hand, the standard techniques for detection of parasites in water are laborious and are not always guaranteed to succeed. Moreover, the dead and empty oocysts are detectable, making it difficult to determine their actual number in the sample.

The detection protocol for SEM involved:

- compaction of the biological material on membrane filters;
- purification of cysts/oocysts by gradient centrifugation;
- applying one drop of as-cleaned suspension on the carbon substrate;
- air drying on SEM specimen holder;
- coating with a thin gold layer (eventual);
- imaging in a high-vacuum mode of VP-SEM (SE and BSE detectors).

3. The advantage of VP-SEM

The essential idea of the VP-technique is shown in Fig. 3. The pumping differential aperture, placed inside the objective lens, enables lower pressure conditions in a specimen chamber of SEM. In a poor vacuum, any gas including water vapor may be present, thus gas molecules interact with incident and emerging electrons. These become ionized and produce a cloud of cations that neutralizes any charge of electrically insulating samples.

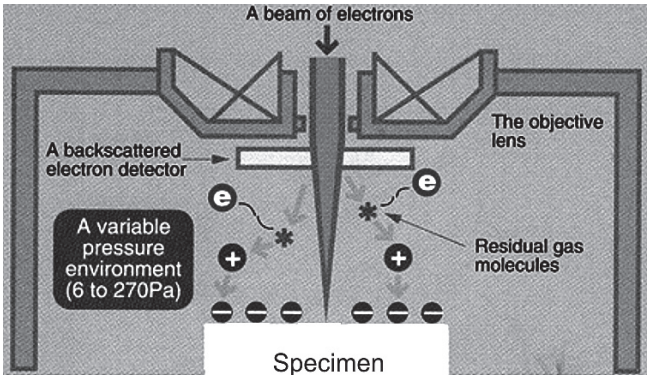

Fig. 3. Schema of the variable pressure operation mode in VP-SEM [Hitachi S-3400N]

The SEM used in this work was the HITACHI S-3400N at the Laboratory for Study Aqueous Suspensions of the Institute of Water Supply and Environmental Protection at the Cracow University of Technology (CUT). The microscope has a conventional tungsten pin thermionic electron gun and can be operated with high vacuum of 1.5×10^{-3} Pa or in VP pressure from 6 Pa to 270 Pa, according to the operator selection. The microscope is equipped with detectors for secondary electrons (SE) and back-scattered electrons (BSE). In VP-mode, the image signal comes from BSE, as having gas inside a vacuum chamber presents a problem for the traditional SE detector. With a help of a standard Peltier cool-stage, temperatures of down to –30°C at maximum pressure of 270 Pa could be obtained [11].

4. Example analysis

4.1. Imaging of *Chironomidae*

As shown in Fig. 2, the *Chironomidae* larva has narrow and elongated body with distinct segments and a capsule-like head. Two pairs of prolegs help larva to catch on: one pair is on the last segment of the abdomen and the other – on the first segment of the thorax.

The images of conductive coated samples were recorded under high vacuum mode using BSE signal in low beam accelerating voltage of 3 kV. The results show that a soft larval body is more sensitive to shrinkage during air-drying than a harder larval head (Fig. 4a),

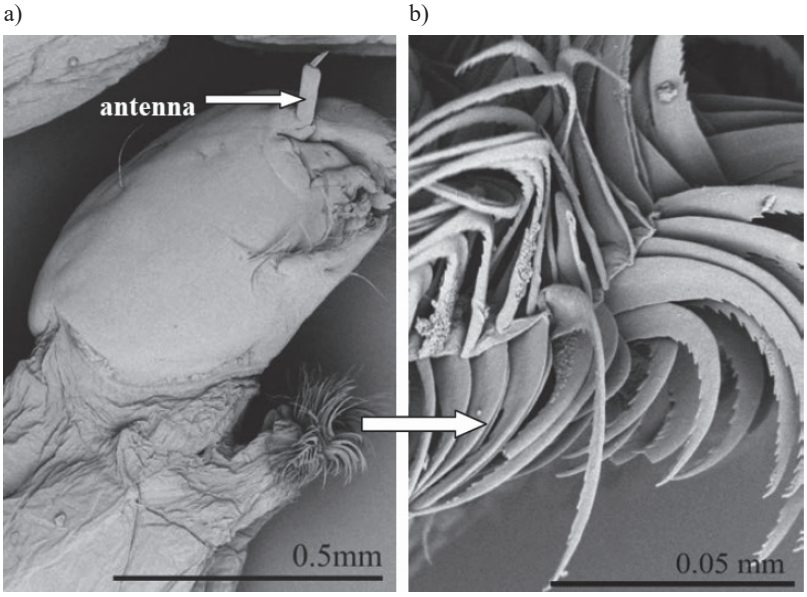

Fig. 4. Images of *Chironomidae* larva observed with BSE detector at 3 kV accelerating voltage, high-vacuum mode: a) the head, lateral view, nominal magnification 100×; b) the claws of anterior parapod, nom. mag. 1000×

on which, in lateral view, a typical antenna [40] and a few fine hears are visualized. Figure 4b shows the tiny hooks of anterior proleg (a parapod found immediately behind the head) in magnification of 1000×. The topology details observed may suggest the presence of particles of dirt (e.g. mud, debris, etc.), collected on the tiny claws. However, the composition differences from eventual surface impurities could not be resolved because of the uniform metal coating of *larvae* sample. A masking of the real structure when coated with gold is a real problem of biological sample studies in high-vacuum SEM [4], whichever detector is used.

Instead, a semi-chemical contrast due to BSE signals allows visualization of adhered particles and other surface artefacts on the biological samples when uncoated (Figs. 5 and 6). Experiments on fresh samples (conserved in alcohol) were performed under constant operation settings: a voltage of 10 kV, a pressure of 15 Pa and a working distance of 9 mm in VP-mode. Fig. 5 shows parts of *Glyptotendipes glaucus*. The satisfactory image resolution and contrast achieved without air-drying of bulk specimens indicate that the less drastic process of dehydration takes place in the specimen chamber environment. Figure 5a shows the hypopygium (a modified 9th abdominal segment) which the copulatory apparatus of many insects, especially dipterous, is associated with. The examples that follow confirm that in VP-mode, magnifications up to 1000× are achieved, insulating wet materials without any problem.

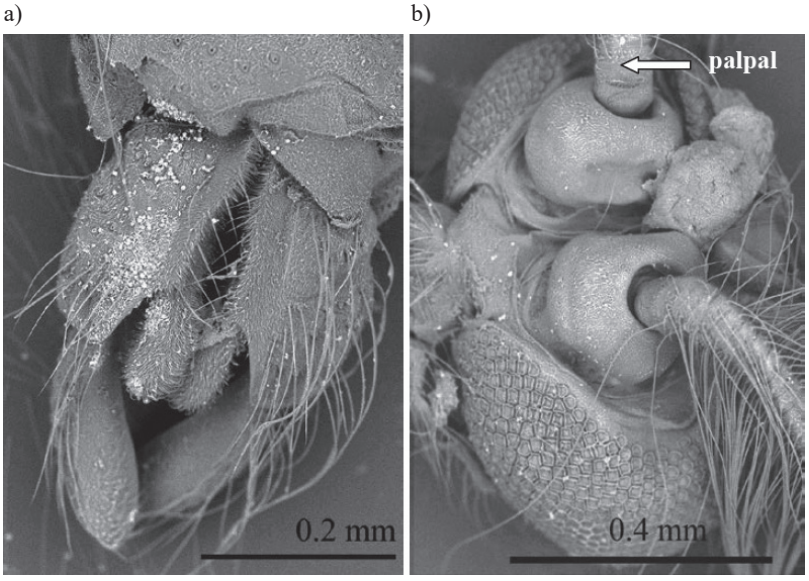

Fig. 5. Images of *Glyptotendipes glaucus*: a) the hypopygium, nom. mag. 200×; b) the head, nom. mag. 140× (sample courtesy of Dr A. Kownacki, PAN)

Figure 6 shows parts of pupal exuvium of *Glyptotendipes glaucus*. For description of the pupal structures of *Chironomidae*, the previously reported SEM and light microscopy (LM) images and entomological drawings [4, 40] were useful. The correlative light-electron microscopy helps to identify new morphological features of various parts of the organisms

studied [4]. For large samples, the most informative surface morphology and structural details are usually found in the magnification range of 100–1500×.

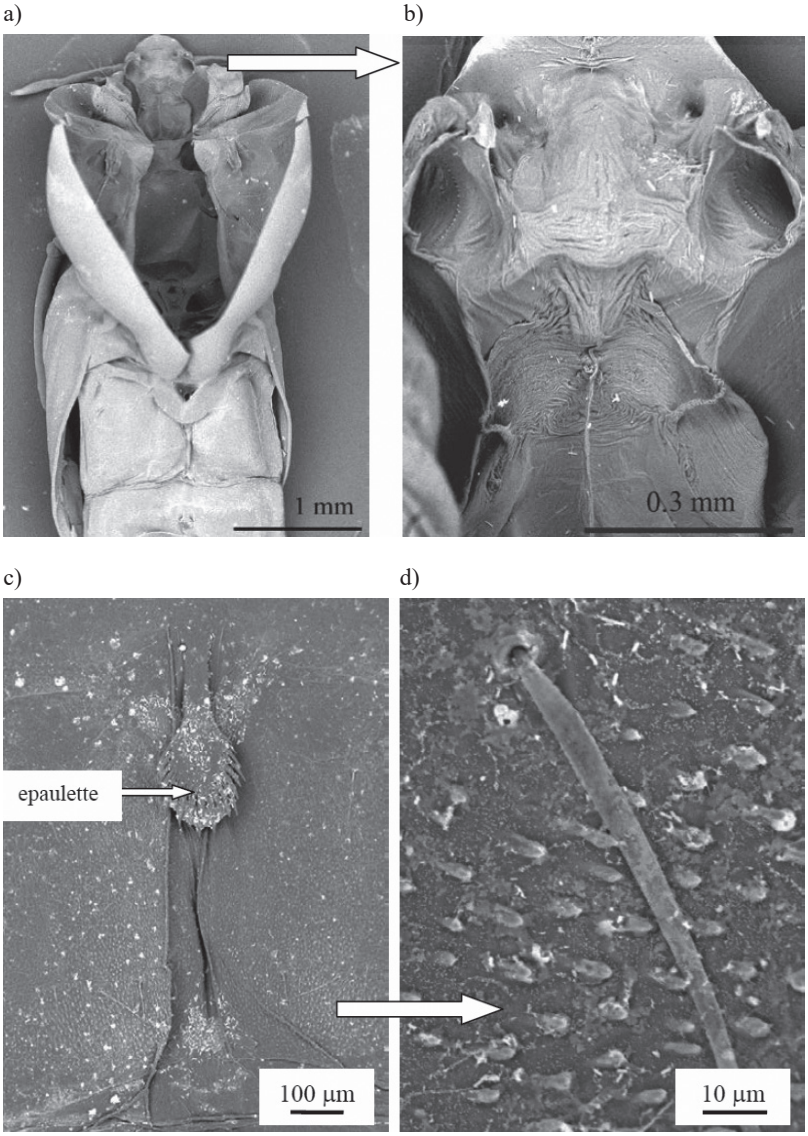

Fig. 6. Images of pupal exuvium of *Glyptotendipes glaucus*: a) anteroventral part of cephalotorax; b) the head in nominal magnification of 1500×; c) tergite in dorsal view, nom. mag. 110×; d) shagreen of tergite, nom. mag. 1000× (sample courtesy of Dr A. Kownacki, PAN)

4.2. Specimen of activated sludge

Images of activated sludge specimen are shown in Figures 7 and 8. The first experiments were performed in high-vacuum, showing the resolution advantage of SE detector at low accelerating voltage. By imaging of bulk structures in order of tenth micrometers (e.g. *Euglenoid algae*, Fig. 7a), charging of the sample occurred at 10 kV immediately. However, lowering a voltage of bombarding electrons to 3 kV permitted many fine particles to be detected in activated sludge (Fig. 7b) and images were taken at magnification of 15 000× (for a short time before next specimen charging). Next, the operation settings were changed to VP-mode after the procedure described in [11].

Figures 7c, d and Figure 8 were recorded at 10 kV and 25 Pa using the BSE signal in VP-mode. The different approach used in this experiment was that specimens were first

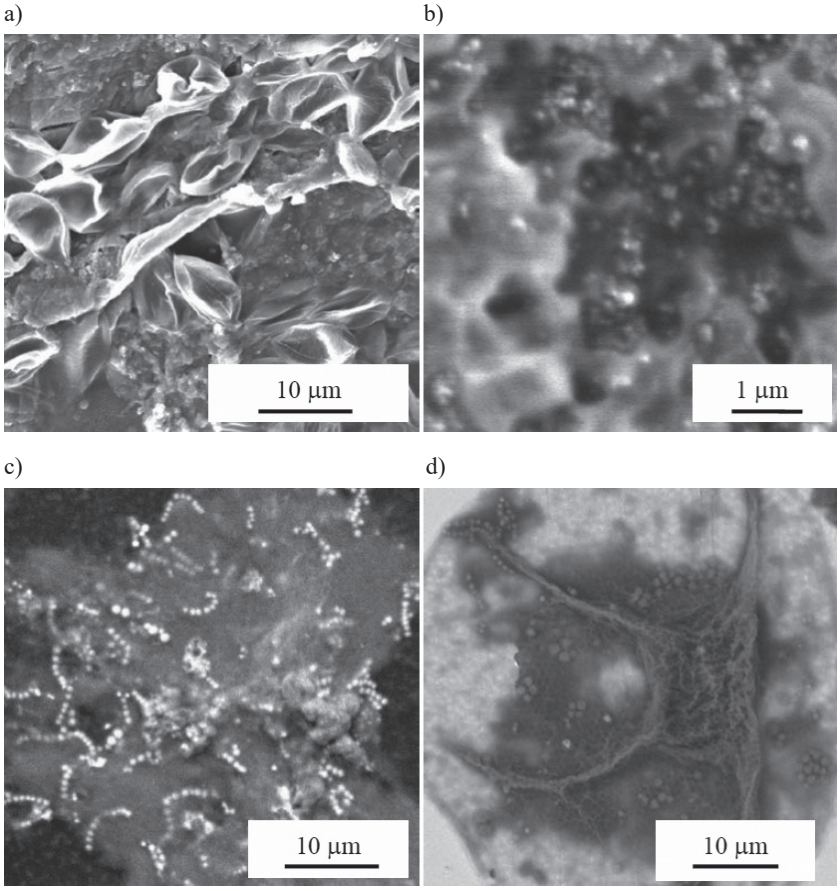

Fig. 7. Images of activated sludge: a) *Euglenoid algae*, SE, 10 kV, nom. mag. 2000×; b) other area, SE, 3 kV, nom. mag. 15000×; c) chains of bacteria attached to the flock, BSE, 10kV, 25 Pa, nom. mag. 2000×; d) *Amoebae* on a gold-coated glass holder, BSE, 10kV, 25 Pa, nom. mag. 2000× (sample courtesy of Prof. A.M. Anielak, CUT)

tested at room temperature and the carbon disc holder was replaced by glass one, priory gold coated (Figs. 7c, d). Results showed that in both cases, fine microstructure of activated sludge appear in good contrast and resolution (nominal magnification of 2000×). It is possible that the same glass holder, with partial surface area made conductive, could provide a useful tool for correlative light-electron microscopy studies in VP-SEM.

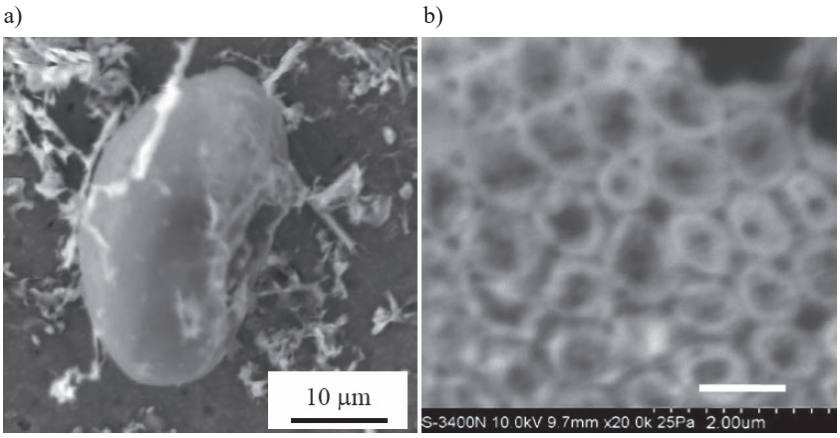

Fig. 8. Images of *Amoebae* cooled down to –25°C in VP-mode: a) the shell of testate *Amoebae*, nom. mag. 2000×; b) surface structure, nom. mag. 20000×, scale bar of 1 μm (sample courtesy of Dr T. Woźniakiewicz)

Figure 8 shows results obtained with the application of a Peltier cooling device. The study confirmed our previous results [11] that settings of 10 kV, 25 Pa and –25°C were enough for imaging less-wet samples with nominal magnification up to 10 000×. For insulating samples, however, the resolution of images acquired at nominal magnifications above 10 000× was not satisfying (Fig. 8b). The resolution of traditional BSE detector in VP-mode (4 nm at 30 kV) is not much less than of SE detector in high-pressure mode (3 nm at 30 kV). However, higher beam voltage could destroy a soft tissue.

4.3. Intestinal protozoan parasites

SEM images of protozoan parasites are presented in Fig. 9. Although the composition of samples under study was known, an unambiguous identification of single parasite cells was difficult.

The BSE image of *G. intestinalis* sample (Fig. 9a) reveals that the base of suspension was not sufficiently removed after one-step spin in distilled water. Single oval forms, which seem "transparent" at accelerating beam voltage of 10 kV, were observed. Apart the appropriate ovoid shape observed, that feature is most probably an artefact, because the too small size of the imaged object. The image of residual suspension constituents is ten times smaller, than the typical dimensions of *Giardia sp.* cysts [38].

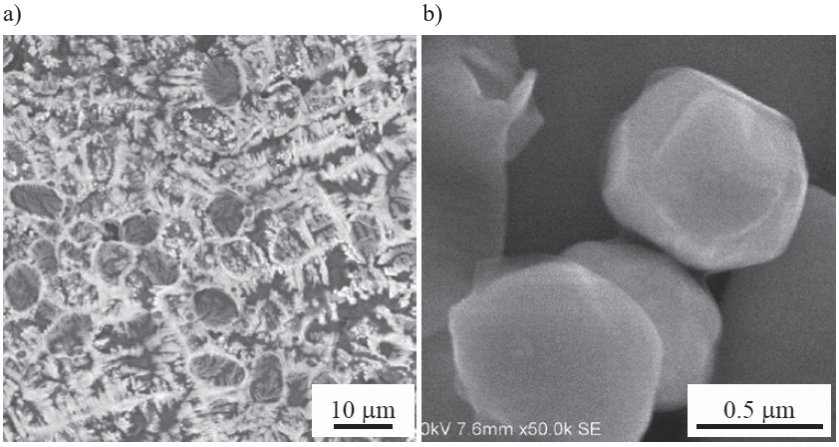

Fig. 9. Images of protozoan species in high-vacuum SEM: a) crystallized residual suspension with *Giardia intestinalis*, BSE, 10 kV, nom. mag. 1000×; b) single organisms in a *C. parvum* sample, SE, 25 kV, nom. mag. 50 000×

Assuming higher analytical depth of BSE for organic matter, the images might show the internal structure of the *Giardia sp.* cysts, which was not the case. To eliminate crystallization effects of residual suspension for SEM studies, much extensive/multistep centrifuging of the specimen is required.

The SE image of the *C. parvum* sample (Fig. 9b) was taken at nominal magnification of 50 000, the highest achieved with satisfactory resolution for biological samples in our VP-SEM. That sample was thoroughly centrifuged and finally conductive coated. A few particles with globular morphology raised the question if the object observed could be protozoan clod plasma or an external armor? Unfortunately, the size of the detected particles adds to the uncertainty as to their nature. Typical *Cryptosporidium* oocysts are ten times larger than the objects of 0.5µm observed in that sample.

Our experiments revealed, that parasite oocysts/cysts are very difficult to detect and diagnose in SEM. Despite its superior image resolution and depth of field, SEM could be used rather for routine microstructural investigations only. It should not be treated as a diagnostic tool for these species, mainly because of laborious sample preparation and many non-characteristic structural features, confirmed by means of immunofluorescent antibody (IFA) technique [39].

5. Conclusions

The variable pressure scanning electron microscope (VP-SEM) is particularly well adapted for observation and experimentation on small and highly hydrated biological specimens. The application of VP-SEM was illustrated by several cases of aquatic organisms, which play an important role in monitoring of water and sewage qualities. Examples demonstrate

that the insulating bulk samples show sufficiently good resolution and contrast in semi-chemical BSE signal for magnifications up to 2000×. The standard carbon disc holder as well as gold evaporated glass (example presented) could be used as conductive specimen substrate in room temperature studies. For magnifications up to 10 000, the best solution would be the use of VP in combination with a Peltier cool-stage.

This work was realized in the frame of the research activity of the Institute of Water Supply and Environmental Protection Ś-3/431/2016/DS Cracow University of Technology (CUT). Authors are grateful to Dr Andrzej Kownacki from Institute of Environmental Protection at Polish Academy of Sciences (PAN), and the colleagues from Institute of Water Supply and Environmental Engineering at CUT, Prof. Anna Maria Anielak and Dr Teresa Woźniakiewicz, who provided the specimens for SEM.

References

[1] Echlin P., *Handbook of Sample Preparation for Scanning Electron Microscopy and X-ray Microanalysis*, Springer, 2009.

[2] Griffin B.J., *Variable Pressure and Environmental Scanning Electron Microscopy*, Methods Mol. Biol., 369, 2007, 467–495.

[3] Bozzola J.J., Russel L., *Electron Microscopy: Principles and Techniques for Biologists*, Jones and Bartlett Publishers, Inc., 1999.

[4] Kownacki A., Szarek-Gwiazda E., Woźnicka O., *The importance of scanning electron microscopy (SEM) in taxonomy and morphology of Chironomidae (Diptera)*, European Journal of Environmental Sciences, 5, 2015, 41–44.

[5] Stokes D.J., *Environmental scanning electron microscopy for biology and polymer science*, Microscopy and Analysis, 1, 2012, 67–71.

[6] Asahina S., Togashi T. et al., *High-resolution low-voltage scanning electron microscope study of nanostructured materials*, Microscopy and Analysis, 2, 2012, S12–S14.

[7] Ensikat H.-J., Weigend M., *Cryo-scanning electron microscopy of plant samples without metal coating, utilizing bulk conductivity*, Microscopy and Analysis, 8, 2013, 7–10.

[8] Ushiki T., Hashizume H. et al., *Low-voltage backscattered electron imaging of non-coated biological samples in a low-vacuum environment using a variable-pressure scanning electron microscope with a YAG-detector*, J. Electron Microsc (Tokyo), 47 (4), 1998, 351–354.

[9] Bogner A., Thollet G. et al., *Wet STEM: A new development in environmental SEM for imaging nano-objects included in a liquid phase*, Ultramicroscopy, 104, 2005, 290–301.

[10] Stokes D.J., *Principles and Practice of Variable Pressure Scanning Electron Microscopy (VP-ESEM)*, John Willey & Sons Ltd., 2008.

[11] Wassilkowska A., Woźniakiewicz T., *Application of Peltier cooling device in a variable-pressure SEM*, Solid State Phenomena, 231, 2015, 139–144.

[12] Podor R., Ravaux J., Brau H.-P., *In Situ Experiments in the Scanning Electron Microscope Chamber, Chapter 3, in Scanning Electron Microscopy*, Kuzmiuk V. (Ed.), InTech, available from: www.intechopen.com

[13] Kownacki A., *Znaczenie i ochrona Chironomidae (Diptera, Insecta) w ekosystemach wodnych Polski*, Forum Faunistyczne, 1, 2011, 4–11.
[14] Information available on: https://swiatmakrodotcom.wordpress.com/muchowki-diptera-2/ (26.06.2016).
[15] Booth S., Brazos B., *Qualitative Procedures for Identifying Particles in Drinking Water*, AWWA, 2005, 34.
[16] Thienemann A., *Chironomus. Leben, Verbreitung und wirtschaftliche Bedeutung der Chironomiden*, Die Binnengewässer, 20, 1954.
[17] Kownacka M., Kownacki A., *Vertical distribution of zoocenoses in the streams of the Tatra, Caucasus and Balkan Mts.*, Verhandlungen des Internationalen Vereins für Limnologie, 18, 1972, 742–750.
[18] Saether O.A., *Chironomid communities as water quality indicators*, Holarctic Ecology, 2, 1979, 65–74.
[19] Kownacki A., *Taxocens of Chironomidae as an indicator for assessing the pollution of rivers and streams. Acta Biologica Debrecina*, Supplementum Oecologica Hungarica, 3, 1989, 219–230.
[20] Szczęsny B. (Ed.), *Degradacja fauny bezkręgowców bentosowych Dunajca w rejonie Pienińskiego Parku Narodowego*, Ochrona Przyrody, 52, 1995, 207–224.
[21] Kownacki A., Soszka H., Fleituch T., Kudelska D., *River biomonitoring and bentic invertebrate communities*, Drukarnia Kolejowa Kraków, Warszawa–Kraków 2002.
[22] Wachałowicz A., Czaplicka-Kotas A., Szalińska E., *Biodostępność chromu z osadów dennych dla larw Chironomus riparius*, Ochrona Środowiska, 3, 2008, 53–58.
[23] Czaplicka-Kotas A., *Wykorzystanie Chironomidae do biomonitoringu środowiska wodnego*, Technologia Wody, 4 (36), 2014, 18–23.
[24] den Besten P.J., Naber A., Grootelaar E.M.M., van de Guchte C., *In situ bioassays with Chironomus riparius: Laboratory-field comparisons of sediment toxicity and effects during wintering*, Aquatic Ecosystem Health & Management, 6(2), 2003, 217–228.
[25] Hudson L.A., Ciborowski J.J.H., *Spatial and taxonomic variations in incidence of mouthpart deformities in midge larvae (Diptera: Chironomidae: Chironomini)*, Can. J. Fish. Aquat. Sci., 53, 1996, 297–304.
[26] Michailova P., Kownacki A., Warchałowska-Śliwa E., Szarek-Gwiazda E., *Genetyczne i behawioralne konsekwencje wpływu metali ciężkich na wybrane gatunki Chironomidae (Diptera) w drobnych stawkach na hałdach*, Materiały XX Zjazdu Hydrobiologów Polskich, 5–8.09.2006, Toruń 2006.
[27] Michailova P., Szarek-Gwiazda E., Kownacki A., *Effect of contaminants on the genome of chironomids (Chironomidae, Diptera) live in sediments of Dunajec River and Czorsztyn Reservoir (Southern Poland)*, Water, Air and Soil Pollution, 202 (1–4), 2009, 245–256.
[28] Buraczewski G., *Biotechnologia osadu czynnego*, Wydawnictwo Naukowe PWN, Warszawa 1994.
[29] Kocwa-Haluch R., Woźniakiewicz T., *Analiza mikroskopowa osadu czynnego i jej rola w kontroli procesu technologicznego oczyszczani ścieków*, Czasopismo Techniczne, 2-Ś/2011, 141–162.
[30] Woźniakiewicz T., Beńko P., Anielak A., Żaba T., *Bioróżnorodność osadu czynnego poddanego bioaugmentacji archeanami lub pracującego w obecności zewnętrznego węgla organicznego*, Przemysł Chemiczny, 12, 2015, 2251–2255.

[31] Polus M., Wassilkowska A., Dąbrowski W., *Challenges in pathogen detection in waste water*, AWE International, Issue 29, march 2012, 33–39.
[32] Brasseur Ph., Uguen Ch., Moreno-Sabater A., Favennec L., Ballet J.J., *Viability of Cryptosporidium parvum oocysts in natural waters*, Folia Parasitologica, 45, 1998, 113–116.
[33] Baxby D., Getty B, et al., *Recognition of whole Cryptosporidium oocysts in feces by negative staining and electron microscopy*, Journal of Clinical Microbiology, April 1984, 566–567.
[34] Hunter P.R., Thompson R.C.A., *The zoonotic transmission of Giardia and Cryptosporidium*, Int J Parasitol., 35, 2005, 1181–1190.
[35] LeChevallier M.W., Norton W.D., *Giardia and Cryptosporidium in raw and finished water*, J AWWA, 87, 1995, 54–68.
[36] Raabe Z., *Metodyka protozoologiczna*, [w:] *Zarys protozoologii*, PWN, Warszawa 1972.
[37] Pitelka D.R., *Electron microscopic structure of protozoa*, Int. Series Monographs on Pure and Applied Biology, Vol. 13, Kerkut G.A. (Ed.), Pergamon Press Book, New York 1963.
[38] Plutzer J., Ongert J., Karanis P., *Giardia taxonomy, phylogeny and epidemiology: Facts and open questions*, Int. J. Hyg. Environ Health., 213 (5), 2010, 321–333.
[39] US EPA, Method 1622, *Cryptosporidium in Water by Filtration/IMS/FA*, EPA, 2005, 815 R 05 001.
[40] Soponis A.R., *A Revision of the Nearctic Species of Orthoclasius van der Wulp (Diptera: Chironomidae)*, The Entomological Society of Canada, Ottawa 1977.

TECHNICAL TRANSACTIONS | CZASOPISMO TECHNICZNE
ENVIRONMENT ENGINEERING | ŚRODOWISKO
1-Ś/2016
DOI: 10.4467/2353737XCT.16.206.5955

BARBARA WILK*

ULTRAFILTRATION MEMBRANES MADE OF: POLYANILINE, IONIC LIQUID AND CELLULOSE

MEMBRANY ULTRAFILTRACYJNE UTWORZONE Z: POLIANILINY, CELULOZY ORAZ CIECZY JONOWEJ

Abstract

The study determined the method of obtaining UF membranes from cellulose, polyaniline and ionic liquid as the gelling agent. The impact of the applied coagulation agent and the conducting polymer (polyaniline) on the transport and separation properties of the obtained membranes was examined.

Keywords: ionic liquids, solvents, ultrafiltration, membrane

Streszczenie

W artykule określono sposób otrzymywania membran ultrafiltracyjnych z surowców: celulozy, polianiliny oraz cieczy jonowej jako substancji żelującej. Zbadano, jaki wpływ na właściwości transportowe i separacyjne otrzymanych membran mają zastosowany koagulant oraz polimer przewodzący (polianilina).

Słowa kluczowe: ciecze jonowe, rozpuszczalniki, ultrafiltracja, membrana

* M.Sc. Eng. Barbara Wilk, Institute of Water Supply and Environmental Protection, Faculty of Environmental Engineering, Cracow University of Technology.

1. Introduction

The development of environmentally friendly materials, products and processes has clearly been motivated by the growing environmental awareness of the society. The principles of "green chemistry" (i.e. chemistry that aims to optimize the processes in order to reduce the pollution of the environment) and the related hazards to human health clearly indicate the need to substitute the volatile organic solvents with environmentally friendly ones (in line with Principle 5 of the green chemistry) [1]. This requires chemical compounds that will not only be easy to obtain, isolate and purify, but will also provide economic benefits.

The recent years have witnessed a breakthrough in the development of chemical sensors with polyaniline as the main component [2]. These next generation sensors make it possible to assay even complex mixtures of substances in biomaterial, soil, air or sewage. The conducting (due to the addition of polyaniline), environmentally neutral (due to the use of ionic liquid as the solvent) UF membranes may have a significant impact on the separation processes. Such membranes could find application as biosensors in certain production processes, in medicine and in the treatment of specific waste.

2. Ionic liquids

Ionic liquids are liquids composed exclusively of ions, being defined as salts with melting point lower than the boiling point of water (100°C). There are also ionic liquids that melt at temperatures below the room temperature (20°C), called the room temperature ionic liquids [4–7]. The most popular molten salts are dialkylimidazolium salts, due to their attractive physical properties and ease of synthesis. Ionic liquids are usually composed of a large, organic cation and an inorganic or organic anion. Number of possible cation – anion combinations equals to 10^{18}. The liquid state of ionic liquids at room temperature arises from the low lattice energy caused by high asymmetry of the ions making up the liquids [8]. Ionic liquid can be either hydrophilic or hydrophobic. The solubility depends on the anion, the length of alkyl substituents of the cation, and the temperature. Ionic liquids also dissolve alcohols, ethyl acetate, chloroform, acetone, DMF, DMSO, inorganic salts, certain polymers and minerals [8, 9]. The boiling point of ionic liquid is also its breakdown temperature (300°C–400°C). The properties of ionic liquids, such as viscosity, density, melting point and miscibility with other substances change depending on the structure of the cation and the anion. As a result, ionic liquids have been dubbed task-specific solvents [10]. Currently, ionic liquids are widely used in organic chemistry as the environment for a number of industrial-grade chemical reactions [6, 11, 12, 14].

3. Polyaniline

Polyaniline is a conductive organic polymer with semiconductor or metallic conductivity along the chain. Polyaniline comes in several forms, differing by the oxidation state, of which

only emeraldine salt (dark green powder) is conductive. It is one of the most temporally stable conductive polymers. Unfortunately, it is a material that is difficult to process. Among the conductive polymers, polyaniline has the widest potential field of application. It is used in anti-corrosion agents for metals, as an ingredient of varnishes, membranes for gas separation and biosensors [2, 3].

4. Cellulose

Cellulose consists of glucose particles (β-D-glucose) linked by glycosidic bonds (β-1,4 bond). It is insoluble in water and common organic solvents. Select ionic liquids dissolve cellulose very well. The literature contains reports that ionic liquids containing imidazolium cation and anions, such as chloride, octane and formate, are characterized as having exceptionally good dissolving properties. Ionic liquid cation and anion structure and its tenacity has an effect on the process of dissolving cellulose in ionic liquids (compounds of lesser tenacity dissolve larger amounts of polymer).Anion of ionic liquid that dissolves cellulose well should have the capability of creating hydrogen bonds with hydroxyl groups. The role of cation is not entirely defined (e.g. aromatic cations – the highest cellulose solubility).

5. Phase inversion method

The most widely used method of membrane production is phase inversion [15]. The method is based on precipitating the polymer (the membrane) from a homogeneous solution. Phase inversion is found in processes such as solvent evaporation, precipitation through controlled evaporation, thermal precipitation, precipitation from the gaseous phase and immersion precipitation. The key process used by the phase inversion is precipitation by immersion in liquid [16–18].

6. Methodology

Membrane preparation by phase inversion (wet method) required the use of an applicator, a feeler gauge, a glass plate and a cuvette for the coagulator for the gelling process.

The first series of membranes was obtained from a membrane-forming solution containing 10% of cellulose (supplied by Merck), dissolved in ionic liquid (1-ethyl-3-methylimidazolium acetate), supplied by Fluka Riedel-de Häen. The solution was used to pour flat membranes with the following thicknesses: 0.2; 0.25; 0.3; 0.35 and 0.4 mm. Following the conditioning, the obtained membranes were tested by filtering deionized water through the membrane to determine the permeability and the relation of the volumetric water flux to the transmembrane pressure. Next, the membranes were coated with a 0.15 mm polyaniline film. For this

purpose, the secondary membrane with 10% polyaniline solution in ionic liquid (1-ethyl-3-methylimidazolium acetate) was poured on cellulose supports. Unfortunately, during the gelling in water bath, the polyaniline layer would partially separate from the cellulose support, rendering this method of obtaining membranes ineffective.

Therefore, it was decided to prepare membrane-forming solutions composed of cellulose, polyaniline and 1-ethyl-3-methylimidazolium acetate. Four types of solutions were prepared, hereafter referred to as solution 1, 2, 3 and 4, respectively. All solutions were 10% cellulose solutions in ionic liquid and differed in terms of polyaniline content, whereby solution 1 did not contain polyaniline at all. Solution 2 contained 1% polyaniline, solution 3–5%, and solution 4–10%. In order to determine the impact of the coagulator on the properties of the membranes, the membranes were gelled in: methanol, ethanol, 1-propanol, 2-propanol, butanol and deionized water. The composition of membrane-forming solutions, the type of applied coagulator and the symbols of obtained membranes that will be used hereafter, are listed in Table 1.

Table 1

Composition of a film-forming solutions and identification of tested membranes

Solution	1-propanol	metanol	H_2O	butanol	2-propanol	pentanol	ethanol
1.10% cellulose	1A	1B	1C	1D	1E	1F	1G
2.10% cellulose + 1% polyaniline	2A	2B	2C	2D	2E	2F	2G
3.10% cellulose + 5% polyaniline	3A	3B	3C	3D	3E	3F	3G
4.10% cellulose + 10% polyaniline	4A	4B	4C	4D	4E	4F	4G

The tests to determine the properties of membranes were conducted with the use of the system illustrated in Fig. 1.

The following parameters were used to assess the transport properties of UF membranes:

– J_v – volumetric water flux, $\frac{\mathrm{m}^3}{\mathrm{m}^2 \cdot \mathrm{s}}$

– L_W – water permeability, $\frac{\mathrm{m}^3}{\mathrm{m}^2 \cdot \mathrm{s} \cdot \mathrm{MPa}}$

The membranes were conditioned with deionized water at room temperature (20°C) in 0.2 MPa and mixing speed of 50 rpm. The filtration was continued until a constant volumetric water flux was achieved. A single membrane was conditioned for 2 to 4 hours.

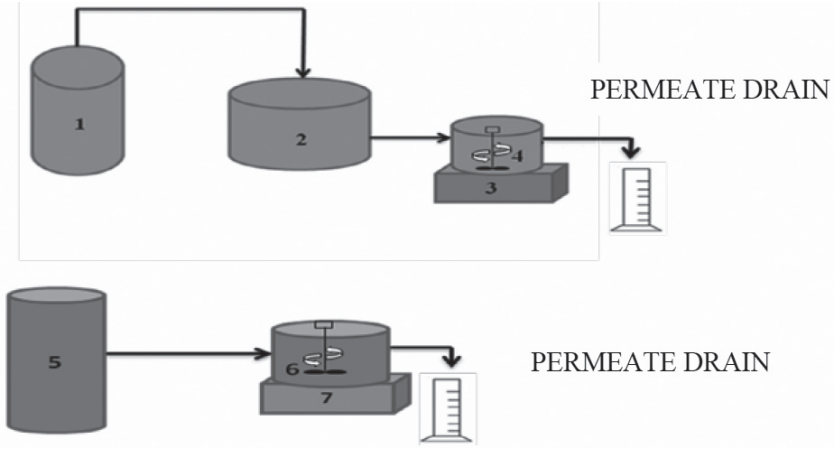

Fig. 1. Measuring position plan: 1, 5 – pressurized gas supply system; 2 – supply tank; 3, 7 – magnetic mixers; 4, 6 – ultrafiltration chambers

The transport properties of membranes were determined by filtering deionized water through the membranes and applying variable transmembrane pressure (ranging from 0.1 to 0.3 MPa) and a constant mixing speed of the filtered medium – 100 rpm. The volume of deionized water filtered over 15 minutes in 2 iterations was assessed. The volumetric water flux was calculated and the relation J_v to the transmembrane pressure was determined.

The separation properties of the membranes were determined by filtering dextran solution with the nominal molecular weight 200,000 Da, through the membranes. The solution mass concentration was 5 g/dm^3. The filtration was conducted with transmembrane pressure of 0.2 MPa. 10% of the feed was received, assaying the shares of individual molecular weights of dextran in the permeate and the retentate, using gel permeation chromatography. On the basis of the recorded chromatograms, the dextran content could be quantified in specific molecular weight thresholds, into which the whole feed and permeate stream had been divided. The retention factor for dextran was calculated from the following correlation [9]:

$$R_0 = \frac{1 - c_p}{c_n} \tag{1}$$

$$R_i = \frac{1 - c_{pi}}{c_{ni}} \tag{2}$$

where:

R_0 – general retention factor,
c_p, c_n – general dextran concentration in permeate and feed, mol/dm^3,
R_i – retention factor determined for individual molecular weight thresholds,
c_{pi}, c_{ni} – dextran concentrations in individual molecular weight thresholds in permeate and feed, mol/dm^3.

On the basis of the values of the retention factor *Ri*, determined for the whole range of the tested molecular weights, the curves were drawn, showing the correlation between the retention level of dextran molecules and their molar weight, and thus the cut-off permeability of the tested membranes. The samples of permeate and feed, collected during membrane testing, were analysed in a gel permeation by Schimadzu, equipped with a NUCLEOGELaqa-OH50-8 column (Machery-Nagel), RID-6A refractive index detector, (Schimadzu), and C-R4A Chromatopac computing integrator (Schimadzu) for data processing.

7. Results and discussion

The results obtained for the first series of membranes are illustrated in Fig. 2, which clearly shows that, with the increase of the membrane thickness, the volumetric water flux drops across the entire range of applied pressure values.

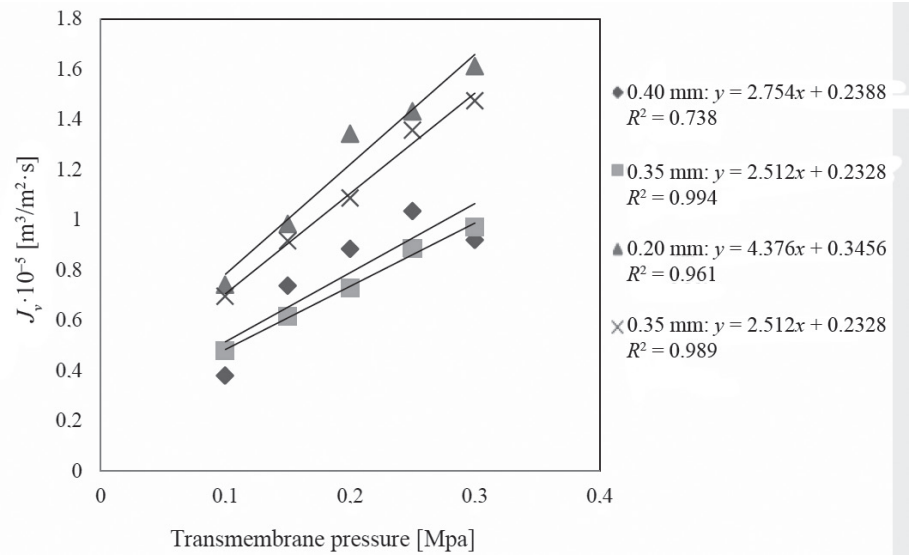

Fig. 2. The dependence of volumetric deionized water flux on pressure for cellulose membranes 0.20–0.40 mm thick

As it can be seen, during the gelling in water bath, the polyaniline layer partially separated from the cellulose support, rendering this method of obtaining membranes ineffective.

Next, the transport and separation properties of the 1A to 4B membranes were assayed. Fig. 3 illustrates the relation of the volumetric water flux to the transmembrane pressure for membranes 1A to 1G.

With the increase of the pressure, the J_v values calculated for all membranes increased as well. The best transport properties were observed in membrane 1D (gelling solution –

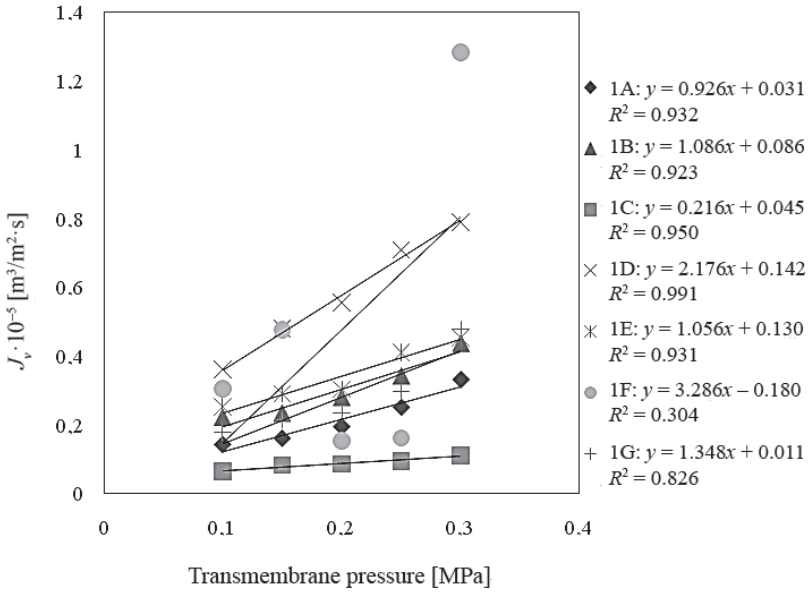

Fig. 3. The dependence of volumetric deionized water flux on pressure for membranes 1A to 1G

butanol) and the poorest in membrane 1C (gelling solution – water). The volumetric water flux ($J_v = 0.087 \cdot 10^{-5}$ m³/m²·s) calculated for membrane 1C was 6 times lower than the J_v value calculated for membrane 1D ($Jv = 0.56 \cdot 10^{-5}$ m³/m²s – for 0.2 MPa transmembrane pressure). Also membrane 1A turned out to be dense (gelling solution – 1-propanol) – $J_v = 0.15 \cdot 10^{-5}$ m³/m²s. The volumetric water flux of other membranes were similar and fell within the range from 0.21 to $0.28 \cdot 10^{-5}$ m³/m²s.

Diagrams 4a, 7a, 10a and 13a illustrate the correlation between the chromatogram peak height and the molecular weight, while diagrams 4b, 7b, 10b and 13b illustrate the cumulative share of molecules in the analysed samples. Figs. 5, 8, 11 and 14 show the cut-off curves, which illustrate the correlation between the dextran retention level and the molecular weight.

Among the membranes obtained from pure cellulose, the best separation properties were observed for membrane 1C (gelled in deionized water). The cut-off molecular weight for that membrane is 9 kDa. Slightly poorer properties were observed in membranes 1B (gelled in methanol) and 1A (gelled in 1-propanol). The cut-off molecular weights for those membranes are: 50 kDa and 80 kDa, respectively. Membrane 1E (gelled in 2-propanol) and 1F (gelled in pentanol) retained only 60% of molecules with 80 kDA molecular weight, while membrane 1D (gelled in butanol) retained only 30% of those molecules.

Fig. 6 illustrates the relation of the volumetric water flux (J_v) to the transmembrane pressure for membranes 2A to 2G. With the pressure rise, the volumetric water flux (J_v) would increase for all membranes. The best transport properties were observed in membrane 2D (gelling solution – butanol) and the poorest in membrane 2G (gelling solution – ethanol). The volumetric water flux ($J_v = 0.668 \cdot 10^{-5}$ m³/m²·s) calculated for membrane 2D was 3.5 times lower than the J_v

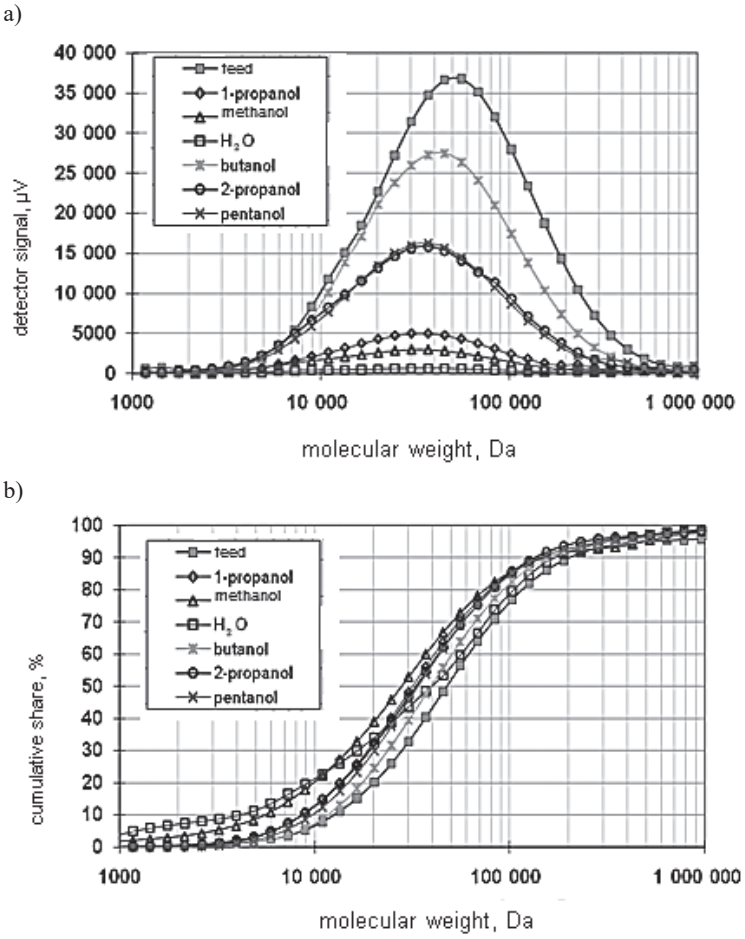

Fig. 4. Dextran molecular weight distribution curves in the feed and the permeates originating from the tests of membranes 1A to 1G (pure cellulose, gelled in various non solvents b) cumulative share of dextran molecules with the given weight

value calculated for membrane 2G (gelling solution – ethanol; J_v = 0.187·10^{-5} m^3/m^{2}s – for 0.2 MPa transmembrane pressure). Transport properties similar to membrane 2G were also observed in membrane 2E (gelling solution – 2-propanol). For the transmembrane pressure p = 0.2 MPa, the calculated J_v was 0.195·10^{-5} m^3/m^{2}s. The volumetric water flux calculated for other membranes were similar and fell within the range from 0.36·10^{-5} m^3/m^{2}s to 0.48·10^{-5} m^3/m^{2}s.

Analysis of Figs. 7 and 8 indicates that among the membranes obtained from the membrane-forming solution, containing 10% of cellulose and 1% of polyaniline, the best separation properties are observed for membrane 2A (gelled in 1-propanol). The cut-off molecular weight for that membrane is 11 kDa. Membranes 2D (gelled in butanol) and 2E (gelled in 2-propanol) retained 75% of molecules with 11,000 Da molecular weight;

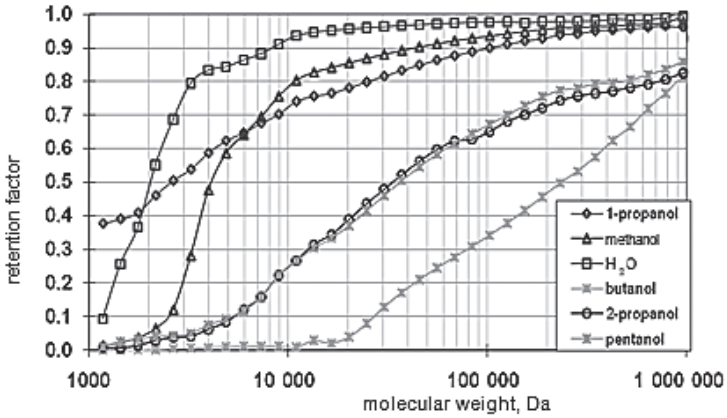

Fig. 5. Relationship between the retention factor and dextran molecular weight, as determined for membranes 1A-1G

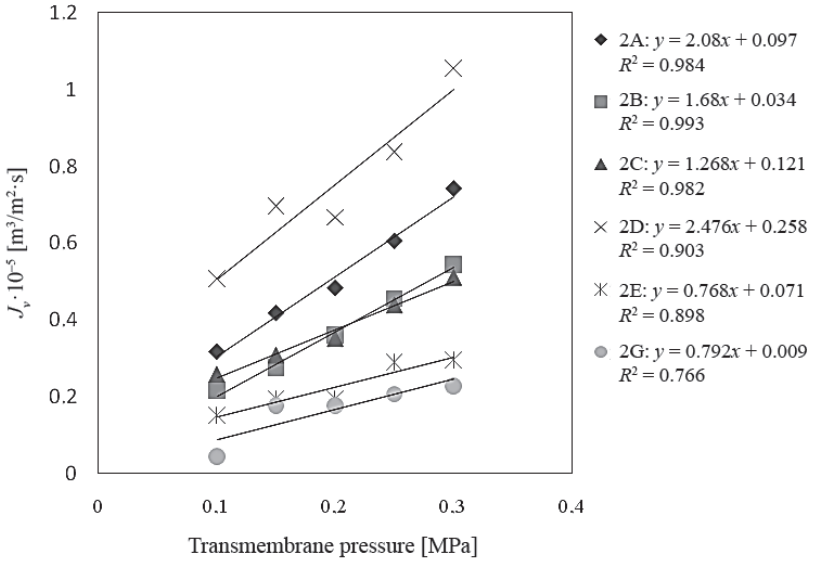

Fig. 6. The dependence of volumetric deionized water flux on pressure for membranes 2A to 2E, 2G

membrane 2G (gelled in ethanol) retained 62% of those molecules, while membrane 2C (gelled in deionized water) retained only 15% of the molecules.

Fig. 9 illustrates the relation of the volumetric water flux (J_v) to the transmembrane pressure for membranes 3B to 3G. With the transmembrane pressure increase, the volumetric water flux (J_v), calculated for all tested membranes, would increase. The best transport properties were observed in membrane 3F (gelling solution – pentanol) and the poorest in membrane 3C (gelling solution – water). The volumetric water flux ($J_v = 0.182 \cdot 10^{-5}$ m^3/m^2·s) calculated

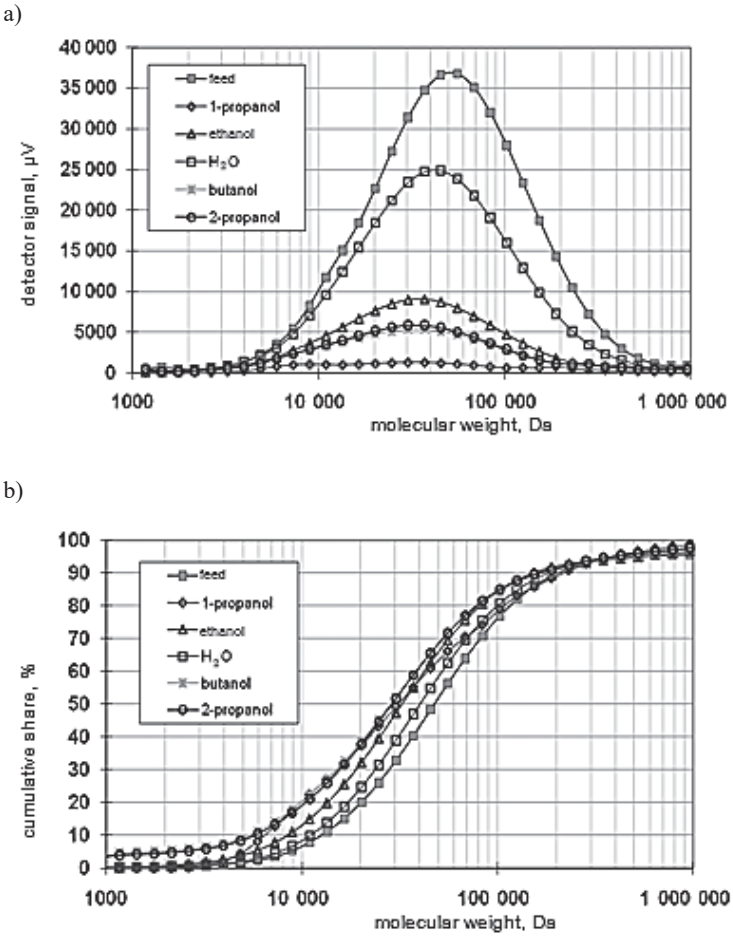

Fig. 7. Dextran molecular weight distribution curves in the feed and the permeate, obtained from the tests of membranes 2A to 2E, 2G: a) correlation of the chromatogram height and dextran molecular weight, b) correlation between the cumulative share of dextran molecules and their molecular weight

for membrane 3C was 4 times lower than the J_v value calculated for membrane 3F (J_v = $0.795 \cdot 10^{-5}$ m^3/m^2s (characteristic values for 0.2 MPa transmembrane pressure). Transport properties similar to membrane 3C were also observed in membrane 3G (gelling solution – ethanol). For the transmembrane pressure p = 0.2 MPa, the calculated J_v was $0.186 \cdot 10^{-5}$ m^3/m^2s. The volumetric water flux calculated for other membranes were similar and fell within the range from $0.597 \cdot 10^{-5}$ m^3/m^2s to $0.612 \cdot 10^{-5}$ m^3/m^2s.

It has been observed that, among the membranes obtained from the membrane-forming solution, containing 10% of cellulose and 5% of polyaniline, the best separation properties are observed for membrane 3G (gelled in ethanol). The cut-off molecular weight for that membrane is 10 kDa. Membrane 3C (gelled in water) retained 85% of molecules with 10 kDa

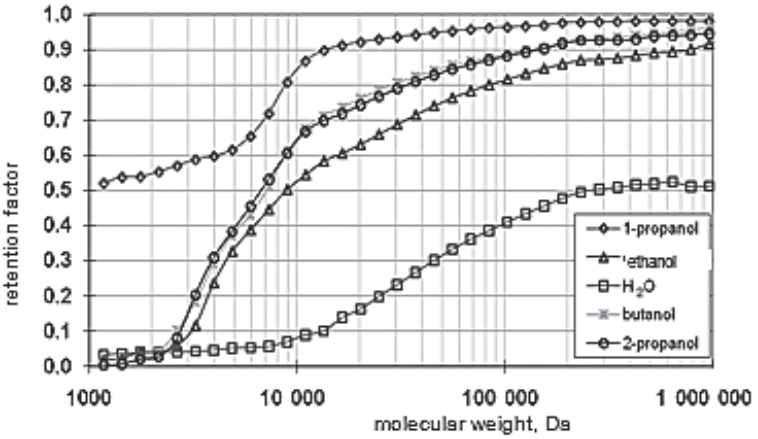

Fig. 8. Relation between the retention factor and dextran molecular weight, as determined for membranes 2A-2E, 2G

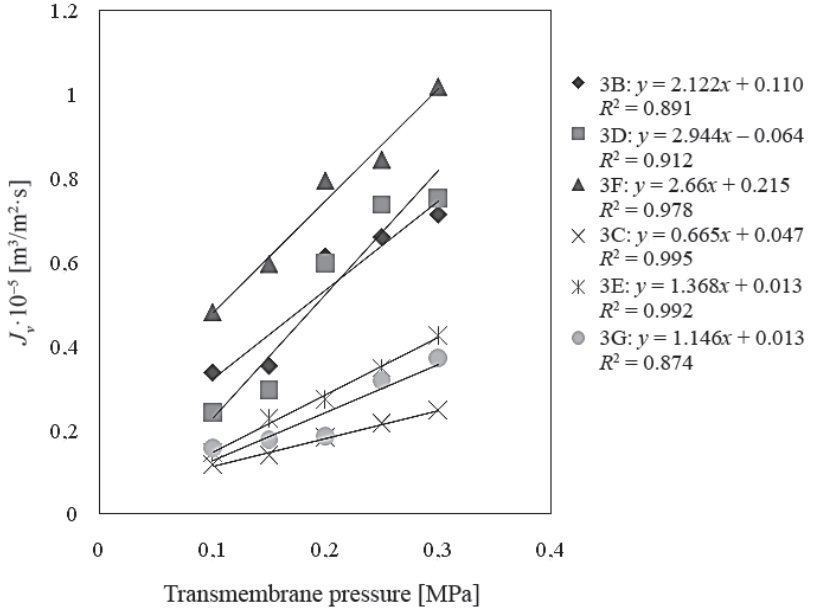

Fig. 9. The dependence of volumetric deionized water flux on pressure for membranes 3B to 3G

molecular weight; membrane 3E (gelled in 2-propanol) retained 30% of those molecules, while membrane 3F (gelled in pentanol) retained only 10% of the molecules. Thus, in this series of membranes, the best separation properties were observed in membrane 3G, while the poorest in membrane 3F.

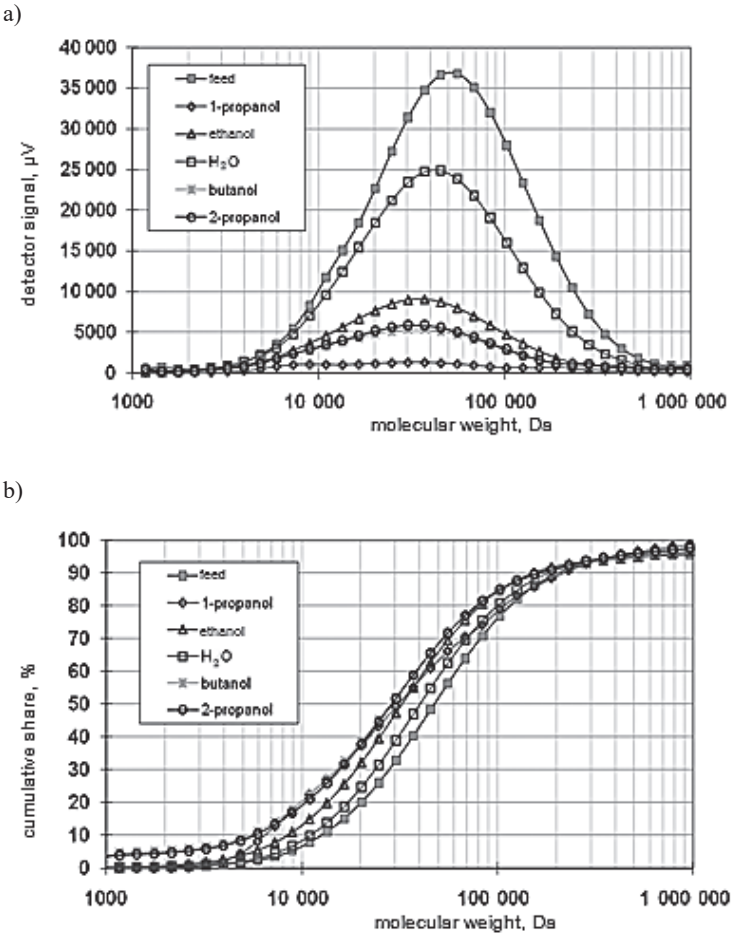

Fig. 10. Dextran molecular weight distribution curves in the feed and the permeate, obtained from the tests of membranes 3B-3G: a) correlation of the chromatogram height and dextran molecular weight, b) correlation between the cumulative share of dextran molecules and their molecular weight

Fig. 12 illustrates the relation of the volumetric water flux (J_v) to the transmembrane pressure for membranes 4A to 4G (cellulose membranes with 10% addition of polyaniline, gelled in various solvents). Similarly to previous cases, the volumetric water flux (J_v) would increase with the pressure increase. The best transport properties were observed in membrane 4D (gelling solution – butanol) and the poorest in membrane 4A (gelling solution – 1-propanol). The volumetric water flux ($J_v = 0.463 \cdot 10^{-5}$ m^3/m^2·s) calculated for membrane 4C was 3 times lower than the J_v value calculated for membrane 4A ($J_v = 0.161 \cdot 10^{-5}$ m^3/m^{2}s (characteristic values for 0.2 MPa transmembrane pressure). Transport properties similar to membrane 4A were observed for membranes 4B, 4E, 4F and 4G. The volumetric water flux

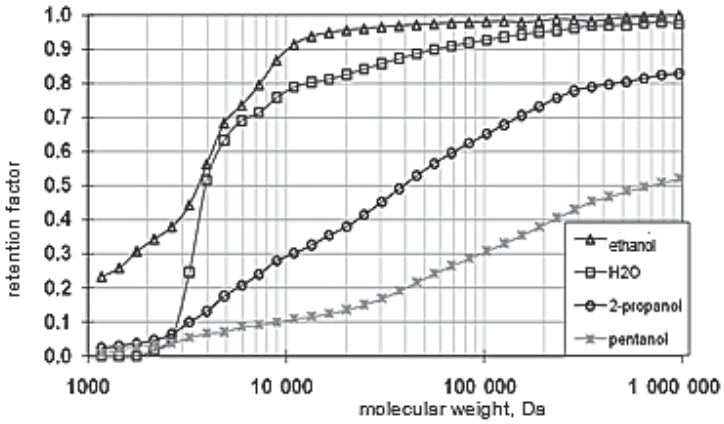

Fig. 11. Relation between the retention factor and dextran molecular weight, as determined for membranes 3B-3G

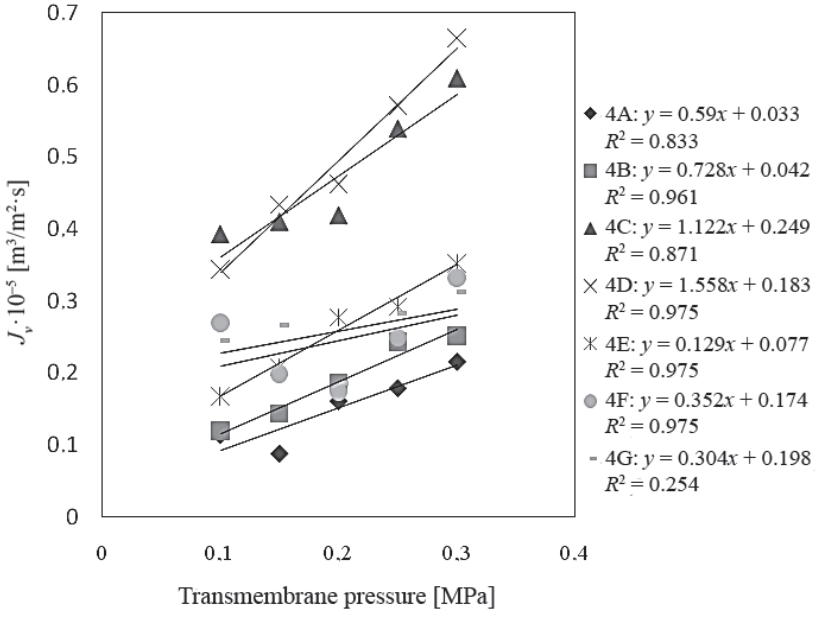

Fig. 12. The dependence of volumetric deionized water flux on pressure for membranes 4A to 4G

calculated for those membranes for p = 0.2 MPa) fell within the range from $0.174 \cdot 10^{-5}$ m^3/m^{2}s to $0.261 \cdot 10^{-5}$ m^3/m^{2}s. Only for membrane 4C (gelling solution – water) the observed transport properties were similar to the most open membrane, i.e. 4D. The J_v calculated for that membrane (for p = 0.2 MPa) was $0.419 \cdot 10^{-5}$ m^3/m^{2}s.

a)

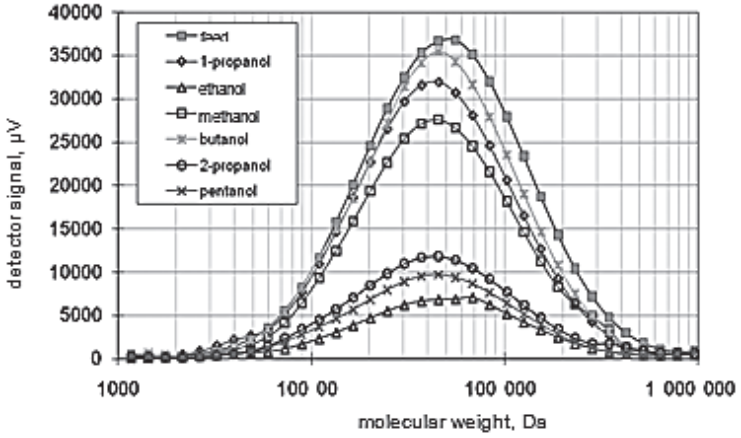

b)

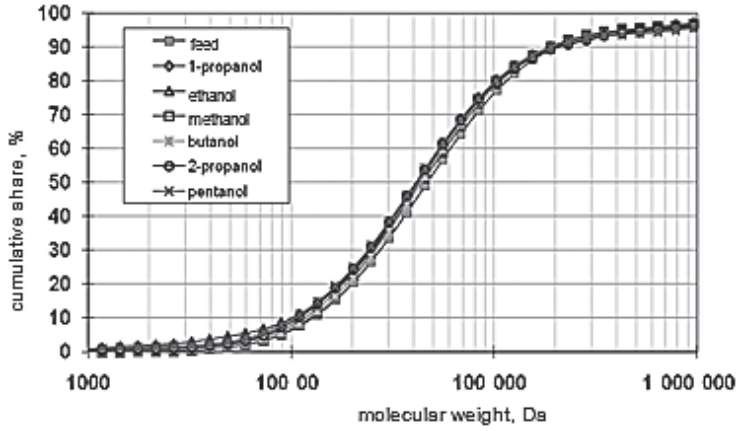

Fig. 13. Dextran molecular weight distribution curves in the feed and the permeate, obtained from the tests of membranes 4A-4G: a) correlation of the chromatogram height and dextran molecular weight, b) correlation between the cumulative share of dextran molecules and their molecular weight

Analysis of chromatograms obtained for this series off membranes (Figs. 13 and 14) indicates that, among the membranes obtained from the membrane-forming solution, containing 10% of cellulose and 10% of polyaniline, the best separation properties are observed for membrane 4G (gelled in ethanol). The membrane retained 80% of molecules with 10 kDa molecular weight. Membranes 4F (gelled in pentanol) and 4E (gelled in 2-propanol) retained 60% and 55% of those molecules, respectively. Membrane 4B (gelled in methanol) retained only 15% of the molecules. The poorest separation properties were observed in membranes

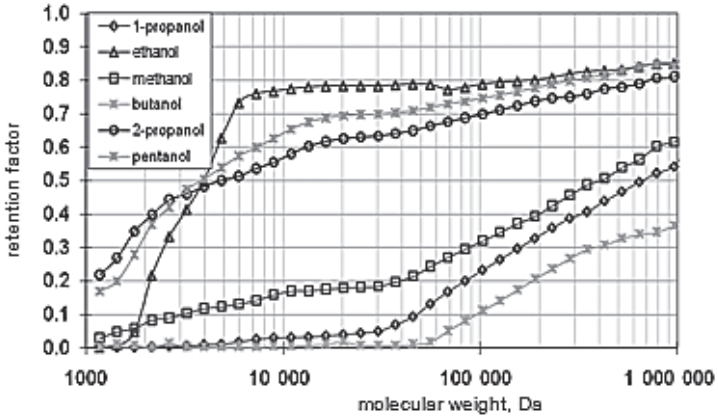

Fig. 14. Relation between the retention factor and dextran molecular weight, as determined for membranes 4A-4G

4A (gelled in 1-propanol) and 4D (gelled in butanol). Those membranes retained only several dozen percent of molecules with 10 kDa molecular weight.

8. Conclusions

The phase inversion method makes it possible to obtain UF membranes from membrane-forming solutions containing cellulose and polyaniline dissolved in ionic liquid and this process cannot be found innovative. It is difficult to clearly determine the impact of the type of gelling liquid on the transport and separation properties of the obtained membranes. Given the uniqueness of the subject, this correlation merits further research, with a reiteration of the performed cycle and expansion of the list of applied coagulants.

The highest retention level of dextran molecules was observed in the following membranes: 1C (membrane obtained from 10% solution of cellulose in ionic liquid), membrane 3G (obtained from 10% solution of cellulose in ionic liquid, with a 5% addition of polyaniline), and membrane 2A (obtained from 10% solution of cellulose in ionic liquid, with a 1% addition of polyaniline). The cut-off molecular weights of those membranes, determined for dextran with the nominal molecular weight of 200,000, were: 9 kDa, 10 kDa and 11 kDa, respectively.

The assessment of the transport properties of the membranes indicates that the water stream volume indeed depends on the transmembrane pressure. The conducted study indicated that the most “open” of the tested membranes is membrane 3F (5% addition of PANI, gelled in pentanol). Similar transport properties were observed for the following membranes: 2D (1% addition of PANI, gelled in butanol) and 3D (5% addition of PANI, gelled in butanol).

The densest membranes include: 1C (membrane without polyaniline addition, gelled in water), 1F (pure cellulose, gelled in pentanol) and 4F (10% addition of PANI, gelled in pentanol). The exact impact of polyaniline addition on the transport properties of membranes cannot be unequivocally determined. For some membranes, polyaniline increases the J_v (e.g. 3F, 2A, 2C, 3B), but for others, it has an opposite effect (e.g. 2E, 2G, 4A, 3G). In addition, it is difficult to establish some kind of relation between the type of the gelling agent and the transport properties of the obtained membranes. During the study, it turned out that the strength properties of membranes 2F (1% addition of PANI, gelled in pentanol) and 3A (5% addition of PANI, gelled in 1-propanol) were insufficient. With higher transmembrane pressure – 0.25 MPa, the membranes would burst.

References

[1] Anastas P.T.,Warner J., *Green Chemistry. Theory and Practice*, Oxford Univ. Press, Oxford 1998.

[2] Zawadzka E., Mazurek B., *Modyfikowana polianilina jako materiał termoelektryczny*, Przegląd elektrotechniczny, 8, 2013.

[3] Sen T., Mishraa S., Shimpi N.G., *Synthesis and sensing applications of polyaniline nanocomposites: a review*, RSC Advances, 6, 2016, 42196–42222.

[4] Majewska E., *Ciecze jonowe w procesach ekstrakcji metali i związków organicznych z procesów spożywczych*, Żywność. Nauka. Technologia. Jakość, 98, 2015, 5–15.

[5] Pinkert A., Marsh K., Pang S., Staiger M., *Ionic liquids and their interaction with cellulose*, Chem. Rev., 109, 2009, 6712–6728.

[6] Ratti R., *Ionic liquids: synthesis and applications in catalysis*, Advances in Chemistry, 2014.

[7] Livazovica S., Lia Z., Behzadb A.R., Peinemannc K.V., Nunesa S.P., *Cellulose multilayer membranes manufacture with ionic liquid*, Journal of Membrane Science, 490, 2015, 282–293.

[8] Rogers R.D., Seddon K., *Ionic liquids–industrial applications for green chemistry*, ACS Symp. Ser, 2002.

[9] Swatloski R., Spear S.K., John D., Holbrey J.D., *Dissolution of cellulose with ionic liquids*, Am. Chem. Soc., 124, 2002.

[10] Kowalska S., Stepnowski P., Buszewski B., *O cieczach jonowych*, Analityka – nauka i praktyka, 3, 2006.

[11] Wu J., Zhang J., Zhang H., He J.S., *Homogeneous acetylation of cellulose in a new ionic liquid*, Biomacromolecules, 5, 2004.

[12] Zhang H., Wu J., Zhang J., He J.S., *1-Allyl-3-methylimidazolium chloride room temperature ionic liquid: A new and powerful nonderivatizing solvent for cellulose*, Macromolecules, 38, 2005.

[13] Surma-Ślusarska B., Danielewicz D., *Rozpuszczalność różnych rodzajów celulozy w cieczach jonowych*, Przegląd Papierniczy, 68, 2012.

[14] Rodriguez H., Williams M., Wilkes J.S., *Green Chemistry*, 10, 2008, 501–507.

[15] Bodzek M., Bohdziewicz J., Konieczny K., *Techniki membranowe w ochronie środowiska*, Wydawnictwo Politechniki Śląskiej, Gliwice 1997.

[16] Narębska A., *Membrany i membranowe techniki rozdziału*, Wydawnictwo Uniwersytetu Mikołaja Kopernika, Toruń 1997.
[17] Anielak A.M., *Wysokoefektywne metody oczyszczania wody*, Wydawnictwo Naukowe PWN SA, Warszawa 2015.
[18] Mohammadi T., Saljoughi E., *Effect of production conditions on morphology and permeability of asymmetric cellulose acetate membranes*, Desalination, 7, 243, 2009, 1–7.

CONTENTS

TREŚĆ

ISSN 0011-4561
ISSN 1897-6336